UNIVERSIDADE DE SÃO PAULO
FACULDADE DE FILOSOFIA, CIÊNCIAS E LETRAS DE RIBEIRÃO PRETO
PROGRAMA DE PÓS-GRADUAÇÃO EM BIOLOGIA COMPARADA

Solos e seus efeitos na vegetação da Caatinga brasileira

Soils and their effects on Brazilian Caatinga vegetation

Alexandre Tadeu Brunello

Tese apresentada à Faculdade de Filosofia, Ciências e Letras de Ribeirão Preto da Universidade de São Paulo, como parte das exigências para obtenção do título de Doutor em Ciências, obtido no Programa de Pós-Graduação em Biologia Comparada.

Ribeirão Preto - SP
2022

UNIVERSIDADE DE SÃO PAULO
FACULDADE DE FILOSOFIA, CIÊNCIAS E LETRAS DE RIBEIRÃO PRETO
PROGRAMA DE PÓS-GRADUAÇÃO EM BIOLOGIA COMPARADA

Solos e seus efeitos na vegetação da Caatinga brasileira

Soils and their effects on Brazilian Caatinga vegetation

Versão corrigida

Alexandre Tadeu Brunello

Tese apresentada à Faculdade de Filosofia, Ciências e Letras de Ribeirão Preto da Universidade de São Paulo, como parte das exigências para obtenção do título de Doutor em Ciências, obtido no Programa de Pós-Graduação em Biologia Comparada.

Orientador: Prof. Dr. Tomas F. Domingues
Coorientador: Prof. Dr. Jonathan J. Lloyd

Ribeirão Preto - SP
2022

O presente trabalho foi realizado com apoio da Coordenação de Aperfeiçoamento de Pessoal de Nível Superior – Brasil (CAPES) – Código de Financiamento 001

Brunello, Alexandre Tadeu
Solos e seus efeitos na vegetação da Caatinga brasileira. Ribeirão Preto, 2022. 194 p. : 34 il.

Tese de Doutorado − Faculdade de Filosofia Ciências e Letras da USP-Ribeirão Preto. Área de concentração: Biologia Comparada.
Orientador: Domingues, Tomas Ferreira
Coorientador: Lloyd, Jonathan James

1. Semiárido brasileiro 2. Caatinga 3. Pedogênese 4. $\delta^{15}N$ do solo 5. Biomassa acima do solo 6. Atributos funcionais 7. Gradientes climáticos 8. Gradientes edáficos

I dedicate this thesis to my parents, ***Rita and Carlos****, not only for all their support and love during all stages of this challenging work but also throughout life.*

Acknowledgements

I must start by thanking my parents, Rita and Carlos Brunello, for supporting me while I was preparing this work and for having them around during the toughest periods of the COVID-19 pandemic. I have no words to express my gratitude to them, who patiently dealt with me during this difficult time.

I also thank my brother Eduardo, who held valuable conversations with me across the way. I also thank him and his wife, Elis, who brought great joy to our family with the birth of my niece, Nina.

I am extremely grateful to my supervisors, Professors Jon Lloyd, Tomas Domingues, and Beto Quesada, who allowed me to study two contrasting but equally astounding Brazilian biomes: Amazônia and Caatinga. In particular, I thank Professor Jon Lloyd for all his help with theory, methods, and valuable comments on my thesis with his 'good old-fashioned way (with pen on paper)'. Professor Tomas Domingues for supporting me when I was fulfilling the academic stages of the Comparative Biology Graduate Program and for providing me with very helpful comments during all stages of my work. Professor Beto Quesada for providing great support for processing and analysing soil samples in the facilities of the Soil and Plant Thematic Laboratory (LTSP) at the National Institute for Research in the Amazon (INPA) and also for providing me with very helpful comments.

From the mentioned laboratory, many thanks to Laura Oliveira, Edivaldo Chaves, Raimundo Filho, Gabriela Gandhi, Roberta Biazutti, Erison Gomes, and especially Jonas de O. M. Filho, who was a 'faithful squire', took care and carried out a considerable part of the soil analyses. This work was only possible thanks to several members and collaborators of the Nordeste Project Network, especially my colleagues Raquel C. Miatto, Luiza H. M. Cosme, Ana C. Aquino, Tony C. de Oliveira, Rodrigo Miranda, Cidney B. Bezerra, Marcelo Mizushima, Moabe F. Fernandes, Desirée M. Ramos, Valdemir F. da Silva, Danielle Pinho and Euvaldo P. C Júnior (who carried the soil sampling in some sites). I also thank Drs. Magna S. B. de Moura, Laura Borma, Domingos Cardoso, Luciano P. de Queiroz, Mário M. do Espírito Santo, Rubens M. dos Santos, Edmar A. de Oliveira, Elmar Veenendaal, Tiina Särkinen, Peter Moonlight and all students and researchers who participated in the Nordeste Project.

Other people not directly involved in the Nordeste Project also provided me with valuable help: Prof. Dr José J. L. L.de Souza and his master's student Renan Figueiredo, who carried out the X-ray fluorescence analysis, Prof. Dr Gabriela B. Nardoto and Dr Fábio Luis de Sousa Santos, who made possible the isotope analysis at the Center for Nuclear Energy in

Agriculture (CENA). Vinicius A. Maia generously helped me with R scripts and discussions about ecology.

To Dr Tony J. F. Cunha (*in memorian*) for teaching a little about the geology and soils of the Pernambuco state.

To my friend Allan Modolo for all the help with maps and geoprocessing expertise.

To Prof. Dr Everardo V. S. B. Sampaio for contributing with important observations on the use of allometric equations.

To all colleagues from the Community Ecology and Ecosystems Functioning Laboratory (ECOFERP, USP, Ribeirão Preto) for their friendship and scientific discussions during our weekly meetings.

To all locals, including those who helped me with the arduous task of digging over 40 soil pits in the 'wild' Caatinga, as well as undergraduate students who helped me to sort out soil samples and participated in laboratory activities. This study was financed in part by the Coordenação de Aperfeiçoamento de Pessoal de Nível Superior – Brasil (CAPES) – Finance Code 001. The Natural Environment Research Council (NERC, Grant NE/N012488/1) and The São Paulo Research Foundation (FAPESP, Grant 2015/50488-5) financed fieldwork and laboratory efforts. I am grateful to these institutions and all members of the Graduate Program on Comparative Biology, FFCLRP-USP, Ribeirão Preto, SP, Brazil.

Lastly, my gratitude and love go to all my friends and family, without whom life would make so much less sense. *Amo vocês*.

'While the lack of water threatens population growth in arid and semiarid regions, the lack of water is the natural state, and the state that imparted the unique properties to arid and semiarid soils. It is also the lack of water that makes arid and semiarid places some of the most open, least developed places on Earth, and some of the last 'wild' places for future generations to enjoy and study.'

Monger, Martinez-Rios and Khresat

Resumo

BRUNELLO, A. T. **Solos e seus efeitos na vegetação da Caatinga brasileira [tese]**. 2022. Doutorado em Biologia Comparada – Faculdade de Filosofia, Ciências e Letras de Ribeirão Preto, Universidade de São Paulo, Ribeirão Preto, 2022.

As propriedades do solo foram negligenciadas por muito tempo em estudos que tentam particionar a influência potencial de múltiplos fatores sobre as propriedades da vegetação. Essa falta de uma abordagem sistemática sobre como os solos influenciam a vegetação é bastante evidente em estudos com foco em florestas tropicais sazonalmente secas (FTSSs). Uma amostragem de solo e vegetação em 29 parcelas de estudo cobrindo grande parte do Domínio da Caatinga sazonalmente seca (isto é, uma abordam de comparação geográfica) possibilitou avaliar variações em várias propriedades do solo entre três afiliações geológicas: sedimentar (S_{SED}), cristalina (S_{CRY}) e cárstica (S_{KAR}) e investigar até que ponto essas propriedades se relacionam com variações na biomassa lenhosa acima do solo (AGB_W), densidade da madeira ponderada pela (CWM_{wd}), diâmetro máximo do tronco (D_{max}), riqueza funcional (F_{Ric}), equitabilidade funcional (F_{Eve}) e divergência funcional (F_{Div}). As propriedades do solo variaram sistemicamente entre as afiliações geológicas. Por exemplo, as métricas associadas ao intemperismo, como capacidade efetiva de troca de cátions (I_E) e reserva total de bases ($\sum_{RB}$), diminuíram de acordo com $S_{KAR} > S_{CRY} > S_{SED}$, enquanto os teores totais de fósforo no solo − $[P]_T$ − foram relativamente mais altos nas áreas S_{KAR}. Além disso, a distribuição dos principais cátions trocáveis (Ca, Mg, K, Na e Al) no complexo sortivo do solo refletiu também refletiu as respectivas afiliações geológicas, com teores de cátions básicos sendo geralmente maiores nas áreas S_{KAR} e S_{CRY}. Em contraste, os níveis de alumínio trocável foram geralmente mais altos nas áreas S_{SED}. A dinâmica do nitrogênio, avaliada através dos valores de $\delta^{15}N$ do solo, foi modulada principalmente por forças climáticas. Neste sentido, os valores de $\delta^{15}N$ do solo foram negativamente influenciados pelo índice de aridez (AI; onde valores mais altos representam condições mais úmidas) e sazonalidade da precipitação (ψ). Além disso, uma influência positiva de I_E sobre os valores de $\delta^{15}N$ do solo também foi detectada, especialmente nos locais mais úmidos. A AGB_W variou de 4.87 a 85.65 Mg ha^{-1}, sendo positivamente influenciada pela precipitação média anual (P_A) e a fertilidade do solo (representada por cálcio trocável – $[Ca]_{ex}$). Além disso, as interações entre o déficit hídrico climático de longo prazo (CWD) e tanto à $[Ca]_{ex}$ quanto ao teor máximo de água disponível no solo (θ_P) sugerem que a AGB_W na Caatinga é determinada por interações complexas. As propriedades do solo também se relacionaram aos índices de diversidade funcional calculados, com CWM_{dmax}, CWM_{wd}, F_{Ric}, F_{Eve} e F_{Div} sendo todos influenciadas pelas propriedades do solo. Neste sentido, foi encontrada uma relação inversa entre cátions básicos do solo e CWM_{wd}. Em contraste, os cátions básicos do solo influenciaram positivamente CWM_{dmax}. Por fim, várias métricas nutricionais do solo influenciaram positivamente F_{Ric}, enquanto apenas alguns elementos influenciaram inversamente F_{Eve} e F_{Div}. Acredita-se que essas relações reflitam as compensações da vegetação entre o investimento em crescimento secundário e estratégias de uso da água. Coletivamente, esses resultados fornecem informações sobre as múltiplas maneiras pelas quais os solos podem afetar a estrutura e o funcionamento da vegetação.

Palavras-chave: 1. Semiárido brasileiro 2. Caatinga 3. Pedogênese 4. $\delta^{15}N$ do solo 5. Biomassa acima do solo 6. Atributos funcionais 7. Gradientes climáticos 8. Gradientes edáficos

Abstract

BRUNELLO, A. T. **Soils and their effects on Brazilian Caatinga vegetation [thesis]**. 2022. Doctoral degree in Comparative Biology – Faculty of Philosophy, Sciences and Letters of Ribeirão Preto, University of São Paulo, Ribeirão Preto, 2022.

Soil properties have long been overlooked in studies that attempt to disentangle the potential influence of multiple drivers on vegetation properties. This lack of a systematic approach to how soils influence vegetation is markedly evident in studies focusing on seasonally dry tropical forests (SDTFs). A soil and vegetation sampling in 29 study plots covering a large part of the seasonally dry Caatinga Domain (that is, a geographic comparison approach) allowed evaluating variations in several soil properties among three geological affiliations: sedimentary (S_{SED}), crystalline (S_{CRY}) and karst (S_{KAR}), and investigating to what extent these properties relate to variations in above-ground woody biomass (AGB_W), community-weighted mean wood density (CWM_{wd}), community-weighted mean maximum stem diameter (D_{max}), functional richness (F_{Ric}), functional evenness (F_{Eve}) and functional divergence (F_{Div}). The soil properties varied systemically among geological affiliations. For example, weathering-associated metrics such as effective cation exchange capacity (I_E) and total reserve base cations ($\sum_{RB}$) were found to decrease following $S_{KAR} > S_{CRY} > S_{SED}$, while total soil phosphorus concentrations ($[P]_T$) were relatively higher at the S_{KAR} sites. Moreover, the distribution of main soil exchangeable cations (Ca, Mg, K, Na, and Al) in the soil sortive complex reflected the respective geological affiliations, with soil base cations being generally higher at the S_{KAR} and S_{CRY} sites. In contrast, exchangeable aluminium levels were generally higher at the S_{SED} sites. Nitrogen dynamics, addressed by soil $\delta^{15}N$ values, was found to be primarily modulated by climatic forces. In this sense, soil $\delta^{15}N$ values were negatively influenced by the aridity index (AI; where higher values represent more humid conditions) and the seasonality of the precipitation (ψ). Moreover, a positive influence of I_E on soil $\delta^{15}N$ values is also suggested, especially at the wetter sites. The AGB_W ranged from 4.87 to 85.65 Mg ha^{-1}, being influenced by the mean annual precipitation (P_A) and soil fertility (represented by exchangeable calcium – $[Ca]_{ex}$). Furthermore, interactions between long-term climatic water deficit (CWD) and both $[Ca]_{ex}$ and the maximum plant-available soil water content (θ_P) suggest that AGB_W in Caatinga is driven by complex interactions. Soil properties were also related to community functional characteristics, with all CWM_{dmax}, CWM_{wd}, F_{Ric}, F_{Eve}, F_{Div} being influenced by soil properties. In this sense, an inverse relationship was found between soil base cations and CWM_{wd}. In contrast, soil base cations had a positive influence on CWM_{dmax}. Finally, several soil nutritional metrics positively influenced F_{Ric}, while only a few elements inversely influenced both F_{Eve} and F_{Div} metrics. These relationships are thought to reflect vegetation trade-offs between investment in secondary growth and water-economy strategies. Collectively, these results provide information on the multiple ways through which soils can affect vegetation structure and functioning.

Keywords: 1. Brazilian semiarid 2. Caatinga 3. Pedogenesis 4. Soil $\delta^{15}N$ 5. Above-ground biomass 6. Functional traits 7. Climatic gradients 8. Edaphic gradients

List of figures

List of tables

List of symbols and abbreviations

S_{SED} –designates soils or sites associated with sedimentary parent materials

S_{CRY} – designates soils or sites associated with crystalline parent materials

S_{KAR} – designates soils or sites associated with karstic parent materials

S_{LAC} – low-activity clay soils

S_{HAC} – high-activity clay soils

S_{ARE} – arenic soils

AGB – above-ground biomass

AGB_W – above-ground woody biomass

CWM – community-weighted trait means

$Sand_f$ – soil sand fraction

$Silt_f$ – soil silt fraction

$Clay_f$ – soil clay fraction

$[Ca]_{ex}$ – soil exchangeable calcium

$[Mg]_{ex}$ – soil exchangeable magnesium

$[K]_{ex}$ – soil exchangeable potassium

$[Na]_{ex}$ – soil exchangeable sodium

$[Al]_{ex}$ – soil exchangeable aluminium

$\sum_B$ – soil sum of bases

$\sum_{RB}$ – soil total reserve of bases

NCR_T – soil total nutrient capital reserves

I_E or ECEC – effective cation exchange capacity

BS% – soil base saturation

m% – soil aluminium saturation

pH_{H2O} – water-measured soil pH

pH_{KCl} – KCl-measured soil pH

$\delta^{15}N$ – the ratio between the two N stable isotopes (^{15}N: ^{14}N)

$[Ca]_T$ – soil total calcium

$[Mg]_T$ – soil total magnesium

$[K]_T$ – soil total potassium

$[Na]_T$ – soil total sodium

$[P]_T$ – soil total phosphorus

$[Fe]_T$ – soil total iron

$[Mn]_T$ – soil total manganese

$[Zn]_T$ – soil total zinc

$[C]_T$ – Soil total carbon

$[C]_N$ – Soil total nitrogen

C/N – soil or plant C: N ratio

T_A – Mean annual temperature

T_{MAX} – Mean temperature of the warmest month

P_A – Mean annual precipitation

AI – Aridity index

ETP_0 – Potential evapotranspiration

CWD – Long-term climatic water deficit

CWD_{adj} – Long-term climatic water deficit with positive sign

θ_v – texture-associated volumetric water content

$W_{\theta V}$ – texture-associated volumetric water content weighted across soil profiles

θ_p – Maximum plant-available soil water

R_{EF} – Measured effective rooting depth

Ψ – Precipitation seasonality (used once for soil matric potential)

a – annum

Ma – mega annum

MEM – Moran Eigenvector Map

OLS – Ordinary least squares

LMM – linear mixed model

SWC – Spatial weighting matrix

AICc – Corrected Akaike Information Criterion

W – Akaike weights

I – Global Moran's I

VIF – Variance Inflation Factor

RIV- Relative importance value

CPRM – Geological Survey of Brazil

IBGE - The Brazilian Institute of Geography and Statistics

RSG – Reference Soil Group

IUSS – International Union of Soil Science

WRB – World Reference Base

SiBCS – Brazilian System of Soil Classification

Summary

Introduction

Although most research in tropical zones has been carried out in evergreen forests and savanna formations, seasonally dry tropical forests (SDTFs; PENNINGTON; PRADO; PENDRY, 2000) have unquestionable ecological and floristic importance. Seasonally dry tropical forests comprise a wide range of plant physiognomies (MURPHY; LUGO, 1986), generally consisting of trees and shrubs with varying height and canopy closure levels, and almost all plant species shedding their leaves during the dry season.

Globally, SDTFs are relatively less studied than other tropical biomes (SANTOS et al., 2011; BECKNELL; KUCEK; POWERS, 2012), although the prevailing water limitation in this type of biome is a strong ecological force that drove the evolution of a unique dry-adapted flora (PENNINGTON; PRADO; PENDRY, 2000; FERNANDES et al., 2022). Furthermore, a considerable part of the available studies did not consider any sort of soil properties.

For example, Becknell, Kucek and Powers (2012) were able to only evaluate climatic variables as explanatory variables of above-ground biomass over an extensive meta-analysis that included 44 pant-tropical studies of SDTFs. The absence of edaphic variables in that study was due to inconsistency among protocols for soil analyses or due to the total lack of soil data. Becknell, Kucek, and Powers (2012) also highlight the need for measurements of soil variables that could potentially explain the biomass stocks of SDTFs.

Most importantly, geologically-derived soil properties are expected to influence vegetation composition, structure, and functioning in multiple ways. For instance, soil properties should influence vegetation not only by providing essential resources (that is, water and nutrients) and mechanical support but also by acting as an environmental selecting species according to particular edaphic conditions (FERNANDES et al., 2022). Furthermore, soil properties have already been shown to influence wood anatomical characteristics (e.g., QUESADA et al., 2012; LIRA-MARTINS, 2019), potentially accounting for variations in many other plant traits (JAGER et al., 2015).

In Brazil, the bulk of SDTFs is found within the Caatinga biome borders, which virtually coincides with the Brazilian semiarid region. This seasonally dry biome occupies an area of approximately 862,818 km² and has marked environmental heterogeneity (IBGE 2019a; 2019b), which is particularly notable when considering the landforms and various soil parent materials found in the region. In simple words, soil parent materials refer to the underlying material, consolidated or not, from which soils are formed (generally bedrock or unconsolidated sediments).

Historically, Caatinga has attracted less attention compared to other biomes in South America (SÄRKINEN et AL. 2011; ALBUQUERQUE et al., 2012), with the study by Santos et al. (2011) providing a series of scores from the '*semiquantitative index describing biodiversity survey efforts and knowledge status'* that support the so-called 'Caatinga negligence', especially compared to other Brazilian regions. Although this situation seems to be improving over the last few years, with several studies being published in important journals of international circulation, the need for the adoption of methodologically consistent protocols for soil analysis remains noticeable. This relative lack of standardised surveys also applies to soils, as there are not many studies reporting on systematic variations in soil properties, and how these properties can account for variations in vegetation structure and function in the region.

Concerning the Caatinga soils themselves, the mosaic pattern of its spatial distribution (Figure 1.3, Chapter 1) is known to be the product of long-lasting intricate evolutionary geological processes (AB' SABER, 1974; SAMPAIO, 1995; OLIVEIRA, 2011). These processes largely determined the chemical, physical, and mineralogical properties of soil, and despite their marked spatial variability, they have been classically categorised into discrete groups to reflect their geological origin. For instance, several studies in ecology and botany classified Caatinga plant communities as 'Crystalline Caatinga', 'Sedimentary Caatinga' and 'Karst Caatinga' (QUEIROZ, 2006; QUEIROZ et al., 2017; FERNANDES et al., 2022).

Importantly, the semiarid climate of Caatinga limits weathering and leaching rates, thus ensuring that soil properties strongly reflect parent material properties. From a general standpoint, soils that overlay the aforementioned geological strata have predictable properties, where 'crystalline soils' are generally assumed to be less weathered (that is, low to intermediate pedogenetic development), while 'sedimentary soils' are generally assumed to be more weathered, noting that many exceptions are common, e.g. soils types with low pedogenetic development can be also found in sedimentary environments.

Soils from karst areas usually show particular properties. This is because the limestones and dolomites typically found in these areas often give rise to soils with high base saturation and high soil pH, ultimately controlling several biogeochemical processes. It should be noted, however, that local relief conditions usually exert a major influence on the properties of these soils. For example, Oliveira et al. (2018) found that solum thickness and mineral assemblage were a function of microrelief variations in karst soils of the Apodi Plateau NE Brazil, with higher weathering rates taking place where surface water tends to accumulate, i.e. concave portions of the terrain.

Therefore, this thesis develops upon the idea that geological processes, in addition to promoting biogeographical shifts (FERNANDES et al., 2022), are a major determinant of soil properties in the semiarid Caatinga. In turn, soil properties are expected to account for variations in a suite of vegetation properties, including stand-level above-ground woody biomass, and community-weighted trait means.

Understanding how climate, soil chemical and physical properties, and their complex interactions altogether determine vegetation structure and functioning is critical to improving our general ecological knowledge in semiarid environments and predicting how global changes may affect the Brazilian Caatinga biome.

Aims and objectives of the thesis

The brief introduction above put forward the outstanding environmental heterogeneity of the Caatinga, which is further detailed in Chapter 1. Despite valuable efforts over the last few decades, the need to improve our understanding of how environmental factors influence the composition, functioning, and structure of vegetation remains noticeable.

Therefore, the general objectives of this thesis are:

1. Employ standard soil and vegetation protocols, with the purpose of investigating soil properties, as well as their relationships with vegetation.
2. Provide a detailed approach for Caatinga soils with particular reference to the study sites sampled as part of the Nordeste Project, aiming to contribute with the soil science in the region.

Thesis outline

Chapter 1 - Literature review

Chapter 2 – Several soil properties were analysed, along with the potential influence of climate on selected soil properties. The analyses were performed in the context of sites associated with distinct geological affiliations (determinants of soil parent materials), that is, soils derived from sedimentary parent materials (S_{SED}), soils derived from crystalline rocks (S_{CRY}), and soils derived from karst environments (S_{KAR}).

Chapter 3 – The influence of climate and soil on above-ground woody biomass (AGB_W) was evaluated through a linear mixed-effect model (LMM), along with a multi-model inference and

approach. Additionally, bivariate relationships were explored considering the entire dataset together and evaluated geological categories separately. Finally, relationships between several soil properties, community-weighted means of plant functional traits, and functional diversity indexes were explored.

Chapter 4 – Concluding remarks

Chapter 1

Literature review

Chapter 1 − Literature review

1.1 Seasonally Dry Tropical Forests

Seasonally dry tropical forests (SDTFs) is a broad term that represents a globally extensive and still less studied biome compared to their tropical humid forests counterparts (PENNINGTON; LEWIS; RATTER, 2006; SANTOS ET AL., 2011; BECKNELL; KUCEK; POWERS, 2012). Although there is no consensus to define SDTFs (SIYUM, 2020), seasonal climatic patterns and long dry periods are elements that are commonly present in bioclimatic definitions of SDTFs. To provide a classical definition, as adopted by Murphy, and Lugo (1986), the term SDTFs encompasses a wide range of vegetation formations, from tall forests in wetter places to succulent scrub where rainfall is reduced, with the annual precipitation levels usually falling within 0.25 to 2.0 m, with 4-7 months with less than 0.1 m precipitation (MURPHY; LUGO, 1986)[1]. Deciduousness is a conspicuous trait of SDTFs, with most woody plant species shedding their leaves during dry periods, which usually is more pronounced as rainfall decreases (MOONEY; BULLOCK; MEDINA, 1995). As a result, leaf litter often accumulates on the forest floor during drier periods, but also because direct sunlight on the forest floor leads to very low humidity levels and low decomposition rates (QUEIROZ, 2006). Xeromorphic traits are also common in SDTFs plants, e.g. the replacement of leaves by spines and the crassulacean acid metabolism (CAM) (SAMPAIO, 1995). The latter is mostly represented by the leafless Cactaceae and Euphorbiaceae families. In addition, ecosystem processes such as net primary productivity take place only during a restricted wet season, i.e., plant growth is markedly seasonal (QUEIROZ, 2006).

Regardless of employed definitions, there is agreement that SDTFs coverage is decreasing worldwide (OCÓN et al., 2021). Also, despite the controversies to estimate the actual extent of these formations, it is noteworthy that these ecosystems have a considerable role in the global carbon budget, with semiarid biomes significantly participating in inter-annual carbon cycle inter-annual variations (POULTER et al., 2014). They also harbour many unique species (SÄRKINEN et al., 2011; DRYFLOR, 2016). More than 50% of the global SDTFs are located within South America, with the other remnants in North America, Central America, Eurasia and Africa (MILES et al., 2006). Figure 1.1 shows the SDTFs distribution across the Neotropics.

[1]Such thresholds may vary according to the bioclimatic definition adopted (ÓCON, 2021).

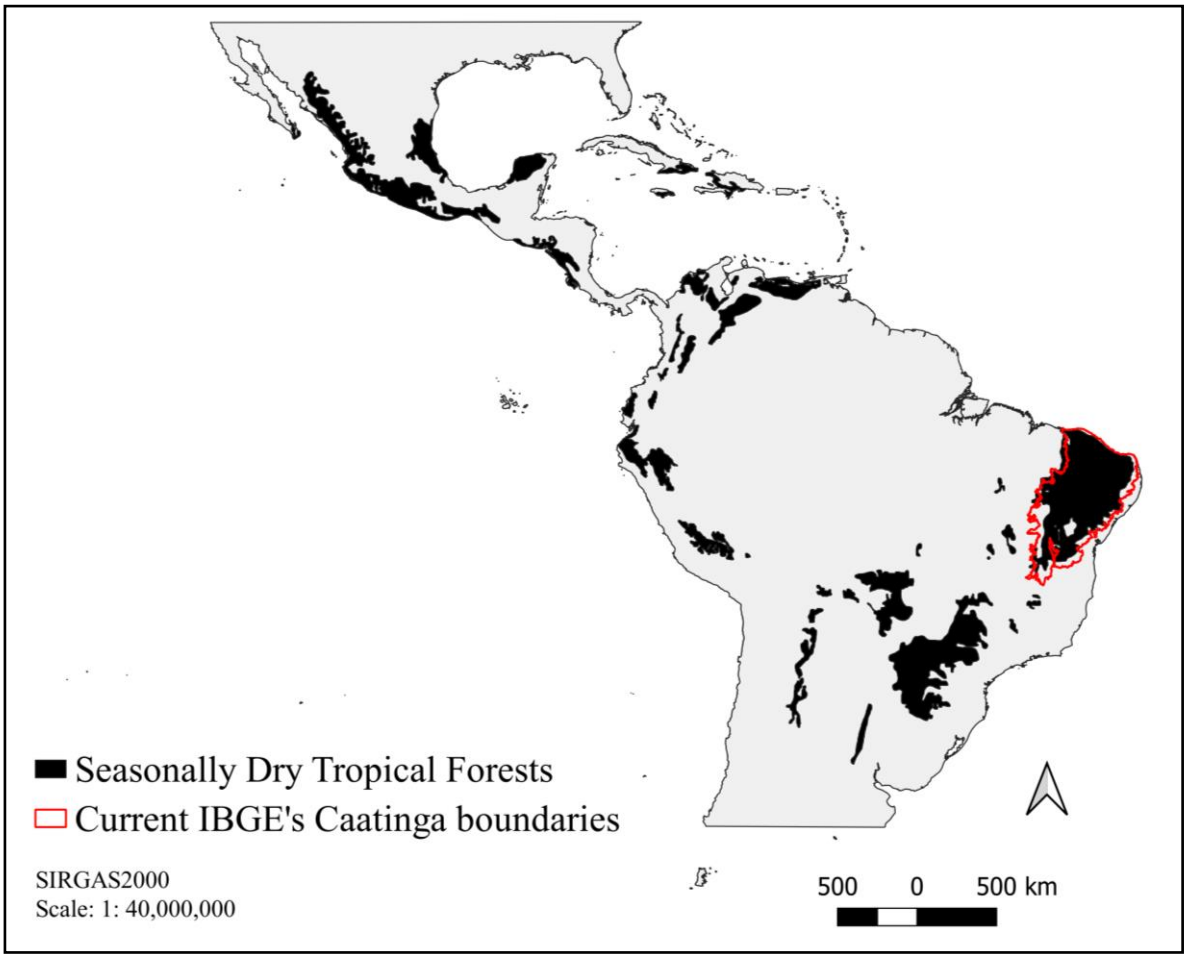

Figure 1.1: Seasonally Dry Tropical Forests distribution in the Neotropics. Redesigned from DRYFLOR et al., 2016. Shapefiles of SDTFs and the Neotropical region were downloaded from the DRYFLOR website (http://www.dryflor.info/data). The Caatinga boundaries shapefile downloaded from the IBGE's website (https://www.ibge.gov.br/geociencias/downloads-geociencias.html).

In South America, these formations occur scattered in disjunct patches. The Brazilian Caatinga is the largest and most continuous nucleus of SDTFs in the New World (QUEIROZ, 2006; QUEIROZ et al., 2017, FERNANDES; CARDOSO; QUEIROZ, 2020), followed by areas known as the Missiones and the Piedmont Nuclei (PRADO; GIBBS, 1993), and areas nearby Venezuela and Colombia coasts (PENNINGTON; PRADO; PENDRY, 2000; DRYFLOR, 2016). Smaller and isolated patches occur scattered with variable plant community structure and composition, largely depending on abiotic conditions (PENNINGTON; PRADO; PENDRY, 2000). Taken together, the unique characteristics of SDTFs, their ecological importance and current levels of climatic and anthropogenic threats, draw attention to the need for a better ecological and biogeochemical understanding as well as the preservation of these ecosystems. Because Caatinga's SDTFs and their relationships with the environment will be

focussed on throughout this work, a brief biotic and environmental characterisation is provided in the following section.

1.2 The Brazilian Caatinga

Even before the arrival of naturalists in Brazil, indigenous groups had already named the typical vegetation growing in Northeastern Brazil *Caatinga*, which means 'whitish forest' in Tupi indigenous language. This is thought to reflect the whitish leafless vegetation aspect during the dry waterless periods (AB'SÁBER; MARIGO, 2011). The word Caatinga names the bulk of SDTFs in Brazil, also naming one of the Brazilian biomes, which occupies an area of ca. 862,818 km², representing about 10.1% of the Brazilian territory according to the Brazilian Institute of Geography and Statistics (IBGE, 2019a)[2]. This biome occurs in all Northeastern Brazil states and is present in the upper part of Minas Gerais state (Southeastern Brazil). Considering the region's observed latitudinal range (ca. 3º to 18º S), the climate is considered azonal since it differs significantly from other regions with the same latitudinal range (AB'SÁBER, 1974). The complex atmospheric circulation largely explains the azonal climate of Caatinga, which is caused by multiple meteorological phenomena (MOURA et al., 2019). In conjunction with orographic effects (i.e. the moisture interception by high plateaus or mountains), the Caatinga region occurs predominantly across a semiarid climate, with scattered wetter environments, or 'exception landscapes' (AB'SÁBER, 1974). As a result of the complex circulation and relief effects patterns, the annual mean precipitation (P_A) is erratic in time and space, usually ranging from 250 – 1000 mm a^{-1}, often concentrated in 3 – 5 months (OLIVEIRA, 2011). Rainfall generally decreases from the Caatinga boundaries to the interior while the temperature rises (SAMPAIO, 1995). At the biome boundaries, the mean annual precipitation is roughly about 1000 mm a^{-1}, coinciding with the so-called 'Drought Polygon' or the 1.0 m isohyet (ANDRADE-LIMA, 1981). Drought events have been reported since the 16th century in the Brazilian semiarid region (MARENGO; CUNHA; ALVES, 2016), with Lima and Magalhães (2018) providing evidence that long-lasting droughts frequency increased significantly over the last centuries. Moreover, the long drought recorded in the 2012-2017 period is believed to be among the longest in history, with the last high-magnitude comparable event dating from the 1720-1727 period (LIMA; MAGALHÃES, 2018; SANTANA; SANTOS, 2020).

[2]The Caatinga area may vary from author to author according to the criteria adopted.

The cloud frequency in Caatinga is usually low so the total annual solar radiation is typically high (OLIVEIRA, 2011). Such high-intensity solar radiation results in high potential evapotranspiration rates (E_p), usually ranging from 1.5 – 2.0 m a^{-1}. Therefore, E_P rates in most cases overcome annual rainfall levels (P_A), resulting in negative water balances of 7 – 11 months year-round (MENEZES et al., 2012). Thus, the P_A / E_p ratio is commonly < 0.65, which characterises the semiarid climate. Furthermore, the high coefficients of variation of rainfall (usually higher than 30%) can be even more critical in conditioning the ecosystem functioning across the region (SAMPAIO, 2010). Considering that many ecological processes occur closely synchronised with adequate water supply, precipitation seasonality is of great importance in these environments (MURPHY; LUGO, 1986), influencing several vegetation features such as canopy coverage, seedling mortality, successional and evolutionary courses (MARKESTEIJN ET AL., 2010; APGAUA et al., 2015).

Some classical overviews of Caatinga have been presented over the past decades (AB'SABER, 1974; ANDRADE, 1977; ANDRADE-LIMA, 1981; SAMPAIO, 1995; ALBUQUERQUE et al., 2012). From these reviews, it can be said that the Brazilian Caatinga stands out in terms of geodiversity (including landforms, rocks, sediments and soil types), which along with the typical semiarid climate, gave rise to an adapted biodiverse and structurally distinct flora. In this context, the geographical soil distribution of Caatinga is commonly referred to as a 'mosaic' (e.g. MEIADO et al., 2012). This terminology can be extended to other components of the ecosystem, such as the complex geological arrangement and the vegetation, also commonly mentioned as a mosaic of plant physiognomies. Furthermore, the unique phytogeographical characteristics of the region appear indisputable among South American SDTF nuclei, as the region harbours several 'Caatingas' (AB'SÁBER, 1974), and many phytophysiognomies have been described and reviewed by some authors (e.g., ANDRADE-LIMA, 1981; VELLOSO et al., 2001; MORO et al., 2014). However, the dry tropical deciduous thorn woodland (Caatinga *stricto sensu*) or *Savana Estépica* in the IBGE definition is estimated to occupy ca. 63% of the Caatinga territory, followed by ecotones and vegetation enclaves (22.6%), deciduous forests (8.0%) and semideciduous forests (2.1%). Savannas and evergreen dense and open forests are also represented to a minor extent throughout the region (IBGE Environmental Information Database, BDiA, Vegetation theme, 2022).

The current knowledge of Caatinga soils is the result of the efforts of several soil scientists and institutions, such as the National Soil Survey and Conservation Service (SNLCS),

currently EMBRAPA soils. The latter has continued the work started in 1947 when the first systematic soil survey was conducted in Brazil (FAVORIM; LAFORET; ARCANJO, 2021). However, much still needs to be done in terms of systematic soil studies that enable our understanding of soil properties and how these properties relate to vegetation structure, functioning and composition.

Beyond their nutritional role, soil characteristics also play a paramount role in the ecosystem water budget, being ultimately the link between rainfall and the available water potentially provided to the ecosystem (WELTZIN et al., 2003; JARAMILLO; MURRAY-TORTAROLO, 2019). But because SDTFs are, intuitively, water-limited ecosystems, soil properties have long been overlooked.

In this scenario, and given that one of the main objectives of this thesis is to provide a detailed approach to Caatinga soils, it is first necessary to describe Caatinga geology and geomorphology, because these largely determine soil properties. From a general standpoint, it may be expected that, as the rainfall levels decrease in a certain region, the climate factor loses strength in determining soil properties, whereas geology (parent materials) and relief assume a more influential role in determining these properties (ARAÚJO FILHO, 2011; ARAÚJO FILHO et al., 2017).

1.3 Geodiversity of Caatinga

The Brazilian Caatinga is characterised by remarkable geological variability, with rock ages ranging from the Paleoarchean Era (3600 – 3200 Ma[3]) to the Quaternary (2.58 Ma BP to the present). Since the 1970s, huge efforts have been made to leverage the mining activities in Brazil through the *RADAM* and *RADAMBRASIL* Projects of the Geological Survey of Brazil (CPRM), Petrobras, universities and several public and private entities. This has yielded diverse maps and a huge volume of data, including the physicochemical properties of rocks (HASUI, 2012).

Brazil was first geologically compartmentalised in the pioneering works of Almeida et al. (1977; 1981), who separated the major geological unit (i.e. the South American Platform) into discrete structural provinces. In simple words, these provinces consist of large continuous domains, with particular compositions along with a shared evolutionary geotectonic history and

[3]Ma = Mega age, i.e. millions of years; 1,000 Ma = 1 Ga

a clear distinction from the surrounding provinces (ALMEIDA et al., 1977; 1981). Although there are several distinct schemes for separating geological provinces (e.g. ALMEIDA et al. 1977; 1981; SCHOBBENHAUS; NEVES, 2003; ALKMIM; MARTINS-NETO, 2004), the current scheme adopted by the IBGE separates Brazil into 13 structural provinces plus the Cenozoic coverage (details below). This scheme is mainly based on Almeida et al. (1977) and incorporates some inputs from other authors. Among these provinces, six plus the Cenozoic coverage occur in Caatinga, that is, São Francisco, Borborema, Parnaíba, Recôncavo Tucano-Jatobá, 'Coastal Province and Continental Margin', Mantiqueira and Cenozoic coverage (Figure 1.2). As already mentioned, these provinces are chiefly differentiated according to the nature of their crystalline basement or sedimentary rocks (i.e. soil parent materials), considering similarities in structures, tectonic plates, and evolutionary geotectonic history (ALMEIDA et al., 1977; 1981). It is noteworthy that, regardless of the specific characteristics of each province, much of their structural evolution has interdependent relationships (ALMEIDA et al., 1981). A brief characterisation of geotectonic processes and geological structural provinces comprised in Caatinga follows.

The São Francisco Province corresponds to its namesake São Francisco Craton in extension and geotectonic characterisation (ALMEIDA et al., 1977; IBGE, 2019b). Materials of various ages overlie the basement of this province. However, where the basement is exposed, it is as old as the Archean (4000 – 2500 Ma BP; ALMEIDA et al., 1977), with subsequent complex events determining the province characteristics, including the collisional Brasiliano orogeny (or Brasiliano cycle) dated from the late Neoproterozoic (670 – 550 Ma BP) (SCHOBBENHAUS; NEVES, 2003). As a result, the South American continent was amalgamated into the African continent, forming the 'São Francisco-Congo/Kasai-Angola' shield. These lumped continents were much later spread during the Pangea's supercontinent splitting (MABESOONE; NEUMANN, 2005), with massive magma amounts being released during these intricate events, allowing the formation of highly migmatised granitic-gneissic complexes (ALMEIDA et al., 1977). Also covering a considerable part of the crystalline basement, representative structures composed of metasediments, metavolcanics, metamorphosed mafic (magnesium and iron-rich rocks), and ultramafic (high iron content; low silicon, potassium and sodium contents) rocks also occur in the province (MABESOONE; NEUMANN, 2005), largely determining the characteristics of soil parent materials. The presence of sedimentary basins across São Francisco Province is also of note, such as the Espinhaço Supergroup, an intracratonic *sag* basin (thick accumulations of sediments) that

shows old Mesoproterozoic (1600 – 1000 Ma) sedimentary structures, mainly formed by arenites and quartz-sericite schist (DUSSIN; DUSSIN, 1995).

The Borborema Province occupies an extensive part of the Caatinga region and was formed during the ancient Brasiliano Orogeny. In simple words, the province's basement is a mosaic resulting from the amalgamation of microcontinents from the Paleoproterozoic (2500 – 1600 Ma BP) (MABESOONE; NEUMANN, 2005). In addition, the Borborema province also comprises sedimentary basins formed during the Cretaceous, where aborted rifts were filled with sediments (ALMEIDA et al., 1977; MABESOONE; NEUMANN, 2005). In this context, the Araripe sedimentary basin represented in Figure 1.2, where the uppermost layers form the Chapada do Araripe, is formed by fluvial sandstone from the late Cretaceous (PEULVAST; BÉTARD, 2015).

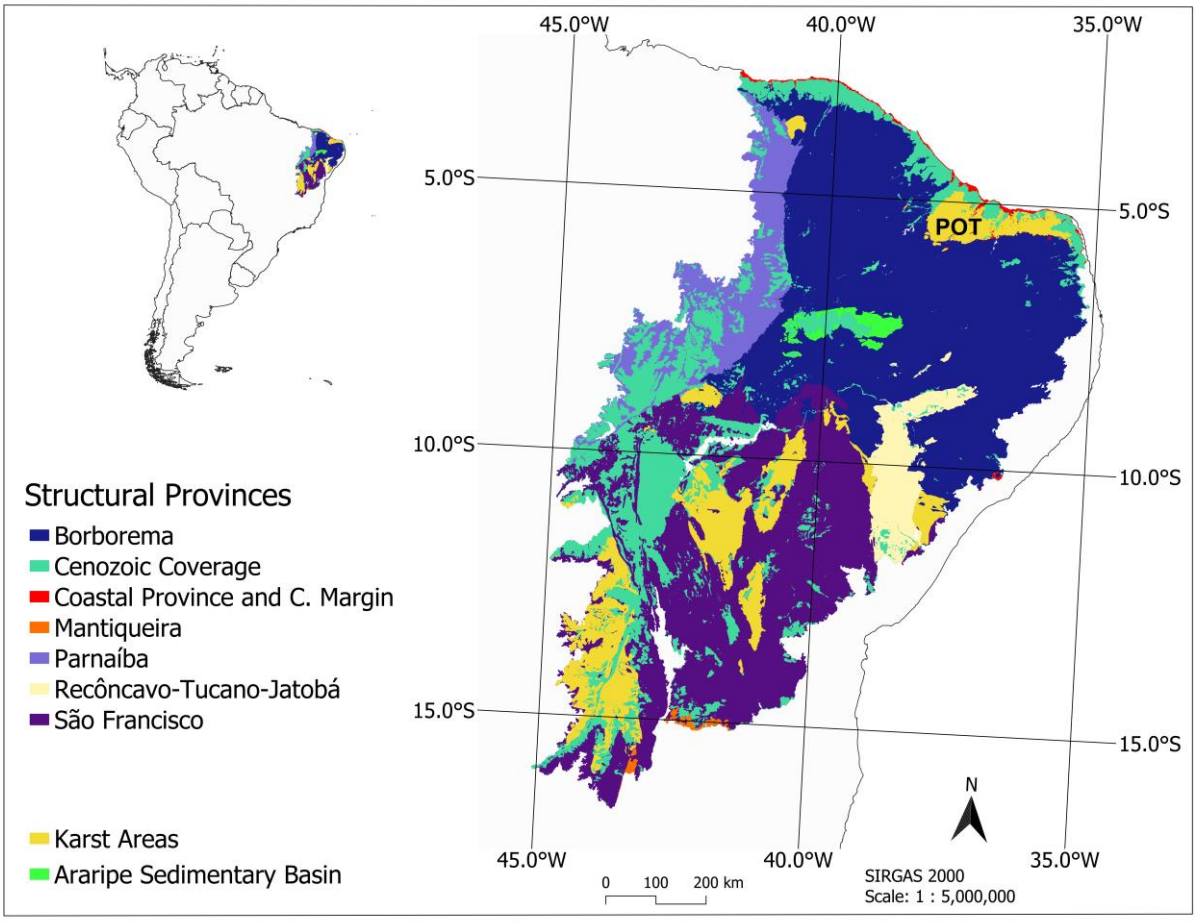

Figure 1.2: Structural provinces encompassed in the Caatinga region. Upper left) South America with emphasis on the Caatinga domain. Right) structural provinces encompassed in the regions. Karst areas and the Araripe sedimentary basin (embedded in the Borborema Province) are also shown. Shapefile source: IBGE's Environmental Information Database – BDiA (theme geology). Map desgin: Brunello, A. T.

Regarding other lithotypes found throughout the Borborema Province, it exhibits rocks as old as the Archean and, predominantly, Paleoproterozoic rocks, overlain by metasedimentary, metavolcanic granitoid intrusions, associated with the Cariris Velhos Cycle (1100 – 930 Ma BP) (HASUI, 2012). Other products include diabase dykes (sheets of rock formed in a fractured pre-existing rock) from the Cretaceous Period, alkalic-basaltic volcanic, and other thin sediment layers from the Tertiary and Quaternary that may occur locally (ALMEIDA et al., 1981). Thus, a great range of rock types is found throughout the Borborema Province.

Along with Paraná Basin and the Amazonas Basin, the Parnaíba Province is one of the large, essentially sedimentary Brazilian basins which virtually overlaps the homonym Parnaíba sedimentary basin, which is essentially formed by Paleozoic strata, occupying ca. 650,000 km² in Piauí, Maranhão and Tocantins, Ceará and Pará states (ALMEIDA et al., 1977; 1981; DA CONCEIÇÃO et al., 2016). The geological strata found throughout the province resulted from coastal and neritic sedimentation, originating sandstones with different grain sizes and conglomeratic associations, followed by thin arenites, siltites and shales, totalising a layer of about 700 m (ALMEIDA et al., 1977; 1981). The region has undergone marine regressions and transgressions episodes along the Devonian Period, resulting in an accumulation of arenites from the seawater (ALMEIDA et al., 1981; MABESOONE; NEUMANN, 2005). Despite the sedimentary origin, the Precambrian basement is also exposed in the northern part of the province. After long-lasting sedimentation (both marine and fluvial), the region has undergone an uplift, with other successional sedimentation events and basaltic magmatism (ALMEIDA et al., 1977). Enormous exposures of sedimentary rocks can be encountered in the region, such as in the Cabeças Formation in the *Parque Nacional das Sete Cidades* (IBGE, 2019b). The geological wealth of the region includes fossil plant-bearing sites, such as the Pedra do Fogo Formation, where large gymnosperm woods were recorded, associated with sedimentary sandstones, siltstones, cherts and limestones (DA CONCEIÇÃO et al., 2016).

The Recôncavo-Tucano-Jatobá Basin consists of extensive sedimentary coverage that partially overlain part of the originally proposed Borborema and São Francisco provinces (IBGE, 2019b). It is estimated that 85% of the basin is in Bahia state. The basin's history goes back to the breakup of the Gondwana supercontinent when aborted rifts (aulacogens) emerged (BIZZI; SCHOBBENHAUS; MOHRIAK, 2003). During this event, the formation of sedimentary basins was enabled, sequentially forming coupled uplifted basins in the South-North direction from Bahia until the Pernambuco states. Caixeta et al. (1994) described the

main lithostratigraphic units (i.e. types of strata or rock layers) present in the basin, from where it can be highlighted the overall occurrence of sandstones and shales with variable grain size and colouration, along with kaolinitic conglomerates, arkose and calcareous also present to a minor extent. Overall, a relief-correlated sandstone has accumulated in this basin (MABESOONE; NEUMANN, 2005).

The Coastal Province and Continental Margin circumscribes the South American Platform divergent margin, directly associated with the ancient Gondwana supercontinent splitting and the rise of the Atlantic Ocean (ca. 140 Ma B.P.) (IBGE, 2019b). Physiographically, the Coastal Province usually exhibits a gently elevated relief closer to the coast, chiefly composed of alluvial and marine deposits. Moving west, the relief becomes higher, represented mainly by tablelands, with a significant presence of continental and marine sediments until the province's boundaries, where the crystalline basement is reached (ALMEIDA et al., 1977; 1981). The continental margin translates into the immersed part of the province, where many sediment types are found, particularly associated with materials from different sedimentation events (MILANI; THOMAZ FILHO, 2000).

The Mantiqueira Province occupies a modest 0.2% of the Caatinga territory and results from the late Neoproterozoic (SCHOBBENHAUS; NEVES, 2003). The province’s territory is predominantly mountainous, with altitudes usually ≥ 1500 a.s.l., which indicates that the relief strongly influences the soil through its rejuvenation originating from erosive processes. Schematic geological cross-sections have shown many crystalline or sedimentary lithologies occurring throughout the province (IBGE, 2019b). Within the main lithotypes found in the northeastern portion of the province, there are alkaline rocks, pelitic to psefitic (i.e. finer to coarse grains) sediments, limestones, mafic volcanic rocks, and other sediments with a variable degree of metamorphism (from greenschist to amphibolite) (ALMEIDA et al., 1977; 1981).

Finally, the Cenozoic Coverage occurs mostly in the southern part of the Parnaíba province and on the western side of the São Francisco Province. To a lesser extent, it occurs in the region’s northern boundary and small inlays within the other provinces. In a simple definition, the Cenozoic coverage represents the sedimentary filling of continental basins during the last 66 Ma in the Cenozoic (IBGE, 2019b). Therefore, geological characteristics (including both landforms and parent material types) are expected to strongly control edaphic properties. Following this rationale, Araújo (2011), Araújo et al. (2017) and Araújo et al. (2019), based on the Northeast Agroecological Zoning (SILVA et al., 1993),

compartmentalised the region into nine landscape units and described the main soil types associated within each type landscape.

In terms of geomorphology, some predominant landforms can be recognised across the Caatinga region: the relief across interplanaltic lowland depressions (locally known as *Depressão Sertaneja*), which is mostly gently undulating, assigned by the intense, long-lasting pediplanation process under semiarid conditions. These processes date from the Cenozoic (Tertiary to Quaternary) and are still active (BEEK; BRAMAO, 1969). As a result, Precambrian crystalline rocks were exposed (i.e. granites, gneisses, and schists), leaving only residuals vestiges (i.e. inselbergs, tablelands, uplands, and mountains) from the younger rocks (BEEK; BRAMAO, 1969; AB'SABER, 1974). Although the soils in these 'depressions'[4] commonly have silty to clayey texture and high fertility, they are commonly shallow, stony, and susceptible to erosion under certain conditions (VELLOSO et al., 2001).

Regarding main soil types found across broad geological types, Leptosols, Regosols and Luvisols, i.e. soils with low medium pedogenetic development, account for a considerable part of crystalline terrains, whereas Arenosols, Ferralsols and Acrisols are soil groups commonly formed in sedimentary terrains, which, in general, are well-weathered, deep, sandy, along with fast-draining conditions (SAMPAIO, 1995, ARAÚJO FILHO, 2011). For example, kaolinitic yellow Ferralsols, developed from Cretaceous ferruginous sandstones, are widespread in the *Chapada do Araripe* (BEEK; BRAMAO, 1969). Although these characteristics predominate, exceptions may occur across the sedimentary portion of Caatinga. For example, in *Complexo de Campo Maior*, a mosaic of ecotones located in the Piauí state, shallow, acidic, finer-textured, and poorly-drained Plinthosols predominate (VELLOSO et al., 2001).

Other sedimentary formations that are important to the Caatinga flora are the aeolian relict continental dunes and karst areas. The former was encompassed in the list of the ecoregions (so-called *Dunas do São Francisco*; VELLOSO et al., 2001). In *Dunas do São Francisco*, disjunct dunes form the landscape, with Arenosols (Neossolos Quartzarênicos) predominating. Such Arenosols are usually deep and poor in nutrients due to their essentially quartzose (SiO_2) composition. In addition, there are some residual elevations across the *Dunas do São Francisco* region, where scattered litolic soils (i.e. Leptosols) and rock outcrops can be found (VELLOSO et al., 2001). Karst areas occur discontinuously in discrete patches across the Caatinga region, specifically in areas in Rio Grande do Norte Ceará (largely represented by

[4]The expression 'flatten surfaces' instead of '*Depressão Sertaneja*' is adopted by some authors.

the Jandaíra Group) and Bahia and Minas Gerais states (largely represented by the Bambuí Group). The Potiguar Basin ('POT' in Figure 1.2) extends across the Rio Grande do Norte and Ceará states, being associated with extensive exposures of carbonate rocks. The basin also corresponds to the portion of the Coastal Province represented in Figure 1.2.

Soils derived from karst tend to be characterised by high base saturation levels due to their original calcium-rich parent materials. Taking the Apodí Plateau as an example, where a vast flattened karst landscape occurs, calcitic and dolomitic limestone rocks often give rise to Cambisols (OLIVEIRA et al., 2018). Vertisols and, to a minor extent, Chernozems and Leptosols also occur (ARAÚJO FILHO, 2011; ARAÚJO FILHO et al., 2017). Soils that originated from karstic materials are exceptions among sedimentary environments due to their high fertility (SAMPAIO, 2010; ARAÚJO FILHO, 2011) and the typical presence of high-activity clays. Soils formed from these materials can assume a wide range of characteristics and fall into different soil groups due to the intensity of pedogenetic processes, with a variable degree of calcite accumulation in the soil profile. These processes are known to be intrinsically related to climatic conditions and topography (BACHMAN; MACHETTE, 1977).

1.4 Classification systems and soil diversity of Caatinga

The great geodiversity of Caatinga, along with its semiarid climate, has resulted in the previously mentioned 'mosaic of soils', which can be observed in Figure 1.3. The figure also shows the distribution of the main soil types across the region. The nomenclature used in Figure 1.3 refers to the first hierarchical level of the Brazilian Soil Classification System (SiBCS). In the SiBCS system, the classification is based on diagnostic attributes and diagnostic horizons and, similarly to the WRB system, was built in hierarchical categorical levels. However, the SiBCS system has six hierarchical categorical levels, namely orders, suborders, great groups, subgroups, families and series. The higher hierarchical levels are based on properties that reflect soil genesis or associated properties (SANTOS et al., 2018).

Also important for this work is the World Reference Base for Soil Resources (WRB-FAO soil classification system; IUSS WORKING GROUP WRB, 2015)[5], where the term reference soil groups (RSGs) are used for classifying soil types based on diagnostic horizons, diagnostic properties and diagnostic materials. The WRB system consists of two hierarchical

[5]International Union of Soil Sciences

levels, where RSGs are the first level (the system has 32 different RSGs in total), and principal and supplementary qualifiers are the second level. Principal qualifiers are ranked in order of importance from right to left before the RSG without brackets, whereas the supplementary qualifiers are placed alphabetically ordered with brackets after the RSG. The WRB system was developed to reflect soil-forming processes also accommodating as far as possible other national systems, such as the Brazilian Soil Classification System (SiBCS; SANTOS et al., 2018). Thus, the correspondence between SiBCS orders and RSGs is more or less straightforward for some groups, but it should be noted that some RSGs are not classified in the Brazilian system (i.e. Cryosols Anthrosols; Technosols Andosols Umbrisols Gypsisols Durisols Calcisols Albeluvisols). Moreover, in the SiBCS, Leptosols, Regosols, Arenosols and Fluvisols of the WRB system are lumped together as 'Neossolos', with the second hierarchical categorical level being 'Litólico', 'Regolítico', 'Quartzarênico' and 'Flúvico', respectively. In this work, I adopted the WRB system mostly because it is intended to serve as a common denominator at the international level (IUSS WORKING GROUP WRB, 2015).

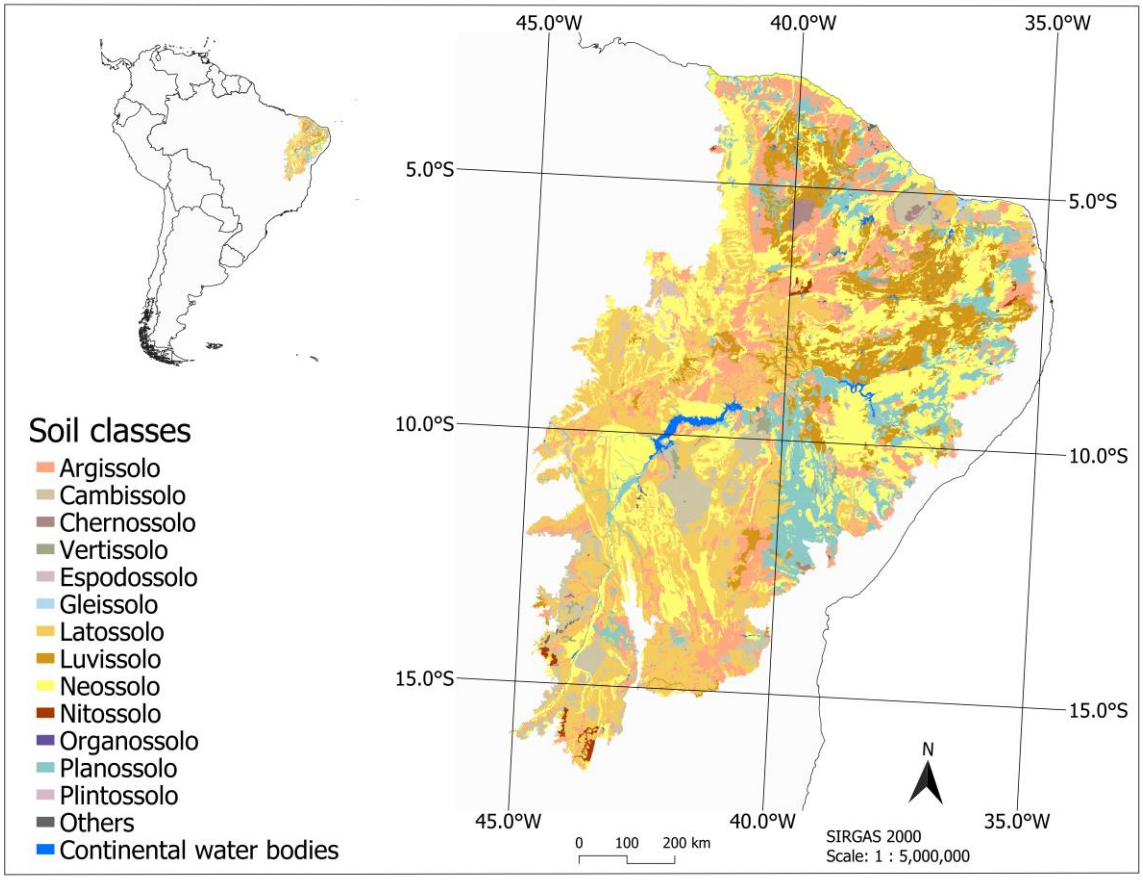

Figure 1.3: Distribution of main soil classes across the Caatinga region. Classes according to the first hierarchical level of Brazilian soil classification system (SiBCS). Shapefile source: IBGE's Environmental Information Database – BDiA (theme pedology). Map design: Brunello, A. T (redesigned from BDiA).

The Caatinga region marked a notable soil diversity (or pedodiversity), meaning that several soil types might occur across the landscape scale. Despite the outstanding soil diversity of Caatinga, six soil groups (i.e. Leptosols, Regosols, Arenosols, Fluvisols, Ferralsols, and Acrisols) account for 68.8% of the region (based on IBGE Environmental Information Database, BDiA, Pedology theme, 2022). A review of each soil group will be not provided here, but for the interested reader, excellent accounts of Caatinga soils are available in national exploratory soil surveys (JACOMINE et al., 1971; 1972a; 1972b; 1973a; 1973b; 1975; 1976; 1977; 1979; 1983; 1986) as well as in Araújo Filho (2011), Araújo Filho et al. (2017; 2019), Jarbas et al. (2010), IBGE (2019b). Excellent global soil reviews are available in Driessen et al. (2001) and the World reference base for soil resources (2015).

Regarding other non-included soil groups in Figure 1.3, it is unlikely that other soil orders occur significantly throughout the region. Nevertheless, the existence of specific environments or microenvironments may give rise to less common soil groups. For example, Souza et al. (2022) described five Umbrisols at Borborema Plateau highlands (> 1,000 m a.s.l). These soils showed unusually high soil organic carbon (SOC) contents under relicts of semideciduous forests and Rupestrian Grasslands. In addition, anthropogenic soils analogous to the Amazon *Terra Preta de Índio* can be found in some regions of paleoenvironmental interest such as Anthrosols found in Paraíba state (SOUZA et al., 2020), with the authors also suggesting the inclusion of ‘Antrosolos’ in the SiBCS.

1.5 Geology and soil diversity across the Caatinga

The complex geological history of the Caatinga has resulted in a large diversity and spatial variability of soils (Figure 1.3). The influence of other soil-forming factors, of course, cannot be left apart. For instance, catena processes, i.e. the soil formation and development along topographic gradients, climate characteristics and the influence of the vegetation on soil properties would help to explain the genesis of some unusual soil classes for the semiarid region, such as the above-mentioned Umbrisols formed at high altitudes described by Souza et al. (2022), or the same parent material giving rise to different soil groups in karst areas according to terrain position as shown by Oliveira et al. (2018).

For practical purposes, the first level of the SiBCS was ‘translated’ to RSG-WRB and its proportional coverages overlaying different rock types and geological structural provinces were calculated from vector-based thematic maps available in the IBGE’s Environmental

Information Database – BDiA; https://bdiaweb.ibge.gov.br/). It resulted that 41% of the Caatinga soils overlain metamorphic rocks, where Acrisols, Leptosols, Ferralsols and Planosols predominate (see Table S1.1). Sedimentary terrains account for 29% of the Caatinga land area (of which ca. 30% are karst zones). Sedimentary terrains are mapped as being mostly overlain by Ferralsols, Arenosols and Leptosols.

Despite many soil classes being potentially found in karst areas, available soil surveys indicated that a few soil groups predominate in these areas, namely Cambisols, Chernozems, Vertisols and Leptosols (FERREIRA, 2013). However, many other soil classes have been already described resulting from carbonate rocks in Brazil, including the Luvisols and Leptosol described by Ferreira et al (2016).

Igneous plutonic terrains account for approximately 14% of the Caatinga's territory, where the most representative soil group are Acrisols, Leptosols, Planosols, Luvisols and Ferralsols. Igneous volcanic terrains account for only 0.03% of the area, where the most representative soils are Leptosols, Vertisols, Luvisols, and Acrisols. Finally, 16% of the Caatinga soils develop from coverages of the Cenozoic age, where Ferralsols and Arenosols account for about 74% of the soils (absolute and relative RSGs coverages for each geological type are shown in Table S1.1 and S1.2).

An interesting pattern can be highlighted from the geology *versus* RSGs across geological structural provinces (Table S1.2). In general, a few soil groups (RSGs) account for 70-90% of all soils in each province. For example, in Borborema Province, where a substantial part of the soils overlain the crystalline core of the Caatinga, Leptosols and Luvisols (i.e., low to intermediate pedogenic stages) account for over 50% of the soils. Ferralsols alone occupy nearly 50% of the Cenozoic Coverage domain, which is mostly represented by sediments that have undergone weathering over the last 66 Ma in the Cenozoic Era (IBGE, 2019b). Arenosols are estimated to occupy approximately 50% of the Recôncavo-Tucano-Jatobá basin's area, which is consistent from a geological standpoint as this basin mostly consists of massive sandstone deposits that accumulated in an aborted rift (CAIXETA et al. 1994; BIZZI; SCHOBB0ENHAUS; MOHRIAK, 2003). Soil-geology associations can be observed in the supplementary 'heat' Tables S1.1 and S2.2, where genetic rock categories and geological provinces, were crossed with RSGs, respectively.

Divergent or slightly divergent terms are not uncommon in publications that mention the fertility of Caatinga soils. In this context, regarding the predominance of 'fertile', 'relatively

fertile' or 'infertile' soils, and considering geologically-distinct parent materials as a determinant force (noting that several exceptions are expected to occur), one can roughly say that Caatinga soils are predominantly fertile given that crystalline materials (metamorphic + igneous plutonic) and karst terrains correspond together for approximately 64% of the Caatinga area. Indeed, most of the Caatinga soils are located in the crystalline basement (DA SILVA; LEAL; TABARELLI, 2017), which has undergone raising and erosion until the Tertiary (SAMPAIO, 1995). Crystalline terrains were calculated to account for 55% of Caatinga's territory.

1.6 Mineralogy and weathering in Caatinga soils

As detailed in Section 1.3, the complex geological history of Caatinga has resulted in the formation of several disparate soil parent material types (or rock types) that can be found across the geological provinces. The resistance of these parent materials to weathering strongly depends on their mineralogical composition. Goldich (1938) showed that the main rock-forming minerals [namely olivine, augite, hornblende, biotite, Ca-plagioclases (anorthite), Na-plagioclases (albite), orthoclases (potassium-rich or K-feldspar), muscovite and quartz] have variable levels of stability (FONTES, 2012), which is strongly influenced by their respective melting points. Thus, minerals that crystallise first (mafic or ferromagnesian minerals; ↓Si; ↑Fe; ↑Mg; arrows indicating higher and lower concentrations) tend to be much less resistant to weathering than those that crystallise later (felsic minerals; ↑Si; ↑Al). Within the felsic minerals, however, Ca-plagioclases (Anorthites) are less resistant to weathering than orthoclases. These two groups were also described by petrologists as the 'Bowen's reactions' series or continuous series of ferromagnesian (mafic) minerals and the discontinuous series of felsic minerals (BOWEN, 1928).

In addition to the intrinsic resistance (or vulnerability) of minerals to weathering, a series of factors such as density, pressure, volume and solubility, together, determine the thermodynamic equilibrium of a given mineral, thus dictating which mineral assemblages will be present in a given space under certain conditions (CEMIC, 2005). Moreover, climatological characteristics also influence weathering intensity. While thermal stress and mechanical weathering are mostly associated with the fragmentation of rocks and the formation of sand and silt particles, clays are formed through chemical weathering (RIGHI; MEUNIER, 1995; WEIL; BRADY, 2016). Within soil particles, sand and silt hold relatively lower specific surface areas (SSA) than clay, but store considerable amounts of weatherable primary minerals such as

feldspars, apatite and micas. Conversely, clay particles have a much higher SSA, but store no weatherable minerals. (PALM et al., 2007).

As anticipated, clay particles are formed through climate-mediated chemical weathering (RIGHI; MEUNIER, 1995) and can be broadly separated into 1: 1 aluminosilicate clays (or low-activity clays, LAC) and 2: 1 aluminosilicate clays (or high-activity clays, HAC) (RIGHI; MEUNIER, 1995; QUESADA et al., 2020). The predominance of these types of clays in a given environment will be determined by both the composition of parent materials composition and climate. In soils of semiarid regions, the relatively low and erratic annual rainfall rates, associated with high potential evapotranspiration rates (so high as 2.0 m a^{-1} in Caatinga) exert a great influence on both leaching, weathering, and chemical reactions involved (ARAÚJO FILHO ET AL., 2017; 2019; RIGH; MEUNIER, 1995). In this respect, an associated important process is partial hydrolysis. For example, the reaction below shows the partial hydrolysis of a K-feldspar:

$$5KAlSi_3O_8 + 16H^+ + 16OH^- + 4H+ \rightarrow KAl_4(Si_7Al)\ O_{20}(OH)_4 + 8H_4SiO_4{}^0 + 4K^+$$

(K-feldspar) (dioctahedral vermiculite)

In the reaction above, the K-spar is hydrolysed releasing soluble silica and potassium, but also forming a 2: 1 dioctahedral vermiculite, a secondary clay mineral (RIGHI; MEUNIER, 1995; FONTES, 2012). A general sequence of clay minerals transformations can be exemplified as in the following sequence: illite → vermiculite → smectite, with these transformations proceeding until the depletion of silica and potassium and a concomitant reduction in the surface charge density over time (WILSON, 1999). Partial hydrolysis occurs in soils where leaching occurs at its minimum rates, thus providing specific conditions (i.e. high concentration of base cations and relatively higher soil pH) for the formation of 2: 1 smectite, as long the parent materials contain enough amounts of base cations (RIGHI; MEUNIER, 1995).

However, 1: 1 clay minerals, mostly represented by kaolinite in several Caatinga soils (MELFI et al., 1983), also occur significantly in Caatinga where losses of bases are more intense and/or where the parent materials intrinsically have greater proportions of 1: 1 clay minerals, such as rocks rich in felsic minerals (ARAÚJO FILHO et al., 2017).

Importantly, clay mineralogy strongly influences the soil surface charge density, effective cation exchange capacity, soil structure and water storage properties (PALM et al., 2007; SANCHEZ, 2019; QUESADA et al., 2020). Regarding the latter, HAC particles are contractible (shrink-swell clays or expansive clays), potentially absorbing plentiful amounts of

water during swelling, but shrinking as the water content decreases[6]. Low-activity clays, however, do not swell as a result of water absorption and generally hold less water than HAC soils. Gaiser, Graef, and Cordeiro (2000) have shown the importance of clay mineralogy along with SOC and soil texture in determining the capacity of soils of semiarid regions to retain water at different matric potentials, with HAC soils potentially storing greater water amounts as opposed do LAC soils. Additionally, numerous Fe and Fe and Al (oxy)hydroxide species, typical of Ferralsols, may occur at different proportions across Caatinga soils depending on soil parent material compositions. Ferralsols of sedimentary domains are thought to have undergone more intense weathering in former wetter conditions (ARAÚJO et al., 2017). Likewise kaolinite, these compounds are variable-charge clays and usually, their I_E is about 3 – 10 $cmol_c\ kg^{-1}$ (SANCHEZ, 2019). Considering that Ferralsol is the predominant soil type of Caatinga, covering ca. 24% of Caatinga's area (BDiA, 2022), variable-charge clays are expected to strongly influence the biogeochemical behaviour of these soils. Despite this relatively high coverage of Ferralsols, it should be noted that they are mainly found developing from sedimentary substrates, which, in general, have undergone higher weathering rates under past wetter conditions (KER, 1997). Moreover, in the Caatinga, soil mineralogies dominated by Fe and Al (oxy)hydroxides are thought to be more relevant in more intensively weathered sedimentary soils.

The high sand contents present in several Caatinga soils make it inappropriate to approach them in terms of clay activity. Rather, the quartz-dominated mineralogy of these soils requires a specific category for them. Quesada et al. (2020) classified a broad suite of soils into 'LAC', 'HAC' and 'Arenic' to study soil carbon concentrations and stabilisation mechanisms in the Amazon. The latter term is used in the WRB system to describe soils *'having a layer ≥ 0.3 m thick, within the ≤ 1.0 m of the mineral surface…'* or in the major part of shallower soils. Therefore, given that the WRB soil classification system is based on soil-forming processes, RSGs can be clustered into LAC, HAC and Arenic categories (QUESADA et al., 2020). Thus, RSGs corresponding to more intensively weathered soil such as Ferralsols and Acrisols are typically classified as LAC soils, whereas soils with low to intermediate pedogenetic development such as Leptosols, Cambisols, Luvisols, Alisols, are usually classified as HAC. It is of note that exceptions may occur such as infertile rocky Leptosols (being LAC rather than HAC) that can be found in the Caatinga. In Quesada et al.(2020) study, LAC, HAC and Arenic

[6] The *shrink-swell* behaviour in Caatinga's Vertisols (which usually show large cracks when dry) are commonly portrayed as the predominant landscape of the Caatinga.

(the latter comprising Arenosols and Podzols) soils had marked differences in terms both in terms of both I_E and SOC stabilisation mechanisms.

1.7 Properties of Caatinga soils

1.7.1 Soil reaction and cation availability

There is a general perception that Caatinga soils are fertile, commonly mentioned as 'fertile', 'nutrient-rich' or 'relatively fertile'. This general perception is associated, in part, with the idea that typical low rainfall levels lead to minimum leaching rates, which in turn lead to the maintenance of nutrients in the soil. This rationale certainly applies to a significant part of the Caatinga soils, where in addition to the relatively high content of base cations, relatively high soil pH values tend to maintain aluminium in low-solubility forms. Moreover, the levels of exchangeable soil bases (i.e., Ca^+, Mg^+, K^+, and Na^+) levels can vary substantially in Caatinga soils, which is thought to reflect the composition of their parent materials. For example, Araújo et al. (2017) summarised the sum of base cations ($\sum_B$) values recorded in representative soils of the Caatinga. In their compilation, the maximum $\sum_B$ values of many soil groups were approximately 50 $mmol_c\ kg^{-1}$. Furthermore, Arenosols and Ferralsols had maximum $\sum_B$ values below 5 $mmol_c\ kg^{-1}$. On the other hand, clay-rich Vertisols and clay-enriched sub-horizons of Luvisols had maximum $\sum_B$values reaching around 400 and 250 $mmol_c\ kg^{-1}$, respectively.

Despite the relatively high $\sum_B$ values that can be found in Caatinga soils, one should also consider that a considerable part of these soils derives from previous weathered and nutrient-poor parent materials (SAMPAIO, 1995; SAMPAIO, 2010; ARAÚJO, 2011; ARAÚJO et al., 2017). In many of these soils, Al^{3+} is likely to predominate in the soil sortive complex. Specifically, in the Caatinga, soil groups having markedly contrasting chemical characteristics can be found at relatively short distances, with parent materials being a major determinant. For example, Ratke et al. (2020) found marked differences in the properties of soils belonging to the *Gurguéia* watershed in the Piauí state. In their study, soil types reflected original parent materials, i.e. sandstones gave rise to Ferralsols and Acrisols, gneiss gave rise to a Cambisol and different alluvial sediments originated a Vertisol and an Arenosol. Moreover, soil parent materials had a sharp relationship with soil chemical properties. Namely, soils formed from sandstone or their sediments (Arenosols and Ferralsols) were associated with

relatively lower organic matter concentrations, low density of permanent charges, high acidity and high aluminium levels.

Acidity is a natural characteristic of most Brazilian soils and is related to several potential negative effects on plant establishment and growth. For example, high aluminium concentrations in acidic soils may be the cause of limitations for root growth (DELHAIZE; RYAN, 1995). Aluminium toxicity may also interfere with cell division, DNA replication, root respiration, enzyme functioning, and plasma membrane function, with implications for water and nutrient uptake, transport and use (BOJÓRQUEZ-QUINTAL et al., 2017). A review of mechanisms undertaken by plants to cope with high Al^{3+} levels is provided in Bojórquez-Quintal et al. (2017). Generally, these mechanisms are separated into avoidance and resistance to aluminium and include changes in the rhizosphere pH, changes in the cell's membrane properties, excretion of metabolites, chelation of Al^{3+} in the cytosol and vacuolar compartmentalisation (BOJÓRQUEZ-QUINTAL et al., 2017). For Cerrado species, where soil aluminium levels often stand out, the study of Oliveira et al. (2019a) showed that 77.4% of native trees and shrubs species (among 31 species) exhibited mechanisms of Al^{3+} avoidance through exclusion as opposed to accumulating this element in their tissues (the remaining species).

Evaluating the influence of soil and climate on the discrimination of plant physiognomies comprised in the Caatinga, Oliveira et al. (2019b) found that soil cations, represented by both base and Al^{3+} saturation and exchangeable potassium (K), were the most important soil attributes. In their work, the occurrence of Cerrado species was tightly associated with higher Al^{3+} saturation levels. According to the authors, such a high concentration of Al^{3+} in the soil also acts as a barrier to the occurrence of SDTFs. In addition, the occurrence of Caatinga *stricto sensu* was associated with higher contents of exchangeable potassium, which was attributed to relatively higher levels of 2: 1 clay minerals and the presence of K-bearing primary weatherable minerals.

Other than these considerations, Al^{3+} tolerance mechanisms by plants may take place in the discussion of biome transitions. It has been hypothesised that in the eventual absence of fire and predominance of sufficiently fertile soils, Cerrado formations might be, if propagules are available, colonised by species of semideciduous, dry forests or even evergreen forests (BUENO et al., 2018). However, if the underlying soils are aluminium-rich, which is thought to be primarily associated with the nature of parent materials, Cerrado species (generally

adapted to high Al^{3+} levels) would be expected to outcompete and dominate the vegetation over time (DEXTER et al., 2018).

1.7.2 Carbon

The soil organic carbon (SOC) contents result from the net balance of organic matter inputs to the soils and its relative decomposition (or mineralisation) rates (SMECK, 1985; BRUUN; ELBERLING; CHRISTENSEN, 2010; SINGH et al., 2018). Notwithstanding, soil general fertility, texture, mineralogy (BRUUN; ELBERLING; CHRISTENSEN, 2010), moisture and climate also are expected to influence losses and accumulation of SOC (QUESADA et al., 2010; QUESADA et al., 2020). It is noteworthy that soils with pH 7.3 or higher potentially contain some inorganic (pedogenic) carbon in the form of carbonates and bicarbonates (SANCHEZ, 2019), which might be the case for many Caatinga soils, especially those developing calcite-rich karst environments.

Due to the relatively low plant biomass and, consequently, low organic matter inputs, the uppermost layers of Caatinga soils tend to hold lower average total organic carbon (in both native and human-modified stands) in comparison to other Brazilian biomes (MENEZES et al., 2012). Within Caatinga soils, and contrary to the authors' expectations, Menezes et al. (2021) did not find significant differences in SOC stocks among the most representative soil orders of the Caatinga, which were more affected by the type of coverage and land use. Biomass production (i.e., the elementary source of SOC) itself might be conditioned by several environmental drivers as will be discussed later in this thesis.

Parent materials and pedogenic stage are expected to influence soil carbon content (QUESADA et al., 2010), who found systematic variation in SOC content across a pedogenic age gradient (reflected by soil types) in forest soils. Nevertheless, soil texture and mineralogy, along with climatic variables are also known to influence SOC levels. Fine-textured soils (i.e. loamy and clayey soils) have a higher specific surface area in comparison to sandy soils (PALM et al., 2007). For this reason, SOC is much more prone to being encapsulated into aggregates of clayey and loamy soils, providing physical protection against mineralisation, which should occur at a much faster rate in sandy soils (SANCHEZ, 2019).

As regards soil mineralogy influences on SOC, although Bruun, Elberling, and Christensen (2010) have found contrary tendencies, soils with abundant high-activity clays (e.g.

smectite group) are expected to hold a greater potential to protect SOC than low-activity clays (e.g. kaolinite). This is assumed to be due to the relatively higher specific surface area found in the former class (SINGH et al., 2018). Also of note is that Fe and Al (oxy)hydroxides tend to associate with clay minerals (e.g. kaolinite), yielding a high capacity to absorb and stabilise organic matter and providing additional protection against biological degradation (BALDOCK; SKJEMSTAD, 2000). Quesada et al. (2020) have shown a significant role of clay to explain SOC storage in highly weathered soils such as Ferralsols and Acrisols, which was assigned to the relatively uniform kaolinitic mineralogy of these soils. On the other hand, less weathered soils (such as Cambisols, Alisols and Plinthosols) had their SOC mainly associated with organo-mineral complexes. In Quesada et al. (2020) study, the carbon content of sandy soils was slightly influenced by clay and silt contents, this likely being associated with particulate organic matter. Those authors did not find, however, relationships between SOC and woody plant productivity, neither above-ground biomass nor temperature and precipitation regimes. Despite related questions that will be addressed in this work, a comprehensive analysis approaching carbon stabilisation mechanisms remains to be undertaken for Caatinga soils.

Soil temperature, moisture and frequency of wetting-drying cycles may also influence SOC. As the temperature rises, an increase in SOC mineralisation can be expected (SANCHEZ, 2019; SINGH et al., 2017) as a result of increased microbial activity, i.e. under tolerable conditions. In Caatinga, the surface soil temperature can achieve temperatures as high as 50°C (SOUTO et al., 2009), which is very likely to inhibit microbial activity.

Wetting and drying processes potentially destroy soil aggregates, but this process should be more important for smectite-rich soils than soils rich in Al and Fe (oxy)hydroxides, which bind SOC much more effectively (SANCHEZ, 2019). In addition, sudden wetting of soils at the onset of rainy seasons may provoke microbial cell lysis, thus releasing nutrients and carbon. These processes are of large importance for soils of semiarid regions due to abrupt changes in soil water status (JARAMILLO; MURRAY-TORTAROLO, 2019).

1.7.3 Nitrogen cycle and causes of soil isotopic discrimination

In contrast to many essential nutrients that originate primarily from soil parent materials (SMECK, 1985), N is derived primarily from biological atmospheric N_2 (BNF) (SPRENT, 2009) and atmospheric deposition (SWAP et al., 1992). It should also be noted that the N cycle in soils is mostly associated with organic pools, as opposed to phosphorus, the latter generally

distributed among organic and inorganic pools (SACHEZ, 2019). Thus, the particular characteristics of the N cycle are of great importance for water-limited ecosystems since the relative availability of nitrogen will depend on biologically mediated mineralisation rates. Globally, gross nitrogen mineralisation of soil was shown to be positively correlated with microbial biomass, total soil carbon, total soil total nitrogen and mean annual precipitation and negatively associated with soil pH and bulk density (ELRYS et al., 2021). However, it seems reasonable to expect that, in semiarid environments, mineralisation rates are mostly limited by climatic aspects, including rainfall total amounts, seasonality patterns, and temperature regimes. Microbial cell lysis due to the sudden increase in soil water potential at the onset of rainy seasons has been proposed as an important process of nutrients release in semiarid ecosystems (DIRZO; YOUNG; MOONEY, 2011; JARAMILLO; MURRAY-TORTAROLO, 2019).

A review of the main pathways associated with inputs, outputs and transformations of soil N highlighted the relatively high N losses commonly measured in SDTFs soils (GEI; POWERS, 2014). Most works undertaken in these ecosystems, however, focus only on the very dry or the wettest end of the rainfall spectrum (i.e. sites with $P_A > 1.8$ m). Moreover, although valuable endeavours have been made to improve knowledge of nutrient cycling in SDTFs in the last years, future efforts would be best directed towards the understanding of the role of water availability on nutrient dynamics and integrative approaches encompassing species to ecosystems levels (GEI; POWERS, 2014).

Another key component of the nitrogen cycle in semiarid environments is the wide presence of Leguminosae. Leguminosae (potentially N_2 fixers) is the most species-rich plant family of SDTFs (PENNINGTON; LAVIN; OLIVEIRA-FILHO, 2009), including Caatinga (QUEIROZ, 2006), but BNF may be limited by different factors, such as the absence of rhizobium infestation (absence of nodules), and/or low BNF efficiency due to shortage of other nutrients (SILVA et al., 2017). A field/experimental study has shown that BNF in Caatinga was associated with P-deficiency rather than the absence of rhizobia bacteria infestation (SILVA et al., 2017), which draws attention to the coupling of cycles of essential nutrients. A BNF study in four fragments of native Caatinga (FREITAS et al., 2010) showed that although species of high BNF capability were present (i.e. *Mimosa tenuiflora*, *Mimosa arenosa* and *Piptadenia stipulacea*), the estimated annual quantities added to leaves biomasses through BNF were relatively low (2.5 to 11.2 kg ha^{-1} yr^{-1}). This was assigned to low proportions of plants that effectively fix N_2 in these communities. The authors also highlighted, however, that these

quantities might reach much higher values in regenerating stands such as 130 kg ha^{-1} $year^{-1}$. Gei, and Powers (2014) also noted that, despite the high observed overall diversity and abundance of Fabaceae in SDTFs, the biologically fixed N in these ecosystems should be modest.

Natural abundances of ^{15}N (expressed by $\delta^{15}N$) provide valuable information on soil nitrogen dynamics. This is because $\delta^{15}N$ integrates a wide range of N transformations over time (HÖGBERG, 1997). In general, SDTFs are assumed to have higher N availability in comparison to humid ecosystems (ARANIBAR et al., 2004; SILVA et al., 2017), and measurements of natural abundances of $\delta^{15}N$ in both soil and leaves have been used to infer the 'openness' of the N cycle and the proportion of biologically fixed N (ARANIBAR et al., 2004; FREITAS et al., 2010; RIVERO-VILLAR et al., 2021). This is because when plants are fixing atmospheric N_2, where the isotopic signature is 0‰, it tends to lower $\delta^{15}N$ values. On the other hand higher $\delta^{15}N$ foliar signatures indicate that most of the N acquired by plants primarily comes from ^{15}N-enriched soil pools where heavy ^{15}N has accumulated due to the process of isotopic discrimination (SWAP et al., 1992; HÖGBERG, 1997). It is of note that, despite the relationships between BNF and isotopic discrimination being commonly used in the literature, Hedin et al. (2009) claimed that the ^{15}N approach oversimplifies the complex soil N dynamics (especially taking considering different pools and fractionating paths) and is not sufficient for *'clearly resolving N fixation at the individual plant level'*.

Soil nitrogen isotope discrimination has been better studied for tropical humid and temperate forest soils compared to semiarid regions, with tropical forest soils showing, on average, $\delta^{15}N$ values 8‰ higher than their temperate counterparts (MARTINELLI et al., 1999). In humid forests, nitrogen availability, expressed by isotope and non-isotope data, has been shown to vary primarily with rainfall at a regional scale. At a landscape scale under the same rainfall conditions, however, soil texture was shown to be the main driver of N availability (NARDOTO et al., 2008). Moreover, in forest soils, there is evidence that $\delta^{15}N$ enrichment patterns are associated with changes in P availability across the pedogenetic development. This process is suggested to ultimately affect N dynamics in soils through intricate stoichiometric controls (QUESADA et al., 2010). In addition, it has been suggested that a trade-off between water and nutrients availability should influence isotopic signatures of N in soils, where nutrients may become more important when water is not a limiting factor (SWAP et al., 2004), which is consistent with findings of QUESADA et al. (2010). Furthermore, potential effects of soil cation exchange capacity have been hypothesised to potentially influence isotopic

discrimination against ^{14}N, though evidence for this effect was minimal (MARTINELLI et al., 1999). Studies in humid regions, however, where environmental conditions are notoriously different than arid and semiarid regions, seem to not contribute significantly to the patterns observed in soils of the latter, where relationships between soil properties and ^{15}N enrichment patterns are far understudied.

Among the available studies, Swap et al. (2004) showed foliar $\delta^{15}N$ values increasing according to a water limitation gradient (P_A ranging from 0.2 m a^{-1} to 1.3 m a^{-1}) in southern Africa. The strong linear relationship found ($r^2 = 0.54$; $p < 0.01$) was somewhat surprising for the authors since their study region included several soil types, land use history and changes and distinct vegetation composition. Similarly, Aranibar et al. (2004) showed a negative correlation between precipitation levels (i.e. increasing aridity) and both soil and plant $\delta^{15}N$ values in the Kalahari region, Southern Africa. The latter study, however, also pointed out that the inverse relationship found between plant $\delta^{15}N$ values and precipitation was even stronger in the sandy soils of 'Kalahari sands' (> 90% of sand) when compared to the results of Swap et al. (2004) for entire southern Africa. This result suggests a role for soil texture in isotopic discrimination. In addition, the authors also found a trend for higher soil $\delta^{15}N$ values with aridity in wetter years, which was suggested to be related to increased mineralisation of old recalcitrant N pools in these unusual years. Collectively, these studies indicate that the N cycle is strongly affected by rainfall total amounts and annual variability in arid and semiarid environments, along with environmental finer-scale factors such as soil texture and general fertility.

Indeed, further evidence suggests that not only climate has a major influence on N isotopic signatures in semiarid environments, but a suite of soil properties can potentially be important. For example, soil $\delta^{15}N$ values are influenced by soil organic matter (SOM) stability. In this respect, Craine et al. (2015) suggest that, in addition to relatively high rates of fractionating gaseous N loss commonly associated with clayey soils, clays are capable to stabilise relatively greater amounts of soil organic matter. Thus, high soil $\delta^{15}N$ values commonly found in semiarid environments can be hypothesised to result from the presence of stable ^{15}N-enriched organo-mineral complexes (CRAINE et al., 2015). Soil pH can also potentially influence isotopic discrimination processes. Because soil pH affects soil microbial community structure, biomass and activity (ACIEGO PIETRI; BROOKES, 2008), in turn affecting mineralisation rates, soils with relatively high pH values can be associated with high soil $\delta^{15}N$ values. This can be explained by higher microbial activity at higher pH resulting in higher SOM decomposition and increased N transformations in the soils. Ammonia

volatilization is also favoured in soils with high pH (HOULTON; MARKLEIN; BAI, 2015). Therefore, any environmental factor that can potentially affect N transformations in soils is likely to define different isotopic signatures of N in soils. Furthermore, it has been suggested that a trade-off between water and nutrients availability should influence isotopic signatures of N in soils, where nutrients may become more important when water is not a limiting factor (SWAP et al., 2004), which is consistent with the findings of Quesada et al. (2010) for Amazon rainforests.

A recent study showed that patterns of $\delta^{15}N$ enrichment in Caatinga soils have a major climatic control (SANTOS et al., 2022). However, soil clay content and soil pH also had a positive and negative relationship with $\delta^{15}N$ values, respectively. The study of Santos et al. (2022) was undertaken along almost the entire longitudinal length of the Pernambuco state, covering distinct physiographic regions (i.e. *Zona da Mata*, *Agreste e Sertão*) and the soil type was Alisol (common to all physiographic regions in their study). Moreover, in that study, the highest $\delta^{15}N$ values were recorded in soils of *Sertão*, where relatively low and erratic rainfall levels, in conjunction with high temperature and alkaline soil reaction, led to favourable conditions for the N transformation reactions in the soils, which in turn yielded higher $\delta^{15}N$ values in these soils. Other potential factors driving isotopic behaviour in semiarid environments are poorly understood. Given the high environmental heterogeneity of Caatinga, it can be expected that isotopic discrimination is influenced by several factors.

1.7.4 Phosphorus

In general, Caatinga soils have been reported as P-deficient (SILVEIRA; ARAÚJO; SAMPAIO, 2006). However, because the Caatinga encompasses a wide range of soil parent materials and stages of pedogenic development, P contents and bioavailable forms (or fractions) are expected to vary significantly across these soils. For example, soil total P concentrations in Caatinga soils were found to range from 123 to 155 mg kg^{-1} (TIESSEN; SALCEDO; SAMPAIO, 1992), 80 to 390 mg kg^{-1} (FRAGA; SALCEDO, 2004), 260 to 390 mg kg^{-1} (ARAÚJO; SCHAEFER; SAMPAIO, 2004), 52 to 1625 mg kg^{-1} (SILVEIRA; ARAÚJO; SAMPAIO, 2006). The latter study evaluated 69 soils encompassing the most common soil orders found in the region. The highest total P contents were found in Fluvisols, Vertisols, Luvisols, and Cambisols; intermediate contents in Acrisols, Leptosols and Ferralsols; and lowest contents in Regosols, Planosols and Arenosols. Despite the high variation found in soil

total P concentrations among the main soil orders of the Caatinga, the majority of soils in the Silveira, Araújo and Sampaio (2006) study had total P concentrations ranging from 100 to 200 mg kg^{-1}.

Along with common weathering indexes (PARKER, 1970; FIANTIS et al., 2010), soil total P has, for decades, been used as an index of weathering stage (e.g. WALKER; SYERS, 1976; CROSS; SCHLESINGER, 1995; QUESADA et al., 2010; PORDER; HILLEY, 2011). This is because as soil weathers, soil P, originally present in primary minerals, tend to redistribute among organic and inorganic forms, also with slow but continuous losses, yielding relatively lower soil total P contents over time. All these authors found relationships between soil total P and weathering levels. However, it is well-established that total P itself does not inform much about its availability for plants and microorganisms (VITOUSEK; SANFORD, 1986; SANCHEZ, 2019).

In addition, only a few studies have employed more detailed approaches to assess P availability in Caatinga soils using classical P fractionation methods such as the sequential Hedley and coworkers' method (HEDLEY; STEWART; CHAUHAN, 1982). Silveira, Araújo, and Sampaio (2006) found marked variability in soil total P as well as its distribution into organic and inorganic forms between and within the main soil groups of the Caatinga. In general, the largest proportion of P was found in the residual fraction (usually considered biologically non-available) and smaller proportions (7 – 12%) in labile fractions (P extracted with anion exchange resin and sodium bicarbonate, usually considered the most bioavailable forms).

Phosphorus inputs to soil systems originate almost entirely from phosphate-bearing primary minerals, particularly apatites (WALKER; SYERS, 1976; SMECK, 1985). Salcedo (2006) reviewed the main mechanisms controlling the availability of P to plants in soils of the Brazilian semiarid region. Considering that the Caatinga holds a vast range of rock types, the variation in the concentration of soil total P should reflect the variation in parent material P concentration. Porder and Ramachandran (2012) led a global compilation assessing the concentration of P in several rock types, noting a 30-fold variation in P concentration. For example, P varied from 120 mg kg^{-1} in many ultramafic rocks to > 3000 mg kg^{-1} in several alkali basalts. Furthermore, silica-rich rocks showed a lower concentration relative to iron-rich rocks. In sedimentary rocks, P concentrations were strongly governed by the grain sizes [i.e. higher in siltstone (finer grains) and lower in sandstone (coarser grains)]. A previous work, assuming a global generic rock classification encountered, on average, 1300 mg kg^{-1} of P in

igneous and metamorphic rocks, 750 mg kg^{-1} in schists, 350 mg kg^{-1} in sandstones and lower 180 mg kg^{-1} in calcareous rocks (JACKSON, 1969, *apud* SALCEDO, 2006). In Porder and Ramachandran's compilation, limestones and dolomites P concentrations were comparably low to sandstones (medians of 500 and 567 mg kg^{-1} for limestones and dolomites, respectively) and even less for other carbonate rocks (median = 290 mg kg^{-1}). Despite the relatively low P contents commonly found in limestones and dolomites, high soil total P concentrations in karst-derived soils are not rare, which may be attributable to the formation of low-solubility calcium phosphates (PANSU; GAUTHEYROU, 2006). Bioavailable forms, however, may be present in relatively small amounts (FERREIRA et al., 2016).

A recent global analysis found that variations in soil total P are largely explained by the combination of soil organic carbon concentrations, parent material, mean annual temperature, and soil sand content (HE et al., 2021). Under similar climatic conditions (i.e. soil and rock P measured in adjacent sites), however, Porder and Ramachandran (2012) found that parent materials alone explained 42% of the variation in soil P. Considering the typical low mean annual precipitation (P_A) levels in the Caatinga, it can be expected that soil P should be related, to a large degree, to parent rock P levels. A comparison between soil total P as related to original parent material in the Caatinga was made in Araújo, Schaefer, and Sampaio (2004), where P fractions of toposequences of Luvisols were compared to their underlying saprolites concentrations, which were greater downslope. Quantifying and comparing soil and rock P can contribute to the understanding of regional and global P variations (PORDER; RAMACHANDRAN, 2012).

In general, phosphate-bearing primary minerals are present as weatherable minerals held in the sand and silt fractions of the soil, whereas secondary phosphorus minerals are formed as discrete clay particles (SANCHEZ, 2019). Depending on the soil mineral assemblage, sand particles may or may not contain significant amounts of P. This is of great importance for Caatinga, where sandy soils occur to a large extent, especially considering geomorphological units such as the arenite-dominated Recôncavo-Tucano-Jatobá Basin (Figure 1.2) and other geological units where sandstones or unconsolidated sands are the main parent materials. As a single mineral usually predominate (i.e. quartz) rather than other primary silicate minerals (e.g. feldspar), the sand fraction often contains few plant-available nutrients (WEIL; BRADY, 2017). In addition to the negative relationship commonly found between quartz and P contents in rocks, sandy soils are more prone to P losses through leaching (HE et al., 2021).

Moreover, phosphate anions are retained in the soils only for a short time either because they become immobilised by microorganisms or plants or are converted into phosphate secondary minerals (SMECK, 1985; SANCHEZ, 2019). Regarding the latter process, it is generally considered that three main forms of phosphate active secondary minerals are formed (ordered from most to least soluble forms): (Ca)-bonded phosphate, (Al)-bonded phosphate and (Fe)-bonded phosphate, and with the proportion of these minerals being determined by soil pH (SMECK, 1985; GUO et al., 2000). In other words, as the soil weathers and becomes more acidic, phosphate anions tend to be bounded in less soluble Al and Fe compounds.

Other geochemical processes are also important to release P into the soils. On the one hand, intense leaching of bases associated with high precipitation regimes may catalyse soil acidification in wetter ecosystems, therefore releasing (Ca)-bonded phosphate into the soil solution (SMECK, 1985; WEIL; BRADY, 2017). On the other hand, this process should be less important in a semiarid ecosystem. SALCEDO (2006) pointed out that the geological substrate (i.e. igneous, metamorphic or sedimentary rocks) is of great importance to understanding P pools and dynamics. In general, it is assumed that slightly weathered soils originating from crystalline terrains should be expected to contain higher (Ca)-bonded phosphate, whereas more intensively weathered soils, common in sedimentary terrains, are expected to contain higher amounts of (Fe) and (Al)-bonded phosphorus forms (TIESSEN; SALCEDO; SAMPAIO, 1992).

Another geochemical process that affects P availability in soils is phosphate sorption. In highly weathered acid tropical soils (e.g. Ferralsols), the large proportion of iron and aluminium (oxy)hydroxides species associated with medium to fine-textured particles are responsible for high phosphate fixation rates (SANCHEZ; UEHARA, 1980; GARCIA-MONTIEL et al., 2000). Phosphate anions become bonded to reactive soil surfaces through ligand exchanges, i.e. phosphate anions replace hydroxyl groups present in (oxy)hydroxides surfaces (SANCHEZ, 2019). With ‘soil ageing’, these phosphate anions can penetrate the mineral matrix of the soil, forming extremely insoluble compounds. In Caatinga soils, P sorption is more important in sedimentary areas, such as in highly weathered Ferralsols of the São Francisco and Parnaíba geological provinces (see Supplementary Table S.2.1).

Phosphorus sorption processes are strongly controlled by three main soi properties, *viz*. texture, SOM and mineralogy. And specifically, sandy soils, which are extensively represented in the Caatinga, should not present phosphate sorption issues, with a low sorption capacity allowing any phosphate anions present in the soil solution to move downwards the soil profile.

Regarding the influence of mineralogy on P sorption, multiple scenarios should exist (or coexist) in the Caatinga since diverse mineral species do occur in its soils, e.g. 2: 1 clay mineral (specially smectite group), 1: 1 clay mineral (kaolinite), seldom hydroxy-interlayered vermiculite (HIV) as well as oxidic fractions such as goethite, hematite and gibbsite (ARAÚJO FILHO et al., 2017). It is worth mentioning that the discrimination of mineral types is significantly influenced by climatic characteristics such as temperature and rainfall distribution (RIGHI; MEUNIER, 1995), with the semiarid climate of the Caatinga region indirectly influencing P sorption processes as described above, via an influence on soil mineralogical properties.

One additional property that influences P sorption is the soil organic carbon (SOC). This is because the negatively charged radicals of SOC compete with phosphate anions for free hydroxyls present at the sesquioxides surfaces. Thus, the higher the SOC, the lower the chance of phosphate anions being sorbed into the soil mineral matrix (MOSHI; WILD; GREENLAND, 1974). The SOC levels of Caatinga soils have been found to be, on average, relatively lower than soils of other Brazilian biomes (MENEZES et al., 2012), perhaps due to relatively low organic matter inputs to the soils.

A considerable portion of the available P is taken up by plants and immobilised by microorganisms. At some point, this P will return to the soil in the form of organic P compounds (P_O). It is believed that P_O plays a paramount role in some more highly weathered P-deficient tropical soils (TIESSEN; SAMPAIO; SALCEDO, 2001). Measurements of both labile and more recalcitrant P_O forms in the Caatinga revealed values ranging from 13% to 60% of the total P (TIESSEN; SALCEDO; SAMPAIO, 1992, SILVEIRA; ARAÚJO; SAMPAIO, 2006). This build-up of P_O is not generally considered to be the result of the soil-forming process (SANCHEZ, 2019). Rather, an accumulation of P_O is related to the ability of some soils to accumulate organic matter (SOM), as evidenced by the relatively fertile Fluvisols and Vertisols sampled by Silveira, Araújo and Sampaio (2006). In those soils, the plant biomass production rates were high, which in turn were reflected by higher SOM and P_O contents as compared to the less fertile soils in their dataset.

Finally, the activity of soil microorganisms is subject to seasonal patterns as it is mediated by the temperature and moisture of the uppermost layers of Caatinga soils. For this reason, the biomass of microorganisms and their enzymatic activity should vary over the year, including the production of alkaline and acid phosphatases, in turn impacting the rates of

mineralisation of organic P as well its storage in the microorganisms' biomass and release across wet and dry seasons (JARAMILLO; MURRAY-TORTAROLO, 2019).

1.7.5 Micronutrients

There has been little research about the role of micronutrients influencing tropical dry ecosystems functioning, with the availability of micronutrients in Caatinga soils and associated biogeochemical processes virtually unknown. Nevertheless, these nutrients may account for some part of the variation in the vegetation (SAMPAIO, 2010), also likely acting in specific biogeochemical processes. Biondi et al. (2011) evaluated the natural contents of metallic micronutrients (i.e., Fe, Mn, Zn, Cu, Ni and Co) in benchmark soil of the Pernambuco state and found significant relationships between these nutrients and the clay fraction in both surface and subsurface horizons of these soils. The soil organic matter, however, was correlated with most micronutrients only in surface horizons. In addition, the contents of such metallic micronutrients in most evaluated soils were found to be relatively lower than soils of other Brazilian regions, which was assigned to the predominant presence of mafic rocks (i.e. containing iron-magnesium minerals) of the latter. Nevertheless, despite variations in rock types among the physiographic regions (*Zona da Mata*, *Agreste* and *Sertão*) evaluated in their study, Biondi et al. (2011) concluded that deficiencies of Fe, Mn and Zn are less likely than Cu, Co and Ni, especially where less advanced weathering and richer parent materials take place.

In addition to the natural concentrations of micronutrients in Caatinga soils, studies considering the contents of these nutrients in plant tissues and their relative biological efficiencies uses are also scarce in Caatinga. Albuquerque et al. (2018), studying tree and shrub species in Acrisols belonging to the geo-environmental unit of the Borborema Plateau, found significant differences in the plant use efficiency of micronutrients following the decreasing order: Mn > Cu > Zn > Fe. Moreover, efficiency levels varied among species, suggesting that some species may perform better than others in edaphically distinct environments, therefore accounting for relatively higher biomass production.

Micronutrients may also affect ecosystem properties through other indirect effects on biogeochemical processes. For example, KASPARI et al. (2008) showed that fertilisation with micronutrients enhanced significantly leaf-litter decomposition in a lowland Panamanian forest. Similarly, a short-term laboratory experiment has demonstrated an increase in leaf-litter decay of tropical dry forests (TDF) species driven by micronutrient supplementation (POWERS;

SALUTE, 2011). In addition to mediating biogeochemical processes, micronutrients (B, Cl, Cu, Fe, Mn, Mo, Zn and Ni) are essential for plant development. The individual role of micronutrients for plants has been stressed in several works (e.g. RÖMHELD; MARSCHNER, 1991; ABREU; LOPES; SANTOS, 2007; BLOOM; SMITH, 2015; WEIL; BRADY, 2017) and will not be detailed here. Nevertheless, it is worth mentioning that all these micronutrients influence both plant structure and metabolism, with many being required for the successful completion of the plant's life cycle (BLOOM; SMITH, 2015).

A few underlying factors that control the concentration and availability of micronutrients in soils are as follows: (1) Mineralogy - similarly to other (macro)nutrients, the main source of micronutrients is the dissolution of primary weatherable minerals present in sand and silt fractions (e.g. feldspars, micas) (SANCHEZ, 2019); (2) Soil pH - except for molybdenum (Mo), the availability of the micronutrients decreases as soil pH increases. Generally speaking, slightly acid soils (soil pH_{H2O} ranging from 6 to 7) are the most optimal for micronutrients uptake; (3) Soil organic matter (SOM) - organic matter is usually micronutrient-rich so low SOM contents may imply a micronutrients shortage (SHUMAN, 2018); (4) Soil texture – coarser-textured soils (e.g. Arenosols) are susceptible to endure micronutrient paucity mostly because these soils generally are associated with low SOM (LÜ et al., 2016) and low ionic retention capacity; (5) Redox status (waterlogged *vs* aerated soils) is also known to control micronutrients availability (SHUMAN, 1991). For example, Fe, Cu, and Mn should be much more available in waterlogged soils rather than in dry oxidated soils. However, waterlogged conditions should have only local importance in exceptional landscapes (AB'SÁBER, 1974) such as floodplains adjacent to hillsides and 'Chapadas' of Caatinga.

In the context of global drylands (i.e. dry sub-humid, semiarid and arid regions), there is some evidence that increases in aridity may limit the availability of metallic micronutrients (Fe, Cu, Mn, and Zn). It has been argued that independent of soil parent materials, increased aridity may affect negatively plant production, leading to lower organic matter inputs in the soils (MORENO-JIMÉNEZ et al., 2019). In addition, aridity-driven limited weathering and changes in soil reaction (i.e. increased soil pH) may also lead to a potential reduction in micronutrient supplies. Because organic matter holds several micronutrients in complex colloidal organic compounds (WEIL; BRADY, 2017) a reduction in SOC contents may represent a limitation in the availability of these nutrients. Concerning the latter effect, it is well-studied that the solubility and availability of most micronutrients are greater in acid conditions so that an increase in soil pH may influence the form of these elements in the soils,

from free ionic forms to hydroxy ions until very stable and insoluble oxides or hydroxides (SHUMAN, 1991; ABREU; LOPES; SANTOS, 2007; WEIL; BRADY, 2017).

1.7.6 Soil water availability and effective rooting depth

Several studies have pointed out that soil water availability is crucial in determining several ecosystem processes (e.g. CHATURVEDI; RAGHUBANSHI, 2014, GAVIRIA; TURNER; ENGELBRECHT, 2017; TERRA et al., 2018). For example, soil water availability significantly influences the survival of seedlings (MCLAREN; MCDONALD, 2003), tree mortality owing to hydraulic failure (VILAGROSA et al., 2012), and long-term terrestrial carbon uptake (GREEN et al., 2019). Extended periods of water deficit may push many species towards their physiological limits, even though it is well-documented that species living in these ecosystems usually possess mechanisms to help them tolerate water shortage effects. For example, drought-deciduousness and/or root systems that are capable to exploit the soils at different depths in search of water (OLIVEIRA et al., 2014), in addition to other traits described in Section 1.1.

Within the factors controlling soil water availability, soil texture is generally assumed as the most important property influencing water retention in soils. As a rule of thumb, finer-textured soils tend to hold more water than fast-draining coarser textured soils (JENNY, 1980). Furthermore, texture indirectly influences soil water-holding capacity since it determines soil bulk density, pore size and distribution (PALM et al., 2007). This, in turn, influences the water movement through soils. Clay mineralogy (Section 1.6) also influences, to a large degree, soil properties such as aggregate stability, structure and porosity (TISDALL; OADES, 1982; PALM et al., 2007), consequently also influencing soil water retention.

Soil organic matter (SOM) is the third soil bulk property that contributes to the soil's hydraulic properties. Interacting with the previously discussed properties, SOM affects soil water storage and release (PALM et al., 2007), for at least two reasons: (1) Organic matter enhances soil structure and enlarges the potential water reservoir (FRANCHINI et al., 2009). (2) Organic matter also is widely known to enhance soil aggregation, cohesion and permeability (BRONICK; LAL, 2005; SCHJØNNING et al., 2018).

The soil properties described above strongly influence the amounts of water that can be stored at different matric potentials (ψ_M). For plants, the most important matric potentials

reflecting soil water availability are the field capacity (FC) - which represents the maximum water content in the soil after drainage ceases (often assumed as ψ_M = -10 kPa); permanent wilting point (PWP) - the lower limit for plant water absorption (ψ_M = -1500 kPa); and plant-available water capacity (AWC) - the plant-available water (interval between FC and PWP in which plants can extract water).

In addition to *in situ* soil properties, terrain physiographical characteristics, e.g. depth to impervious layers to water drainage (e.g. bedrock or hardpans) influence the size of the water reservoir [the maximum plant-available soil water (θ_P)], in turn influencing the ecosystem-level water availability. In general, shallow soils (e.g. < 1.0 m deep), if not replenished in time through rainfall, are expected to supply water for plants only for a few weeks, while deep soils (≥ 2.0 m) might store water for long periods as long as the root system can exploit a large volume of soil (SAMPAIO, 2010).

Only a few studies have been published reporting on soil water availability in both natural and human-modified environments of Caatinga (e.g. GÜNTNER; BRONSTERT, 2004, PINHEIRO et al., 2017, ALCÂNTARA et al., 2021), but some works in other tropical biomes also shed some light on this discussion. For example, Lloyd et al. (2015) showed through numerical simulations that the presence of shallow impermeable layers might actually be beneficial for the soil water budget as long the reductions in water losses by drainage are not being fully compensated by negative effects (e.g. strong runoff and erosion) in the case of heavy rainfall events. Costa et al. (2022) showed that a shallow water table (WT) might be beneficial during moderate drought by buffering water shortage. Nevertheless, that work also showed that during severe drought, forests with shallow WT (dominated by species with shallow root systems and intolerant-drought traits) might endure negative effects such as increased mortality.

In addition to the overall soil water holding capacity of soils, a variety of ecosystem properties such as nutrient availability, vegetation type and climate also influence root growth (GUSWA, 2010). By equating the marginal cost of carbon to invest in deeper roots compared to the benefit of these roots to continued transpiration, Guswa (2010) found deeper roots in ecosystems where the potential evapotranspiration was nearly equal to rainfall rates, which is consistent with a global analysis of roots distribution for terrestrial biomes (JACKSON et al., 1996). This is because, in wetter ecosystems, water is regularly found near the surface, whereas in drier ecosystems, there is usually no water at depth (GUSWA, 2010). Schenk and Jackson (2002) found deeper rooting depths in water-limited ecosystems when compared to their wetter counterparts, also noting that the deeper 95% rooting depths were found in sandy soils

compared to clayey soils and across shallow organic horizons compared to deeper organic horizons. Pinheiro et al. (2013) found effective root depths ranging from 0.6 to 0.78 m in non-restrictive Caatinga soils with 65% of the cumulative root biomass in the soil upper 0.3 m, an intermediate value for tropical deciduous forests and savannas (JACKSON et al., 1996). It is thus readily apparent that climate plays a marked role in root development and dynamics, which then interact with species characteristics and other soil properties (e.g. aluminium levels and overall fertility) in determining the capacity of roots to exploit the soil in search for water and nutrients.

1.8 Above-ground woody biomass (AGB_W)

Above-ground biomass (AGB) is a pivotal property of terrestrial ecosystems, reflecting manifold ecosystem services including carbon uptake and storage (POORTER et al., 2015). More often than not, studies that focus on environmental controls on AGB in Caatinga (as in seasonally dry tropical forests worldwide), have tested only climate variables rather than soils and potential soil-climate interactions. This is either because of the lack of the requisite *in situ* soils or because of inconsistent soil sampling protocols and laboratory analyses across sites. The largest collection of standardised soil information is available in the Brazilian System of Soil Information (EMBRAPA, 2022). Oliveira et al. (2019) using EMBRAPA's soil data set showed that, rather than climate or soil separately, a combination of soil and climate predictors, performed better in separating plant physiognomies comprised in the Brazilian semiarid zone.

An important consideration to be made regarding the Caatinga vegetation is that, due to the history of the region itself, there is a high probability that any area in the region must have undergone severe modifications over the past. In this sense, Andrade (1977), based on reports of former authors, presents a series of examples of severe anthropogenic disturbance in the past mainly either because of abusive and uninterrupted intensive grazing practices or by the irrational extraction of charcoal. They also report places where a larger/more robust vegetation was replaced by a thinner/more xerophytic vegetation. Moreover, the widespread presence of cattle and goats implies that vegetation must be to some extent impacted when accessed by these animals. Even recently, except for protected areas, animal activity and selective logging remain important disturbances sources (MENEZES, personal communication, 2022).

Considering the modified nature of the region, Souza et al. (2019) pointed out that AGB can be a multi-driven characteristic in a given ecosystem, especially where human disturbances

took place. The authors tested species richness, successional stages, plant functional composition, rainfall, soil fertility, and grazing impacts as potential biomass drivers in Caatinga and found a high variation between stands (28.48 ± 23.32 Mg ha^{-1}) mostly explained by successional stage, species richness and rainfall.

Castanho et al. (2020a) compiled information from 104 published data reporting on Caatinga AGB values and found a variation between 5 – 118 Mg ha^{-1} across a variety of plant physiognomies. Furthermore, through a satellite product, Castanho et al. (2020a) estimated that around the year 2000, over 50% of the Caatinga region had AGB levels as low as < 2 Mg ha^{-1} (accounting for ca. 1% of total Caatinga's AGB), 20% of the region had AGB in the range of 40-80 Mg ha^{-1} (accounting for 55% of the region's total AGB), and only 7% of the region had AGB ranging from 80 to 130 Mg ha^{-1}, representing another 31% of the region's total AGB of the region (the remaining AGB was in stands with 2-40 Mg ha^{-1}).

These results illustrate the high spatial variability of AGB in the Caatinga, reflected by at least three hierarchical levels, i.e. macro, meso and micro-variability, these being with climate and soil effects, current land-use of a given stand and the successional age, respectively (CASTANHO et al., 2020a). Therefore, any inferences concerning AGB in the Caatinga must necessarily specify which factors are being tested.

A common distinction often made is 'Dense Caatinga' and 'Open Caatinga'. The former generally refers to those stands with closed (or nearly closed) canopies, whereas the latter refers to those stands with intermediate regeneration levels or those with natural limitations for plant growth such as very limited soil depth (MENEZES et al., 2021). Commonly, AGB values between Dense and Open Caatingas vary significantly. For example, Menezes et al. (2021) reported average AGB values of 42.3 ± 6.2 and 22.7 ± 6.0 Mg ha^{-1} for Dense and Open Caatingas, respectively (using a conversion factor of 0.47 since the authors provided C stocks values). Also noted in Menezes et al. (2021) discussion is that, on average, AGB values of old-growth Dense and Open Caatingas tend to be lower compared to other SDTFs in South America. This was attributed to the Brazilian Caatinga region being markedly drier than other places in the continent, with water being a major limiting factor in this semiarid ecosystem. That said, one should also bear in mind that water availability does not depend on precipitation itself, but on rainfall seasonality, soil water storage characteristics, and actual evapotranspiration.

Concerning studies reporting on potential constraints for above-ground woody biomass in SDTFs, Becknell, Kucek; Powers (2012), examining 44 SDTFs worldwide have shown that mean annual precipitation (P_A) itself explained over 50% of the above-ground biomass in old-growth SDTFs. This finding is consistent with other research supporting that biomass accumulation is related to rainfall gradients (BROWN; LUGO, 1982; POORTER et al., 2016; MOORE et al., 2018). However, it is noteworthy that some studies, beyond considering P_A itself, also considered other water availability metrics, such as climatic water deficit (CWD). Indeed, it seems sensible that water availability does not depend on precipitation itself but on the final water budget. For example, Poorter et al. (2016) showed that biomass accumulation in regeneration forests resulted from water availability (represented by lower climatic water deficit and higher rainfall). Some works have, however, looked at the influence of soil properties on vegetation characteristics of SDTFs at local scales. For example, PEÑA-CLAROS et al. (2012) found a considerable role for soil nutrients in a suite of vegetation properties. Interestingly, the soil chemistry effects were more pronounced in drier than moister forests, contrary to the authors' predictions. De Souza et al. (2019) showed the influence of small-scale heterogeneity of soils influencing standing biomass, sprouting rates, and community composition. Maia et al. (2020a) have found interactions between soil and climate variables (i.e. texture, precipitation seasonality and precipitation in the driest quarter), accounting for variations in both above-ground woody biomass and species richness. Most studies, however, covered limited geographical ranges and further research upon larger spatial scales is needed to disentangle the most predominant environmental forces influencing the structural properties of Caatinga's SDTFs, across the biome.

1.9 AGB_W, functional diversity and soil properties

Alternative hypotheses have already been tested in the sense of disentangling standing AGB_W drivers and related dynamic processes in dry forests (i.e. recruitment, mortality, and growth of surviving trees). Prado-Junior et al. (2016) tested four contrasting hypotheses that could potentially explain these dynamics and found that the initial standing AGB_W was the most influential factor that determined all AGB_W-associated demographic processes in mature stands. Initial standing AGB_W translates into the 'vegetation quantity hypothesis' (LOHBECK et al., 2015). The premise of this hypothesis is that the quantity of vegetation is the most influential factor in determining ecosystem processes, as opposed to the quality of the vegetation. Lohbeck et al. (2015) also found that the amount of vegetation in a site is the most

important driver of ecosystem process rates, that is, wood and litter productivity and litter decomposition. Interestingly, despite showing relatively similar results, the studies of Lohbeck et al. (2015) and Prado-Junior et al. (2016) were carried out under very different conditions (that is, the former in wetter successional forests and the latter in dry mature forests). Thus, if it generally applies to dry Caatinga forests, any environmental force driving the initial standing AGB_W may indirectly influence dynamic processes.

Regarding other hypotheses that potentially explain variations in AGB_W, the soil fertility hypothesis, which is comprehensively tested in this thesis, has already been tested in a multitude of studies in humid (e.g. LAURANCE et al., 1999; ROGGY et al., 1999; CLARK; CLARK, 2000; QUESADA et al., 2012) and dry ecosystems (Section 3.1, Chapter 3).

The mass ratio hypothesis (or biomass ratio hypothesis) is based on the idea that the predominant traits in a given community exert a dominant role in ecosystem processes, therefore contributing more significantly to primary production (GRIME, 1998). This could potentially reflect greater biomass accumulation over time. In practice, functional traits are considered the mechanistic connection between plant species assembly and ecosystem functioning (LOHBECK et al., 2015; DÍAZ et al., 2006).

The niche complementarity hypothesis (TILMAN et al., 1997), reflected by the community functional richness (F_{Ric}), is thought to be driven by multiple factors, such as positive symbiotic interactions, improved use of limiting resources, decreased diseases, herbivory, and positive feedbacks in nutrient cycling (TILMAN; ISBELL; COWLES, 2014).

Soil properties have already been shown to influence the functional composition of plant communities. For example, Quesada et al. (2012) found a negative relationship between many soil nutrients and stand-level wood density in humid forests, which was primarily attributed to water-economic strategies. Furthermore, low-density trees were associated with higher turnover rates on physically unfavourable soils (QUESADA et al., 2012). Lira-Martins (2019) also found low wood density values associated with potassium and sodium leaf contents in humid pantropical forests, suggesting that these relationships were mainly mediated by an inverse relationship between parenchymatic tissues and wood density, the former associated with water, nutrients and carbohydrates storage. However, these patterns seem to be less studied in seasonally dry environments. In a recent study, Angelico et al. (2021) found evidence that soil fertility influences tree growth and wood anatomical characteristics in individuals of *Enterolobium contortisiliquum* (Vell.) ('Tamboril'), a species that occurs widely in Brazil, including several areas in Caatinga (CARVALHO et al., 2003). For example, Angelico et al. (2021) found that soil fertility positively influenced stem diameter, tree height, storage

compounds associated with parenchymatic cells, fibre walls, and diameter of intervessel pits, these being associated with low values of wood density. The authors also highlighted the need to establish reliable relationships between soil conditions and species wood anatomical features, this strongly reflecting water-economic strategies and nutrient uptake.

The distribution of a given trait value (or a set of trait values) over the niche space can be summarised into orthogonal axes, these representing functional diversity indexes (MASON et al., 2005). Specifically, functional richness (F_{Ric}) represents how much of a multivariate-trait space is filled in a given community; functional evenness (F_{Fve}) reflects the degree to which the basal area is distributed across the multivariate-trait space; and functional divergence (F_{Div}) indicates if the basal area is concentrated at the extremes of the multivariate-trait space (that is, high F_{Div}) or if the basal area is concentrated towards the centre of the multivariate-trait space (*sensu* MASON et al., 2005). In this context, determining the influence of soil properties on specific functional traits, as well as its derived functional diversity metrics, is part of the object of study of this thesis.

Supplementary Table S1.1: Reference soil groups (RSGs) coverages according to geological classes. Total area and fraction cover refer to the proportion of the Caatinga land covered by each RSG. Colours represent relative coverage proportions of each RSG within geologic affiliations, whereby warmer colours means relatively higher coverages whereas cooler colours represent relatively lower coverages. Calculations based on BDiA/IBGE. Coverage values in km².

RSG	Coverages	Fraction cover	RSG	Igneous Plutonic	Fraction cover	RSG	Igenous Volcanic	Fraction cover
Ferralsol	77,223.91	0.56	Acrisol	26,040.73	0.21	Leptosol	71.72	0.29
Arenosol	24,480.95	0.18	Leptosol	25,491.54	0.21	Vertisol	60.98	0.24
Acrisol	8,969.72	0.07	Planosol	20,301.29	0.16	Luvisol	39.47	0.16
Cambisol	7,532.86	0.05	Luvisol	18,034.44	0.15	Acrisol	28.28	0.11
Leptosol	5,066.62	0.04	Ferralsol	15,692.94	0.13	Arenosol	21.60	0.09
Planosol	4,074.14	0.03	Regosol	8,925.05	0.07	Ferralsol	15.03	0.06
Fluvisol	3,565.04	0.03	Cambisol	4,753.65	0.04	Planosol	7.26	0.03
Vertisol	1,465.68	0.01	Nitisol	1,297.19	0.01	Fluvisol	3.88	0.02
Urban areas/water bodies	1,413.76	0.01	Arenosol	1,259.44	0.01	Nitisol	0.90	0.00
Plinthosol	1,260.78	0.01	Urban areas/water bodies	907.04	0.01	Urban areas/water bodies	0.26	0.00
Luvisol	992.80	0.01	Rock Outcrops	404.84	0.00	Plinthosol	0.13	0.00
Dunes	743.46	0.01	Fluvisol	330.91	0.00	Rock Outcrops	0.00	0.00
Gleysol	363.43	0.00	Vertisol	300.64	0.00	Cambisol	0.00	0.00
Nitisol	232.35	0.00	Chernozem	172.65	0.00	Chernozem	0.00	0.00
Regosol	199.59	0.00	Plinthosol	94.30	0.00	Dunes	0.00	0.00
Histosol	15.50	0.00	Gleysol	6.90	0.00	Gleysol	0.00	0.00
Chernozem	12.21	0.00	Dunes	0.00	0.00	Regosol	0.00	0.00
Rock Outcrops	7.91	0.00	Histosol	0.00	0.00	Histosol	0.00	0.00
Total area	137,620.71	1.00	Total area	124,013.55	1.00	Total area	249.50	1.00
RSG	**Metamorphic**	**Fraction cover**	**RSG**	**Sedimentary**	**Fraction cover**	**RSG**	**Total**	**Fraction cover**
Acrisol	76,007.22	0.22	Ferralsol	65,662.85	0.27	Ferralsol	205,594.32	0.24
Leptosol	73,597.36	0.21	Leptosol	48,437.54	0.20	Leptosol	152,664.79	0.18
Luvisol	70,562.45	0.20	Arenosol	36,805.05	0.15	Acrisol	142,262.13	0.16
Planosol	53,799.10	0.15	Acrisol	31,216.20	0.13	Luvisol	93,915.53	0.11
Ferralsol	46,999.59	0.13	Cambisol	29,392.66	0.12	Planosol	88,218.36	0.10
Cambisol	8,751.97	0.03	Planosol	10,036.58	0.04	Arenosol	64,795.43	0.08
Regosol	7,854.81	0.02	Fluvisol	5,749.94	0.02	Cambisol	50,431.14	0.06
Urban areas/water bodies	2,896.70	0.01	Luvisol	4,286.38	0.02	Regosol	17,538.35	0.02
Chernozem	2,728.08	0.01	Plinthosol	4,210.12	0.02	Urban areas/water bodies	13,297.11	0.02
Arenosol	2,228.40	0.01	Vertisol	3,218.79	0.01	Fluvisol	10,266.29	0.01
Vertisol	1,822.35	0.01	Urban areas/water bodies	2,712.42	0.01	Vertisol	6,868.44	0.01
Nitisol	1,167.96	0.00	Gleysol	1,303.55	0.01	Plinthosol	6,343.42	0.01
Plinthosol	778.09	0.00	Chernozem	993.16	0.00	Chernozem	3,906.10	0.00
Fluvisol	616.51	0.00	Regosol	558.91	0.00	Nitisol	3,186.08	0.00
Gleysol	30.30	0.00	Nitisol	487.69	0.00	Gleysol	1,704.18	0.00
Rock Outcrops	22.57	0.00	Rock Outcrops	239.11	0.00	Dunes	938.76	0.00
Dunes	9.83	0.00	Dunes	185.46	0.00	Rock Outcrops	674.43	0.00
Histosol	0.00	0.00	Histosol	19.19	0.00	Histosol	34.68	0.00
Total area	349,873.26	1.00	Total area	245,515.58	1.00	Total area	862,639.53	1.00

Supplementary Table S1.2**:** Reference soil groups (RSGs) coverages in each geologic province encompassed in Caatinga. Total area and fraction cover refer to the proportion of the Caatinga land covered by each RSG. Colours represent relative coverage proportions of each RSG within geologic provinces, whereby warmer colours means relatively higher coverages whereas cooler colours represent relatively lower coverages. Calculations based on BDiA/IBGE. Coverage values in km².

WRB classification	Borborema	Cenozoic Coverage	C. Province and C. Margin	Mantiqueira	Parnaíba	R. Tucano-Jatobá	São Francisco	Total area	Fraction cover
Ferralsol	12,350.05	98,551.00	1,201.75	441.21	15,864.23	2,195.81	75,011.55	205,647.32	0.24
Leptsosol	78,519.67	5,719.00	90.68	706.89	20,240.34	4,468.07	43,073.32	152,867.40	0.18
Acrisol	69,544.96	20,003.01	2,474.27	407.31	4,769.38	2,675.64	42,412.80	142,421.72	0.17
Luvisol	83,339.88	1,575.37	17.31	21.56	477.40	1,223.68	7,380.09	94,072.47	0.11
Planosol	42,696.66	8,116.65	183.04	-	1,075.19	3,078.87	33,098.64	88,355.41	0.10
Arenosol	2,596.76	32,333.33	1,331.99	-	10,776.74	14,651.57	3,189.43	64,910.93	0.08
Cambisol	1,508.56	8,636.46	5,591.30	134.85	8.03	337.09	34,186.91	50,435.09	0.06
Regosol	12,864.50	170.40	28.57	-	-	477.13	3,996.33	17,538.71	0.02
Water bodies	777.21	708.68	55.84	-	21.70	1.58	159.22	10,700.23	0.01
Fluvisol	872.60	7,468.71	170.11	-	993.25	28.68	1,033.51	10,620.31	0.01
Vertisol	2,077.64	2,024.92	616.79	-	84.35	431.32	1,639.43	6,876.77	0.01
Plinthosol	189.47	1,480.92	41.21	-	3,989.63	-	647.09	6,349.31	0.01
Chernosol	2,515.19	30.62	991.67	-	-	-	368.56	3,906.11	0.00
Nitisol	954.37	129.11	-	0.85	60.45	-	2,041.34	3,186.14	0.00
Gleysol	15.09	619.07	1,125.84	-	85.61	-	1.82	1,856.67	0.00
Urban area	68.50	193.26	92.68	0.13	34.12	-	85.86	1,193.71	0.00
Dunes	12.35	78.64	886.61	-	-	-	-	991.31	0.00
Rock outcrops	96.78	11.75	-	-	-	-	565.90	674.43	0.00
Histosol	-	32.67	2.80	-	-	-	-	35.47	0.00
Total	311,000.23	187,883.61	14,902.46	1,712.80	58,480.41	29,569.45	248,891.82	862,639.53	1.00

Chapter 2

Chemical and physical properties of geologically distinct Caatinga soils

Chapter 2 – Chemical and physical properties of geologically distinct Caatinga soils

2.1. Introduction

The semiarid Caatinga soils have a marked spatial variability (Figure 1.3, Chapter 1), which makes it common to be referred to as a 'soil mosaic' (e.g., SAMPAIO, 1995; OLIVEIRA, 2011; MEIADO et al., 2012). Such a pattern can be considered as an interactive product of the prevailing semiarid climate and considerable geodiversity, the latter corresponding to both landforms and geologically-determined soil parent materials.

In an attempt to compartmentalise the Northeast Brazil region into discrete units sharing biotic and abiotic features, Veloso et al. (2002) proposed the Ecoregions for the Caatinga biome. This work was mostly based on the Northeast Agroecological Zoning (ZANE) (SILVA et al., 1993) and separated the Caatinga region into eight distinct ecoregions, each of them showing particular biotic and abiotic characteristics, including typically associated soil types. Despite these existing schemes, Caatinga has traditionally been divided into (i) Precambrian lowland crystalline rock depressions; (ii) ancient sedimentary basins and dunes; (iii) karst deposits (FERNANDES et al., 2022). The most typical landscape and ecological conditions are, however, associated with Precambrian crystalline terrains ['the Caatinga core' (AB SABER, 1974)]. Indeed, most of the Caatinga soils are derived from crystalline areas (Chapter 1, Section 1.5; DA SILVA; LEAL; TABARELLI, 2017).

From the pedological standpoint, soil types associated with (i), (ii) and (iii) are expected to show predictable properties. For example, Leptosols, Planosols and Luvisols are expected to occur in crystalline terrains (i) to a large extent. These RSGs have low to intermediary pedogenetic stages, being commonly shallow but with reasonable fertility conditions. On the other hand, soils developed from sedimentary parent materials (ii) are, in general, deeper but with less favourable soil fertility conditions (e.g. Ferralsols, Arenosols, Acrisols). Karst environments can potentially give rise to distinct RSGs, including Leptosols, Chernozems and Cambisols, with the latter usually predominating (ARAÚJO FILHO, 2011; ARAÚJO FILHO et al., 2017; OLIVEIRA et al., 2018). Due to their original base-rich parent materials, karst soils usually show high base saturation levels and high soil pH, which is particularly important for several biogeochemical processes.

These geological categories have been extensively considered in ecological and botanical studies (KENZO et al., 2017; QUEIROZ, 2006, QUEIROZ et al., 2017, FERNANDES et al., 2020; 2022), sometimes to reflect the influence of nutritional and

hydrological soil properties upon vegetation stands (e.g. MORO et al., 2015). But in any case, it seems reasonable to expect that geological features and associated discrete units may reflect soil type distribution across Caatinga. In turn, RSGs are, to a large degree, associated with soil chemical and physical properties since they should reflect soil-forming processes (Section 1.4, Chapter 1).

In this respect, the general idea of *a priori* marked differences among soils originating from different geological types, direct qualitative and quantitative comparisons have rarely been made. Moreover, although some global relationships among soil properties are well-established, studies exploring these relationships are required to improve our understanding of the pedogenetic process in semiarid environments, especially as regards the underlying biogeochemical processes. For example, if parent material largely determines soil texture and associated biological-mediated processes such as the decomposition of organic matter and nutrient cycling (PALM et al., 2007; SANCHEZ, 2019), then soil geologic affiliation can potentially influence soil organic carbon and nitrogen dynamics. This may more often be the case in semiarid environments, where the influence of parent material on soil properties is expected to be more pronounced than in wetter environments (ARAÚJO et al., 2017). As weathering forces in semiarid environments are of smaller relevance compared to humid tropics, levels of exchangeable and total chemical species of macro and micronutrients are mostly driven by the composition of soil parent materials. In addition, under these conditions, leaching and losses of soil bases take place at low rates giving rise to the formation of 2: 1 silicate clay minerals (or expansive clays) through partial hydrolysis reactions (RIGHI; MEUNIER, 1995; FONTES, 2012). Expansive clays are often present in Caatinga soils (ARAÚJO et al., 2017). Along with soil organic matter (SOM), clay mineralogy and soil texture are considered soil core properties (PALM et al., 2007; WEIL; BRADY, 2016). These properties covary but interplay with many other soil properties such as pH, and effective cation exchange capacity (I_E).

For instance, the size of the soil sortive complex reflected by I_E is influenced by both soil particle size distribution and soil mineral assemblage, including silicate clay minerals and species of Al and Fe (oxy)hydroxides. Thus, differences in the relative proportion of these constituents, which are thought to reflect geologic affiliations, are expected to influence soil properties such as soil surface charge density and associated I_E. Effective cation exchange capacity is also sensitive to soil pH, i.e., through hydrolysis, H^+ ions replace cations in the silicate lattice, which can be leached out of the system or form clay minerals (QUESADA et

al., 2010). Since the hydrolysis process should occur at a prevailing low rate in Caatinga soils, the quality of soil parent materials will strongly affect I_E and its interactions with other soil properties. Indeed, I_E seems to be primarily influenced by pedogenic stages, whereas the relative proportions of bases and aluminium seem to be associated with soil parent material and its mineral assemblage (QUESADA et al., 2010).

Similarly, apatite-bearing minerals concentrations in soil parent materials should reflect soil total phosphorus concentrations $[P]_T$, which have already been reported to be three to five-fold higher in soils derived from crystalline terrains compared to soils derived from sediments in the Caatinga (SALCEDO, 2006). Nevertheless, manifold factors should influence phosphorus availability in soils. For instance, soil pH ultimately governs the predominance of (by decreasing solubility): (Ca)-bonded > (Al)-bonded > (Fe)-bonded phosphates (SMECK, 1985; GUO et al., 2000). Moreover, parent materials quality and mineral assemblage are expected to influence these associations. In addition, if an ecosystem has evolved so a relatively high amount of P circulates through the organic pathway (P_O), it might be expected that $[P]_T$ correlate to soil total organic carbon (SOC), as reported in Menezes et al. (2012). Nevertheless, it has also been suggested that the build-up of P_o in soils depends on high inorganic P supplies (MCGILL; COLE, 1981). Soil texture, general fertility, and mineral assemblage are also known to influence processes related to SOC dynamics and accumulation in soils (SMECK, 1985; BRUUN; ELBERLING; CHRISTENSEN, 2010; SINGH et al., 2018). Therefore, the interrelationships among geologically-determined soil parent materials, RSGs and soil properties are also expected to relate to SOC concentrations and dynamics.

Several potential causes of variation in soil N isotopic signature in (seasonally) dry environments were described in Chapter 1, Section 1.7.3. The literature shows that soil ^{15}N enrichment can be driven by both edaphic and climatic factors, with the latter usually prevailing in arid or semiarid regions (e.g. SWAP et al., 2004; ARANIBAR et al. 2004; SANTOS et al. 2022). Edaphic effects, however, cannot be disregarded, but the potential mechanisms involved are not fully understood. For example, Aranibar et al (2004) report higher soil and plant $\delta^{15}N$ values associated with sandy soils. By contrast, Santos et al. (2022) found higher $\delta^{15}N$ values positively associated with more clayey soils in Caatinga (SANTOS et al., 2022). Alternative pathways were suggested accounting for the clay effects. For instance, Houlton et al. (2015) pointed out that, in addition to potential higher N fractionating in clayey soils, the latter can also contain stabilised N^{15}-enriched complexes. Importantly, if geologically-determined soil properties (e.g. texture and mineral assemblage) account for variation in isotopic discrimination

patterns, then variations in soil ^{15}N values might be reflected by geological origins and associated RSGs.

Spatial information concerning soil $\delta^{15}N$ values for the Caatinga region is still sparse, with the work of Santos et al. (2022) reporting on map-modelled soil $\delta^{15}N$ values generated from Alisols of Pernambuco state under different land uses and varying climatological conditions. Information over a biome-wide scale can be useful to provide insights into N dynamics on a subcontinental scale.

Regarding weathering relationships explored in this work, weatherable primary minerals are known to be associated with sand and silt particles, whereas secondary minerals are known to be mostly associated with clay particles (SANCHEZ, 2019). Thus, given the prevailing quartz (SiO_2) composition of most sands, nutrient capital reserves can be markedly influenced by weatherable primary minerals present in the soil silt fraction, likely reflecting the contents of other chemical species.

Potential environmental drivers that control effective rooting depth across soil profiles are also explored in this chapter. Effective rooting depth is thought to reflect a balance between benefits acquired with deeper rooting relative to carbon costs associated with root tissue construction and autotrophic respiration (GUSWA, 2010). Considering the typical negative water balances of the Caatinga, lower mean annual climatic water deficits (CWD) translate into potential evapotranspiration rates closer to mean annual precipitation (P_A) year-round, which in turn might favour deeper root systems.

A sampling effort spanning a wide latitudinal and longitudinal range across the Brazilian Caatinga territory gave rise to the unique opportunity to study the variability of several soil properties across geologically distinct soil groups. Sites sampled here also encompassed both rainfall and temperature gradients, allowing for the investigation of potential systematic relationships between soil parent materials, current climate conditions and selected soil properties.

Specifically, in this chapter, I address the following questions:

1) How does geology (as a determinant of the types of soil parent material) influence a suite of soil chemical and physical properties of the soil?

2) How do soil properties interrelate in the context of different geological affiliations?

3) Do climate [represented by mean annual precipitation (P_A), mean annual temperature (T_A), climatic water deficit (CWD) and Aridity Index (AI)] exert significant influence on specific soil properties, that is, total carbon $[C]_T$, total nitrogen $[N]_T$, C/N ratio, and effective rooting depth (R_{EF})?

4) Accounting for the (expected) climate influence, how do soil properties relate to N dynamics (evaluated through *time-integrated* soil $\delta^{15}N$ measurements)?

This study is by no means intended to generalise soil properties for all Caatinga soils belonging to broad geological affiliations. As already mentioned, the astounding environmental heterogeneity of the Caatinga would make this task impossible. Instead, this study is intended to evaluate the above-mentioned questions and serve as a baseline soil survey for current and future research in the established permanent plots achieved by the Nordeste Project (FAPESP Grant 2015/50488-5 / NERC Grant NE/N012488/1).

2.2 Material and methods

2.2.1 Study sites

Data analysed here come from 29 study plots spanning latitudinal and longitudinal ranges, encompassing much of the geographic extent of the Caatinga region. The allocation of the study sites was defined in the sense of capturing as far as possible variations in P_A levels and soil conditions but also taking into account logistical aspects. Thus, P_A varied from 0.512 m a^{-1} at CND-01, Bahia to 1.363 m a^{-1} at PSC-02, Piauí, also including many soil types (described below). The soil sampling was undertaken in three intensive fieldwork campaigns (2017, 2018, and 2019). Despite other vegetation types being common throughout the Caatinga domain, only soils under drought-deciduous Seasonally Dry Tropical Forests (herein SDTFs) were analysed in this work. The geographical location of the study sites/plots is shown in Figure 2.1, and additional information is available in Table 2.2.1 and Table 2.2.2 below.

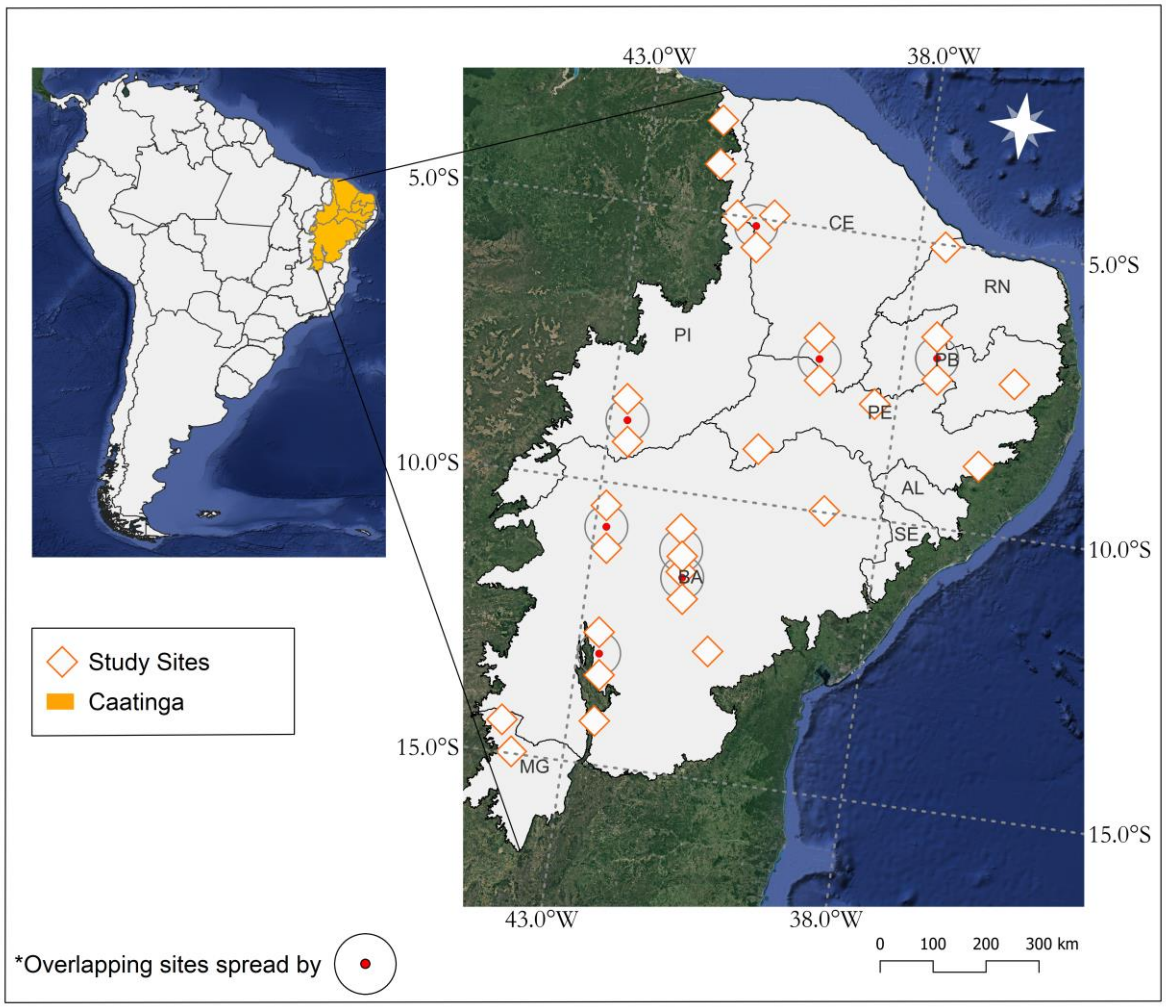

Figure 2.1: Study sites across the Caatinga region. Federated states are shown: PI = Piauí; CE = Ceará; RN = Rio Grande do Norte; PB = Paraíba; PE = Pernambuco; AL = Alagoas; SE = Sergipe; BA = Bahia; MG = Minas Gerais.

Table 2.1: Plot codes, site names/federated states, latitude, longitude, mean annual precipitation (P_A), mean annual temperature (T_A), altitude, structural provinces, geological formation, and geological class. Study plots were grouped according to their respective structural provinces.

Plot Code	Site Name/States	Lat	Long	P_A (m)	T_A (°C)	Alt (m a.s.l.)	Province	Formation	Class
LGE-01	Embrapa Semiárido - PE	-9.048	-40.32	0.59	25.1	384	Borborema	Barra Bonita	Crystalline
ARI-03	Araripe 3 - CE	-7.271	-39.453	1.08	22	680	Borborema	Missão Velha	Sedimentary
SJO-01	São João - PE	-8.81	-36.405	0.79	21.4	495	Borborema	Belém do São Francisco	Crystalline
SET-01	Serra Talhada - PE	-7.97	-38.385	0.75	23.7	275	Borborema	São Caetano	Crystalline
CGR-01	INSA/Campina Grande - PB	-7.28	-35.976	0.6	22.8	256	Borborema	São Caetano	Crystalline
PAT-01	Patos 1 - PB	-7.007	-37.396	0.79	26.2	311	Borborema	Jurucutu	Crystalline
PAT-02	Patos 2 - PB	-7.023	-37.403	0.81	26.2	460	Borborema	Serra dos Quinos	Crystalline
SDA-03	R. N. Serra das Almas - CE	-5.117	-40.873	0.82	25.5	760	Borborema	Tamboril Santa-Quitéria	Crystalline
ARI-04	Araripe 4 - CE	-7.36	-39.477	1.01	21.4	901	Cenozoic Coverage	Cobertura D.L. Paleogênica	Sedimentary
IBD-01	Ibiraba Dunes 1- BA	-10.787	-42.819	0.7	25.5	425	Cenozoic Coverage	Vazantes-Dunas	Sedimentary
IBD-02	Ibiraba Dunes 2 - BA	-10.785	-42.776	0.68	25.6	421	Cenozoic Coverage	Vazantes-Dunas	Sedimentary
PFF-01	Furna Feia National Park - RN	-5.041	-37.521	0.86	26.8	106	Coastal Province	Jandaíra	Karst
SCP-02	Serra da Capivara N. Park - PI	-8.862	-42.676	0.77	25.6	500	Parnaíba	Pimenteiras	Sedimentary
SDA-01	R. N. Serra das Almas - CE	-5.147	-40.928	0.97	23	620	Parnaíba	Tianguá	Sedimentary
PSC-02	Sete Cidades National Park - PI	-4.134	-41.684	1.36	26	98	Parnaíba	Cabeças	Sedimentary
SCP-01	Serra da Capivara N. Park - PI	-8.865	-42.702	0.79	25.4	620	Parnaíba	Pimenteiras	Sedimentary
BTI-01	Buriti dos Lopes - PI	-3.362	-41.743	1.22	26.6	237	Parnaíba	Cabeças	Sedimentary
SDA-02	R. N. Serra das Almas - CE	-5.141	-40.915	0.97	23.3	510	Parnaíba	Tianguá	Sedimentary
CND-01	Canudos - BA	-9.971	-39.006	0.51	22.7	533	R. Tucano-Jabobá	São Sebastião	Sedimentary
BVT-01	Fazenda Boa Esperança - BA	-12.725	-40.711	0.72	22.2	489	São Francisco	Mairi	Crystalline
CJU-01	Lagoa do Cajueiro S. Park - MG	-14.965	-43.916	0.83	24.2	459	São Francisco	Paraopeba	Sedimentary
MCS-02	Macaúbas 2 - BA	-13.061	-42.517	0.78	24.4	545	São Francisco	Pedra Branca	Crystalline
MOR-01	Morro do Chapéu 1 - BA	-11.493	-41.331	0.6	20.5	926	São Francisco	Morro do Chapéu	Sedimentary
CTI-01	Caetité - BA	-14.225	-42.53	0.94	20.9	638	São Francisco	Sítio Novo	Crystalline
GBR-01	Gruta dos Brejões - BA	-11.014	-41.439	0.52	23.3	791	São Francisco	Gabriel	Karst
GBR-02	Gruta dos Brejões - BA	-11.021	-41.411	0.52	22.9	880	São Francisco	Nova América	Karst
MCS-01	Macaúbas 1 - BA	-13.002	-42.707	0.79	23.1	524	São Francisco	Pajeú	Crystalline
MOR-02	Morro do Chapéu 2 - BA	-11.495	-41.346	0.59	20.8	857	São Francisco	Morro do Chapéu	Sedimentary
JUV-01	Juvenília - MG	-14.425	-44.157	0.9	24.2	593	São Francisco	Paraopeba	Sedimentary

Table 2.1 (continued): average plot slope (APS) soil classification (WRB/FAO System), clay activity and main regional parent materials. Notes: Within each soil classification, Reference Soil Groups (RSGs) are shown in bold; HAC = high-activity clays; LAC = low-activity clays; ARE = arenic; F = flat; SS = slightly slope.

Plot Code	APS	WRB Soil Classification	Clay Activity	Main Regional Parent Materials
LGE-01	F	Skeletic Abruptic **Luvisol** (Clayic, Hypereutric, Ochric)	HAC	Phyllite, Marble, Mica Schist
ARI-03	SS	Haplic **Alisol** (Arenic - ARE, Ochric)	LAC	Sandstone, Siltite
SJO-01	F	Eutric Protic **Arenosol** (Ochric)	ARE	Orthogneiss, Migmatite, Metadiorite
SET-01	F	Rhodic Leptic **Luvisol** (Arenic, Hypereutric, Ochric, Profondic)	HAC	Metabasalt, Metagrabbo, Paragneiss
CGR-01	F	Leptic Abruptic **Luvisol** (Clayic, Differentic, Hypereutric, Ochric, Magnesic)	HAC	Metabasalt, Metagabbro, Paragneiss
PAT-01	F	Rhodic Stagnic Leptic Abruptic **Luvisol** (Loamic, Hypereutric, Humic)	HAC	Schist, Marble, Paragneiss
PAT-02	F	Rhodic Stagnic Leptic **Luvisol** (Loamic, Densic, Hypereutric, Ochric)	HAC	Schist, Marble, Paragneiss
SDA-03	F	Chromic Abruptic **Luvisol** (Loamic, Differentic, Hypereutric, Ochric)	HAC	Schist, Paragneiss
ARI-04	F	Haplic **Acrisol** (Loamic, Ochric, Vetic)	LAC	Sandstone, Siltite
IBD-01	SS	Hypereutric Protic **Arenosol** (Aeolic)	ARE	Aeolian Sediment
IBD-02	F	Hypereutric Protic **Arenosol** (Aeolic)	ARE	Aeolian Sediment
PFF-01	F	Skeletic **Calcisol** (Clayic)	HAC	Calcarenite, Calcilutite, Shale
SCP-02	F	Xanthic Leptic **Acrisol** (Loamic, Differentic, Ochric, Profondic, Vetic)	LAC	Sandstone, Shale, Sandy Siltite, Conglomerate
SDA-01	F	Orthodystric Rhodic **Arenosol** (Humic)	ARE	Sandstone, Shale, Sandy Siltite, Conglomerate
PSC-02	F	Orthodystric **Regosol** (Ochric)	LAC	Sandstone
SCP-01	F	Orthodystric Skeletic Sideralic Pisoplinthic **Cambisol** (Loamic, Ochric)	LAC	Sandstone, Shale, Siltite
BTI-01	SS	Orthodystric Hyperskeletic **Leptosol** (Loamic, Profundihumic)	HAC	Sandstone, Shale
SDA-02	F	Hyperdystric Leptic **Leptosol** (Loamic, Ochric)	HAC	Sandstone, Shale, Sandy siltite, Conglomerate
CND-01	F	Orthodystric Chromic Sideralic **Arenosol** (Aridic)	ARE	Sandstone, Argillite, Shale, Siltite
BVT-01	SS	Xanthic **Acrisol** (Loamic, Hyperdystric, Humic, Vetic)	LAC	Orthogneiss
CJU-01	F	Hyperdystric **Arenosol** (Ochric)	ARE	Sandstone, Arkose, Calcarenite, Dolomite, Shale
MCS-02	F	Hypereutric **Arenosol** (Ochric)	ARE	Gneiss, Migamatite, Orthogneiss
MOR-01	F	Orthodystric Sideralic **Arenosol** (Humic)	ARE	Quartz-sandstone
CTI-01	SS	Hyperdystric **Regosol** (Loamic, Profundihumic, Magnesic)	LAC	Phyllite, Metaconglomerate
GBR-01	F	Calcaric Chromic Eutric **Cambisol** (Loamic, Humic)	HAC	Calcarenite, Calcilutite
GBR-02	F	Hypereutric Calcaric Lithic **Leptosol** (Loamic, Profundihumic)	HAC	Calcarenite, Calcilutite
MCS-01	SS	Hyperdystric Hyperskeletic **Leptosol** (Loamic, Ochric)	LAC	Mica-quartzite, Quartize-feldspar, Metaconglomerate
MOR-02	SS	Hyperdystric Hyperskeletic **Leptosol** (Loamic, Humic)	LAC	Arkose arenite, Pelite
JUV-01	SS	Rhodic **Luvisol** (Loamic, Hypereutric, Humic, Profondic)	HAC	Arkose, Argillite, Calcarenite, Dolomite, Shale

2.2.2 Soil sampling

Taking into account the morphological particularities of individual soils, soil sampling was carried out according to a standard protocol (available at https://rainfor.org/wp-content/uploads/sites/129/2022/07/soilandfoliarsampling.pdf) as has been widely used in former field sampling in tropical biomes research such as the RAINFOR and TROBIT Projects (e.g. QUESADA et al., 2010; 2011; LLOYD et al., 2015). Typically, 4–7 soil cores were taken in each 100 x 50 m (0.5 ha) plot. Specifically, four auger cores were established as baseline sampling, with one to three additional cores drilled in cases of within-plot marked spatial variability (e.g. irregular topography, rock outcrops, vegetation changes, etc). In addition, a soil pit was dug just outside each plot to allow for soil profile description, also serving as an additional sampling location for soil physical and chemical analysis (in the same depth as for auger samplings). The maximum sampling depth was set to 2 m. It should, however, be noted that shallower soils are quite common in the region, with bedrock or other hardpans commonly found within the upper 1 m or shallower.

Soil collection at specific depths was undertaken with the aid of an auger set (VanWalt Ltd), with proper drills for different soil types, i.e., sandy, loamy, clayey, stony and rocky. Samples were separated at the depths: 0.00 – 0.05; 0.05 – 0.10; 0.10 – 0.20; 0.20 – 0.30; 0.30 – 0.50; 0.50 – 1.00; 1.00 – 1.50; 1.50 – 2.00 m (according to the maximum depth reached). Soil pits were described following the Guidelines for Soil Description (JAHN et al., 2006). Important properties such as horizons width, diagnostic horizons and materials, soil structure, colour, roots depth and distribution, soil total depth and the presence (or absence) of any hardened impervious layer were always recorded. After collection, all samples were air-dried as soon as practical and sent to the Soil and Plant Thematic Laboratory (LTSP) of the National Institute for Research in the Amazon (INPA, Manaus, Brazil).

2.2.3 Laboratory analysis

Samples were loosened, sieved in 2 mm (10 mesh), and had residues removed (i.e. stones, vegetation or faunal debris, etc). Most soil chemical and physical analyses were performed in the facilities of the LTSP-INPA, usually starting a few days after the fieldwork campaigns or as soon as practical. All analyses were carried out following specific protocols described in ‘Procedures for Soil Analysis’ (REEUWIJK, 2002). Calibration procedures and standard samples were routinely used to ensure the results. The X-ray fluorescence analysis

(XRF) was undertaken at the Soil Department of the Federal University of Viçosa (UFV), Minas Gerais, Brazil and the isotope analysis at the Center for Nuclear Energy in Agriculture (CENA), Piracicaba, São Paulo, Brazil.

2.2.3.1 Soil pH

Soil pH was determined both in water and in 1 M KCl. This method consists of measuring the pH in the supernatant suspension of a 1:2.5 soil-deionised water (or 1 M KCl). Samples were shaken for one hour in a reciprocating shaking machine, and the measurements were undertaken with the aid of a glass electrode. Soil pH in 1 M KCl was also determined as the soil ΔpH ($\Delta pH = pH_{H2O} - pH_{KCL}$) is sometimes required for classification purposes. This measure is also used as an indicator of the predominance of soil charges. That is, the lower the ΔpH, the more electronegative the soil is.

2.2.3.2 Soil exchangeable cations

Soil exchangeable cations were determined by the Silver-Tioureia (AgTU) method (PLEYSIER; JUO, 1980). This is a rapid and efficient cations extraction based on the affinity of the AgTU complex with the negatively charged soil colloids. It allows a complete cations extraction (including aluminium) in a single-step centrifuge extraction with an unbuffered 0.01 M AgTU solution (PLEYSIER; JUO, 1980). The concentration of each cation in the samples was then determined using an Atomic Absorption Spectrophotometer (AAS, Model 100b, Perkin Elmer, Norwalk, CT, USA). Subsequently, the soil sum of bases ($\sum_B$), effective cation exchange capacity (I_E), base (BS%) and aluminium (m%) saturation were calculated as follows:

$$\sum_B = [Ca]_{ex} + [Mg]_{ex} + [K]_{ex} + [Na]_{ex}, \quad \text{Eqn. (2.1)}$$

$$I_E = \sum_B + [Al]_{ex}, \quad \text{Eqn. (2.2)}$$

where $[X]_{ex}$ represents the respective exchangeable cation content.

The effective base saturation is:

$$BS\% = \frac{[Ca] + [Mg] + [K] + [Na]}{[Ca] + [Mg] + [K] + [Na] + [Al]} \times 100. \quad \text{Eqn. (2.3)}$$

Where BS% = effective soil sum of bases (%). Effective aluminium saturation (m%) was calculated as m% = 100 – BS%.

2.2.3.3 Soil carbon and nitrogen

Total soil carbon and nitrogen were determined using an automated analyser (Vario Max CN, Element Analyzer; PELLA, 1990; NELSON; SOMMERS, 1996). A subset of samples with higher pH (karst-associated soils) was tested in the sense of detecting the potential presence of carbonates by adding 1 *M* HCl.

2.2.3.4 Isotopic composition ($\delta^{15}N$)

Soil $\delta\ ^{15}N$ was analysed from composite air-dried samples from the upper 0.00 - 0.05; 0.05 - 0.10; 0.10 – 0.20; 0.20 – 0.30 m soil layers (to be consistent with the other analyses) at the Isotopic Ecology Laboratory of the Center of Nuclear Energy in Agriculture (CENA-USP). Measurements were undertaken with an elemental analyser (Carlo Erba, 1100 model, Milan, Italy), along with a coupled isotopic mass spectrometer (Thermo Quest-Finnigan Delta Plus). The abundance of ^{15}N compared to the lighter ^{14}N was expressed as thousand deviations (‰) relative to the atmospheric standard through the equation:

$$\delta^{15}N\ (‰) = (R_{\ sample}/\ R_{\ standard}\ -1)\ x\ 1000 \qquad \text{Eqn. (2.4)}$$

where $\delta^{15}N$ is the stable isotopic composition in deviations per thousand and R_{sample} and $R_{standard}$ are the respective ^{15}N:^{14}N ratios of the samples and standard, the latter being internationally adopted as the atmospheric N.

2.2.3.5 Phosphorus

Total soil phosphorus (P) was determined using composite samples from the upper 0.00 - 0.05; 0.05 - 0.10; 0.10 – 0.20; 0.20 – 0.30 m soil layers. Samples were digested with concentrated sulfuric acid, followed by peroxide hydrogen additions (TIESSEN; MOIR, 1993). After this process, the total P contents were determined by colourimetry using molybdenum blue colour development as described by Olsen and Sommers (1982), using a spectrometer (Model 1240, Shimadzu, Kyoto, Japan).

2.2.3.6 Total reserve bases and soil elemental ratios

The main soil total base cations concentrations and total Fe, Zn and Mn were obtained through concentrated sulfuric acid digestion, followed by peroxide hydrogen additions (TIESSEN; MOIR, 1993). Extract concentrations were determined using an Atomic Absorption Spectrophotometer (AAS, Model 100b, Perkin Elmer, Norwalk, CT, USA), with the sum of total Ca, Mg, K, and Na ($\sum_{RB}$) calculated as an indicator of soil chemical weathering (DELVAUX; HERBILLON; VIELVOYE, 1989). The $\sum_{RB}$ index was calculated as:

$$\sum_{RB} = [Ca_T] + [Mg_T] + [K_T] + [Na_T], \quad \text{Eqn. (2.5)}$$

where $\sum_{RB}$ = Total reserve bases, and $[X_T]$ is the total content of a given base (usually in $mmol_c\ kg^{-1}$ or $cmol_c\ kg^{-1}$).

Soil total elemental composition was also obtained through X-ray fluorescence (XRF) using an automated analyser (μ-EDX-1300, Shimadzu, Kyoto, Japan). To help understand weathering status across the studied soils, elemental ratios were calculated from oxides concentrations, these being iron to zircon (Fe_2O_3/ZrO_2), potassium to zircon (K_2O/ZrO_2) and silicon to aluminium (SiO_2/Al_2O_3). The rationale for using zircon (Zn) as a denominator in the ratios is that this element is highly resistant to weathering and immobile in the soil (SHAHID et al., 2013). Using [Zr] as a common denominator provides a straightforward way to compare groups of soils derived from relatively close parent materials.

2.2.3.7 Soil texture

Soil texture was determined using the sieve-pipette method (GEE; BAUDER, 1986). Ten grams of soil were treated with 20 mL of sodium pyrophosphate 5% (a dispersant) and completed to ca. 200 ml in Erlenmeyer flasks and left overnight. Subsequently, samples were shaken for 15 minutes and had the sand fraction ($sand_f$) separated with a 212 μm sieve. The remaining water, soil and dispersant were, subsequently, transferred to a measuring cylinder and completed to 1 L, agitated and left to rest for a pre-established period according to the mixture temperature. After that, the clay fraction ($clay_f$) of each sample was obtained by pipetting 20 mL from the upper part of the cylinder and the silt fraction ($silt_f$) was obtained by subtracting $sand_f$ and $silt_f$ from the initial sample weight.

2.2.3.8 Soil bulk density

Soil bulk density was determined through the volumetric ring method (Eijkelkamp Agrisearch Equipment BV, Giesbeek, Netherlands). For this purpose, samples were collected from the trench walls at specific depths, i.e. 0.00 – 0.10, 0.10 – 0.20, 0.20 – 0.30, 0.30 – 0.50, 0.50 – 1.00, 1.00 – 1.50, 1.50 – 2.00 m. In the laboratory, the samples were oven-dried at 105°C until constant weight, and the bulk density was obtained by the division of dried soil mass by the ring of known volume.

2.2.4 Soil classification

The soil classification was attained through the WRB/FAO System 2014 (updated in 2015). The classification procedure is mainly based on the characterisation of diagnostic horizons, properties both observed in the field and determined in the laboratory. These attributes relate to soil-forming processes (e.g. clay illuviation giving rise to *argic* horizons). Initially, the Reference Soil Groups (RSGs) were determined, followed by principal and complementary qualifiers. This system was designed to accommodate national systems instead of substituting them and serving as an international denominator for soil science (IUSS Working Group WRB, 2015). Effective base saturation (BS%) was then calculated to differentiate clay-enriched subsurface diagnostic horizons (i.e. Acrisols, Alisols, Luvisols and Nitisols) and Eutric to Dystric qualifiers (rather than the previously employed base saturation at pH 7). BS% combines exchangeable bases ($[Ca]_{ex}$ + $[Mg]_{ex}$ + $[K]_{ex}$ + $[Na]_{ex}$) extracted by 1 *M* NH_4OAc (ammonium acetate) at buffer pH 7 and exchangeable aluminium ($[Al]_{ex}$) extracted by 1 *M* KCl. The addition of 1 *M* HCl was also undertaken in some samples to detect the eventual presence of calcic horizons (i.e. calcium carbonate equivalent in the fine earth fraction ≥ 15%). The soil classification was performed with the aid of the WRB Tool 1.1.2.0 for Windows (OrlovDO, 2017; https://apps.microsoft.com/store/detail/wrb-tool/), which follows the WRB key in a structured way.

2.2.5 Geological surveying

The geoscience system (GeoSGB) of the Geological Survey of Brazil (CPRM) was used as a reference to achieve proper geological characterisations. In brief, the surveying consisted of identifying the sheets of the International Map of the World (IMW) comprised in the RADAMBRASIL Project (viz. SA.24 – Fortaleza; SB.24 – Jaguaribe; SB.25 – Natal; SC.24 – Aracaju; SC.23 - Rio São Francisco; SD.24 – Salvador; SD.23 – Brasília). Thus, the respective geological charts were thoroughly analysed, and relevant attributes were extracted, such as geological units/formations, initial and final geologic formation times, and predominant rock types (soil parent materials). This process allowed for uncovering the main lithostratigraphic units, i.e. associated rock and sediment types. When feasible, soil parent materials were documented and identified in the field. In addition, local publications, larger-scale geological charts, and personal communication with a few experts also helped in the sense of adding any relevant information to attain appropriate geologic characterisations.

2.2.6 Soil depth and plant water availability

Because direct soil water availability measurements in the field were impractical, a pedotransfer function (PTF) was used, which indirectly allowed for obtaining soil available water contents (AWC) as given in Hodnett and Tomasella (2002). Volumetric soil water (θ_V) content associated with specific soil textural classes (following USDA soil textural classes) was calculated assuming plant-available soil water as the range between field capacity (-10 kPa) and the permanent wilting point (-1,500 kPa). In addition, texture-associated volumetric soil water contents were weighted across each soil profile ($W\theta_V$) according to sampling depths. In Hodnett and Tomasella's work, 771 horizons were included encompassing several reference soil groups (RSGs) and distinct clay mineralogies, i.e. kaolinite and montmorillonite clays. The calculations were attained according to the widely used Van Genutchen model (VAN GENUCHTEN, 1980) as given in Eqn 2.6.

$$\theta_v = \theta_r \frac{\theta_s - \theta_r}{[1+(\alpha|\psi|)^n]^m}, \qquad \text{Eqn. (2.6)}$$

where θ_v= volumetric soil water content ($m^3\ m^{-3}$); θ_s and θ_r= the saturated and residual water content, respectively; ψ = a given absolute matric potential; α, n and m stand for shape parameters (m generally assumed as $1 - {}^{1}/_{n}$). After that, volumetric soil water content θ_v was

calculated for each sample to the maximum measured profile depth (m), thus providing the plant-available water storage capacity (θ_P) in $m^3\ m^{-2}$ (or m) integrated across the soil profile.

2.2.7 Climatological data

Climatological data were extracted from WorldClim Version 2.1 (released in January 2020). Initially, 19 bioclimatic variables (BIO1-BIO19) were obtained for each site (each variable's meaning can be seen at https://www.worldclim.org/data/bioclim.html). These variables represent the historical averages for the 1970 – 2000 period with 30 arc-seconds (~1 km^2) resolution (FICK; HIJMANS, 2017), with the current version providing a refined version of the previous WorldClim Version 1 database due to the increased number of meteorological stations over the past decade (FICK; HIJMANS, 2017). In this chapter, I use mean annual precipitation (BIO12, P_A) and mean annual temperature (BIO1, T_A).

An estimate of the long-term climatic water deficit (CWD) was also extracted from raster files for each study site. CWD represents the net balance between precipitation and potential evapotranspiration (ETP_0) in the driest months (i.e. months where ETP_0 exceeds rainfall, usually in mm a^{-1} (CWD is negative by definition) and was obtained from http://chave.ups-tlse.fr/pantropical_allometry.htm with 2.5 arc-minute resolution. For easier interpretation, I here use CWD with opposite positive signs (CWD_{adj}), where CWD_{adj} serves as a measure of the water deficit to which the vegetation is subjected. In addition, ETP_0 and the Global Aridity Index (AI) Version 3 were obtained from https://cgiarcsi.community/2019/01/24/global-aridity-index-and-potential-evapotranspiration-climate-database-v3/ with 30 arc-seconds resolution. The index represents the ratio between precipitation and potential evapotranspiration, with higher values representing more humid conditions (ZOMER; TRABUCCO, 2022). Site elevation was obtained from the Shuttle Radar Topography Mission (SRTM) data.

2.2.8 Data analysis

Data were first grouped into geologic affiliations (i.e. sedimentary – S_{SED}, crystalline – S_{CRY} and karst - S_{KAR}) and according to clay mineralogy (i.e. low-activity clays – S_{LAC}, High-activity clays – S_{HAC} and 'arenic' – S_{ARE}. As detailed in Section 1.6, Chapter 1, S_{HAC} soils are dominated by 2: 1 silicate clay minerals, with low to moderate weathering status, whereas S_{LAC}

soils are dominated by 1: 1 silicate clay minerals, with more advanced weathering. Thus, soils with less than 24 $cmol_c\ kg^{-1}$ CEC_{clay} were considered S_{HAC} (mainly associated with crystalline terrains of the Caatinga), whereas values below this threshold were considered S_{LAC} soils (mainly associated with sedimentary terrains of the Caatinga). Soils with predominant loamy sand texture or coarser were classified as S_{ARE} (typically Arenosols; mainly associated with sedimentary terrains of the Caatinga).

Subsequently, selected soil properties belonging to the above-mentioned geologic affiliations were compared through a non-parametric robust Kruskal-Wallis test (χ^2), followed by the Wilcoxon-Mann-Whitney rank-sum test with Benjamini-Hochberg (BH) correction for multiple comparisons.

Bivariate relationships amongst the studied soil properties were evaluated using Kendall's rank correlation coefficient (τ), with ordinary least squares (OLS) linear models used to evaluate potentially meaningful relationships at the entire dataset level, as well as considering soil geological affiliations separately. In a few cases, some data points were not considered in the regression analyses based on justifications as explained throughout the results session. Regression assumptions, i.e. normality of residuals and homoscedasticity, with logarithmical transformations used when necessary. The spatial independence of the residuals was also checked. Thus, the function *listw.candidates* function of the *adespatial* R package (DRAY et al., 2021) was used to generate spatial weighting matrices (SWC). When spatial structures were detected in model residuals, spatial filtering techniques were undertaken using Moran's Eigenvectors Maps (MEMs), which were introduced into the models to correct for spatial autocorrelations. All analyses refer to the upper 0.3 m mean values.

Soil $\delta^{15}N$ values were modelled using an OLS multiple linear regression approach. Initially, a series of climatic and edaphic candidate variables that could potentially account for variations in soil $\delta^{15}N$ were selected, *viz*. P_A, AI, ETP_0, ψ, T_A, $sand_f$, $clay_f$, I_E and all associated exchangeable cations, soil pH_{H20}, $[P]_T$, $[C]_T$ and soil C/N ratio. Aiming to facilitate the model's coefficients interpretation, predictor variables were standardised, i.e. the means of each variable were subtracted from individual observations and then divided by its standard deviation, thus providing comparative scores ('effect size') among predictors using the *caret* package (MAX et al., 2020). Subsequently, a global model expressed in Eqn. (2.7) was constructed for the subsequent steps:

$$\delta^{15}\mathrm{N} = \beta_0 + \beta_1 \mathrm{AI} + \beta_2 \mathrm{ETP}_0 + \beta_3 \psi + \beta_4 T_\mathrm{A} + \beta_5 \mathrm{clay_f} + \beta_6 I_\mathrm{E} + \beta_7 [\mathrm{P}]_\mathrm{T} + \beta_8 [\mathrm{C}]_\mathrm{T} + \beta_9 \mathrm{pH_{H20}} + \beta_{10} \mathrm{C/N} + \beta_{11} \mathrm{AI} \times \psi + \beta_{12} \mathrm{AI} \times \mathrm{sand_f} \quad \text{Eqn. (2.7)}$$

From the global model of Eqn. (2.7), all possible combinations among candidate variables (including interaction terms) were tested using the *dredge* function of the *MuMIn* package (BARTON; BARTON, 2021), with this process generating 121 unique models. Subsequently, an information-theoretic (I-T) approach was used to select those models with ΔAICc < 4, which retained only five models. Note that, despite some relatively high correlations existing between variables included in the global model of Eqn. (2.7), only Pearson's (| r | <0.6) variables were allowed to be included simultaneously in the same models, with the variance inflation factor (VIF) also being checked afterwards. Moreover, the maximum number of predictor variables included simultaneously in each model was set to three, thus controlling potential overfitting issues. Moreover, since P_A and AI showed a nearly perfect correlation (r = 0.97, p < 0.000), they were evaluated by replacing one for the other and comparing their performance in the model. Similarly, the replacement of I_E for alternative cations (or $\sum_\mathrm{B}$) and $\mathrm{sand_f}$ by $\mathrm{clay_f}$ was undertaken, with these attempts not justifying the inclusion of any of these alternative terms in the global model. Subsequently, the potential presence of spatial structures in the model's residuals (represented by the Global Moran's *I*) was checked in the selected models, with spatial filters (MEMs) being incorporated in those models showing spatially structured residuals. These procedures were comprehensively described by Bauman et al. (2018a) and Bauman et al. (2018b). After corrections, models were re-ranked according to their ΔAICc and Akaike weights (*W*). Subsequently, the model's predictions were extrapolated for the entire Caatinga region, with the best-ranked model including only climatic variables (i.e. AI and ψ). Attempting to identify additional sources of noise in predictions provided by Model 1, the dataset was categorised in terms of P_A classes assuming 'high P_A' > 0.8 m a^{-1} and 'low P_A' < 0.8 m a^{-1}, with a non-parametric robust Kruskal-Wallis test (χ^2) being undertaken to check differences in soil δ^{15}N values according to established P_A classes. OLS linear regressions were used to investigate the influence of soil pH, soil individual cations and composite indexes (i.e. $\sum_\mathrm{B}$ and I_E) on soil δ^{15}N values considering the established P_A classes. The map-modelled values of soil δ^{15}N for the Caatinga region were produced using functionalities of the *plyr*, *tidyverse*, *sf*, *geobr*, ggplot2, and *ggspatial* R packages. All graphs were produced with the *ggplot2* package (WICKHAM et al., 2021) and all analyses were performed in the environment R

version 4.1.1 (R CORE TEAM, 2021). The QGIS 3.16.10-Hannover was also used for geoprocessing and map tools.

2.3 Results

2.3.1 Cations availability and soil texture

The Kruskal-Wallis test revealed consistent differences in some of the studied soil properties associated with the three distinct geologic affiliations. Median values, interquartile ranges (IQR), and statistical comparisons of median values for all variables are shown in Table 2.2. For example, median values for $[Ca]_{ex}$ decreased following $S_{KAR} \geq S_{CRY} \geq S_{SED}$ ($p = 0.001$); median values for $[Mg]_{ex}$ decreased following $S_{KAR} = S_{CRY} \geq S_{SED}$ ($p = 0.005$); differences in the median values of $[K]_{ex}$ and $[Na]_{ex}$ were not significant at $p \leq 0.05$; medians for $[Al]_{ex}$ decreased following $S_{SED} \geq S_{KAR}$, $S_{SED} = S_{CRY}$, $S_{CRY} = S_{KAR}$, ($p = 0.028$). Proportions of soil bases in the sortive complex typically followed $[Ca]_{ex} \geq [Mg]_{ex} \geq [K]_{ex} \geq [Na]_{ex}$, with a few exceptions (Figure 2.2). The median values were comparably low for $[Na]_{ex}$ for all geologic affiliations (i.e. ≤ 1.0 $mmol_c$ kg^{-1}). Regardless of geologic affiliation, bases and aluminium contents, in general, showed opposite trends, i.e. when base concentrations were high, aluminium concentrations tended to be lower. Soil pH_{H2O} was strongly associated with both $[Al]_{ex}$ and $\sum_B$ [Figure 2.3; Kendall's $\tau = -0.63$ ($p = 0.000$) for $[Al]_{ex}$, and $\tau = 0.57$; ($p = 0.000$) for $\sum_B$], with soil pH_{H2O} decreasing markedly from $S_{KAR} \geq S_{CRY} \geq S_{SED}$ (Table 2.2, $p = 0.004$). Exchangeable aluminium concentrations in S_{KAR} sites and some S_{CRY} sites were virtually negligible and were found to be more pronounced in S_{SED} sites, with S_{CRY} sites showing relatively high values only in a few cases. Figure 2.2-b shows that, in general, effective base saturation was proportionately higher than aluminium saturation, even for soils with relatively higher [Al]ex contents.

Table 2.2: Selected soil properties compared among distinct geological affiliations (i.e. S_{SED} = sedimentary; S_{CRY} = crystalline; S_{KAR} = karst). Letters within lines represent significant differences at $p \leq 0.05$ detected through the Wilcoxon-Mann-Whitney rank-sum test with Benjamini-Hochberg (BH) correction for multiple comparisons. The absence of letters within lines indicates that there were no statistical differences. Kruskal-Wallis chi-squared (χ^2), *p-values*, median values and interquartile ranges (IQR) for each group are shown.

Variable	χ^2	*p*	S_{SED} (n=15)		S_{CRY} (n=11)		S_{KAR} (n=3)	
			Median	IQR	Median	IQR	Median	IQR
Availability of cations and soil reaction								
$[Ca]_{ex}$ ($mmol_c\ kg^{-1}$)	14.49	**0.001**	2.54 **c**	3.86	12.35 **b**	20.57	55.78 **a**	4.96
$[Mg]_{ex}$ ($mmol_c\ kg^{-1}$)	10.71	**0.005**	1.15 **b**	1.81	5.83 **a**	5.06	9.59 **a**	1.42
$[K]_{ex}$ ($mmol_c\ kg^{-1}$)	6.95	**0.031**	0.7	1.34	1.82	1.1	2.58	1.21
$[Na]_{ex}$ ($mmol_c\ kg^{-1}$)	4.79	0.091	0.25	0.27	0.47	0.49	0.27	0.36
$[Al]_{ex}$ ($mmol_c\ kg^{-1}$)	7.17	**0.028**	4.75 **a**	7.39	2.02 **ab**	5.62	0.09 **b**	0.4
$\sum_B$ ($mmol_c\ kg^{-1}$)	14.99	**0.001**	5.37 **c**	3.51	18.46 **b**	26.15	68.54 **a**	7.67
I_E ($mmol_c\ kg^{-1}$)	13.34	**0.001**	11.72 **c**	9.59	21.97 **b**	21.3	68.64 **a**	8.07
pH_{H2O}	11.19	**0.004**	4.51 **c**	0.43	5.47 **b**	1.29	7.77 **a**	0.2
BS%	10.6	**0.005**	53.94 **b**	30.03	87.6 **a**	33.37	99.86 **a**	0.48
m%	10.6	**0.005**	46.06 **a**	30.03	12.4 **b**	33.37	0.14 **b**	0.48
Carbon and nitrogen								
$[C]_T$ ($mg\ g^{-1}$)	4.09	0.129	11.38	9.01	9.55	4.84	16.75	4.01
$[N]_T$ ($mg\ g^{-1}$)	6.17	**0.046**	0.92 **ab**	0.51	0.87 **b**	0.38	1.55 **a**	0.22
C/N ratio	2.45	0.293	12.13	3.10	11.44	1.95	9.38	2.64
Soil $\delta^{15}N$ (‰)	1.27	0.539	8.82	7.38	8.27	2.98	11.11	1.25
Phosphorus								
$[P]_T$	7.8	**0.020**	101.3 **b**	104.22	148.38 **b**	86.05	468.56 **a**	416.79
Weathering metrics								
$\sum_{RB}$ ($mmol_c\ kg^{-1}$)	12.81	**0.002**	60.66 **c**	74.73	176.27 **b**	51.17	377.76 **a**	1043.73
$[Fe]_T$ (g kg-1)	4.66	0.097	42.64	63.44	44.56	30.26	105.4	62.06
$[Zn]_T$ (mg kg-1)	9.28	**0.010**	60 **b**	68	128 **b**	48	268 **a**	78
$[Mn]_T$ (mg kg-1)	9.22	**0.010**	412 **b**	234	912 **b**	932	2684 **a**	226
XRF K/Zr	19.94	**0.000**	6.18 **b**	10.65	40.77 **a**	35.82	73.19 **a**	21.19
XRF Ca/K	3.80	**0.149**	0.28	0.47	0.23	0.20	0.32	0.44
Water availability								
$W\theta_v$ ($m^3\ m^{-3}$)	5.26	**0.072**	0.10	0.06	0.12	0.03	0.20	0.05
θ_P ($m^3\ m^{-2}$)	0.37	0.832	0.13	0.11	0.12	0.01	0.11	0.01

$[X]_{ex}$ = concentration exchangeable cation inside the brackets; $\sum_B$ soil sum of bases; I_E = effective cation; pH_{H2O} = water-measured soil pH; BS% = base saturation; m% = aluminium saturation; $[C]_T$ = soil total carbon concentration; $[N]_T$ soil total nitrogen concentration; C/N ration = soil carbon to nitrogen ratio; soil $\delta^{15}N$ = the ratio between the two N stable isotopes (^{15}N: ^{14}N) in the soil; $\sum_{RB}$ = total reserve bases; $[Fe]_T$ = total iron concentration; $[Zn]_T$ = total zinc concentration; $[Mn]_T$ = total manganese concentration; XRF K/Zr = X-ray fluorescence measured potassium to zircon ratio; XRF Ca/K = X-ray fluorescence measured calcium to potassium ratio; $W\theta_v$ = weighted volumetric soil water content weighted across soil profiles; θ_P = maximum plant-available soil water.

Figure 2.2-b also shows that slight increases in soil pH_{H2O} are associated with marked changes in the dominance of bases or aluminium in the soil sortive complex and, when soil pH_{H2O} approaches 6.0, $[Al]_{ex}$ levels are negligible.

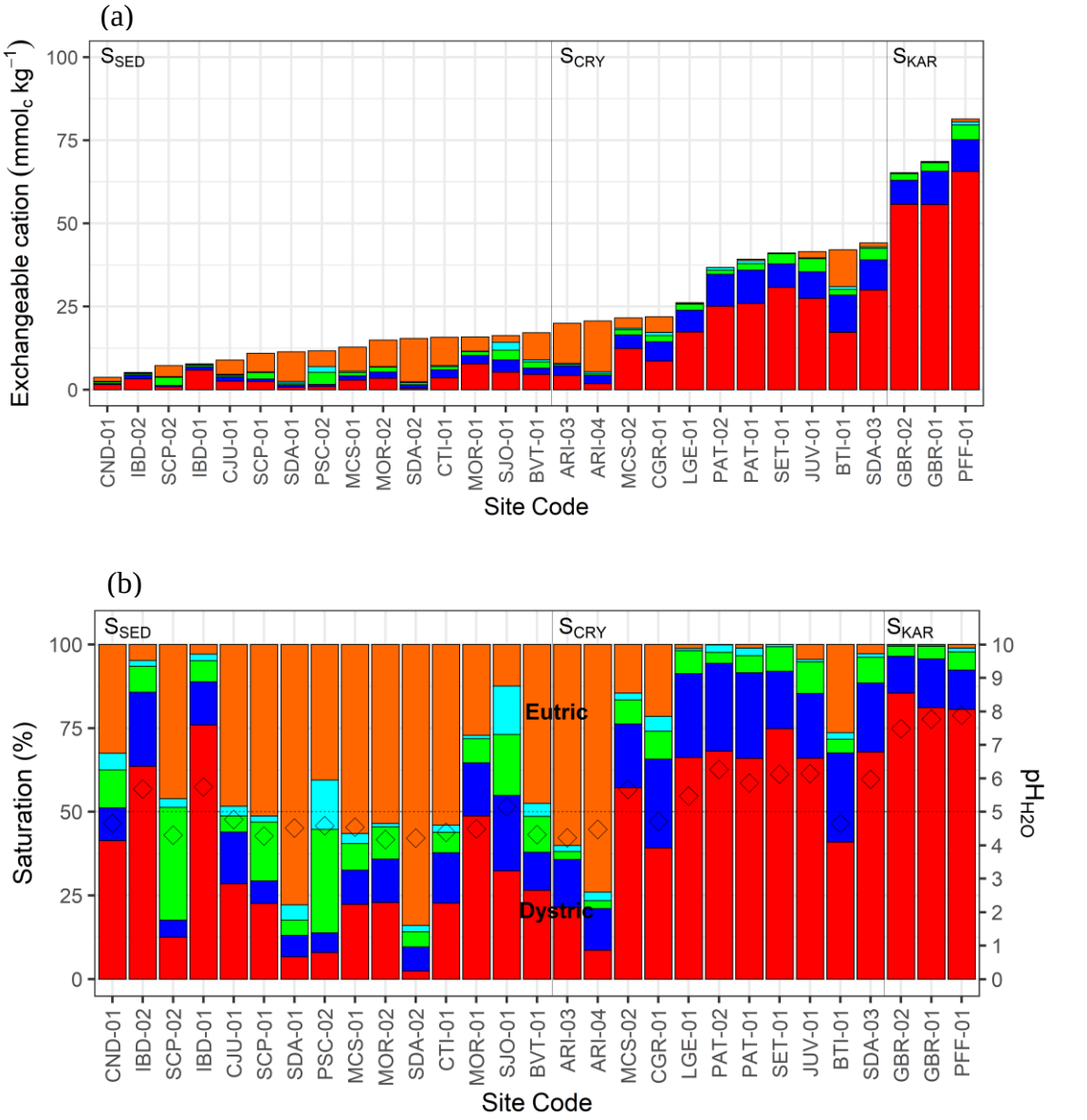

Figure 2.2. a) Contents of main exchangeable cations according to soil geological affiliations [sedimentary (S_{SED}); crystalline (S_{CRY}) and karst (S_{KAR})]; b) AgTU measured soil bases (BS%) and aluminium saturation (m%) and soil pH. In both cases, study sites are ordered according to increasing effective cation exchange capacity. In Figure 2.2-b, soils with BS% greater than 50% refer to the 'Eutric' qualifier, whereas soils with BS% lower than 50% relate the 'Dystric' qualifier. Note: 'Eutric' and 'Distric' qualifiers are usually used for diagnostic subsurficial horizons and here was used for the soil upper 0.3 m layer only for differentiation purposes.

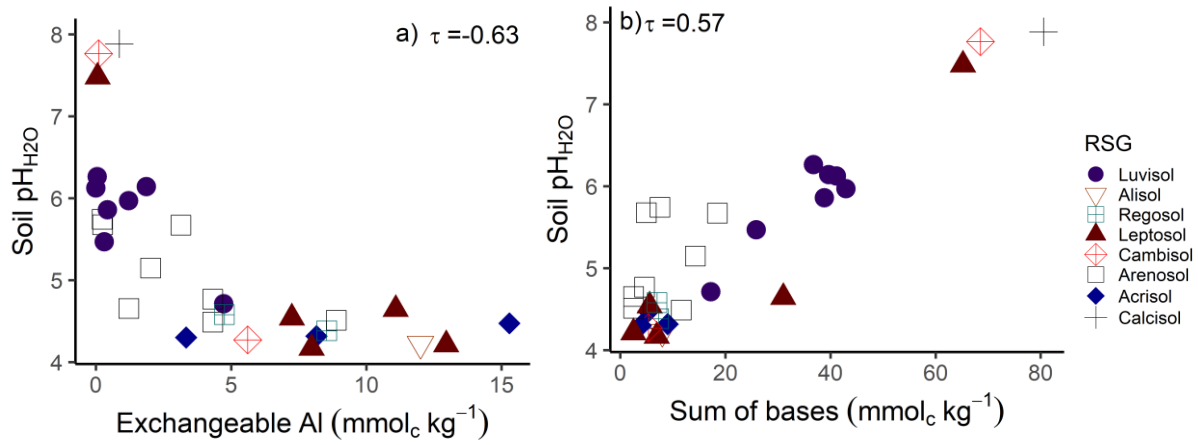

Figure 2.3. a) Water-measured soil pH and exchangeable aluminium – $[Al]_{ex}$; b) Water-measured soil pH and soil sum of bases ($\sum_B$). RSGs are shown.

The relative proportion of individual soil cations is further illustrated in Figure 2.4, where $[Ca]_{ex}$ appears as the bulk of I_E for most study soils. Although $[Al]_{ex}$ accounts for the higher proportion of I_E in a few soils, neither $[Mg]_{ex}$ nor $[K]_{ex}$ and even less $[Na]_{ex}$ correlates with I_E as $[Ca]_{ex}$ does, with a simple linear regression showing that $[Ca]_{ex}$ accounts for 94% (r^2 = 0.94; $p < 0.000$) of the variance in I_E (Figure 2.4). As regards the composite indexes $\sum_B$ and I_E, median values decreased in both cases from $S_{KAR} \geq S_{CRY} \geq S_{SED}$ (Table 2.2, p = 0.001 and p = 0.001, respectively), with S_{KAR} values being ca. three-fold higher than S_{CRY} sites and even higher relative to S_{SED} sites. Two S_{SED} sites (BTI-01 and JUV-01) had significantly higher cation contents compared to other S_{SED} sites. Base saturation was close to 100% for S_{KAR} sites but also high for S_{CRY} sites (median = 88%) and significantly lower for S_{SED} sites (median = 54%, p = 0.005). Conversely, aluminium saturation decreased from $S_{SED} \geq S_{CRY} = S_{KAR}$ (p = 0.005), with S_{KAR} showing negligible values.

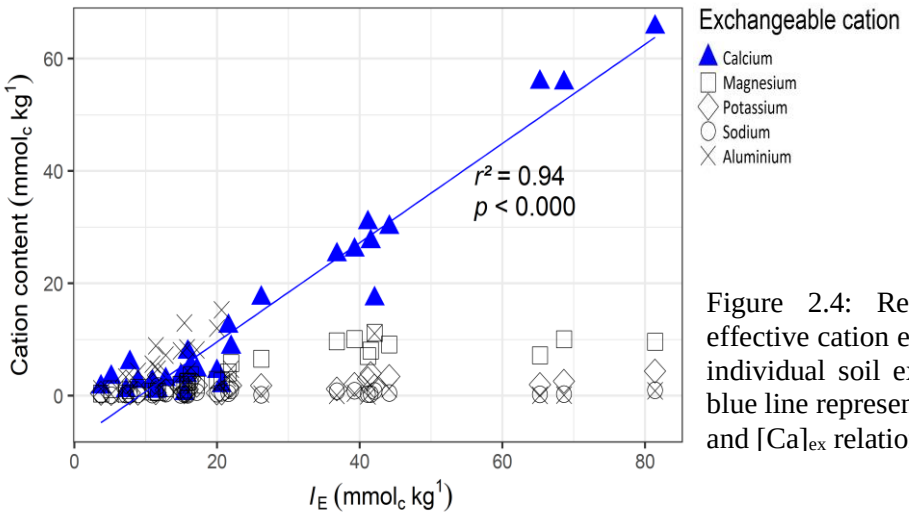

Figure 2.4: Relationship between soil effective cation exchange capacity (I_E) and individual soil exchangeable cations. The blue line represents a linear model fit for I_E and $[Ca]_{ex}$ relationship.

Regarding soil texture, and except for S_{KAR} sites, the majority of soil samples analysed for particle size distribution fell into the 'Sandy Loam' class or coarser, as shown in the USDA textural triangle of Figure 2.5.

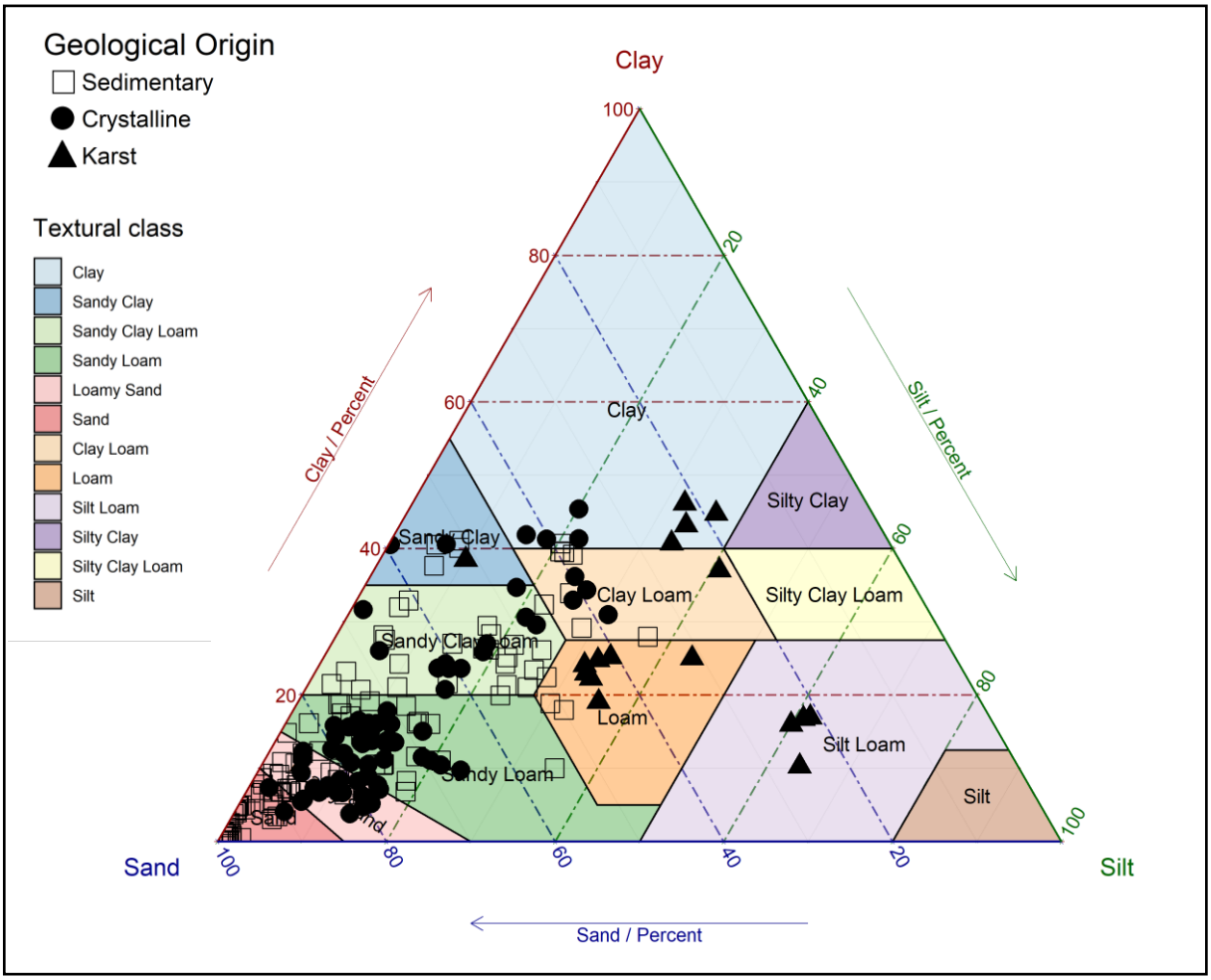

Figure 2.5: Textural classes of soil samples from 29 profiles distributed in the Caatinga region. Samples were discriminated according to their geological affiliations.

Regarding the tested bivariate relationships, all three textural fractions (that is, $sand_f$, $silt_f$, and $clay_f$) accounted for variations in I_E at the whole data set level and at the S_{SED} sites, while only $silt_f$ was associated with I_E at the S_{CRY} sites (Table 2.3, Figure 2.6). In addition, XRF measured Fe_2O_3 and Al_2O_3 also appeared as reasonable predictors of I_E in the entire dataset (Table 2.3-a) as well as both S_{CRY} and S_{SED} separately (Figure 2.6). For the lowest AICc model (Al_2O_3 only), when Al_2O_3 is equal to its dataset average (8.03%), the model predicts that I_E = 19.49 $mmol_c\ kg^{-1}$ (geometric mean) calculated by $I_E = \exp(\beta_0 = 2.970)$. The model also predicts that I_E increases by ca. 19% for every 1% increase in Al_2O_3 since $\exp(\beta_1 = 0.172)$. Considering the second-best AICc-ranked predictor, for each 10% increase in $sand_f$, I_E should increase by

27% in a proportional sense since exp($\beta_1 \times 10 = -0.31$). A similar interpretation can be taken for all I_E predictors in Table 2.3.

Table 2.3: Pairwise relationships between selected soil properties at the full sampling level. Predictors have been centred so that intercept (β_0) reflects predicted response variables when predictors are at their means and slope (β_1) represents increases in response variables as predictors increases by one unit. Units: $sand_f$, $silt_f$ and $clay_f$, Fe_2O_3 and AlO_3 in %; Mean annual temperature (T_A) in °C; Mean annual precipitation (P_A) in m; $[C]_T$ in mg g^{-1}; $[N]_T$ in dag kg^{-1}; $[P]_T$ in mg kg^{-1}; I_E and $\sum_{RB}$ in $mmol_c$ kg^{-1}; $[Fe]_T$ in g kg^{-1}; $[Zn]_T$ and $[Mn]_T$ in mg kg^{-1}, C/N; K/Zr and Ca/K unitless.

	x	y	$S_{SED} + S_{CRY} + S_{KAR}$				
			β_0	β_1	r^2_{adj}	p	AICc
a)	$sand_f$	$\ln(I_E)$	2.970	-0.031	0.60	**0.000**	45.74
	$silt_f$	$\ln(I_E)$	2.970	0.045	0.56	**0.000**	48.54
	$clay_f$	$\ln(I_E)$	2.970	0.048	0.29	**0.001**	62.19
	Fe_2O_3	$\ln(I_E)$	2.970	0.382	0.48	**0.000**	53.38
	Al_2O_3	$\ln(I_E)$	2.970	0.172	0.60	**0.000**	45.63
b)	Fe_2O_3	$[P]_T$	142.606	61.094	0.83	**0.000**	288.9
	Al_2O_3	$[P]_T$	142.606	17.521	0.43	**0.000**	315.5
	CaO	$\ln[P]_T$	4.723	1.003	0.12	**0.040**	-
	SOC	$\ln[P]_T$	4.723	0.034	0.03	0.191	-
	$sand_f$	$[P]_T$	142.607	-4.859	0.63	**0.000**	305.6
	$silt_f$	$[P]_T$	142.606	8.552	0.75	**0.000**	301.8
	$clay_f$	$[P]_T$	142.606	6.990	0.39	**0.002**	319.0
c)	$sand_f$	$\ln[C]_T$	2.270	-0.019	0.32	**0.001**	39.6
	$silt_f$	$\ln[C]_T$	2.270	0.020	0.19	**0.011**	44.2
	$clay_f$	$\ln[C]_T$	2.270	0.038	0.25	**0.004**	42.2
	T_A	$\ln[C]_T$	2.270	-0.052	-0.01	0.370	50.4
	P_A	$\ln[C]_T$	2.270	0.533	0.00	0.302	50.1
	Fe_2O_3	$\ln[C]_T$	2.270	0.188	0.16	**0.019**	45.2
	Al_2O_3	$\ln[C]_T$	2.270	0.060	0.11	**0.051**	47.1
d)	T_A	$\ln[N]_T$	2.153	-0.025	-0.03	0.652	48.2
	P_A	$\ln[N]_T$	2.153	0.371	-0.02	0.452	47.8
	I_E	$\ln[N]_T$	2.153	0.014	0.20	**0.010**	41.2
	$[P]_T$	$\ln[N]_T$	2.153	0.001	0.15	**0.024**	42.9
	SOC	$\ln[N]_T$	2.153	0.080	0.77	**0.000**	6.3
e)	T_A	ln(C/N)	2.432	-0.028	0.05	0.141	-12.8
	P_A	ln(C/N)	2.432	0.169	0.00	0.325	-11.5
f)	$silt_f$	ln(TRB)	4.794	0.061	0.71	**0.000**	-
	$\sum_{RB}$	$\ln[Fe]_T$	3.805	0.001	0.19	**0.010**	-
	$\sum_{RB}$	$\ln[Zn]_T$	4.628	0.001	0.24	**0.004**	-
	$\sum_{RB}$	$\ln[Mn]_T$	6.358	0.001	0.20	**0.009**	-
	$\sum_{RB}$	ln(K/Zr)	2.837	0.001	0.08	0.070	-
	$\sum_{RB}$	ln(Ca/K)	1.103	0.001	0.06	0.099	-
	$\sum_{RB}$	$[P]_T$	142.607	0.688	0.57	**0.000**	-
	I_E	$[P]_T$	142.607	4.614	0.69	**0.000**	-

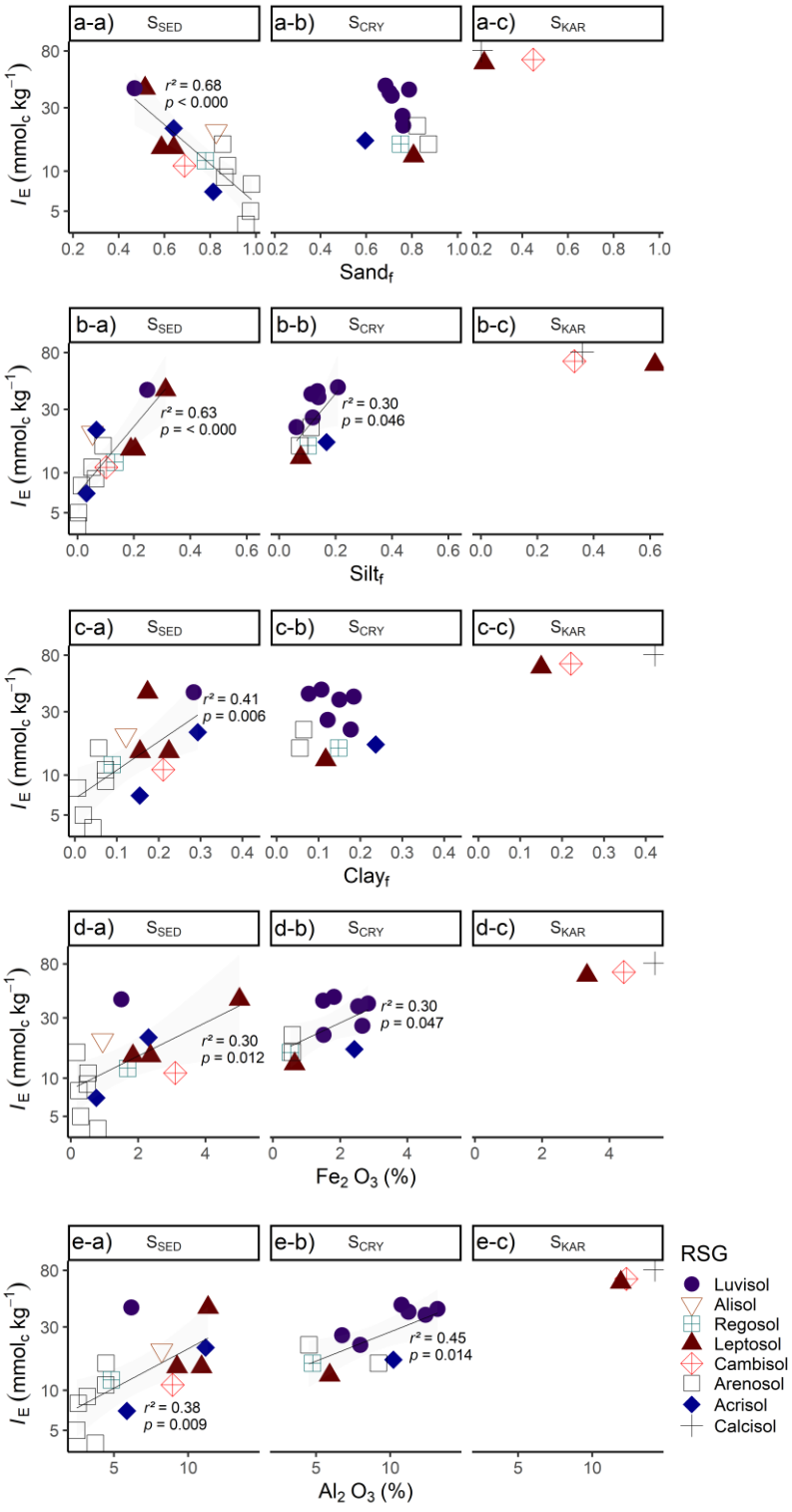

Figure 2.6: Soil effective cation exchange capacity (I_E), soil texture ($sand_f$, $silt_f$ and $clay_f$) and total XRF measured Fe_2O_3 and Al_2O_3 relationships (a, b, c, d and e, respectively). Study soils have been discriminated according to their respective geological affiliation (i.e. S_{SED}, S_{CRY} and S_{KAR}) across panels. Note that *y-axis* is in log10 scale.

Main soil base cations availability was modelled as a function of the total reservoir of bases ($\sum_{RB}$) and soil pH_{H2O} (Figure 2.7 and Table 2.4). It is noteworthy that considering $\sum_{RB}$ and pH_{H2O} individually, the predictive power was relatively high ($r^2 = 0.60$; $p < 0.001$ for pH_{H2O} and $r^2 = 0.70$; $p < 0.001$ for $\sum_{RB}$). However, when $\sum_{RB}$ and pH_{H2O} were included interactively in the model, the model accounted for 94% of the variation in the sum of bases. As predictors were centred at their means and scaled by their standard deviations (SD), Table 2.4 shows that holding all predictors at their dataset averages, modelled $\sum_{B}$ was 17.62 $mmol_c\ kg^{-1}$ and an increase of 1 SD in $\sum_{RB}$ (i.e. 113.72 $mmol_c\ kg^{-1}$) representing an increase of 8.81 $mmol_c\ kg^{-1}$ in $\sum_{B}$.

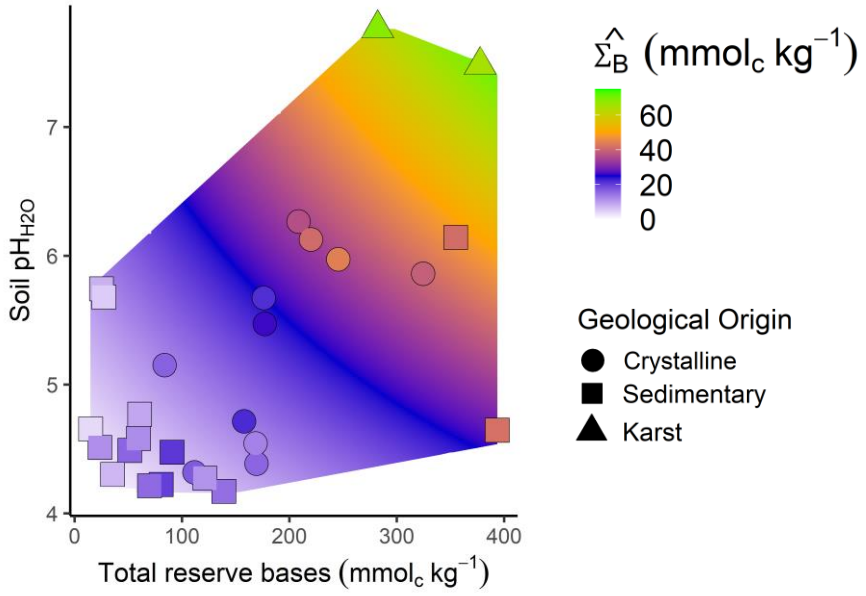

Figure 2.7: Predicted soil sum of bases ($\sum_{B}$) as a function of total reserve bases ($\sum_{RB}$) and soil pH_{H2O}. Field measured $\sum_{B}$ overlain their respective $\sum_{RB}$ × pH_{H2O} environment. Geological affiliation is represented.

Table 2.4: Regression metrics relating soil sum of bases ($\sum_{B}$) to soil total reserve bases ($\sum_{RB}$) and water-measured soil pH. Predictor variables have been centred at their means and scaled by their SD so as intercept reflects $\sum_{B}$ values when all variables are at their means and predictors β coefficients represent changes in $\sum_{B}$ values as predictors increase one SD. Regression residues were free of spatial structure issues. Variance inflation factor (VIF) and corrected Akaike Information Criterion (AICc) are also shown.

$\sum_{B:}$ $r^2 = 0.94$; $p < 0.000$; AICc = 175.73					
	Standardised coefficients				
	β	t	p	SD	VIF
Intercept	17.63	16.0	< 0.000	1.10	-
pH_{H2O}	9.88	7.6	< 0.000	1.16	1.56
$\sum_{RB}$	8.81	7.3	< 0.000	1.35	2.14
$pH_{H2O} \times \sum_{RB}$	2.54	2.4	0.027	1.08	1.69

The model also predicts that an increase of 0.98 in soil pH_{H2O} leads to an increase of 9.88 $mmol_c\ kg^{-1}$ in $\sum_B$. Regarding the interactive effect of $\sum_{RB} \times pH_{H2O}$, it can be seen that, at a similar total reserve of bases, soil pH exerts a major influence on the concentration of the exchangeable bases (Figure 2.7). For example, when $\sum_{RB} \approx 300\ mmol_c\ kg^{-1}$, the model predicts $\sum_B = 20.85\ mmol_c\ kg^{-1}$ when soil pH_{H2O} 4.91, whereas, at the same $\sum_{RB} \approx 300\ mmol_c\ kg^{-1}$, the model predicts $\sum_B = 52.68\ mmol_c\ kg^{-1}$ when soil $pH_{H2O} = 6.91$. The field-measured values largely correspond to the modelled responses, and a clear distinction can be seen in the $\sum_{RB} \times pH_{H2O}$ environmental space of S_{SED}, S_{CRY} and S_{KAR} sites (Figure 2.7).

2.3.2 Phosphorus

Soil $[P]_T$ contents ranged from 15 $mg\ kg^{-1}$ in CJU-01 (Hyperdystric Arenosol) to 1194 $mg\ kg^{-1}$ in GBR-02 (Hypereutric Calcaric Lithic Leptosol) (Figure 2.8), with median values decreasing from $S_{KAR} \geq S_{CRY} = S_{SED}$ ($p = 0.02$; Table 2.2). Regarding OLS relationships exploring the associations between selected soil attributes and soil $[P]_T$ (Table 2.3-d), there was a strong association between $[P]_T$ and Fe_2O_3 (XRF-measured), with an increase of 1% in Fe_2O_3 accounting for an increase of 61.1 $mg\ kg^{-1}$ in soil $[P]_T$. To a lower degree, Al_2O_3 and (even lower) CaO were also related to soil $[P]_T$ at the entire dataset level (Table 2.3-b). These relationships were partially maintained across soil geologic affiliations (Figure 2.9), with Al_2O_3 predicting $[P]_T$ in both S_{SED} and S_{CRY} with similar predictive ability, but with Fe_2O_3 only significant in predicting $[P]_T$ of S_{SED} soils ($r^2 = 0.71$; $p = 0.000$). The XRF CaO was associated with $[P]_T$ only for the S_{CRY} sites ($r^2 = 0.55$; $p = 0.005$). All S_{SED} had virtually negligible Ca whereas unusually high CaO content (2.50%) was found in a Calcisol in PFF-01 (S_{KAR}).

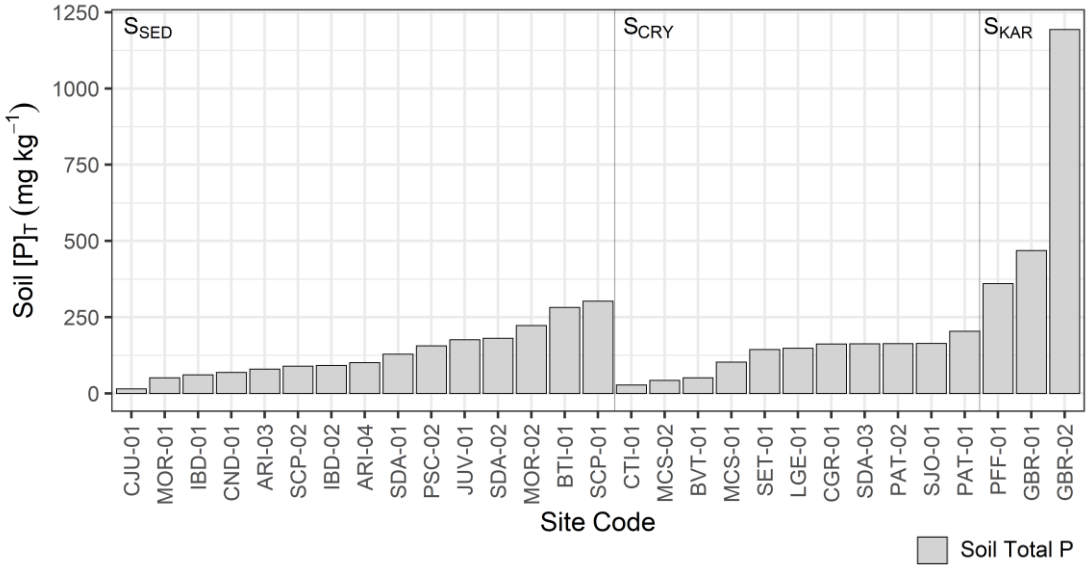

Figure 2.8: Total soil phosphorus concentrations. Sites are ordered according to increasing $[P]_T$ within each geological affiliation (S_{SED} = sedimentary; S_{CRY} = crystalline; S_{KAR} = karst).

Regarding soil texture effects, $sand_f$, $clay_f$ and $silt_f$ were all related to soil $[P]_T$ at the entire dataset level, with $silt_f$ showing the strongest relationship with $[P]_T$ ($r^2 = 0.75$; $p < 0.001$) and the model predicts an increase of 85 mg kg^{-1} for every 10% increase in the $silt_f$ content. Relationships between soil texture and $[P]_T$, however, were maintained only for S_{SED} sites (Figure 2.9-e, f, g).

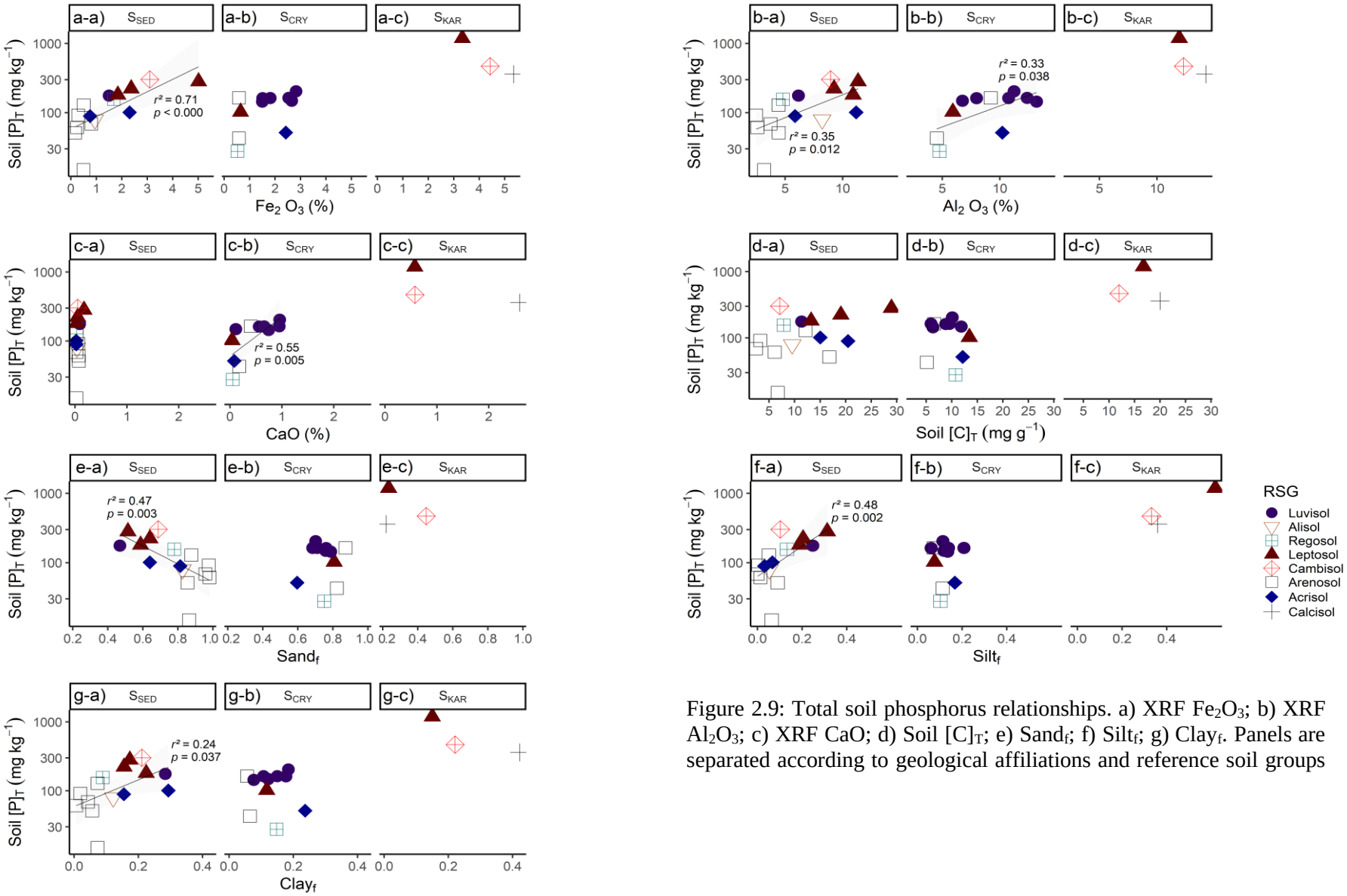

Figure 2.9: Total soil phosphorus relationships. a) XRF Fe_2O_3; b) XRF Al_2O_3; c) XRF CaO; d) Soil $[C]_T$; e) $Sand_f$; f) $Silt_f$; g) $Clay_f$. Panels are separated according to geological affiliations and reference soil groups

2.3.3 Soil C, N, C/N and soil $\delta^{15}N$

Differences in $[C]_T$ contents among geologically distinct soils were not significant at $p \leq 0.05$ (Table 2.2), with the median values of 16.75 mg g^{-1}; 11.38 mg g^{-1} and 9.01 mg g^{-1} for $S_{KAR,}$ S_{SED} and S_{CRY}, respectively (Table 2.2; Figure 2.10). Soil $[N]_T$ contents were, however, significantly higher for S_{KAR} than for S_{CRY} sites, but equal to S_{SED} sites, with median values were 1.55 mg g^{-1}; 0.87 mg g^{-1} and 0.92 mg g^{-1} for $S_{KAR,}$ S_{CRY} and $S_{SED,}$ respectively (Table 2.2). Differences in soil C/N were not significant at $p \leq 0.05$ among the studied groups, with median values equal to 12, 11, and 9 for S_{SED}, S_{CRY}, S_{KAR}, respectively (Table 2.2). With regards to soil nitrogen isotopic composition, $\delta^{15}N$ tended to be slightly higher for S_{KAR} sites than for S_{CRY} and S_{SED} sites (median values were 11.11‰, 8.82‰ and 8.27‰ for S_{KAR}, S_{SED} and S_{CRY}, respectively), but these differences were not significant at $p \leq 0.05$ (Table 2.2).

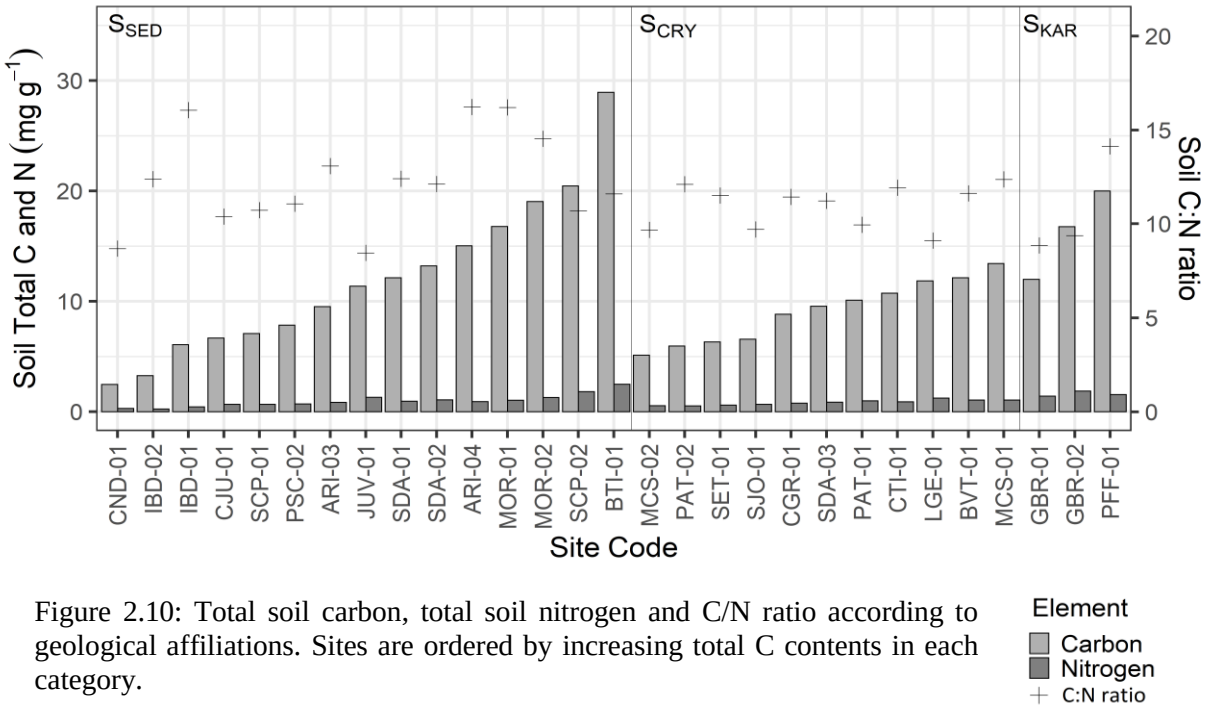

Figure 2.10: Total soil carbon, total soil nitrogen and C/N ratio according to geological affiliations. Sites are ordered by increasing total C contents in each category.

Across the entire dataset level, $sand_f$ showed the best ability to predict $[C]_T$ ($r^2 = 0.32$; $p = 0.001$; AICc = 39.6; Table 2.3-c). As $\exp(\beta_1 \times 10) = (-0.019 \times 10) = 0.83$, the model predicts a proportional reduction of 17% for every 10% increase in $sand_f$. According to AICc values, better $[C]_T$ predictions can be achieved in the following order: $sand_f > clay_f > silt_f > Fe_2O_3 > Al_2O_3$. All these relationships were maintained for S_{SED} sites, where $sand_f$ was again the best predictor ($r^2 = 0.37$; $p = 0.00$; Figure 2.11).

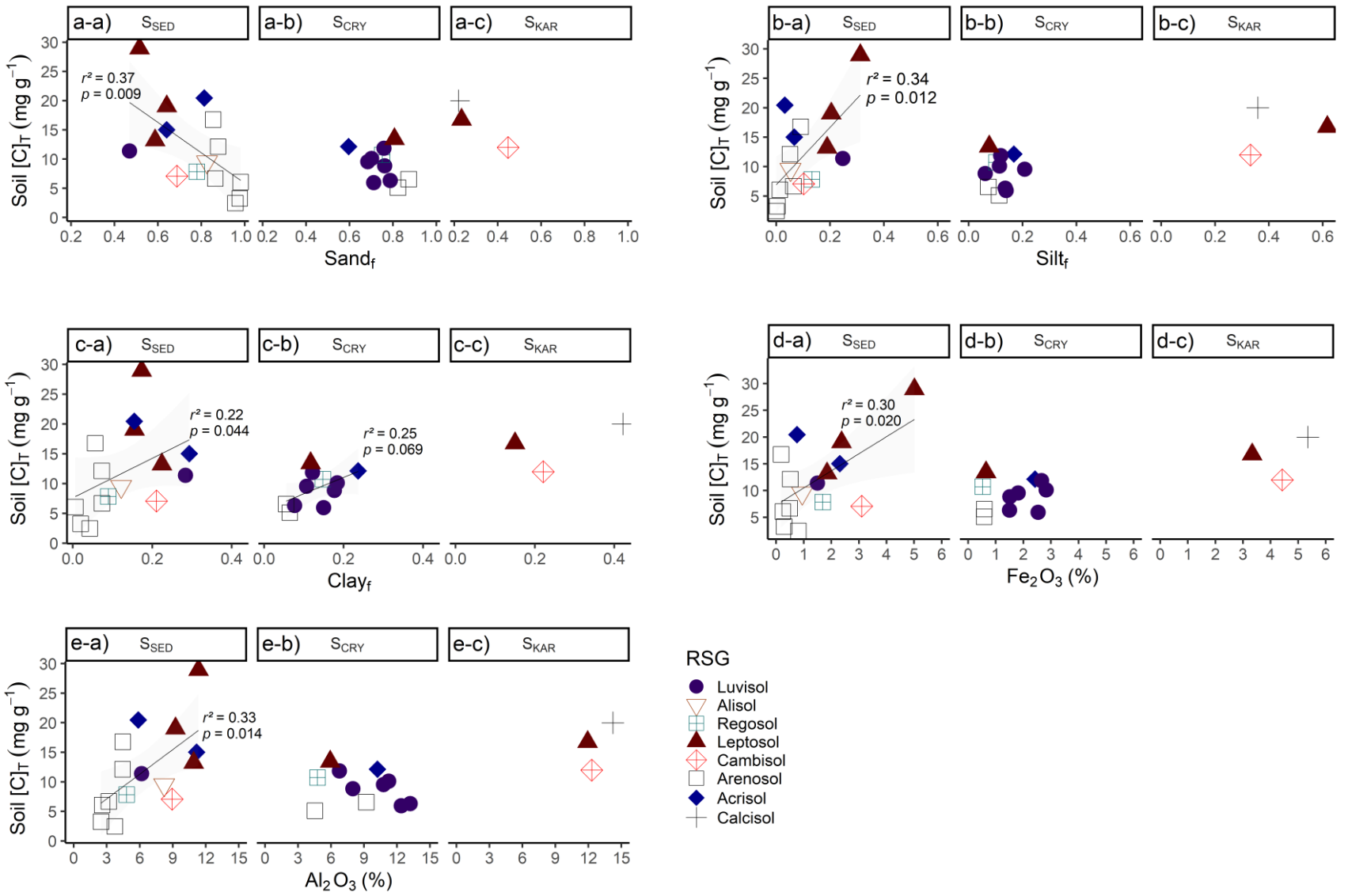

Figure 2.11: Total soil carbon relationships. a) sand fraction; b) silt fraction; c) clay fraction; d) XRF Fe_2O_3 and e) XRF Al_2O_3. Panels are separated according to geological affiliations and reference soil groups (RSG) are shown. Significant OLS regression lines at $p \leq 0.05$ are shown within each panel.

Both soil $[P]_T$ and I_E were associated with $[N]_T$ concentrations when the full dataset was analysed (Table 2.3-d). The relationship was slightly stronger for I_E (r^2 = 0.20; p = 0.010) compared to $[P]_T$ (r^2 = 0.15; p = 0.024). Both relationships remained present considering only S_{SED} sites (Figure 2.12). Also for the case of the S_{SED} sites, the relationship was stronger for I_E (r^2 = 0.40; p = 0.007) compared to $[P]_T$ (r^2 = 0.16; p = 0.074).

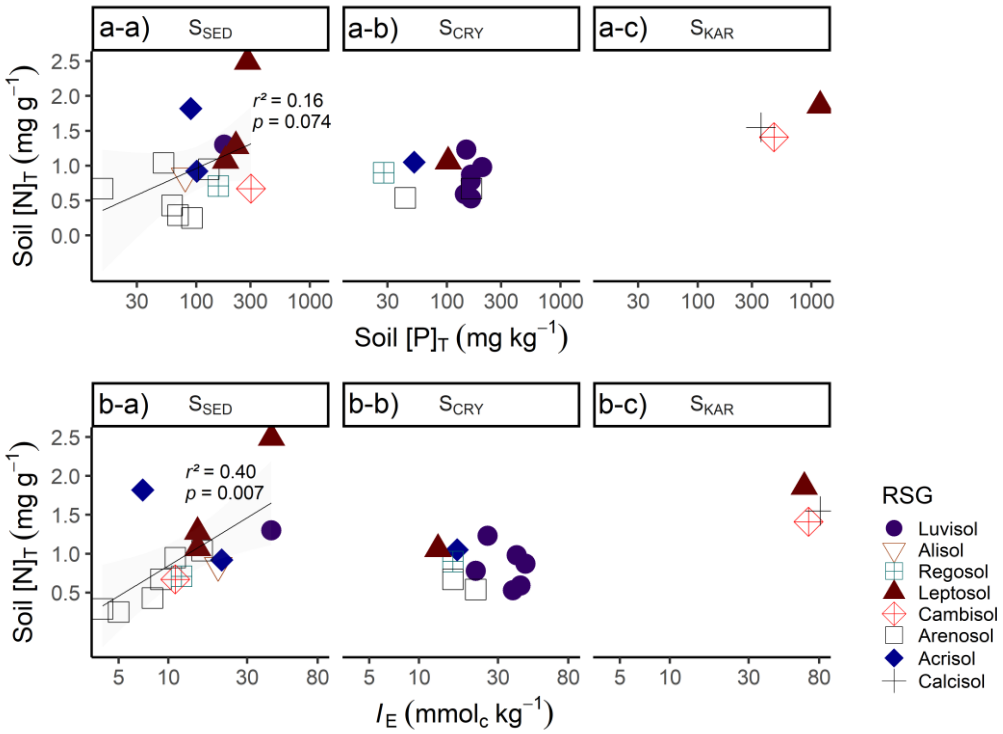

Figure 2.12: a) Relationship between soil total N and soil total P; b) relationship between soil total N and I_E. Panels are separated according to geological affiliations and reference soil groups (RSG) are shown.

Climatic parameters (i.e. P_A and T_A) were not related to $[C]_T$, $[N]_T$ and soil C/N ratio at the entire dataset level (Table 2.3-c,d,e). Nevertheless, an additional analysis considering the 0.9 percentile showed a negative relationship between T_A and $[C]_T$ (r^2 = 0.26; p = 0.005; Figure 2.13). Such exclusion of the upper 0.9 quantile omitted PFF-01, SCP-02 and BTI-01 from the analysis, which is justified by the likely confounding presence of pedogenic carbon ($CaCO_3$) in PFF-01 as well as the unusually high values of $[C]_T$ measured in BTI-01 and SCP-02 (28.94 and 20.46 mg g^{-1}, respectively). The 0.9 percentile filtered data set was also used to test the same relationships across the soil geological classes, with T_A showing a negative influence on both $[C]_T$ and $[N]_T$. The relationship was stronger for $[C]_T$ (r^2 = 0.49; p = 0.004) compared to $[N]_T$ (r^2 = 0.23; p = 0.055) (Figure 2.13). Climatic parameters (i.e. P_A and T_A) were not significantly related to C/N ratios at $p \leq 0.05$ (Table 2.3-e).

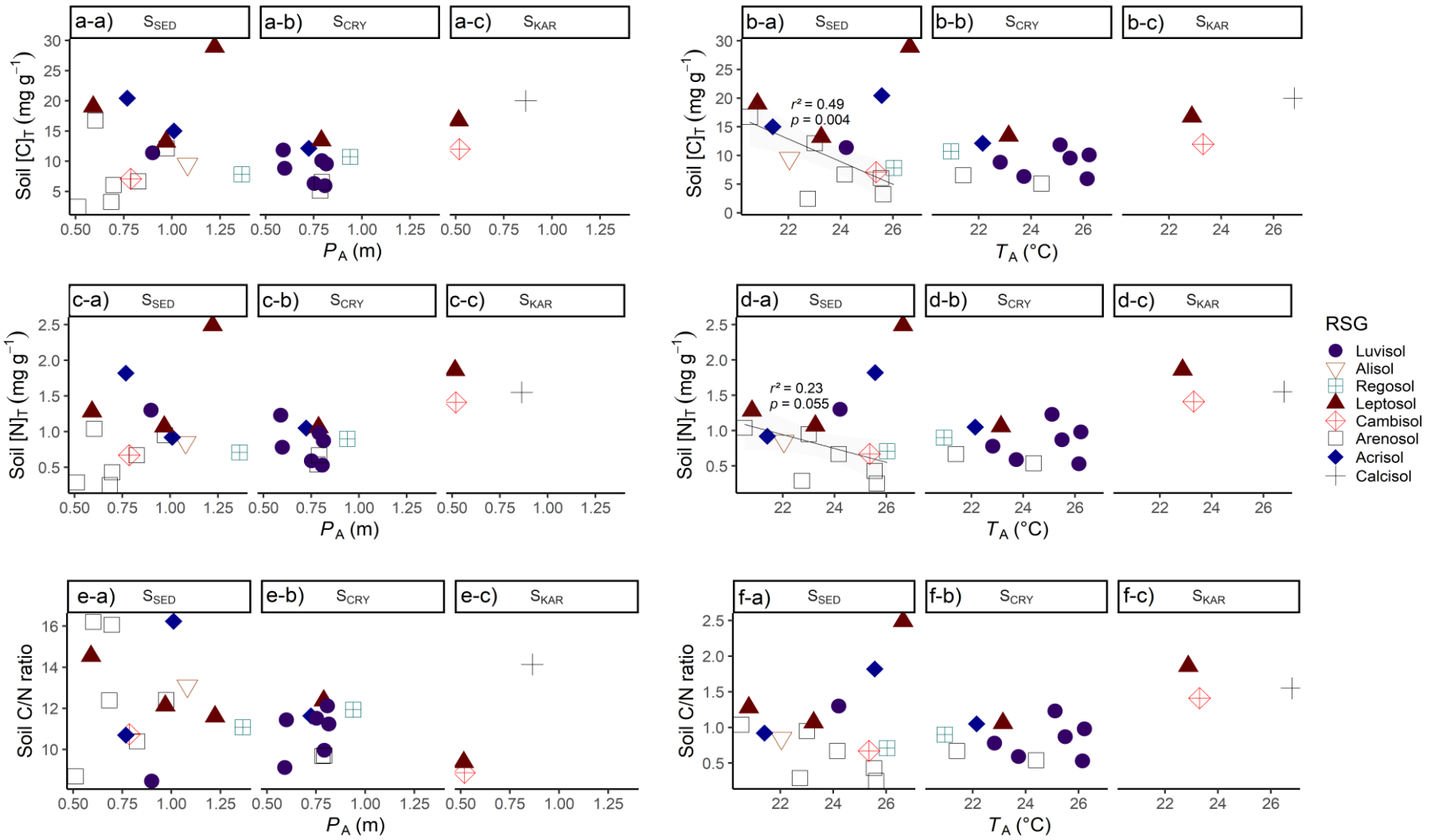

Figure 2.13: Effects of P_A and T_A on $[C]_T$ (a-b), $[N]_T$ (c-d) and soil C/N ratio (e-f). Regression lines refer to 0.9 quantile OLS linear regressions. Panels are separated according to geological affiliations and RSG are shown.

Regarding the relationships between soil $\delta^{15}N$ and selected climatic and edaphic predictors, only climatic predictors had significant relationships with soil $\delta^{15}N$ at the entire data set levels. After required spatial correction for models' residuals, the predictive power decreased following ψ (r^2 = 0.74; p < 0.000; AICc = 128.80) > P_A (r^2 = 0.72; p < 0.000; AICc = 131.51) > AI (r^2 = 0.69; p < 0.000; AICc = 133.83). No edaphic variables, even after spatial correction, were significant at $p \leq 0.05$. A similar trend was found for S_{SED} and S_{CRY} evaluated separately (Figure 2.14).

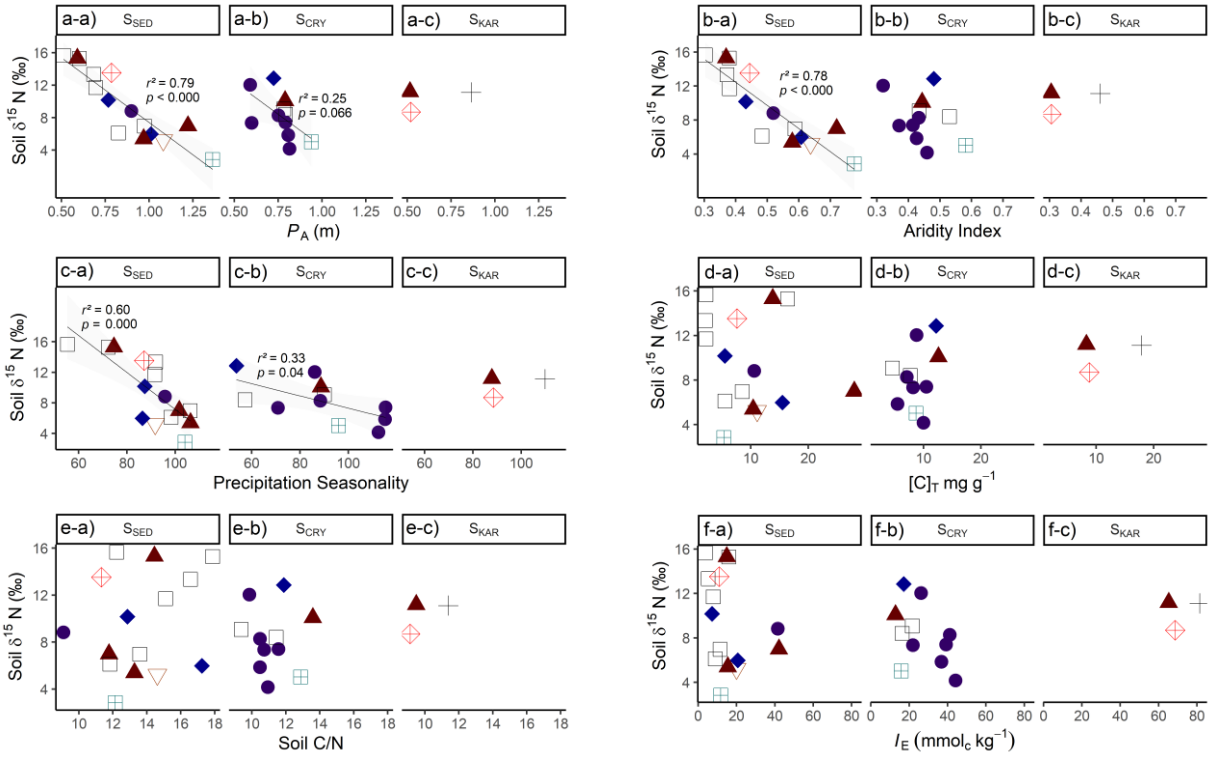

Figure 2.14: Potential edaphic and climatic predictors of soil $\delta^{15}N$. a) Mean annual precipitation (P_A); b) aridity index (AI); c) precipitation seasonality (ψ); d) Soil total carbon $[C]_T$; e) Soil C/N ratio; f) Effective cation exchange capacity (I_E). Panels are separated according to geological affiliations (S_{SED} = sedimentary; S_{CRY} = crystalline and S_{KAR} = karst) and reference soil groups (RSG) are shown.

Results from the OLS multiple linear regression modelling (Table 2.5), however, suggest a slightly different picture, with some edaphic variables (i.e. $[C]_T$, C/N ratio and I_E) also included in the ΔAICc < 4 range. A purely climatic model was better ranked in terms of AICc, i.e., after spatial correction for models' residuals, the best-ranked model retained only AI and ψ (r^2 = 0.81; p < 0.000; AICc = 122.0). Standardised coefficients were -1.882 and -1.657 for ψ and AI, respectively. Additional information and model metrics are provided in Table 2.5.

Table 2.5: Best AICc-ranked models accounting for variations in soil $\delta^{15}N$ values of Caatinga. Model intercept (β_0) and standardised regression coefficients are shown: AI = aridity index; P_A = mean annual precipitation; ψ = precipitation seasonality; $[C]_T$ = soil total carbon; C/N = soil C/N ratio; I_E = effective cation exchange capacity; pH_{H2O} = water-measured soil pH. Selected spatial filters, i.e. Moran Eigenvector Maps (MEMs) were incorporated into models with spatially structured residues. Predictor variables have been centred at their means and scaled by their SD so that the intercept reflects soil $\delta^{15}N$ values when all variables are at their means and predictors coefficients represent changes in units of soil $\delta^{15}N$ values as predictors variables increase by one SD. Note that models 1,2 and 4 correspond to corrected versions (for residual spatial structures) of models 8, 7 and 9, respectively. AICc = Corrected Akaike Information Criterion; W = Akaike weights; I = Global Moran's I. Letter a) includes models with ΔAICc < 4, whereas 'b)' includes models with ΔAICc > 4. Significant Moran's I at $p \leq 0.05$ are shown in bold.

Model		β_0	AI	P_A	ψ	$[C]_T$	C/N	I_E	AI x ψ	MEM11	MEM7	MEM1	MEM12	R^2_{adj}	p	AICc	ΔAICc	W	I
a)	1	9.133	-1.657	-	-1.882	-	-	-	-	1.290	-0.752	-0.686	-0.670	0.81	< 0.000	122.0	0	0.42	-0.06
	2	9.133	-1.983	-	-1.978	0.707	-	-	-	1.317	-0.694	-0.687	-	0.81	< 0.000	122.2	0.28	0.37	0.15
	3	9.133	-	-1.749	-1.557	-	-	-	-	1.329	-0.818	-0.668	-0.748	0.80	<0.000	124.1	2.09	0.15	0.04
	4	8.954	-1.854	-	-1.862	-	-	-	0.566	1.298	-0.783	-0.673	-	0.79	< 0.000	125.8	3.86	0.06	-0.06
b)	5	9.133	-2.106	-	-1.306	-	0.896	-	-	-	-	-	-	0.63	< 0.000	135.5	13.50	0.00	0.37
	6	9.133	-3.257	-	-	1.673	-	-1.633	-	-	-	-	-	0.61	< 0.000	136.5	14.57	0.00	-0.06
	7	9.133	-2.188	-	-1.474	0.795	-	-	-	-	-	-	-	0.61	< 0.000	136.8	14.87	0.00	**0.58**
	8	9.133	-1.887	-	-1.492	-	-	-	-	-	-	-	-	0.58	< 0.000	137.3	15.31	0.00	**0.56**
	9	8.947	-2.008	-	1.385	-	-	-	0.589	-	-	-	-	0.58	< 0.000	139.0	17.04	0.00	**0.48**

Nevertheless, the second-best model takes into account ψ, AI and $[C]_T$ (r^2 = 0.81; p < 0.000; AICc 122.2), also showing a low ΔAICc (0.28 in the scale of information). This provides evidence that $[C]_T$ is likely to account for variations in soil $\delta^{15}N$ values of the studied soils. Any other models including alternative edaphic variables (i.e. I_E and C/N ratio) had ΔAICc > 2 units relative to the first two best-ranked models, thus being considered less likely to reflect the reality. Also of note is that a version of the best-ranked model replacing AI for P_A yielded a worse model in terms of AICc (124.1), supporting the inclusion of the former rather than the latter. Figure 2.15 shows measured soil $\delta^{15}N$ versus model simulated $\delta^{15}N$ values using the parameters of Model 1 (r^2 = 0.81; p < 0.000; AICc = 122.0).

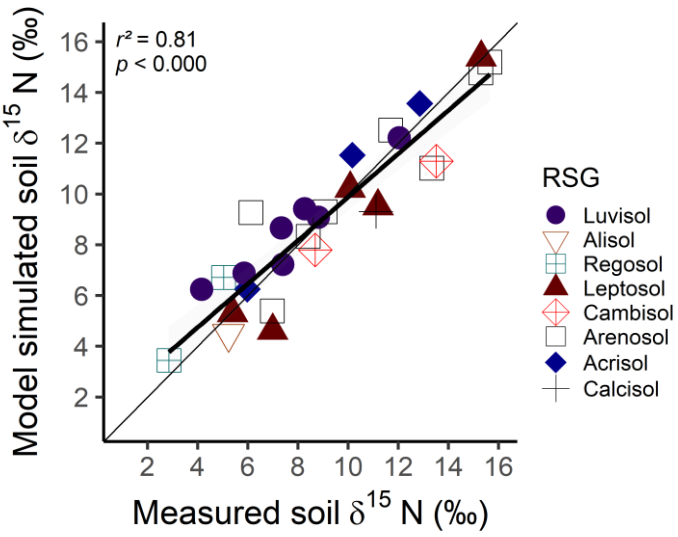

Figure 2.15: Measured soil δ ^{15}N values *versus* model simulated soil δ ^{15}N values. The coarser line represents the model fit and the thinner line is the 1: 1 line. Reference soil groups are shown.

Subsequently, coefficients of Model 1 (Table 2.5) were used to produce map-modelled responses. Figure 2.16, therefore, shows soil $\delta^{15}N$ map-modelled responses extrapolated for the entire Caatinga region. In Figure 2.16, field-measured $\delta^{15}N$ values overlain modelled responses values with reasonable accuracy.

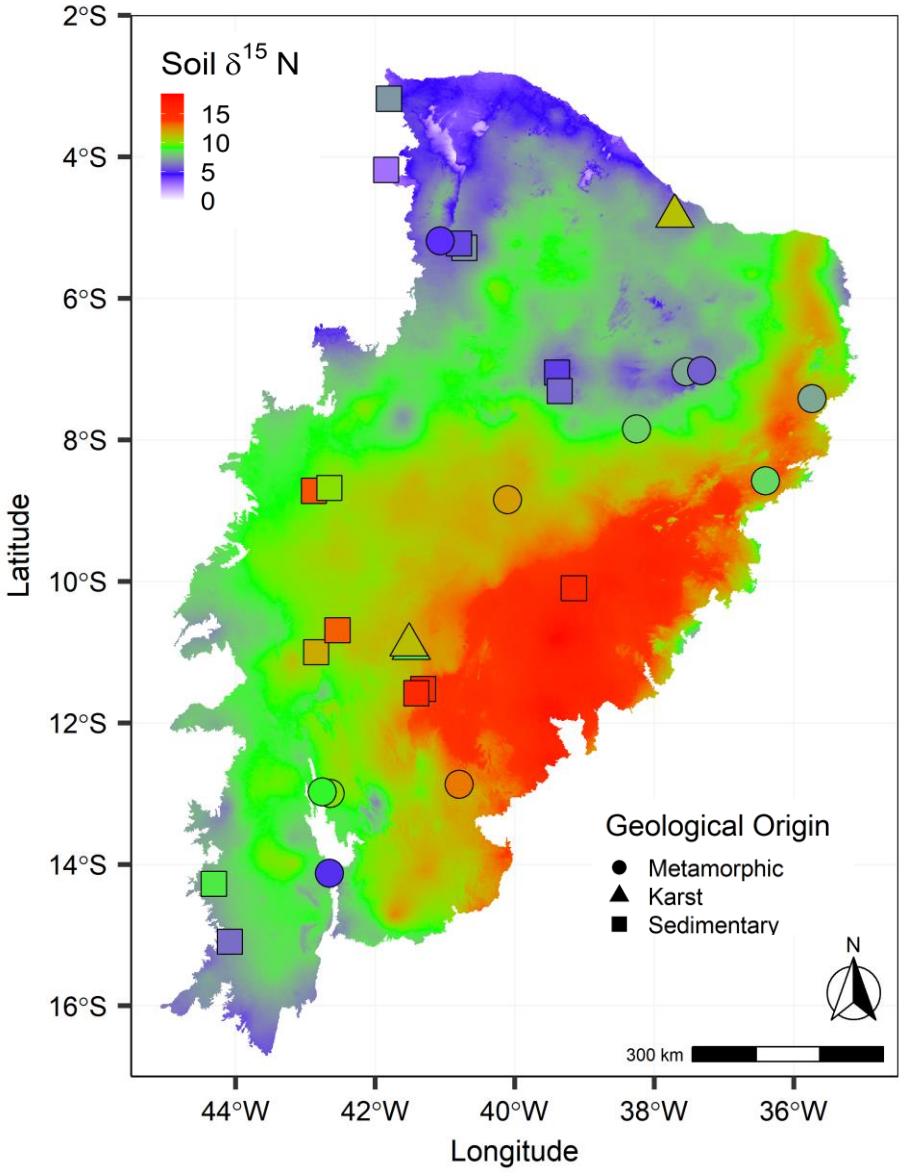

Figure 2.16: Model simulated soil $\delta^{15}N$ values for the Caatinga region. Soil measured $\delta^{15}N$ values overlain their respective geographical space. Modelled responses obtained with spatially explicit variables included in the Model 1 (Table 2.5): Soil $\delta^{15}N$ = 9.133 -1.657*AI -1.882*ψ. Model metrics: R^2_{adj} = 0.81; p < 0.001; AICc = 122.00; W = 0.42; Global Moran's I = -0.06 after residual spatial correction.

Finally, a comparison between $\delta^{15}N$ values in soils under high and low P_A (i.e. > 0.8 m a^{-1} and < 0.8 m a^{-1}) has shown that soil $\delta^{15}N$ values were lower in the drier former (Figure 2.17-a; χ^2 = 15.53; p < 0.000). An OLS linear regression model showed that, within the high-P_A category, effective cation exchange capacity (I_E) explained 44% of the variance in soil $\delta^{15}N$ values (Figure 2.17-b; r^2 = 0.44; p < 0.000), whereas in the drier category, I_E was not associated with soil $\delta^{15}N$ values. In Figure 2.17, labels correspond to S_{KAR} sites (PFF-01, GBR-01 and GBR-02).

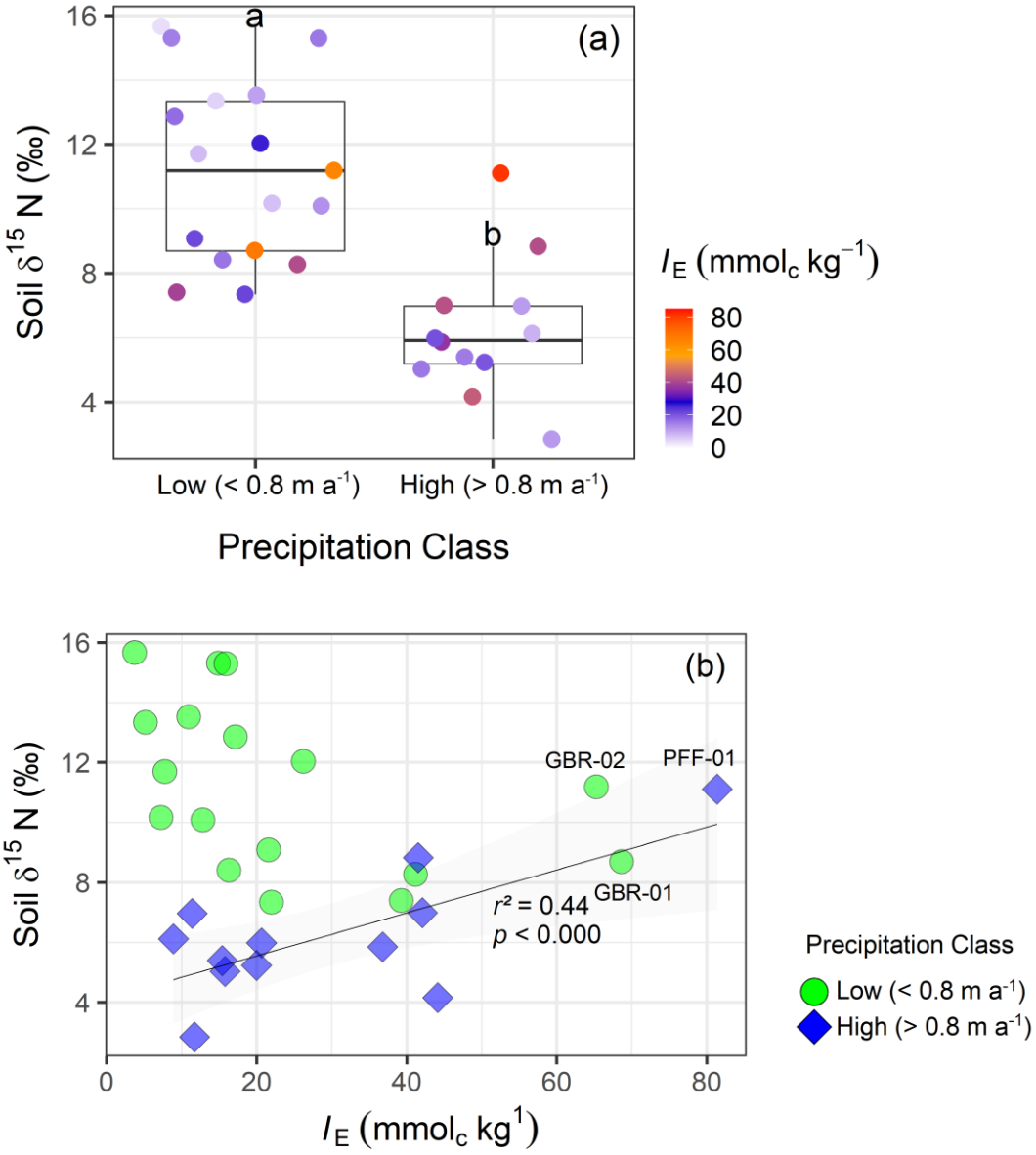

Figure 2.17: a) Soil $\delta^{15}N$ values according to low (< 0.8 m a^{-1}) and high (> 0.8 m a^{-1}) precipitation classes and effective cation exchange capacity (I_E). Letters associated with boxplots represent significant differences (at $p \leq 0.05$) detected through a Kruskal-Wallis test (χ^2); b) Soil $\delta^{15}N$ values according to I_E under high and low precipitation levels. Regression line represents an OLS linear model fit where $\delta^{15}N = 4.120 + I_E*0.813$. Regression's residuals met normality at $p \leq 0.05$ and were free of spatial structures (Moran's $I = -0.06$; $p = 0.55$). Labels indicate S_{KAR} sites.

2.3.4 Weathering metrics

Significant differences in soil total reserve bases ($\sum_{RB}$) were evident among soils of different geologic affiliations, with $\sum_{RB}$ sharply decreasing for $S_{KAR} \geq S_{CRY} \geq S_{SED}$ ($p = 0.002$), with median values of 377.76, 176.27 and 60.66 $mmol_c\ kg^{-1}$, respectively (Table 2.2). Both $[Zn]_T$ and $[Mn]_T$ median values decreased following $S_{KAR} \geq S_{CRY} = S_{SED}$ ($p = 0.01$ for both cases). Median values for $[Zn]_T$ were 268, 128 and 60 mg kg^{-1} for S_{KAR}, S_{CRY} and S_{SED}, respectively (Table 2.2). Median values for $[Mn]_T$ were 2684, 912 and 412 mg kg^{-1} for S_{KAR}, S_{CRY} and S_{SED}, respectively (Table 2.2). Differences in $[Fe]_T$ were not significant at $p \leq 0.05$, with median values of 42.64, 44.56 and 105.4 g kg^{-1} for S_{SED}, S_{CRY} and S_{KAR}, respectively (Table 2.2). Median values for the K/Zr elemental ratio decreased from $S_{KAR} = S_{CRY} \geq S_{SED,}$ ($p = 0.000$), with median values of 6.18, 40.77 and 73.19 for S_{SED}, S_{CRY} and S_{KAR}, respectively (Table 2.2). Finally, differences in the Ca/K ratio, taken here as an indication of the current proportion of weathering products of plagioclases to K-feldspars primary mineral were not significant at $p \leq 0.05$, with median values of 0.28, 0.23 and 0.32 for S_{SED}, S_{CRY} and S_{KAR}, respectively (Table 2.2).

Similarly to previous soil properties, differences in weathering-associated key properties among soils of distinct geologic affiliations were verified with potentially meaningful OLS models investigated for both the entire dataset level as well S_{SED}, S_{CRY} and S_{KAR} separately. For example, OLS fits have shown that $silt_f$ was strongly associated with $\sum_{RB}$ levels at the entire dataset level ($r^2 = 0.71$; $p = 0.000$), with an increase of 10% in $silt_f$, representing a proportional increase of 84% $\sum_{RB}$. This relationship was even stronger for S_{SED} sites ($r^2 = 0.91$; $p < 0.000$; Figure 2.18-a), where the model predicts that an increase of 10% in $silt_f$ is associated with a proportional increase of 141% in $\sum_{RB}$ levels. Increases in $\sum_{RB}$ levels represented relatively small but significant increases in $[Fe]_T$, $[Zn]_T$, and $[Mn]_T$ levels (regression metrics Table 2.3-f), but these relationships were maintained only for S_{SED} for $[Fe]_T$ and $[Zn]_T$ cases and only for S_{CRY} soils for the $[Mn]_T$ case (Figure 2.18-d). Total reserve base levels were not associated with XRF-analysed K/Zr and Ca/K elemental ratios, despite being marginally significant (Table 2.3-f). Considering only S_{SED}, however, K/Zr increased reasonably with increasing $\sum_{RB}$ ($r^2 = 0.28$; $p = 0.024$; Figure 2.19-e; function not shown). Finally, $[P]_T$ was associated with both $\sum_{RB}$ ($r^2 = 0.69$; $p = 0.000$) and I_E ($r^2 = 0.57$; $p = 0.000$). Relationships involving weathering metrics were more evident at the entire dataset level than considering geological affiliations separately.

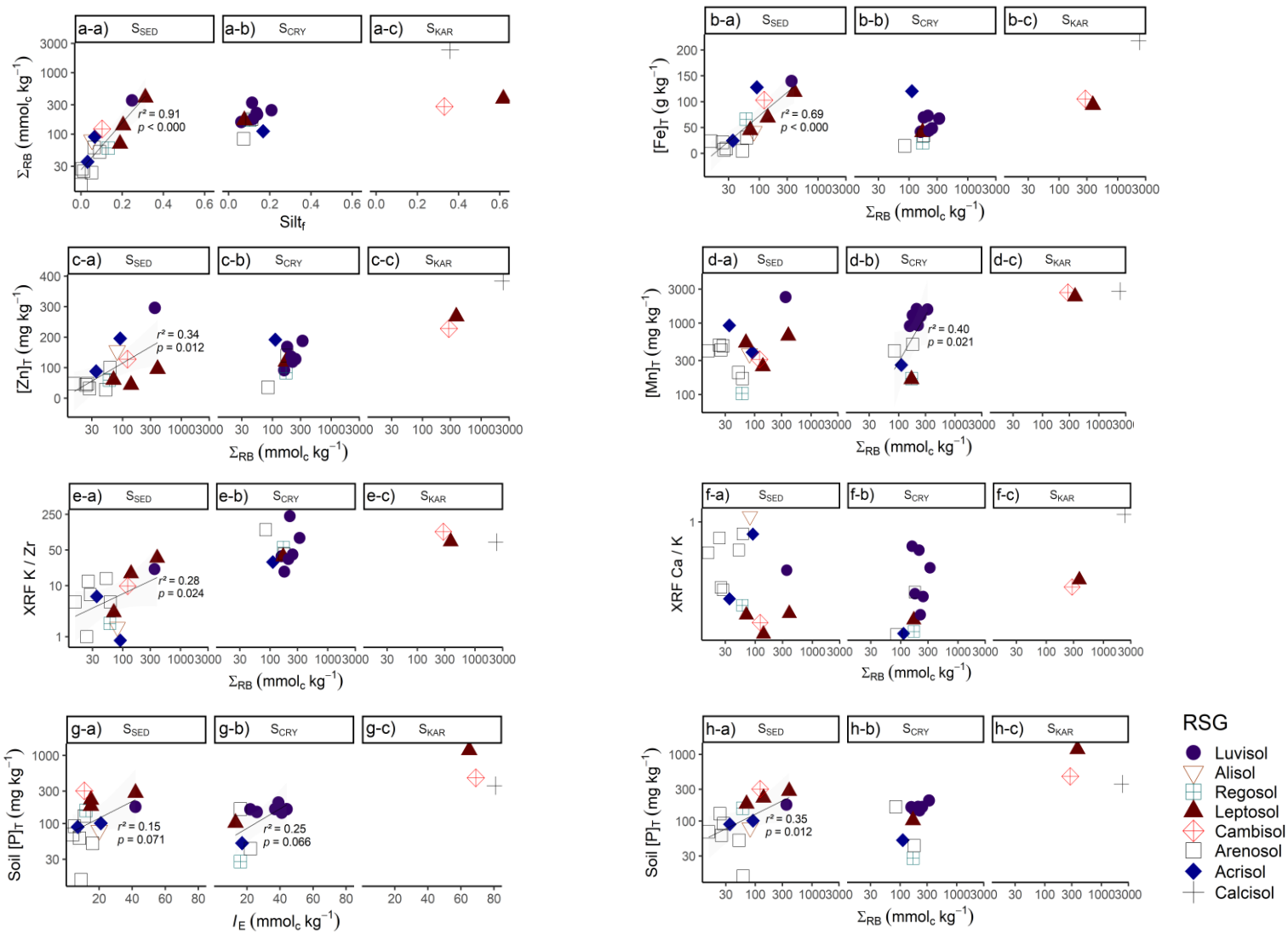

Figure 2.18: Weathering-associated relationships. a) Soil $silt_f$ and total reserve bases ($\sum_{RB}$); b) $\sum_{RB}$ and $[Fe]_T$; c) $\sum_{RB}$ and $[Zn]_T$; d) $\sum_{RB}$ and $[Zn]_T$; e) $\sum_{RB}$ and XRF K/Zr); f) $\sum_{RB}$ and XRF Ca/K); g) $\sum_{RB}$ and I_E; h) $\sum_{RB}$ and $[P]_T$. R-squared, *p-values* and regression lines are shown for significant relationships at $p \leq 0.05$, along with 0.95 confidence interval bands. Panels are separated according to geological affiliations and reference soil groups (RSG) are shown.

2.3.5 Soil morphology, effective rooting depth (R_{EF}) and water availability

Maximum measured soil and effective rooting depths are shown in Figure 2.19. As expected, there was a marked tendency for deeper soils at the S_{SED} sites rather than their S_{CRY} and S_{KAR} counterparts. The effective rooting depth, however, was considerably variable in all S_{CRY}, S_{SED} and S_{KAR} categories, i.e. in some cases, roots generally occupied all exploitable profiles and, in other cases, it was concentrated in the upper soil layers (regardless of the soil total depth). Moreover, R_{EF} did not show systematic variations among RSGs, suggesting that soil types are not a sensible surrogate to predict predicting R_{EF} in Caatinga soils, at least for the profiles studied.

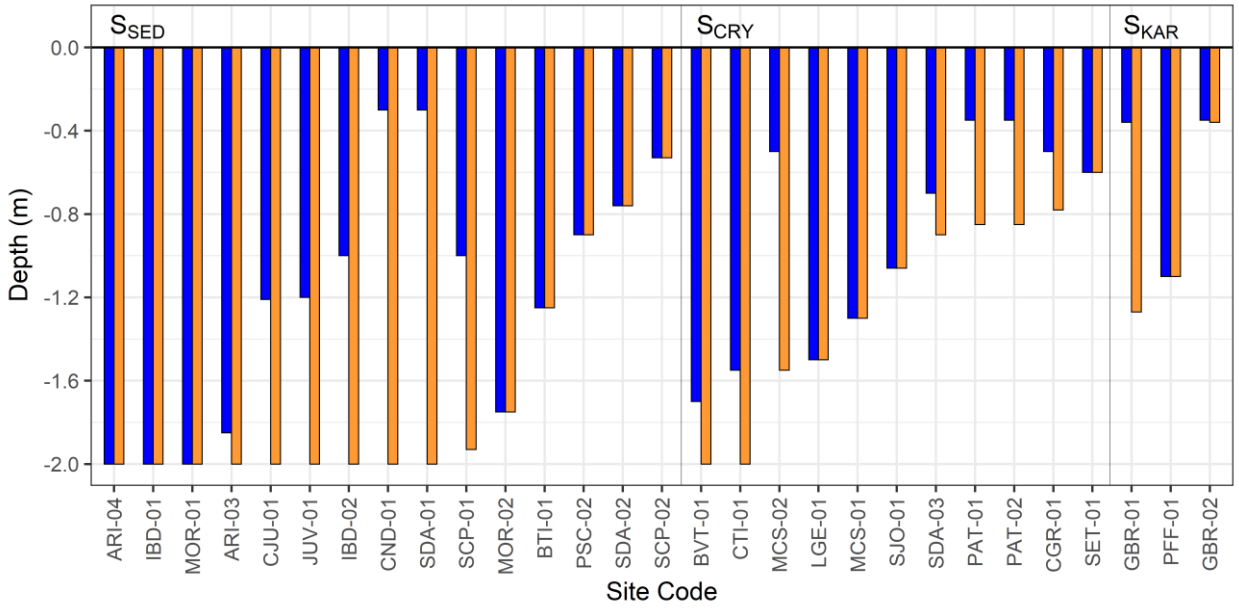

Figure 2.19: Maximum measured soil depth and maximum measured effective rooting depth (R_{EF}) for each studied site. Study sites are ordered according to maximum measured soil depth within each geologic category [Sedimentary (S_{SED}); Crystalline (S_{CRY}) and Karst (S_{KAR})]. The '0.0 horizontal line' correspond to the soil surface.

Furthermore, R_{EF} did not appear to be related to soil bases or aluminium, soil bulk density or soil texture. Rather, Figure 2.20, suggests a climatic control on R_{EF}. Here, data have been categorised into 'restrictive' soil profiles for root growth, i.e. presence of impervious layers (e.g. bedrock; saprolites) within the 2 m from the soil surface and 'non-restrictive', i.e. absence of impervious layers within the upper 2 m from the soil surface. For the latter, a simple linear regression model showed that CWD_{adj} accounted for a substantial component of the variation in R_{EF} ($r^2 = 0.25$; $p = 0.065$) in the non-restrictive group. Considering the 0.9 quantile data [i.e. excluding two semideciduous forests (ARI-03 and ARI-04), and IBD-01, a loose

dune], the predictive power of CWD_{adj} to account for differences R_{EF} increased significantly (r^2 = 0.56; p = 0.020; Figure 2.20).

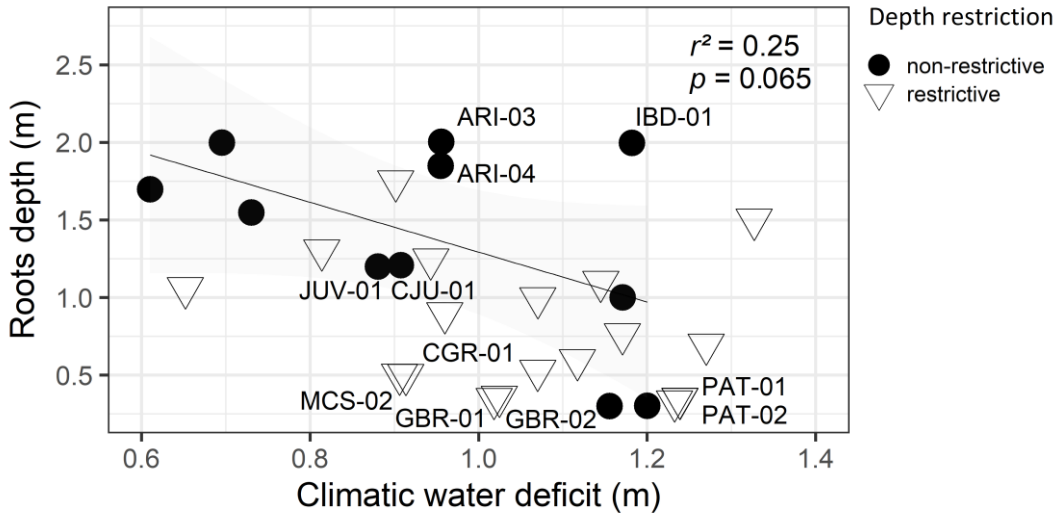

Figure 2.20: Relationship between roots depth and climatic water deficit (the higher CWD, the higher the water stress). Regression line stands for a simple linear regression considering the non-restrictive soils [i.e., absence of shallow impeditive layers (< 2.0 m) for root growth]. Confidence interval bands at 0.95 of probability is shown. A 0.9 quantile regression for the 'non-restrictive' group yielded r^2 = 0.56; p = 0.020 (function not shown).

Differences in texture-associated volumetric soil water storage capacity weighted across soil profiles ($W\theta_v$) were, however, marginally significant among the studied categories, with median values decreasing from $S_{KAR} \geq S_{CRY} \geq S_{SED}$ (p = 0.072; Table 2.2). Median values of $W\theta v$ were 0.20, 0.12 and 0.10 $m^3\ m^{-3}$ for S_{KAR}, S_{CRY} and S_{SED}, respectively (Table 2.2). Moreover, differences in maximum plant-available soil water (θ_P) were not significant at $p \leq$ 0.05 across S_{SED}, S_{CRY} and S_{KAR}, with median values of 0.13, 0.12 and 0.11 $m^3\ m^{-2}$ for S_{SED}, S_{CRY} and S_{KAR}, respectively (Table 2.2). Figure 2.21 illustrates the relative importance of texture-associated volumetric soil water and soil depth in accounting for the total plant-available soil water. It is of note that these results involve calculations only to the maximum sampled soil depth of 2.0 m. If deeper profiles are considered, then likely larger maximum plant-available soil water reservoirs may be found, especially in S_{SED} terrains.

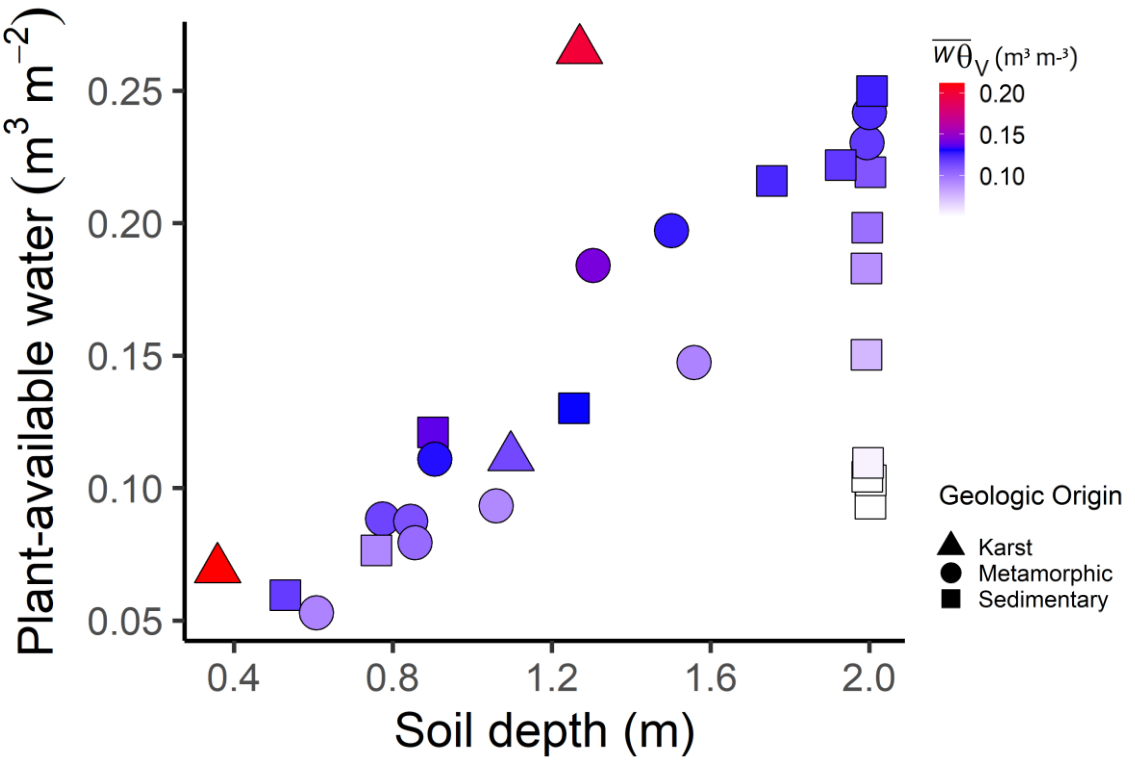

Figure 2.21: Maximum plant-available soil water content (θ_P) as a function of soil depth and volumetric soil water content (θ_V) calculated from across-profile textural volumetric soil water. Symbols representing distinct geological affiliations were coloured according to the textural volumetric soil water weighted across each soil profile ($W\theta_V$).

2.4 Discussion

In this chapter, I aimed to investigate to which extent soil parent materials (reflected by the geological background) account for differences in a suite of soil properties. In addition, a series of bivariate relationships were employed amongst several soil properties to evaluate pedogenetic aspects and weathering products. Potential drivers of variations in soil $\delta^{15}N$ values were evaluated through a multiple linear regression approach and a map with modelled soil $\delta^{15}N$ values was produced for the Caatinga region. Finally, the potential influence of climatological parameters (i.e. P_A, T_A and CWD_{adj}) on selected soil properties (i.e. soil pH, $[C]_T$, $[N]_T$, soil C/N ratio and R_{EF}) were evaluated in the context of soil geological affiliations.

2.4.1 The influence of geology on soil properties

2.4.1.1 Cations availability and soil reaction

Across the study sites, RSGs occurrence and their properties considerably mirrored the geological origin, though some of the studied properties varied more than others. For example, except for $[K]_{ex}$ and $[Na]_{ex}$, most main exchangeable soil cations, effective cations exchange capacity and associated base and aluminium saturation varied systematically across geological classes (Figures 2.2-a and 2.2-b). These results are aligned with the expected variability of soil cations levels according to geological classes as pointed out in several works reporting on Caatinga soils (e.g. SAMPAIO, 1995; SAMPAIO, 2010; ARAÚJO, 2011; ARAÚJO et al., 2017; 2019).

Regarding the exceptions, both $[K]_{ex}$ and $[Na]_{ex}$ were, in general, present in proportionately lower concentrations compared to other base cations. The largest part of K in soils is known to be present in primary and secondary minerals (Structural K), with only a small fraction present in both the soil solution (Solution K) and electrostatically bonded as an outer-sphere complex on the negatively charged soil particles (Exchangeable K) (SPARKS, 2002). The latter is considered to be readily available for plants, replenishing K to the soils when it is lost by leaching or taken up by plants (ERNANI; ALMEIDA; SANTOS, 2007). This is considered a dynamical chemical equilibrium (NAJAFI-GHIRI et al., 2019), where weatherable K-bearing minerals should constitute a major factor in determining K availability in the long term. Higher concentrations of K are reported in igneous (e.g. granites and sianites), intermediate in pelitic sedimentary rocks such as (e.g. shales, argillites and siltites) and lower in calcareous rocks (ERNANI; ALMEIDA; SANTOS, 2007). Therefore, the prevailing quartz-rich composition of many soils in this study helps explain the relatively low K contents.

Similarly, $[Na]_{ex}$ was present only in small concentrations (except for PSC-02 and SJO-01, all soils had $[Na]_{ex} \leq 1$ $mmol_c$ kg^{-1}). Despite losses through leaching being expected to occur at a relatively low pace in the Caatinga, the electrostatically bonded Na may be more prone to be lost from the soil system compared to divalent cations (i.e. Ca^{2+} and Mg^{2+}), the latter more strongly adsorbed onto soil particles. Coarse-textured soils, largely represented in this study, are unlikely to exhibit salt accumulation (FREIRE; FREIRE, 2007). Sodium is found in a wide range of both felsic and mafic igneous rocks, as well as in their crystalline counterparts (SMITH et al., 2019). The latter may also contain silicate Na-bearing minerals, such as Na-Plagioclases, a major source of Na in soils (SMITH et al., 2019). Regardless of the mineralogical aspects, Na is expected to be easily weathered (QUESADA et al. 2010) and leached through the soil

profiles, though this process should be relatively slower in the Caatinga compared to soils of wetter regions.

Contrary to most S_{SED} sites, JUV-01 and BTI-01 have shown relatively higher exchangeable cations concentrations. The likely reason is that the former is situated in the Bambuí Group geologic formation (on the Minas Gerais side) where, along with limestones and dolomites, arkose – a detrital sedimentary rock rich in feldspar and other base-rich materials also occurs to a large extent. Regarding BTI-01, the study plot is situated nearby the limits of Cabeças and Pimenteiras Formations (Piauí State), and soil parent materials such as siltites, conglomerates and shales widely occur (CPRM, 2004), with the latter recorded in the BTI-01 soil. Both JUV-01 and BTI-01 had comparable I_E, with BTI-01, however, holding a relatively higher content of $[Al]_{ex}$. These results reinforce that, despite the predominance of certain soil characteristics in sedimentary areas, several exceptions may occur across the Caatinga. It has been asserted that 'crystalline soils' have more varying properties than 'sedimentary soils' (SAMPAIO, 2010). Nevertheless, considerable variability in soil properties of S_{SED} sampled in this study is also evident. Moreover, regardless of the geological affiliations, a marked predominance of coarse-textured soils was noted (see the textural triangle in Figure 2.5). The tendency of coarse-textured soils in the Caatinga has been previously observed (JARAMILLO; MURRAY-TORTAROLO, 2019), which is of great importance for several biogeochemical processes as soil texture largely influences the surface charge density, adsorption capacity as well as elemental fluxes between organic and inorganic pools (WEIL; BRADY, 2016; SANCHEZ, 2019).

As pointed out in the Amazon forest study of QUESADA et al. (2010), high I_E levels usually reflect mineral weathering still taking place, with the dominance of the soil sortive complex by either bases or aluminium reflecting the current product of the active weathering. Clay activity is known to influence the overall soil sortive complex's size and composition, but contrary to findings in Western Amazon soils (MARQUES et al., 2002), the high-activity clay soils identified in this work had relatively much lower (often negligible) aluminium contents compared to their low-activity clay counterparts. Of note in this respect, is that most soil pH_{H2O} in Marques and coworkers' study occupied the 4.4 to 4.7 range, with an increase of 0.3 pH_{H2O} being associated with a doubling of exchangeable aluminium concentration (from 91 to 181 $mmol_c\ kg^{-1}$). In this study, soil pH_{H2O} values were often around 5.0 and ≥ 5.6 in 11 soils, a value that virtually indicates the absence of any aluminium in soluble forms. Figure 2.1-b shows that

small changes in soil pH may lead to large changes in aluminium or base dominance in the soil sortive complex.

In addition to the chemical nature and composition of parent materials, soil pH is a major determinant of cation availability. Figure 2.7 shows measured values of soil bases ($\sum_B$) along with modelled responses of $\sum_B$ as a function of $\sum_{RB}$ and soil $pH_{H2O.}$ Considering a few exceptions, the geochemical environments of S_{SED}, S_{CRY} and S_{KAR} were found to be reasonably delimited. These results, together, illustrate significant differences in the geochemical characteristics of geologic-edaphically distinct environments, which are thought to be of pivotal importance for several biological processes of both plant and soil microorganisms.

2.4.1.2 Phosphorus

Despite a wide range of observed $[P]_T$ contents, the majority of both S_{CRY} and S_{SED} soils had relatively low to moderate contents of $[P]_T$ (ranging from 100 to 200 mg kg^{-1}). These values are in agreement with other studies in the region considering the upper soil layer or A horizons (e.g. TIESSEN; SAMPAIO; SALCEDO, 1992; FRAGA; SALCEDO, 2004; ARAÚJO; SCHAEFER; SAMPAIO, 2004; SILVEIRA; ARAÚJO; SAMPAIO, 2006). Soil $[P]_T$ contents were, however, markedly higher for the S_{KAR} sites [median of 469 mg kg^{-1} and notorious 1194 mg kg^{-1} measured in GBR-02 soil (Hypereutric Calcaric Lithic Leptosol)]. Karst-derived soils can be considered a special case since the high $[P]_T$ levels commonly found in these soils usually do not reflect P availability (FERREIRA, 2013). If parent material (geology) P concentration reflects soil $[P]_T$ concentration (PORDER; RAMACHANDRAN, 2013), this probably is not the case for karst-derived soils, in which original limestone and dolomite P levels were shown to be comparable to P-depleted sandstone contents (PORDER; RAMACHANDRAN, 2013). Assuming a generic rock classification, Jackson (1969) encountered, on average, 1300 mg kg^{-1} of P in igneous and metamorphic rocks, 750 mg kg^{-1} in schists, 350 mg kg^{-1} in sandstones and a comparably low 180 mg kg^{-1} in calcareous rocks (JACKSON, 1969, *apud* SALCEDO, 2006). The most likely underlying reason is the tendency of calcareous soils to accumulate calcium phosphates (Ca-P) of low solubility (PANSU; GAUTHEYROU, 2006). Former pedological studies have shown that the typical high P of tropical calcareous soils were, in fact, the product of the secondary accumulation of P in insoluble compounds originally present in the limestones strata (SCHROO, 1963). A comprehensive assessment of bioavailable P-forms as well as P distribution across organic (P_o) and inorganic (P_i) pools would, however, require specific

methods such as Olsen-P (OLSEN; SOMMERS, 1982) and Hedley's fractionation (HEDLEY et al., 1982).

Indeed, despite the very high $[P]_T$ levels of S_{KAR}, the availability of this nutrient might be a concern in these soils, which is likely to be counteracted by biological players. For example, phosphorus-bearing minerals (i.e. apatites) are dissolved by soil natural acidity as well as by enzymatic activity (i.e. phosphatases) of both roots, mycorrhizae and microorganisms (SANCHEZ, 2019). In addition, 'biocrusts' (BELNAP, 2013; SZYJA et al., 2019) have been observed in several semiarid areas. These are communities of non-photosynthetic and photosynthetic organisms that, in contrast to wetter ecosystems, often thrive in arid and semiarid soils because of the presence of spaced canopy covers. Specifically, discontinuous canopy coverages leave sun-exposed soil surfaces available for biocrusts colonisation (BELNAP, 2013), and these communities are involved in several ecological processes, including carbon and nitrogen fixation as well as promoting increases in phosphorus availability (ZHANG et al., 2016; BELNAP et al., 2016). The latter takes place at least through two pathways: (1) Some microorganisms can secrete phosphatases so that P-availability in soils underlying biocrusts sheets might be higher than surrounding soils as well as the associated higher P concentration on overlying plant tissues (ZHANG et al., 2016); (2) Intricate symbiotic mechanisms have been proposed among biocrusts species such as the possibility of free-living fungi delivering P to immobile lichen and bryophyte (comparable to mycorrhiza delivering P to plants at the expense of plant-derived carbon) or the fungi-produced phosphatases enhancing P availability across the biocrust but also likely improving the soil general fertility (BELNAP et al., 2016). These processes could be of great importance in karst-derived soils of the Caatinga, potentially participating in weathering processes as shown for karst exposed to wetting-drying cycles (CHEN et al., 2014). Furthermore, biocrusts might be considerably important across the entire region, potentially catalysing fluxes from both organic and inorganic unavailable P into available pools. Biocrusts were found to be conspicuous in the Caatinga, including several taxa and potentially covering about 10% of old-growth and secondary-growth topsoil total surfaces (SZYJA et al., 2019).

2.4.1.3 Carbon and nitrogen

In this study, $[C]_T$ contents were not different neither considering geological classes nor their associated RSGs. These results are in agreement with MENEZES et al. (2021), who did not find differences in soil carbon storage among the main soil groups of the Caatinga, also

noting that Menezes et al. (2021) report on carbon stocks whereas carbon concentrations are evaluated here.

Calcareous soils are known to enhance the stability of carbon, potentially causing nutrient limitation (HU et al., 2012). Despite a tendency for higher $[C]_T$ values in S_{KAR} sites, the current results suggest that carbon dynamics and storage should not present significant differences in a reasonable range of soils in the Caatinga. Total nitrogen levels did not differ between S_{CRY} and S_{SED} sites. However, $[N]_T$ contents in S_{KAR} sites were 68% and 78% greater than S_{SED} and S_{CRY}, respectively. Soil N is often considered a limiting nutrient in karst ecosystems this being attributable to $CaCO_3$ enhancing the stability of soil organic matter (PAN et al., 2016). Measures of N availability such as potential mineralisation rates were not included in this study, but the high contents of $[N]_T$ measured in S_{KAR} are potentially present in stable organic compounds. Nitrogen availability in calcareous may be improved through the exudation of oxalic acid from hyphae and roots, potentially playing a crucial role in N acquisition (CLARHOLM; SKYLLBERG; ROSLING, 2015; PAN et al., 2016).

2.4.2 Causes of isotopic discrimination in Caatinga soils

Soil $\delta^{15}N$ values were, in general, similar across geological soil affiliations with no clear patterns across pedogenetic conditions reflected by RSGs. Most measured soil $\delta^{15}N$ values were higher than values commonly measured in soils of wetter tropical regions such as those reported by Martinelli et al. (1999) and Quesada et al. 2010). Soil $\delta^{15}N$ values varied from $\delta^{15}N$ = 2.85 ‰ at PSC-02 (Orthodystric Regosol) to 15.66 ‰ in CND-01 (Orthodystric Chromic Sideralic Arenosol). Interestingly, the lowest and the highest measured soil $\delta^{15}N$ values in the dataset were found at the sites with the highest and lowest P_A levels, respectively.

Here of note is that high $\delta^{15}N$ values do not necessarily translate into high N availability. High $\delta^{15}N$ values have been historically considered an indicator of an ‘open N cycle’, i.e. relatively high N fluxes (MARTINELLI et al., 1999). This terminology, however, has begun to be more cautiously used by experts, since to provide a consistent assessment of ‘openness’, not only stocks, transformations and fluxes but a comprehensive understanding of N turnover would be also required.

The low N fixation rates by legumes often found in Caatinga may be due to the high stress by other factors under which these plants are held making N fixation too costly to bring any advantage. Nitrogen biological fixation was suggested to occur at a much higher rate in natural stands under regeneration (FREITAS et al., 2010).

The values presented in this study were also consistent with those reported by Santos et al. (2022), who measured a maximum soil $\delta^{15}N$ value of 17.3 ‰ in an Alisol in the *Sertão Pernambucano* under native Caatinga and P_A = 0.71 m a^{-1}. Freitas et al. (2015) also reported soil $\delta^{15}N$ values ranging from 4 ‰ to 16 ‰ along a rainfall gradient encompassing a vegetation transition in Northeast Brazil. It is of note that both Freitas et al. (2015) and Santos et al. (2022) adopted soil $\delta^{15}N$ mean values relative to the upper 0.20 m layers, whereas, in this study, I used data from the upper 0.3 m layer. The association between mean soil $\delta^{15}N$ values from the 0.20 and the 0.30 m layers in this study, however, was very high (r^2 = 0.99; $p < 0.000$), with potential implications for the interpretation of the results being considered negligible.

Similarly to this study, Santos et al. (2022) have found a marked influence of climatic variables on soil $\delta^{15}N$ values. This pattern has already been noticed in several studies in arid and semiarid regions over the past decades (e.g. SHEARER et al., 1993; SWAP et al., 2004; ARANIBAR et al., 2004; FREITAS et al., 2015; SANTOS et al., 2022), and also for a wide range of environmental conditions at global and subcontinental scales, e.g. Handley et al., 1999; Nardoto et al., 2008, the latter study reporting on foliar $\delta^{15}N$. Also using foliar $\delta^{15}N$ data, Martinelli et al. (2021) found the highest $\delta^{15}N$ values for Caatinga leaves compared to other Brazilian biomes, which was attributed to longer N residence time in soil associated with lower leaching rates and plant uptake. It is worth mentioning that, with no exception, all Caatinga sites included in the study of Martinelli and coworkers' (2021) are also part of this study, which is thought to largely explain the similarities found between the $\delta^{15}N$ range in both studies.

The aridity index (AI) and precipitation seasonality (ψ) were significantly related to soil $\delta^{15}N$ values. The former is a quantification of the precipitation availability over the atmosphere demand (ZOMER; TRABUCCO, 2022), where higher values translate into more humid conditions, whereas low values represent higher aridity. On the other hand, precipitation seasonality is a measure of the long-term rainfall variability throughout the year, where greater values represent greater precipitation variability, i.e. the precipitation is more concentrated over a part of the year (O'DONNELL; IGNIZIO, 2012), and lower values mean that precipitation is more evenly distributed throughout the year. The AI was strongly associated with P_A (r^2 = 0.95; $p < 0.000$), therefore was not allowed to be included simultaneously in models attempting to account for variations in soil $\delta^{15}N$. These variables are thought to contain redundant information as the index is simply the mean annual precipitation divided by mean annual reference evapotranspiration (ETP_0). The latter was found to be relatively constant across the dataset, with minimum and maximum values reaching 1.49 and 1.91 m a^{-1}, respectively. Anyway, both

variables are expected to influence N processing in soils as well as the biologically-mediated soil organic nitrogen (SON) mineralisation. Indeed, in addition to total annual rainfall amounts, precipitation temporal variability has been suggested as a key driver influencing N processing in dry regions (ARANIBAR et al., 2004; SANTOS et al., 2022). Swap et al. (2004) suggest that the gradual increase of soil $\delta^{15}N$ in dry regions is the result of intense episodic microbial activity during the onset of the wetter season after long-lasting dry spells in southern Africa. However, under extreme seasonal conditions, the rainy period may not be long enough to process all available N in the soils, thus causing isotopic signatures toward higher $\delta^{15}N$ values. (SWAP et al., 2004).

The results presented here are consistent with the premise that, in drier environments, the N dynamics are strongly controlled by water availability. Additional input from the literature may help explain the results of this study. For example, studies show that, as rainfall decreases, mineralisation and nitrification rates tend to increase as long the water deficit is not extreme (MARTINELLI et al., 2021). Other potential mechanisms leading to higher fractionating rates (consequently higher soil $\delta^{15}N$ values) are high N volatilization rates commonly found in dry tropical regions. Moreover, reduced N losses through leaching can be associated with a longer N residence time in the soils (MARTINELLI et al., 2021), which also can yield ^{15}N-enriched pools. In this study, P_A covaried positively with ψ suggesting that lower precipitation rates but with a better distribution throughout the year may promote favourable conditions for N discrimination processes, thus yielding higher soil $\delta^{15}N$ over time.

The mechanisms underlying soil $\delta^{15}N$ enrichment conditioned by climatic forces remain somewhat enigmatic, but the main line of thought suggests that such enrichment is influenced by complex biogeophysical controls, thereby rainfall (or aridity) affects N pools processing and the openness of the N cycle (SWAP et al., 2004). In this regard, it has been proposed that either decrease in the overall fluxes of N into organic pools or a greater flux of N from organic to minerals pools can induce changes in isotopic signatures, with N mineral forms susceptible to being lost as leachate or gaseous emissions (HÖGBERG, 1997; HANDLEY et al., 1999; MARTINELLI et al., 1999). Thus, whenever N loss rates surpass N incoming in a given ecosystem, then internal cycling tends to discriminate against ^{15}N, causing its enrichment in the soil (QUESADA et al., 2010).

The map-modelled soil $\delta^{15}N$ values for the Caatinga region presented in Figure 2.16 were produced with a purely climatic model that includes AI and ψ variables (Model 1; Table 2.5; $r^2 = 0.81$; $p < 0.000$; AICc = 122.0). Because the ΔAICc of the second best-ranked model

was only 0.28 (scale of information), this model could be also considered feasible in explaining variations in soil $\delta^{15}N$ if information theory is strictly considered. Similarly to Model 1, Model 2 (Table 2.5; $r^2 = 0.81$; $p < 0.000$; AICc = 122.2) includes the AI and ψ variables, but also soil total carbon - $[C]_T$. Some lines of evidence may help explain such an influence. Higher levels of $[C]_T$ in soils are likely to reflect the presence of more stable/recalcitrant organic compounds for a longer period. In turn, soil organic carbon stability can be conditioned by a variety of factors, including chemical recalcitrance, physical protection and interaction with soil mineral surfaces (LÜTZOW et al., 2006). In this study, clay content accounted for a considerable proportion of the variation in $[C]_T$ ($r^2 = 0.35$; $p = 0.000$). The positive influence of $[C]_T$ on $\delta^{15}N$ values, therefore, can potentially be associated with direct and indirect effects. On the one hand, old recalcitrant N pools tend to become more ^{15}N enriched. On the other hand, higher clay contents, beyond promoting greater N gaseous losses during fractionating processes (CRAINE et al., 2015), are suggested to influence the persistence of stable long-lasting ^{15}N-enriched organic compounds (BAISDEN et al., 2002; MARIN-SPIOTTA et al., 2009). Santos et al. (2022) reported an effect for clay in increasing $\delta^{15}N$ values in Caatinga, but also highlight that it may be due to the greater stability of organic matter in clayey soils. The higher δ^{15} in this study, however, was found in an Arenosol (> 90% of sand). Alternative explanations for sandy soils also giving rise to ^{15}N-enriched soils are provided by Aranibar et al. (2004). In summary, SOM compounds are, in general, less physically protected in coarse-textured soils. Thus, the easier biological attack (i.e. SOM mineralisation) can also potentially give rise to higher $\delta^{15}N$ values in the remaining N pools of these soils.

The model simulated soil $\delta^{15}N$ values for the Caatinga Domain presented in Figure 2.16 provides the first approximation of the isotopic behaviour across the region. Modelled $\delta^{15}N$ values over the region were made possible due to the inclusion of only spatially explicit predictors variables in the lowest-AIC model (i.e. AI and ψ). Field-measured $\delta^{15}N$ values overlying modelled responses indicate that the model can reasonably predict $\delta^{15}N$ values in Caatinga, with measured soil ^{15}N *versus* model simulated soil $\delta^{15}N$ shown in Figure 2.15 providing additional support for the model accuracy.

The spatial representation of $\delta^{15}N$ for the Pernambuco state of SANTOS et al. (2022) provided a clear picture of the climatic control on isotopic discrimination in semiarid places. In their work, this control remained even under distinct land uses and over three physiographic regions. However, soil isotopic composition is thought to be the result of a multitude of processes (BAUMGARTNER et al., 2021). For instance, geomorphological features are also

likely to control soil isotopic discrimination processes. Despite the prevailing apparent regional climatic control on soil $\delta^{15}N$ values on regional scales, the topography may be important at a local scale (BAUMGARTNER et al., 2021). Erosive forces may operate at different rates across slope gradients, therefore influencing soil rejuvenation processes (AMUNDSON et al., 2003). Furthermore, relief dictates orographic rainfall, therefore exerting indirect control on isotopic composition.

The results of Santos et al. (2022) provide further insights concerning potential differences in soil $\delta^{15}N$ values arising from geomorphological characteristics. For example, the Zona da Mata physiographic region has a warm and humid climate and showed the lowest soil $\delta^{15}N$ value. In contrast, the Sertão physiographic region has a hot and dry semiarid climate and showed the highest soil $\delta^{15}N$ value. The Agreste physiographic region is the transition zone between Zona da Mata and Sertão covering much of the Planalto da Borborema mountain range (SANTOS et al., 2022). Accordingly, regions surrounding higher terrains areas are susceptible to experiencing orographic rainfall, potentially influencing isotopic signatures. In addition, influence from erosive processes is thought to potentially influence isotopic signatures in these sloping terrain areas.

Finally, despite the somewhat expected variations in soil $\delta^{15}N$ values between the two P_A categories (Figure 2.17-a; $\chi^2 = 15.53$; $p < 0.000$), subsequent evaluation of the pedogenetic influence (expressed by effective cation exchange capacity; I_E) considering these two levels of P_A provided further insights into isotopic discrimination processes in Caatinga. For instance, considering the 'high-rainfall' category (i.e. $P_A > 0.8$), effective cation exchange capacity appeared to explain 44% of the variation in soil $\delta^{15}N$ values ($r^2 = 0.44$; $p < 0.000$; Figure 2.17-b). Indeed, it has been suggested that soil properties (including nutrient availability) may become more important in ecosystems where water is not a limiting factor (SWAP et al., 2004). Interestingly, soil $\delta^{15}N$ values were relatively high for all S_{KAR} sites under different precipitation conditions, potentially reflecting the influence of nutritional status on the isotopic discrimination at these places. Collectively, the results presented here, in addition to evidence from the literature, suggest that differences in nutrient availability and geomorphologic-environmental variation may account for unexplained variances when attempting to predict $\delta^{15}N$ values using purely climatic models.

2.4.3 Weathering and total nutrient capital reserves (NCR_T)

Within the weathering metrics evaluated in this study, $\sum_{RB}$, $[Zn]_T$, $[Mn]_T$ and the K/Zr elemental ratio were higher for S_{KAR} sites, with S_{CRY} sites also showing higher $\sum_{RB}$ and K/Zr than the S_{SED} sites. These metrics clearly show the influence of parent materials on nutrient capital reserves. Importantly, the weathering course in semiarid regions is likely substantially distinct from warm humid places. Specific conditions such as very high ETP_0 to relatively low annual P_A, barriers to water drainage and typical soil reactions range (moderately acid to moderately alkaline) are all geochemical processes that favour the persistence of bases in the soils, thus controlling the formation of 2: 1 (expansive) silicate clay minerals such as smectite (SCHULZE, 2005), a representative group found in many Caatinga soils. (ARAÚJO et al., 2017).

2.4.4 Interrelationships between soil properties

Figure 2.6 shows that soil texture across soils derived from crystalline rocks (S_{CRY}) had considerably less variation in the contents of sand, clay and silt, not surprisingly then soil texture accounted more strongly for variations in I_E of S_{SED} sites. Soil texture is known to widely account for the surface charge density of soils. Specifically, sand and silt particles hold relatively much lower specific surface area (SSA) than clay particles, but might store considerable amounts of weatherable minerals, potentially releasing essential nutrients for plant growth into the soil solution over time (PALM et al., 2007). Conversely, clay particles are not constituted of weatherable minerals but have a large SSA and plenty of charged edges, thus allowing clay-rich soils to hold relatively large amounts of ions (SANCHEZ, 2019).

Figure 2.9 provides a picture of how soil $[P]_T$ relates to several soil constituents, namely soil total iron, aluminium and calcium oxides percentages (XRF-measured), soil $sand_f$, $silt_f$ and $clay_f$ and $[C]_T$. Such constituents reflect a series of potential P associations. Nevertheless, $[C]_T$ and soil $[P]_T$ were not related considering the full dataset together neither S_{SED} nor S_{CRY} separately. These results are contrary to results reported by Menezes et al. (2005; *apud* Menezes et al., 2012), who reported a strong significant positive relationship between soil carbon and soil P_T (r = 0.89**) calculated from several soil surveys covering the main soil orders of Caatinga. This relationship could indicate proportional increases in P contents as soil SOC increases, presumably in organic P-forms (P_o), also suggesting a minor or absent contribution of P in primary minerals, i.e. apatites. Such discordant results probably are associated with differences in texture and mineral assemblages of the soils included in the Menezes and

coworkers' compilation. As shown in Figure 2.5, the soils sampled in this work were mostly coarse-textured, which influences SOC storage and most likely also P_o forms. The importance of P_o for tropical soils has been widely considered (NZIGUHEBA; BÜNEMANN, 2005; QUESADA et al., 2010) with P_o often considered to be the major pool in advanced weathered soils (SANCHEZ, 2019).

The current literature concerning P_o and P_i pools, however, reports mostly on soils of humid tropics and cannot be simply extrapolated for semiarid regions such as the Caatinga (SILVEIRA; ARAÚJO; SAMPAIO, 2006). In general, the P_o fractions of Caatinga soils are lower than P_i. For example, Araújo, Schaefer and Sampaio (2004), in a toposequence study, found relatively low proportions of P_o in pedogenetically distant Ferralsols and Luvisols (25% and 28% of the total P, respectively), despite P_o levels increasing downslope. It has been suggested that unlike $[P]_T$, P_o is not closely associated with the degree of weathering (SANCHEZ, 2019. Rather, biologically-produced P_o should be related to soil organic matter build-up processes. For example, Silveira, Araújo, Sampaio (2006) reported soils of relatively high $[P]_T$ but with only 13% and 17% of P_o and soils with relatively low $[P]_T$ with 26% and 33% of P_o. The above-mentioned studies help explain the lack of relationship encountered between $[C]_T$ and $[P]_T$, which seems to be primarily associated with soil mineral constituents.

All measured soil textural fractions (i.e. $sand_f$, $silt_f$ and $clay_f$) were associated with $[P]_T$ at the level of the full dataset. However, considering the geological classes separately, the association existed only for S_{SED} sites. A likely underlying reason is that the S_{CRY} group had a less varying texture, whereas the S_{SED} group had a larger textural spectrum, allowing for a more easy evaluation of textural influence on $[P]_T$ levels. The highest predictive power was assigned to $silt_f$, followed by $sand_f$ and $clay_f$ at both the entire sampling level as well as only for $S_{SED.}$

Primary minerals are those whose mineral compositions have not changed significantly since their extrusion as molten lava (WEIL; BRADY, 2016; NANZYO; KANNO, 2018). The silt fraction can potentially hold P-bearing primary minerals, then yielding the relationship. However, P-bearing primary minerals have been rarely reported in practice in Caatinga soils. In addition, it is not possible to determine to what extent the method used here (sulfuric acid digestion) reflects the eventual presence of P minerals in its primary form.

On the other hand, $[P]_T$ contents decrease proportionately as $sand_f$ increases, which seems fairly logical as sandy soils hold a low charge density along with a low adsorption capability (QUESADA et al., 2010), also suggesting that negligible or even absent P are present in the form of weatherable minerals in the sand fraction of the studied soils.

As regards the modest relationship between $[P]_T$ and $clay_f$, it should reflect different proportions of clay-sized particles with descending SSA from allophane to aluminium and iron oxy(hydroxides) (PALM et al.,2007; (SINGH et al., 2017). In general, $clay_f$ is expected to determine phosphorus sorption capacity for soils of similar mineralogy. In addition, this association is maintained through the formation of secondary phosphorus clay minerals, namely (Ca)-bonded, (Al)-bonded and (Fe)-bonded phosphates (SANCHEZ, 2019). The proportional occurrence of these forms is known to be conditioned by soil pH, where acid reactions allow for (Ca)-phosphate hydrolysis, giving rise to (Al)-bonded and (Fe)-bonded phosphates (GUO et al., 2000; SALCEDO, 2006), the latter usually being of lowest solubility (SANCHEZ, 2019). Considering that the soils of this study were collected in Caatinga, measured soil pH_{H2O} values were somewhat low, which may help explain the higher predictive ability of Fe_2O_3 to account for $[P]_T$ rather than the Al_2O_3 and CaO (Table 2.3). In addition, a compilation of P contents in several common rock types has shown that median P contents were marked higher in Fe-rich rocks as opposed to Si-rich rocks (PORDER; RAMACHANDRAN, 2013), which suggests proportional abundances of $[P]_T$ and $[Fe]_T$, thus giving rise to (Fe)-P compounds.

The $[P]_T$ × CaO relationship was, however, weak at the overall sampling level (r^2 = 0.12; p = 0.04), but was relatively high considering S_{CRY} sites only (Figure 2.9-c; r^2 = 0.53; p = 0.005). But CaO at all S_{SED} sites was negligible, indicating low weatherable calcium capital reserves. As already mentioned, a more conclusive evaluation of P-forms distribution across specific fractions requires sequential P fractionations. Nevertheless, these results illustrate differences in geochemical conditions of S_{CRY}, S_{SED} and S_{KAR}. As the movement of P from primary minerals towards less soluble (Fe) and (Al)-bonded compounds requires continuous losses of Ca^{2+} and soil acidification, it is expected that soils with relatively higher pH (i.e. S_{CRY} and S_{KAR}) should have higher levels of (Ca)-bonded compounds as opposed to S_{SED} sites. These results are consistent with the theoretical framework provided by Salcedo (2006). An example of the complex P chemistry and behaviour is provided by Agbenin and Tiessen (1994), who measured P-rich silt particles, concomitantly containing Ca, Fe and Al, which was suggested to be a mixture/impregnation of P-bearing primary minerals onto (oxy)hydroxides during erosive processes with limited leaching intensities typical of the Brazilian semiarid region.

As previously shown, differences in total $[C]_T$ and $[N]_T$ were not associated with the different geologic classes and/or RSGs. Soil texture, on the other hand, markedly influenced $[C]_T$ contents. Clayey soils, as mentioned already, have a relatively much higher SSA, allowing the formation of organo-mineral complexes, as well as providing physical protection for carbon

particles inside their micropores. On the other hand, sandy soils have much lower SSA, along with a very reduced physical protection against SOC mineralisation (PALM et al., 2007, SANCHEZ, 2019). The current results echo these theoretical conceptions as both soil $sand_f$, $silt_f$ and $clay_f$ showed significant relationships with $[C]_T$ in the overall sampling context, with sand having a strong negative association with $[C]_T$. Contrary to the authors' expectations, Menezes et al. (2021) found large SOC levels in coarse-textured Arenosols underlain Dense Caatinga. This superiority of SOC contents in Arenosols in Menezes and coworkers (2021) was assigned to the unsuitability of these soils for agriculture, corresponding to longer fallow periods, thus accumulating C for a longer time.

Within S_{CRY} sites, clay content tended to better account for variations in $[C]_T$ (Figure 2.11-c). Since all S_{ARE}, S_{LAC} and S_{HAC} soils are present in the S_{CRY} category, the observed differences may reflect a spectrum of increasing SSA. Within the S_{CRY} category, however, the highest $[C]_T$ content (13.42 mg kg^{-1}) was found in a quartzite-derived S_{LAC} Leptosol (MCS-01), which might be hypothesised as being due to lower mineralisation rates. The conventional assumption that S_{HAC} soils stabilise more carbon than LAC kaolinitic-illitic soils was counteracted by Singh et al. (2017), who showed that contents of clay-sized smectites led to higher soil moisture, which in turn increased soil respiration and microbial biomass. The current results do not support the idea that S_{HAC} soils necessarily store more SOC than S_{LAC} soils, which appeared to be much more associated with particle size effects, levels of Fe and Al-bearing minerals and T_A. Although specific methods are required to specifically characterise clay mineralogy and (oxihydr)oxides species, soil total iron includes these forms as well as iron present in silicate minerals (SCHULTE, 2004). In conjunction with clay-sized aluminium species (e.g. kaolinite and gibbsite), (oxihydr)oxides are believed to be the most important soil constituents in the long-term persistence of SOC (KIRSTEN et al., 2021). Despite Caatinga soils generally not containing large amounts of Fe and Al (oxihydr)oxides, these constituents should be important in SOC storage and dynamics. Ultimately, SOC levels should be controlled by the prevalent semiarid climate (i.e. high temperature and low moisture levels), proportions of free Fe and Al (oxy)hydroxides, Fe and Al bearing minerals, as well as varying levels of clay minerals from crystalline to amorphous allophane. The latter are usually assumed to hold the largest specific surface area among clay minerals (SINGH et al., 2017). Additionally, organic matter quantity and quality are also factors controlling the SOC contents and dynamics in soils (DAVIDSON; JANSSENS, 2006.

Climatic conditions have long been recognised as a major factor determining SOC build-up and decomposition (JENNY, 1980). In this respect, Figure 2.13 shows no apparent effect of P_A for $[C]_T$, $[N]_T$ and soil C/N ratio, whereas mean annual temperature (T_A) was associated with a decrease in $[C]_T$ levels for all sites considered together, but with a steeper relationship considering only S_{SED} sites. Despite the relatively small variation in mean annual temperature among sites (from 20.5°C to 26.8 °C), these differences are hypothesised to be sufficient for catalysing SOC mineralisation, considering that mean values are affected by extreme values (as those in the warmest month and warmest year quarter), despite potential limitations arising from the minimum soil moisture levels required for biological activity. It has been reported that the release of physically protected and/or more recalcitrant SOC forms (such as aromatic compounds) is temperature-sensitive (DAVIDSON; JANSSENS, 2006; SANCHEZ, 2019). Thus, these forms may have lower rates of accumulation, yielding lower SOC contents over time at higher temperatures. An important concept underlying SOC decomposition is the temperature sensitivity of SOC decomposition, commonly expressed as changes in SOC decomposition every 10°C increases (Q_{10}), with studies showing a codependence of soil moisture and SOC recalcitrance (DAN et al., 2016; MOINET et al., 2020). Mean annual temperature also had a negative effect on $[N]_T$ contents, but only for S_{SED} sites. Moreover, the relationship was stronger for $[C]_T$ rather than $[N]_T$, which suggests higher net carbon losses relative to nitrogen, potentially present in more stable compounds. In addition, NO_X fluxes are considered an important biogenic source of nitrogen leaving arid and semiarid ecosystems (FEIG; MAMTIMIN; MEIXNER, 2008). NO_X and fluxes have been reported to be highly sensitive to temperature changes in these ecosystems, at least in part attributable to the fact that microbial populations should have distinct optimal temperatures, thus affecting gaseous N-fluxes (ARANIBAR et al., 2004).

An important consideration related to these results is that the nitrogen incorporated into soil organic pools represents an integrative ecosystem property, which is expected to reflect an integration of biogeochemical processes over time [e.g. nitrogen biological fixation (NBF)]. Some works reporting on NBF have been published for Caatinga over the last decade (e.g., FREITAS et al., 2010; DE SOUZA et al., 2012; FREITAS et al., 2012; DA SILVA et al., 2017), from which it is clear that despite the outstanding richness and abundance of legumes in Caatinga (QUEIROZ, 2006), the proportion of N_2-fixing plants that effectively do so is commonly low. Nitrogen biological fixation is a highly-demanding process, which is more

likely to occur under higher rainfall levels (MCKEY, 1994), which may explain the low rates of NBF as found in the above-mentioned studies.

Relatively low phosphorus and high nitrogen availability have been found to influence symbiotic mechanisms instead of lacking nodulation in potentially N_2-fixing species (SILVA et al., 2017). Figures 2.12-a and 2.12-b provide further evidence of the coupled nature of the nitrogen, phosphorus and cations cycles (here represented by I_E). Both relationships were significant considering the whole dataset (Table 2.3-d), however, when considering geologically distinct soils separately, the relationship was significant only in S_{SED} sites. These results suggest that the influence of phosphorus and general fertility on the nitrogen cycle may be regulated under different geochemical circumstances, with some 'sedimentary Caatingas' sites possibly susceptible to a relatively sluggish ecosystem nitrogen enrichment as compared to nutrient-rich sites across Caatinga.

Figure 2.18 (a-h) shows a series of weathering-associated relationships discriminated according to soil geologic affiliations. As anticipated in Section 2.4.4, $silt_f$ can be taken as a reasonable indicator of pedogenetic development, with less developed soils, in general, holding relatively higher silt contents as compared to highly weathered soils. Therefore, there is a strong association between soil $silt_f$ and $\sum_{RB}$, with the highest latter values being found in the three calcareous-derived S_{KAR} (Calcisol, Cambisol and Leptosol; PFF-01, GBR-1 and GBR-02, respectively). Such elevated contents, however, are thought to be the result of calcite secondary accumulation in stable compounds. The relatively high contents of silt in PFF-01, GBR-01 and GBR-02 soils are likely attributable to the presence of underlying calcilutites (i.e. predominantly silt or clay-sized limestones) widely present in the Jandaíra, Gabriel and Nova América geologic formations (PFF-01, GBR-01 and GBR-02, respectively). The $silt_f \times \sum_{RB}$ relationship was even stronger for S_{SED} sites, which encompass varying pedogenetic conditions, including quartz-rich Arenosols with nearly negligible silt contents (e.g. Arenosols of 'Vazante Dunas' geologic unit), and pedogenically younger soils (i.e. Leptosol, Luvisol, Cambisol).

Regarding the relationships found between $\sum_{RB}$ and total contents of iron zinc and manganese (Fe_T, Zn_T and Mn_T), it is noteworthy that soil total micronutrients reservoirs are the complex product of initial concentrations in parent materials and their subsequent interactions with pedogenic processes (WHITE; ZASOSKI, 1999). Indeed, both Fe_T and Zn_T had linear increases with $\sum_{RB}$ across S_{SED} sites. On the other hand, Mn_T increased with $\sum_{RB}$ increases only for the S_{CRY} sites, suggesting generally lower levels of Mn in S_{SED} soils (except for a Luvisol in JUV-01).

Despite higher micronutrient capital reserves, the S_{KAR} sites were slightly alkaline, potentially giving rise to limitations in the availability of most metallic micronutrients (optimally in slightly acid or acid soils). It has been shown that increases in aridity may indirectly lead to a shortage of metallic micronutrients mostly because of lower SOC inputs as well as aridity-induced soil pH increases (WHITE; ZASOSKI, 1999; MORENO-JIMÉNEZ et al., 2019). Thus, high soil pH caused by increased aridity might be a concern in a future scenario of lower precipitation amounts, at least in some Caatinga soils. The mechanisms whereby soil organic matter (SOM) improves metallic micronutrient availability have been comprehensively reviewed in DHALIWAL et al. (2019). In summary, SOM influences physicochemical reactions that improve levels of exchangeable and water-soluble plant-available micronutrients. Similar biogenic mechanisms may catalyse the conversion of unavailable to available micronutrient forms, thus counteracting potential micronutrient shortage issues in alkaline soils.

The elemental ratios of Figure 2.18 (e, f,) are additional weathering metrics. K/Zr ratios were markedly higher and less varying in S_{CRY} and S_{KAR} sites. On the other hand, S_{SED} sites have shown more varying K/Zr ratios across the $\sum_{RB}$ spectrum. This could be attributable to the predominance of quartz-rich Arenosols in the lower part of the spectrum, with K-bearing minerals (i.e. potassium feldspar or 'K-spar') virtually absent. The higher part of the spectrum is associated with Leptosols, Cambisols and Luvisols, i.e. less weathered soils associated with high values of K/Zr, which suggests higher levels of weatherable K-spars (in addition to available forms). The Ca/K relationship discriminates soils derived from plagioclase-bearing materials from those derived from K-spars-rich materials. Regardless of soil geologic affiliations, there were no differences in Ca/K with similar ranges for the S_{CRY} and S_{SED} sites. It should be highlighted that, even under the same environmental conditions, weathering rates are not uniform. Rather, its susceptibility depends upon factors such as mineral assemblage, colour and texture (FONTES, 2012). Thus, minerals can be ordered according to weathering resistance. Goldich (1938) conceived a pioneer study where the resistance of primary minerals to weathering was linked to the magma crystallisation sequence. Generally speaking, mafic or ferromagnesian minerals (↓Si; ↑Fe; ↑Mg), which are formed first, are much more prone to weathering, tending to first disappear from $sand_f$ and $silt_f$ (FONTES, 2012), whereas felsic minerals (↑Si; ↑Al) tend to resist more to weathering. Still, according to the weathering resistance sequence of Goldich (1938), K-spars are more resistant to Albite (Sodic Plagioclase), which in turn is more resistant than Anorthite (Calcic Plagioclase). As anticipated in Section 1.6, it is worth mentioning that the resistance of minerals to weathering not only depends on

their intrinsic characteristics but also on thermodynamic equilibrium, the latter determined by factors such as solubility, pressure, volume and others (CEMIC, 2005).

In summary, the Ca/K ratios shown in Figure 2.18-f), not only reveal the current lower abundance of plagioclase products for virtually all sampled soils but it is also suggested that orthoclase K-spars minerals might persist for longer periods in soils.

Concerning the relationships among $\sum_{RB}$, $[P]_T$ and I_E (Figure 2.18-g and h), it has been suggested that similar general processes control these variables, which are strongly influenced by soil pH changes (QUESADA et al., 2010). At more alkaline pH, soil P reactions are mostly towards Ca-bonded compounds, which are more soluble as soil pH declines, as compared to Al and Fe-bonded P compounds, both later formed under acid reactions. Thus, with soil ageing and the tendency of base impoverishment and soil acidification, Ca-bonded P-forms compounds tend to be solubilised with an increasing abundance of Fe and Al-bonded P forms which have a higher P retention capacity, also undergoing slow but continuous losses of P out of the system (WALKER; SYERS, 1976; SANCHEZ; UEHARA, 1980). In parallel, clay activity tends to diminish (2: 1 clay → 1: 1 clay), along with a decrease in specific surface area and associated surface charge density. As a result, a decrease in cations and anions retention capability is expected.

2.4.5 Soil morphology, effective rooting depth (R_{EF}) and water availability

Except for Caatinga sedimentary terrains where soils are appreciably deep (≥ 2.0 m), Caatinga soils are morphologically particular, with conspicuous shallow soils (i.e. ≤ 0.5 m) or less shallow (i.e. ≥ 0.5 and ≤ 1.0) dominating in the region (ARAÚJO FILHO et al., 2017). This characteristic itself may impose a marked physical constraint for root development, also affecting both soil physical support capability as well as the volume of exploitable soils for water and nutrient uptake. A general opposite trend between physical and chemical constraints can be observed in this study. These patterns are largely represented across the S_{CRY} and S_{SED} dichotomy, where the former usually exhibits favourable chemical conditions for plant growth, whereas the latter (excluding non-aggregated loose sands) tend to show more appropriate physical conditions to support plant growth as well as larger volumes of root-exploitable soils. These characteristics are known to be influenced by geomorphological features, where sloping terrains are more prone to continuous pedological rejuvenation processes and soil parent material exposure, and potentially also affect vegetation dynamics (i.e. NPP, mortality and recruitment rates). An evaluation of the impact of soil physical properties on vegetation

dynamics these dynamics remains to be undertaken in forthcoming work in the established permanent plots.

The results presented in Section 2.3.5 are consistent with observational field data and theoretical findings (GUSWA, 2010; SCHENK; JACKSON, 2002). Although R_{EF} can be assumed as a result of multiple factors, i.e. mean annual rainfall, soil texture class, depth of soil physical barriers such as compacted layers or differences in porosity, growth forms (e.g. tree, shrubs, herbs, grasses), stand species composition, water table depth (FAN et al., 2017), it seems logical that, in water-limited ecosystems, the climatic and hydrologic components may exert a pivotal influence on $R_{EF.}$ From the water standpoint, optimal R_{EF} is thought to be achieved by the trade-off between carbon investments in root tissues and associated water uptake benefits as suggested by GUSWA (2010), who also found that deepest root systems were found when potential evapotranspiration approaches rainfall rates. And indeed, Figure 2.30 shows that deeper rooting zones tend to be found at lower CWD levels, i.e. towards a balance between rainfall and evapotranspiration levels. Laio, D'Odorico, and Ridolfi (2006) found the deepest root systems in coarse-textured soils where the rainfall rates were slightly lower than evaporative demands. Given the marked predominance of coarse-textured soils in the sampled soils of this work, the textural effect on R_{EF} may be obfuscated. As shown in Figure 2.19, R_{EF} values were highly variable across the sampled sites (0.3 – 2.0 m in non-restrictive soils; 0.35 to 1.75 in restrictive soils), even under similar climatic conditions. Beyond species characteristics, this overall variability may reflect local soil water status, infiltration rates and shallow water tables depth, and relief-driven drainage barriers, as has been suggested by FAN et al. (2017). Interestingly, paired sites with similar or distinct soil conditions were located in similar positions across the CWD × R_{EF} environmental space (labelled in Figure 2.30), providing some evidence that nutritional characteristics may be less influential in R_{EF}, at least for the studied soils. For example, JUV-01 and CJU-01 (Luvisol and Arenosol, respectively) and CGR-01 and MCS-02 (also Luvisol and Arenosol, respectively), had quite dissimilar chemical and physical characteristics, but similar R_{EF}. Nevertheless, soils with similar conditions (namely PAT-01 and PAT-02, both Luvisols) also showed equivalent $R_{EF,}$ GBR-01 and GBR-02 (Cambisol and Leptosol), which are chemically comparable but morphologically distinct (in terms of depth) also had equivalent R_{EF}. ARI-03 and ARI-04 (Alisol and Acrisol, respectively) support floristically similar semideciduous forests and have an equivalent P_A to CWD values, which may justify similar R_{EF} depths. Taken together, these results provide evidence of a climate-driven below-ground carbon investment in SDTFs of Caatinga. Pinheiro,

Costa e Araújo (2013) further suggested that R_{EF} may vary across different soil vegetation associations, with a marked capability of Caatinga to adapt to shallow soil profiles and a lack of spatial variability in R_{EF} within stands. Improved comprehension of plant rooting depth drivers is crucial to understanding global changes as Earth system models are particularly sensitive to the root depth parameter (FAN et al., 2017).

Finally, given that R_{EF} and general vegetation performance are believed to be largely driven by hydrologic parameters, Figure 2.31 shows that, contrary to what is often assumed, soils developed in sedimentary terrains, do not necessarily hold the higher maximum plant-available soil water contents (θ_P). Rather, the final water-holding capability is a function of both soil depth and soil texture-associated volumetric soil water (θ_v). Thus, θ_v among the deepest soil profiles (that is, 2 m) varied from 0.05 to 0.13 $m^3\ m^{-3}$, whereas soils as shallow as 0.8 m were able to hold water volumes comparable to the deepest profiles (Figure 2.31). Overall θ_v was found to be low compared to clayey soils of other Brazilian regions, which is markedly due to the tendency of overall coarse textures found in many Caatinga soils, at least across the current sampling. These results can potentially contribute to regional modelling efforts to characterise soil hydrologic characteristics of Caatinga.

Conclusions

In this chapter, it was shown that the common distinction often made between soils from ‘crystalline’ and ‘sedimentary’ terrains should be valid in most cases. However, there may be several exceptions. The properties of soils derived from sedimentary parent materials, crystalline and calcareous rocks had marked differences, especially in terms of available cations, soil pH, and total (macro and micro) nutrient contents. These results illustrate the high variability characteristics in Caatinga soils, even within sedimentary environments, often assumed to be more homogeneous.

Total phosphorus contents measured in this work are consistent with previous work that also measured $[P]_T$ in Caatinga soils. Karst-derived soils (S_{KAR}), however, had relatively higher P contents. These high contents are believed to be mostly present in low-solubility P forms, which should be counteracted by biological players. Additional sampling in karst environments (including the biological component) is desirable for understanding the peculiar dynamics of essential nutrients in these ecosystems, which should be strongly influenced by specific geochemical conditions of associated soils.

Total soil carbon concentrations were best explained by the soil sand fraction. The mean annual temperature, however, also appeared to be related to both $[C]_T$ and $[N]_T$ in sedimentary environments. This is suggested to be due to the likely lower physical protection in soils resulting from sedimentary parent materials. Considering that soils of semiarid regions may play a considerable role in the global carbon sink (MENEZES et al., 2021), understanding the dynamics underlying the persistence of SOC in these soils is considerably important for global carbon emissions issues.

Soil $\delta^{15}N$ values were shown to be driven primarily by climatic parameters in Caatinga, with a smaller effect from the carbon pool size. This result is consistent with several studies showing the control of the climate on N isotopic signatures. Considering the extreme environmental variability of Caatinga, and echoing Swap et al. (2004), how could climate forces account so strongly for variation in isotopic composition changes? The soil $\delta^{15}N$ map produced for the Caatinga region may potentially contribute to the understanding of the N cycle in this region. Furthermore, the results presented here suggest a mark of 0.8 m a^{-1} P_A, which is suggested to potentially be the point where I_E becomes more relevant than the climate in determining the isotopic discrimination in Caatinga soils. However, soils with I_E in the 40 – 80 $mmol_c\ kg^{-1}$ range are particularly lacking in this study (Figure 2.17) and additional sampling in soils within this I_E range would be helpful to clarify the isotopic behaviour in less weathered or more fertile soils covering the variations in P_A within the region.

Regarding soil water, the results presented here illustrate that soils located in sedimentary terrains do not necessarily have a greater maximum plant-available soil water. If on the one hand, deeper soils translate into potentially larger physical reservoirs, on the other hand, many deep soils in the Caatinga are expected to hold coarse textures (that is, lower volumetric soil water content associated with soil texture).

Finally, the simple model proposed in Table 2.4, including the $\sum_{RB} \times pH_{H20}$ term, represented 94% of the variation in soil $\sum_B$ (available Ca + Mg + K + Na). Considering that methods to estimate the available and total bases are extremely time-consuming (especially sulfuric acid digestion – SAD) and given the high predictive power of the generated proposed model, the parameters could serve as a surrogate tool for estimating values from one method to another (if soil pH_{H2O} values are also available).

Chapter 3

Soil and climate influence on above-ground woody biomass of Brazilian SDTFs: a regional assessment in geologically distinct stands

Chapter 3 – Soil and climate influence on above-ground woody biomass of Brazilian Seasonally Dry Tropical Forests: a regional assessment in geologically distinct stands

3.1 Introduction

Stand-level above-ground biomass (AGB) integrates several processes, including primary productivity, tree recruitment, and mortality (LLOYD et al., 2009). Much of the research in the tropics concerning AGB has been carried out in rainforests (e.g. BARALOTO et al., 2011; LAURANCE et al., 1999; QUESADA et al., 2012; SULLIVAN et al., 2020), but seasonally dry tropical forests (herein SDTFs) are an important component of tropical vegetation, although with lower carbon stocks. This type of vegetation is usually associated with semiarid climates and, although they once have been estimated to represent 42% of the landmass covered by tropical forests (MURPHY; LUGO, 1986a), nowadays it is estimated that they are reduced to less than 10% of their original coverage in many countries (DRYFLOR, 2016), with a global gross loss of its coverage estimated to be 11% between 2001 and 2020 compared to the year 2000 (OCÓN et al., 2021). Moreover, despite storing relatively less carbon and having a simpler structure compared to their wetter counterparts (BECKNELL; KUCEK; POWERS, 2012a), SDTFs have been suggested to be increasingly relevant in carbon cycle inter-annual variability, with a substantial component of the record land carbon sink of 2011 (LE QUÉRÉ et al., 2013) associated with ecosystems of the Southern Hemisphere semiarid (POULTER et al., 2014). Therefore, understanding which environmental factors influence AGB accumulation is critical to understanding how global changes could affect this property and associated ecological services.

Above-ground ground biomass in the Caatinga is known to be a multi-driven property, especially considering the human-modified characteristic of the region (SOUZA et al., 2019; CASTANHO et al., 2020a). An estimate from a satellite product showed that, in the year 2000, the stand-level AGB distribution was extremely heterogeneous across Caatinga (CASTANHO et al., 2000; Section 1.8, Chapter 1). Such a heterogenous distribution of AGB reflects human modifications, which led to a mosaic of stands ages, but also reflects the environmental influence, i.e. geologically derived soil substrates, AGB potential of species, and climate. The latter is considerably associated with different plant physiognomies and standing AGB across the region (CASTANHO et al., 2020b). For this reason, the opportunity to evaluate the influence of environmental drivers on the vegetation attributes of mature stands is relatively rare in the region. Considering that the Caatinga usually exhibits negative water balances and high precipitation seasonality (SAMPAIO, 1995), SDTFs growing in the region should be

primarily limited by water availability, as for other SDTFs worldwide (MOONEY; BULLOCK; MEDINA, 1995, BECKNELL; KUCEK; POWERS, 2012; ALLEN et al., 2017).

Importantly, forecasted climate scenarios warn of potential changes in rainfall regimes in the tropical range by the end of the 21st century, and geographically comparative studies are essential to understand how SDTFs are sensitive or resistant to these changes (ALLEN et al., 2017). So far, most studies comprising larger or even global scales have only tested climate variables as AGB predictors (e.g. BECKNELL et al., 2012).

Among the few studies that have evaluated the influence of soil properties on AGB in semi-arid zones, Souza et al. (2019a) showed that soil properties (summarised as orthogonal axes) affect AGB, vegetation sprouting capacity, and community composition. Similarly, Maia et al. (2020a) reported interactions between soil attributes and climate-shaping above-ground woody biomass and community assembly of SDTFs in the transition zone between the Cerrado and Caatinga biogeographic domains. Souza et al. (2019b) found a minor role in soil fertility to explain AGB in SDTFs in Catimbau National Park, Pernambuco state. Prado-Júnior et al. (2016) suggested a negative effect of soil calcium on SDTFs productivity, with no direct influence on initial standing AGB. Peña-Claros et al. (2012) have found a considerable role of soil fertility and texture to explain a suite of dry forest properties including basal area, stems density, species richness and taxonomic diversity. Interestingly, the effect of soil fertility was more pronounced in dry than in moist forests. Peña-Claros et al. (2012) argued that this counterintuitive effect was because the soils of moister forests in their study had a general high-fertility status, thus being less responsive to site variations in nutrient concentrations. Nevertheless, all these works were limited to relatively small geographic ranges. If climate factors are believed to drive AGB over larger scales, factors such as soil properties and topography are likely to exert a greater influence at smaller scales, i.e., local to regional (SIEFERT et al., 2012). As the Brazilian Caatinga occupies an area of approximately. 862,818 km², covering ca. 10.1% of Brazil's territory (IBGE, 2019a), both soil and climate are likely to affect AGB in the region.

In this context, noting the extreme environmental variability of Caatinga (Chapter 1), it should also be noted that not only has the complex geological history influenced the present flora assembly but also determined the soil parent materials found in the region. Therefore, accounting for the ability of most species to tolerate water-stressed conditions, geologically-derived soil parent materials are believed to be the main factor for plant species diversity and endemism (FERNANDES et al., 2022).

Generally speaking, it can be expected that the taxonomic/phylogenetic composition of a given community will reflect its respective functional attributes, with the latter ultimately being considered the mechanistic connection between plant species assembly and ecosystem functioning (LOHBECK et al., 2015; DÍAZ et al., 2006). Soil properties have already been demonstrated to influence the functional composition of plant communities (Section 1.9, Chapter 1). For example, an inverse correlation between soil cations and wood density was reported by Quesada et al. (2012) and Lira-Martins et al. (2019). In turn, wood density might reflect different life histories and strategies to cope with environmental adversities. Soil nutrients may also influence other plant attributes, with Jager et al. (2015) examined the responses of functional traits to soil fertility and found a clear trend of species associated with low-fertility soils showing 'slow leaves traits', i.e. high wood density, low P, low N and high leaf mass dry content (LMDC) as opposed to species occupying high fertility soils.

Conceptually, if geologically-derived soil properties influence community attributes characteristics and the latter influence vegetation dynamics and standing biomass, geology can be seen as a major factor in shaping soil properties and, ultimately, influencing vegetation properties. Therefore, both community-weighted trait means (CWM), i.e. the mean trait values weighted by their relative abundance in a given community (LAVOREL et al., 2008), and functional diversity indexes (MASON et al., 2005), that is, the patterns of how a given community fills a certain niche space can potentially provide valuable information in exploring these relationships (Section 1.9, Chapter 1).

Concerning the role of specific soil nutrients in driving vegetation properties, several studies have pointed out how the availability of soil nutrients can modulate vegetation performance and attributes. Nitrogen (N) and phosphorus (P) are essential nutrients without which plants cannot complete their life cycle. Both elements are involved in the key physiological process, with a marked influence on photosynthetic rates (DOMINGUES et al., 2010) and numerous other processes. For example, N is present in chlorophyll, nucleic acids (DNA and RNA), proteins and enzymes that regulate water and nutrient uptake, while P constitutes sugar phosphates, and nucleic acids, with a key role in energy absorption, storage, and conversion to adenosine triphosphate (ATP), a crucial biomolecule in biochemical reactions in plants (TAIZ; ZEIGER, 2014). Given that some Caatinga soils tend to show relatively low P contents (Chapters 1 and 2; SILVEIRA; ARAÚJO; SAMPAIO, 2006), phosphorus might be a concern in these soils, although field-based validation for this possibility in natural stands is

rare. On the other hand, N-availability in SDTFs is considered even higher than in humid places (ARANIBAR et al., 2004; SWAP et al., 2004; DA SILVA et al., 2017), which is also evidenced by high nitrogen concentrations and high $\delta^{15}N$ values commonly found in the leaves of Caatinga species (MARTINELLI et al., 2021).

Soil cations are also likely to play an important role in water-stressed environments. Potassium (K) is an osmotically active ion involved in several physiological processes and has already been shown to be an important modulator of the structure of tropical woody vegetation (LLOYD et al., 2015). Calcium (Ca), in turn, is involved in wood construction and the onset of cambial activity after periods of reduced physiological activity (FROMM, 2010). Furthermore, Ca is involved in the regulation of complex physiological responses to various abiotic stresses (SHARMA; KUMAR, 2021). Magnesium (Mg) is involved in essential plant processes such as photosynthesis and enzyme activation, so its deficiency can limit plant performance (CHEN et al., 2018). Although sodium (Na) is not an essential nutrient for plants, it has been reported to potentially substitute some K functions in plants (WAKEEL et al., 2011). High concentrations of Na salts are believed to be an issue in many semiarid areas, but only specific environments in the Caatinga are reported to exhibit high Na concentrations (i.e. low valleys), largely due to the modern exorheic drainage pattern of the region (AB'SÁBER, 1974). Aluminium (Al) can impair root development when present in toxic concentrations (BOJÓRQUEZ-QUINTAL et al., 2017). In the Caatinga, Al toxicity is more likely to potentially occur in some regions (e.g. in acid Alisols and Acrisols of the Parnaíba Basin) rather than in others with neutral to alkaline soils, where Al activity should be negligible. Essential micronutrients (B, Fe, Zn, Mn, Mo, Cu, and Cl) have been hypothesised to explain some variations in vegetation attributes, but little is known about this possible influence on Caatinga vegetation (SAMPAIO, 2010). Except for molybdenum, low availability of micronutrients is likely to occur at high soil pH (> 7), which can be the case for more alkaline soils in Caatinga.

In addition to the role of soils in fulfilling plant nutritional needs, soil properties play a decisive role in water availability. Soil texture, largely determined by original parental materials, is likely to be the most important soil property (PALM et al., 2007) influencing soil fertility, water-holding capability, and the movement of water and gases (UPADHYAY; RAGHUBANSHI, 2020). Soil mineralogy and soil organic matter (SOM) are the two additional properties that contribute to soil water-holding capacity (PALM et al., 2007).

Landscape physiography may also influence water retention in a given environment as topography influences the runoff and drainage processes, also redistributing solutes in the

landscape (MARKESTEIJN et al., 2010). Soil depth is also important, ultimately controlling the size of the potential plant-available water reservoir, and shallow soils are believed to be beneficial under certain circumstances. For example, Lloyd et al. (2015) demonstrated through numerical simulations that soil water availability is improved by a shallow impermeable layer as it constrains water losses due to drainage. In contrast to deep well-drained soils typical of other Brazilian regions (e.g. *Cerrado* and *Amazônia*), impermeable layers are often found in the Caatinga region, particularly in soils of the Crystalline Domain, with soil depth commonly reaching 0.5 - 1.0 m. In such conditions, barriers to water drainage can be beneficial in provisioning water to the vegetation, but such water is rapidly depleted in a few weeks if new rains do not occur (SAMPAIO, 2010).

Potentially complicating the analyses here is the fact that environmental predictors (and response variables) sampled over large geographical extensions have a high probability to show spatially autocorrelated data. QUESADA et al. (2012) provide a detailed overview of this matter and discuss alternative approaches to deal with spatially structured data. Briefly, spatial structures may be attributable to predictors, dependent variables only, and model residuals only, with these approaches, differently relating to underlying processes accounting for variation in a given response variable.

The current study reports on the climate, soil and vegetation properties of 29 SDTFs stands in the semiarid Caatinga that covers a rainfall gradient and different geological affiliations (i.e. crystalline – S_{CRY}, sedimentary – S_{SED} and karst – S_{KAR}), consequently exhibiting disparate edaphic properties. The following questions were addressed:

1) Do soil chemical and physical properties, climate, and their interactions influence the observed variability of stand-level above-ground woody biomass (AGB_W)?

2) Is the effect of climatic and edaphic factors the same for stands of different geological affiliations?

3) Do soil chemical characteristics and soil texture influence community-weighted mean traits, namely maximum stem diameter of adults (CWM_{dmax}) and wood density (CWM_{wd}) and their associated functional diversity metrics, namely functional richness (F_{Ric}), functional evenness (F_{Eve}) and functional divergence (F_{Div})

4) Do functional properties account for variations in AGB_W?

3.2 Material and Methods

3.2.1 Study sites

Data used here come from 29 sites distributed along the Brazilian Caatinga (Figure 1.2, Chapter 1), encompassing a wide range of edaphic conditions, from only slightly weathered soils mostly developed from crystalline rocks (S_{CRY}) to much more weathered soils from sedimentary parent materials (S_{SED}). Sampling included three vegetation stands in karst areas (S_{KAR}). Respective reference soil groups (RSGs) for each site can be accessed in Table 2.1, Chapter 2. Mean annual precipitation (P_A) ranged from 0.512 m a^{-1} at CND-01 (Bahia) to 1.363 m a^{-1} m in PSC-02 (Piauí), whereas the mean annual temperature (T_A) ranged from 20.5 °C in MOR-01 (Bahia) to 26.8 °C at PFF-01 (Rio Grande do Norte). Above-sea level elevation of the sites varied from 99 m in PFF-01 to 944 m in MOR-01 (Table 2.1, Chapter 2). Vegetation structure varied from open canopies of only 4 – 7 m in height up to 25 – 30 m closed canopies. Study sites consisted of well-conserved old-growth stands. Sporadic grazing and occasional timber logging, however, could not be disregarded for some sites. The slope at the studied sites was typically flat, with a few exceptions (Table 2.1, Chapter 2). Vegetation inventory and soil sampling were undertaken in three intensive fieldwork campaigns (2017, 2018, and 2019), each for *ca*. two, three, and one month, respectively. Vegetation sampling was undertaken during the late wet season to reflect the maximum vegetative development.

3.2.2 Stand structure

Standardised floristic and structural inventories were carried out following the 'The DryFlor Field Manual for Plot Establishment and Remeasurement' (MOONLIGHT et al., 2021). Briefly, a 100 x 50 m (0.5 ha) plot was established and sub-partitioned into 50 subplots (10 x 10 m or 0.01 ha) at each site. All trees having stems with a diameter either at breast height (DBH − 1.30 m from the ground level) or at 0.3 m from the ground level (DGL) ≥ 5 cm were measured in all subplots. Trees were identified in the field at the species level and voucher specimens were incorporated into the Herbarium of Feira de Santana State University (HUEFS; Feira de Santana, Bahia, Brazil) collection.

3.2.3 Soil sampling and laboratory analyses

Comprehensively described in Sections 2.2.2 and 2.2.3, Chapter 2.

3.2.4 Maximum plant-available soil water (θ_P)

Comprehensively described in Section 2.2.6, Chapter 2.

3.2.5 Climatological data

Comprehensively described in Section 2.2.7, Chapter 2.

3.2.6 Geological surveying

Comprehensively described in Section 2.2.5, Chapter 2.

3.2.7 Above-ground woody biomass calculations

Estimates of individual tree above-ground woody biomass (AGB_W) were obtained using an allometric equation as provided in SAMPAIO and SILVA (2005). The Eqn. (3.1) considers only the diameter at the ground level (DGL) as the input variable according to:

$$AGB_W = 0.0644 \times DGL^{2.3948}, \quad \text{Eqn. (3.1)}$$

where AGB_W stands for the oven-dry above-ground tree biomass (kg), and DGL is the diameter at the ground level (cm).

A second equation provided in SAMPAIO and SILVA (2005) was used for estimating the biomass of cactus individuals. Such an equation was developed from individuals of *Cereus jamacaru* DC.:

$$AGB_C = 0.0268 \times DGL^{2.3440} \quad \text{Eqn. (3.2)}$$

Finally, palm tree biomass (only 35 individuals in the dataset) was estimated using equation 3.4 from SALDARRIAGA et al. (1988), *viz.*

$$\ln AGB_P = -6.3789 - 0.877 \ln X1 + 2.151 \ln X2, \quad \text{Eqn. (3.3)}$$

where AGB_P stands for the oven-dry above-ground palm tree biomass (kg), $X1$ stands for 1/DBH² (diameter at breast height taken at 1.30 m from the ground), and $X2$ represents the palm tree height (H).

Further information on the chosen equations and a comparison with the dry forest global allometric equation (CHAVE et al., 2014) is provided in Supplementary Section S3.1 and Figure S3.1.

3.2.8 Community-weighted trait means (CWM) and functional diversity

Two community-weighted trait means were calculated: community-weighted maximum stem diameter (CWM_{dmax}) and community-weighted mean wood density (CWM_{wd}). Both are considered a 'whole plant trait'. Species' wood density values were extracted from the global wood density database (CHAVE et al., 2009, ZANNE et al., 2009). When unavailable at the species level, wood density values of genus or family were used. Botanical names were checked and adjusted according to the Brazilian Flora 2021 with the flora package version 0.3.5 (CARVALHO, 2020). The species' maximum stem diameter reflects adult sizes and was calculated as the upper 0.95 percentile of those trees with a stem diameter ≥ 0.1 × the diameter (cm) of the thickest tree observed in a given population. This approach was chosen because, within alternative approaches, it was shown to be the least sensitive to sample sizes as well as providing robust estimates for both large and smaller species (KING; DAVIES; NOOR, 2006). Each trait was weighted according to the individual species' basal area, which is believed to better indicate plant performance than abundance (PRADO-JÚNIOR et al., 2016). Functional diversity indexes, i.e. functional richness (F_{Ric}), functional divergence (F_{Div}) and functional evenness (F_{Eve}) were calculated using the *FD* package (LALIBERTÉ; LEGENDRE; SHIPLEY, 2022).

3.2.9 Data analysis

During the exploratory phase of the data, a correlation matrix reporting Kendall's rank correlation coefficients (τ) and associated probabilities was built. In addition, OLS linear regressions and graphical inspections were used to first assess the predictive ability of individual soil and climate variables to predict $AGB_{W.}$ Then, a linear mixed-effect model (LMM), along with a multi-model inference approach was used to investigate to which extent soil and climate associations account for AGB_W across the studied sites. Within each 0.5 ha plot (29 in total), two subplots of 0.25 ha were considered (n=58). The analytical design was thus subplots (0.25 ha) nested within plots (0.5 ha). This procedure was adopted to allow the inclusion of a higher number of variables into the same models with low risks of overfitting issues (Section 1.4.1 of Burnham and Anderson, 2002).

As many AGB_W candidate predictors were strongly correlated, pairwise variables with Pearson correlation ($r \geq |0.70|$) were never simultaneously included as candidate variables. Mean annual precipitation (P_A) and climatic water deficit CWD_{adj} were included to represent the overall water input and climatic water balance in studied ecosystems. The maximum

temperature of the warmest month (T_{MAX}) was included as the key thermal variable. T_{MAX} reflects high-temperature events throughout the year and can be used to examine if the function of a given community is affected by high-temperature anomalies (O'DONNELL; IGNIZIO, 2012).

Soil predictors (mean values for the upper 0.3 m layer) were selected using similar criteria. Given that some soil properties were correlated to each other [i.e. exchangeable cations, sum of bases ($\sum_B$), effective cation exchange capacity (I_E), and soil pH_{H2O}], individual performances of these collinear predictors were assessed by replacing them one by one across the 'global model' of Eqn. (3.4) presented below. Thus, relative importance values (RIV), variance inflation values (VIF), global model marginal r^2 (r^2m), global model AICc values, and graphical analysis of modelled responses were undertaken to compare the model performance of each alternative model. The *importance* function of the *MuMin* package (BARTON et al., 2020) represents the sum of the Akaike weights of all models that include a given variable in a given ΔAICc range. Relative importance values decreased following I_E > $[Ca]_{ex}$ > $\sum_B$ > pH_{H2O} > $[Mg]_{ex}$ > $[Na]_{ex}$ > $[K]_{ex}$ > $[Al]_{ex}$ (0.96, 0.95, 0.87, 0.64, 0.46, 0.39, 0.31 and 0.15 respectively). Despite I_E showing a slightly higher RIV than $[Ca]_{ex}$ (0.96 *versus* 0.95, respectively), the remaining evaluated criteria suggested that $[Ca]_{ex}$ is a better predictor. For instance, I_E had a higher VIF than $[Ca]_{ex}$ (3.51 and 3.25, respectively). Moreover, the global model of Eqn (3.4) including $[Ca]_{ex}$ as the 'cation term' showed r^2_m = 0.49 and AICc = 92.95, *versus* r^2_m = 0.46 and AICc = 94.67 for I_E. Also of note is that $[Ca]_{ex}$ had a higher effect size in both full and conditional average models. That is, $[Ca]_{ex}$ showed β_1 = 0.38 and β_1 = 0.39 for the full and conditional average models, respectively, whereas I_E showed β_1 = 0.35 and β_1 = 0.37 for the full and conditional average models, respectively. Based on these metrics and $[Ca]_{ex}$ being the dominant cation in the soil sortive complex of most study sites (Table 2.2 and Figure 2.4), subsequent analyses were performed by adopting the inclusion of $[Ca]_{ex}$. The alternative inclusion of I_E would lead to relatively similar results quantitatively speaking, but with small differences in interpretation due to the properties of the predictors.

Given the important role of these nutrients in plant functioning, soil total phosphorus $[P]_T$ and soil total nitrogen $[N]_T$ were also included as potential AGB_W predictors. Concerning soil physical properties, maximum plant-available soil water (θ_P) was calculated considering the full profile, i.e. the water until the maximum soil profile depth (any hardened layers usually impervious to water drainage or a maximum of two meters deep). Plant-available soil water considering only the layer whereby roots were observed ($^*\theta_P$) and potential interactions along

with soil depth and the presence (or absence) of a shallow impermeable layer (I_{LAYER}) were also tested.

Soil and climate values were considered at the plot level considering that subplots largely share similar climate and soil properties, especially considering the marked differences existing among sites. Variance inflation factor values (VIF) were also verified among the selected predictors, whereby none of them exceeded VIF ≥ 3 (the exception was $[\mathrm{Ca}]_{ex}$; VIF = 3.25). Much higher VIF values (i.e. ≥ 10) are usually considered a critical threshold (DORMANN et al., 2013).

To facilitate the interpretation of model coefficients, predictors were standardised (i.e. the mean of each predictor was subtracted from each observed value and then divided by the standard deviation), providing comparative scores, 'effect size', among predictors using the *caret* package (MAX et al., 2020). Because the analysis strategy tacitly implied non-independent observations, sites were included as random structures in the model (HARRISON et al., 2018), accounting for the nestedness present in the analytical approach here undertaken (observations were correlated within sites).

Equation 3.4 expresses the global model built for the subsequent analysis:

$$\log(\mathrm{AGB_w}) = \beta_0 + \beta_1\theta_\mathrm{P} + \beta_2 P_\mathrm{A} + \beta_3[\mathrm{Ca}]_{ex} + \beta_4\mathrm{CWD_{adj}} + \beta_5\theta_\mathrm{P} \times \mathrm{CWD_{adj}} + \beta_6[\mathrm{Ca}]_{ex} \times \mathrm{CWD_{adj}} + \beta_7 T_\mathrm{MAX} + \beta_8\log[\mathrm{N}]_t + \beta_9\log[\mathrm{P}]_t + (1|\mathrm{site}) + \varepsilon \quad \text{Eqn. (3.4)}$$

where β_0 represents the model intercept, $\beta_{1\ldots(n)}$ represents coefficients associated with model terms and ε is the residual error.

Once fitted, the distribution of the model residual distribution was both statistically and graphically evaluated. The response variable was log-transformed to attain the assumption of normality and reduce the heterogeneity in the variance. Spatial correlograms with distance class increments as available in the *ncf* package (BJORNSTAD; CAI, 2020) were used to check for any spatial structuring of the models' residues. Additionally, the potential presence of spatial structures was also evaluated through the recently developed approaches as described in Bauman et al. (2018a) and Bauman et al. (2018b). The *listw.candidates* function of the *adespatial* package (DRAY et al., 2021) was undertaken to test a small number of distance and graph-based spatial weighting matrices (SWM), resulting in no significant spatial dependencies in the model's residues.

All possible combinations of predictors (including interaction terms) were tested with the aid of the *MuMIn* package (BARTON, 2020). As an additional control of potential (multi)collinearity issues, predictors with Pearson's correlation coefficient ($|r| \geq 0.6$) were prevented to be simultaneously included in the same models. This process generated 137 unique models, with the maximum number of predictors in each model being constrained to 6, thus ensuring approximately 10 observations *per* model term.

Subsequently, an information-theoretic (I-T) approach was used to deal with model uncertainty by selecting those models with ΔAICc < 4 (BURNHAM; ANDERSON; HUYVAERT, 2011; HARRISON et al., 2018). Analyses were also run using ΔAICc < 2 as a cutoff value with very similar results with no consequences for the interpretation of the results. From the 19 models retained (ΔAICc < 4), coefficients were averaged through the *model.avg* function available in the *MuMin* package (BARTON, 2020). Model averaging was achieved through the function *model.avg* available in the *MuMIn* R package (BARTON, 2020). The results of both full and conditional ('subset') average models are presented. The 'full' averaging approach dictates that each variable is included in every model (setting the coefficients to zero in the models where the term is absent), whereas the 'conditional' average approach considers only those models where the parameter appears (BARTON, 2020). In both cases, averaged coefficients were weighted according to Akaike weights. The full average is a type of shrinkage estimator, and coefficients of variables with weak support tend towards zero. The global model's marginal (r^2_m) and conditional (r^2_c) determination coefficients are also reported. The former reports only on fixed effects, while the latter refers to both fixed and random effects. The r^2 reported here consists of a revised statistic based on (NAKAGAWA; SCHIELZETH, 2013).

The *importance* function (also available in *MuMin*) was also used to calculate the relative importance value (RIV) of each model term. Model predictions were performed using the coefficients from the full average model. Importantly, the conditional average model coefficients are usually considered inappropriate for model predictions, whereas the full model coefficients (with shrinkage) are recommended in such instances (MAZEROLLE, 2020). Indeed, associated R packages do not even provide a function to make predictions with conditional model coefficients. Consequently, less supported averaged coefficients have little influence on modelled responses.

In addition, potential differences in AGB_W according to the geological grouping undertaken in this study (i.e. S_{SED}, S_{CRY} and S_{KAR}) were evaluated through a non-parametric robust Kruskal-Wallis test (χ^2). Subsequently, a series of LMM linear regressions were used to assess the predictive ability of individual soil and climate predictors on AGB_W within each category, with relationships, also shown for the entire dataset level.

Both evaluated CWM traits and functional diversity indexes were also compared among geological categories using the Kruskal-Wallis test (χ^2), followed by the Wilcoxon-Mann-Whitney rank-sum test with Benjamini-Hochberg (BH) correction for multiple comparisons. In addition, bivariate linear relationships between CWM traits and functional diversity indexes were tested through ordinary least squares (OLS) linear regression models. Finally, a Spearman's rank correlation coefficient (ρ) matrix was built to evaluate potential associations between soil chemical and physical properties and community functional properties. For the graphical representation of results, the *alphahull* package (PATEIRO-LÓPES; RODRÍGUEZ-CASAL, 2022) was used to constrain the heat maps simulations to the actual environmental envelope found in the dataset. Finally, all graphs were constructed using the *ggplot2* package (WICKHAM et al., 2021), and all analyses were carried out in the environment R version 4.1.1 (R CORE TEAM, 2021).

3.3 Results

In this work, the inclusion (or not) of spatial filters (here Moran Eigenvectors Maps; MEMs) in those models with spatially structured residuals was adopted. This is thought to reflect the influence of environmental predictors on a given response once the potential effects of other sources of variation have been filtered (e.g., endogenous processes attributable to plant species) (QUESADA et al., 2012). Interestingly, the studied response variable (AGB_W) did not show spatial structures, likely reflecting the spatial variability of AGB_W in Caatinga (CASTANHO et al., 2020a; CASTANHO et al., 2020b). On the other hand, some edaphic variables (mainly associated with cations) have shown moderate values of Global Moran's *I* (coefficient of spatial autocorrelation) (0.40 to 0.50; $p < 0.05$), likely reflecting patches of soils conditioned by geological substrates. Global Moran's *I* values for climatic variables were relatively higher (i.e > 0.60; $p < 0.05$), which is expected for the interpolated climatic values adopted in this study.

3.3.1 Above-ground woody biomass

In total, 18,201 stems (DGL ≥ 5 cm) were recorded across 29 plots of 0.5 ha, of which 1,098 individuals were *cacti* and 35 were palm trees. The mean AGB_W was 32.55 ± 22.35 Mg ha^{-1} (minimum = 4.87 Mg ha^{-1} at CJU-01 and maximum = 85.65 Mg ha^{-1} at JUV-01). Mean stem density (counts ha^{-1}) was 1255 ± 489 (minimum of 492 at CJU-01 and maximum = 2534 at SDA-02); mean basal area (B_A) was 12.9 ± 7.1 m^2 ha^{-1} (minimum of 2.44 m^2 ha^{-1} at CJU-01 and maximum of 28.79 at JUV-01). Above-ground woody biomass values did not differ among geological categories as indicated by a Kruskal-Wallis test ($\chi 2$) at $p < 0.05$ (Figure 3.1).

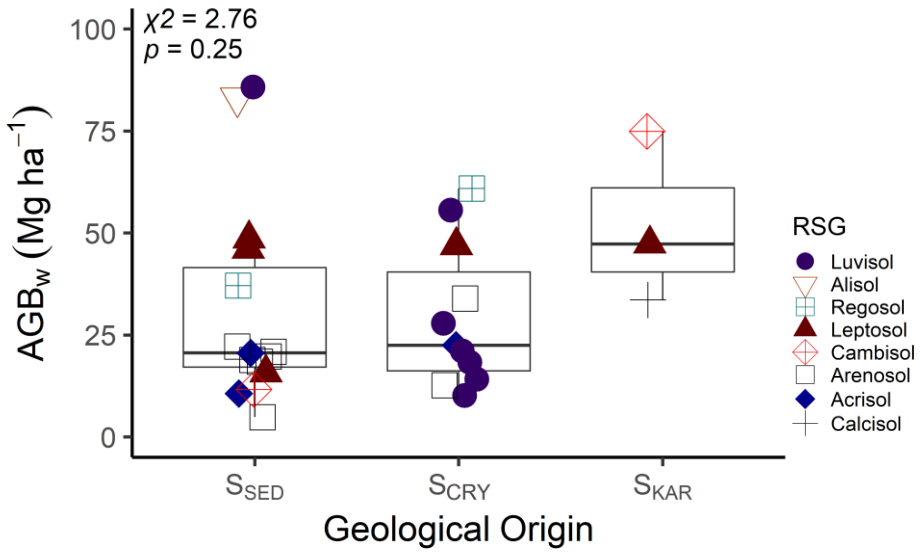

Figure 3.1: Above-ground woody biomass (AGB_W) values according to soil geological affiliation. Reference soil groups (RSGs) are shown.

Figures 3.2-a and 3.2-b show averaged coefficients, standard errors and confidence intervals resulting from conditional and full average models, respectively. The conditional model (Figure 3.2-a) provides the β coefficients averaged only from within those models where the variable appeared, i.e. P_A (β = 0.28); $[Ca]_{ex}$ (β = 0.40); $\Theta_P \times CWD_{adj}$ (β = -0.25); $[Ca]_{ex} \times CWD_{adj}$ (β = -0.43) and $[P]_t$ (β = 0.23). The β coefficients from the full averaged model (Figure 3.2-b) were shrunk towards zero for model terms with low frequency across the selected models.

Nevertheless, P_A ($\beta = 0.25$); $[Ca]_{ex}$ ($\beta = 0.38$) and $[Ca]_{ex} \times CWD_{adj}$ interaction ($\beta = -0.17$) remained as the most supported terms as they had relatively high β coefficients even in the full average model.

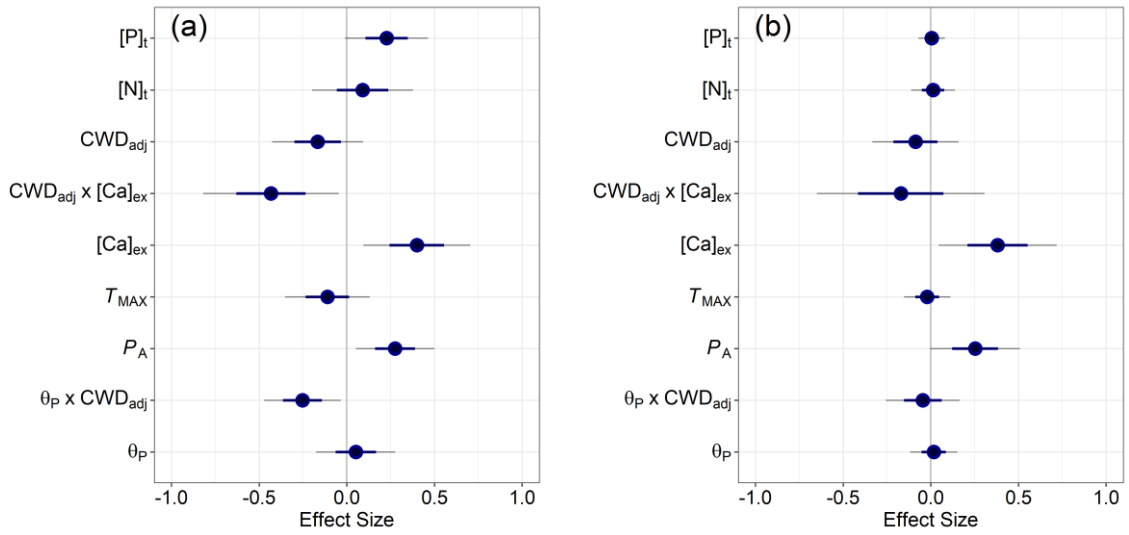

Figure 3.2: Edaphic and climatic effects on AGB_W of Caatinga stands. Points represent coefficients of averaged linear mixed effects models. a) Conditional average model coefficients; b) Full average model coefficients. In the full average model, poorly supported coefficients tend to be shrunken towards zero. Coefficients were standardised, thus representing changes in log (AGB_W) for one standard deviation change in the predictor variable (effect size). Error bars show standard error (dark blue) and 95% confidence interval (thin gray). Further information on 'conditional' and 'full' average models is provided in Section 3.2.9 of this thesis.

Figure 3.3 shows RIV for all terms included in the global model of Eqn. (3.5) above. The retention of a variable across the models and associated RIV depends on the other variables included as 'candidate predictors', which may help explain some variables with relatively high RIV and low effect size (e.g. CWD_{adj}). It is of note that $[Ca]_{ex}$ and P_A, which showed the highest standardised coefficients for both conditional and full averaged models, also had the highest RIV (0.95 and 0.92, respectively). The RIV values below ≤ 0.9 were, in descending order, $CWD_{adj} = 0.53$, $[Ca]_{ex} \times CWD_{adj} = 0.40$, $\Theta_P = 0.33$, $T_{MAX} = 0.18$, $\Theta_P \times CWD_{adj} = 0.18$. The lowest RIV values were attributed to $[N]_t = 0.15$ and $[P]_t = 0.02$, which also corresponded to small effect sizes.

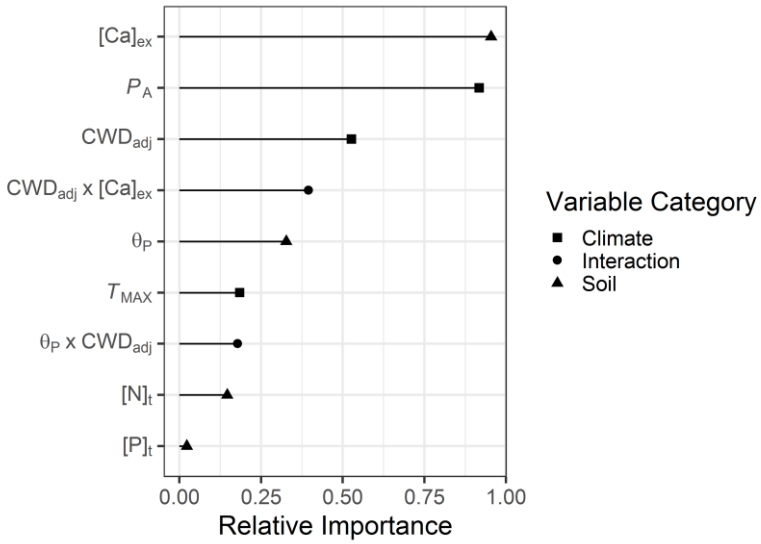

Figure 3.3: Relative importance values (RIV) of each variable included in the global model of Eqn. (3.5). Symbols represent variable categories.

As the interactive effects detected among variables were complex, Figures 3.4 and 3.5 illustrates the predicted responses of AGB_W through *heat maps*. This analysis shows the AGB_W predicted responses ($\hat{AGB}_W$) related to environmental gradients by varying the interaction terms with all other model terms held constant (for instance, at their dataset average). Figure 3.4 shows $\hat{AGB}_W$ as influenced by P_A held at: a) the dataset average - 1 standard deviation (SD); b) dataset average; c) dataset average + 1 SD; d) dataset average + 2 SD (0.6, 0.8, 1.01, 1.21 m a^{-1}, respectively). Simulations for all possible combinations within the maximum and minimum observed CWD_{adj} and Θ_P environmental domain were performed. Actual AGB_W values are also shown in the specific panels associated with their respective P_A regimes.

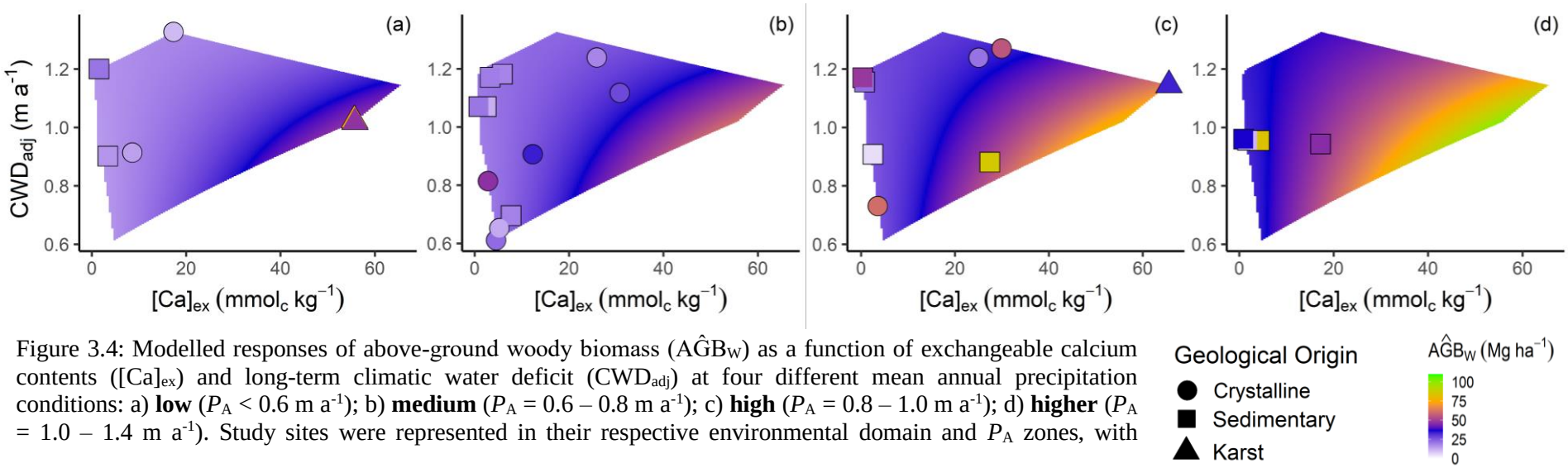

Figure 3.4: Modelled responses of above-ground woody biomass ($A\hat{G}B_W$) as a function of exchangeable calcium contents ($[Ca]_{ex}$) and long-term climatic water deficit (CWD_{adj}) at four different mean annual precipitation conditions: a) **low** (P_A < 0.6 m a^{-1}); b) **medium** (P_A = 0.6 – 0.8 m a^{-1}); c) **high** (P_A = 0.8 – 1.0 m a^{-1}); d) **higher** (P_A = 1.0 – 1.4 m a^{-1}). Study sites were represented in their respective environmental domain and P_A zones, with

The modelled responses presented in Figure 3.4 suggest that $[Ca]_{ex}$ levels strongly influence $A\hat{G}B_W$ at any examined P_A zones. This effect, however, was also modulated by the intensity of the long-term climatic water deficit (CWD_{adj}). For example, when $[Ca]_{ex}$ is low (e.g. 5 $mmol_c\ kg^{-1}$), $A\hat{G}B_W$ was not inferred to vary markedly with changes in CWD_{adj}. However, at higher $[Ca]_{ex}$ (e.g. 40 $mmol_c\ kg^{-1}$), the modelled influence of CWD_{adj} on $A\hat{G}B_W$ increases. The magnitude of the effect was also sensitive (in an absolute sense) to the P_A regime. For example, at the lowest precipitation (P_A = 0.6 m a^{-1}) and taking $[Ca]_{ex}$ as constant in 50.37 $mmol_c\ kg^{-1}$, $A\hat{G}B_W$ varies from 28.2 to 46.1 Mg ha^{-1} across the CWD_{adj} range (1.20 to 0.98 m a^{-1}). Nevertheless, for the highest precipitation zone (P_A = 1.2 m a^{-1}), when $[Ca]_{ex}$ is 50.37 $mmol_c\ kg^{-1}$, AGB_W varies from 60.10 to 98.41 Mg ha^{-1} across the CWD_{adj} range (1.20 to 0.98 m a^{-1}). As the model has a log-linear nature, the exponentiated AGB_W values (geometric means) differ in magnitude according to different levels of P_A, but the ratio of these variations was constant (64% for both cases). It is noteworthy that S_{SED} sites occur across almost the full range of CWD_{adj}, but with $[Ca]_{ex}$ levels, as expected (and except for JUV-01), at relatively low values ($\leq$ 10 $mmol_c\ kg^{-1}$). On the other hand, S_{CRY} sites showed large variability in CWD_{adj}, with $[Ca]_{ex}$ levels generally $\geq$ 10 $mmol_c\ kg^{-1}$, whereas S_{KAR} sites always had invariably $[Ca]_{ex} \geq$ 50 $mmol_c\ kg^{-1}$ and high CWD_{adj} values ($\geq$ 1.0 m a-1). Moreover, only S_{SED} sites were encountered in the highest P_A zone (Figure 3.4-d).

Following the same approach, Figure 3.5 shows the interaction between maximum plant-available soil water (Θ_P) and annual climatic water deficit (CWD_{adj}) under four different P_A regimes. Model predictions at all P_A zones show that $A\hat{G}B_W$ levels increase with higher Θ_P and lower CWD_{adj}. Nonetheless, even sites with relatively high Θ_P tend to show low $A\hat{G}B_W$ values when CWD_{adj} is high. For example, assuming two extremes P_A zones (Figure 3.5-a and 3.5-d), using Θ_P = 0.20 m as a reference in the lower precipitation zone (Figure 3.5-a), when CWD_{adj} is at its minimum (0.62 m a^{-1}), the model predicts AGB_W = 27.80 Mg ha^{-1}. Conversely, when CWD_{adj} is at its maximum (1.29 m a^{-1}), the model predicts $A\hat{G}B_W$ = 16.60 Mg ha^{-1}. Using a similar approach for the wetter P_A zone (Figure 3.5-d), when Θ_P = 0.2 m, the model predicts $A\hat{G}B_W$ = 35.79 Mg ha^{-1} when CWD_{adj} is in its maximum (1.29 m a^{-1}) and predicts $A\hat{G}B_W$ = 59.87 Mg ha^{-1} when CWD_{adj} is in its minimum (0.62 m a^{-1}). Therefore, the modelled responses observed in Figure 3.5 suggest that the absolute magnitude of the interactive effect of $CWD_{adj} \times \Theta_P$ depends upon the prevailing P_A, with these differences proportionally occurring across all panels.

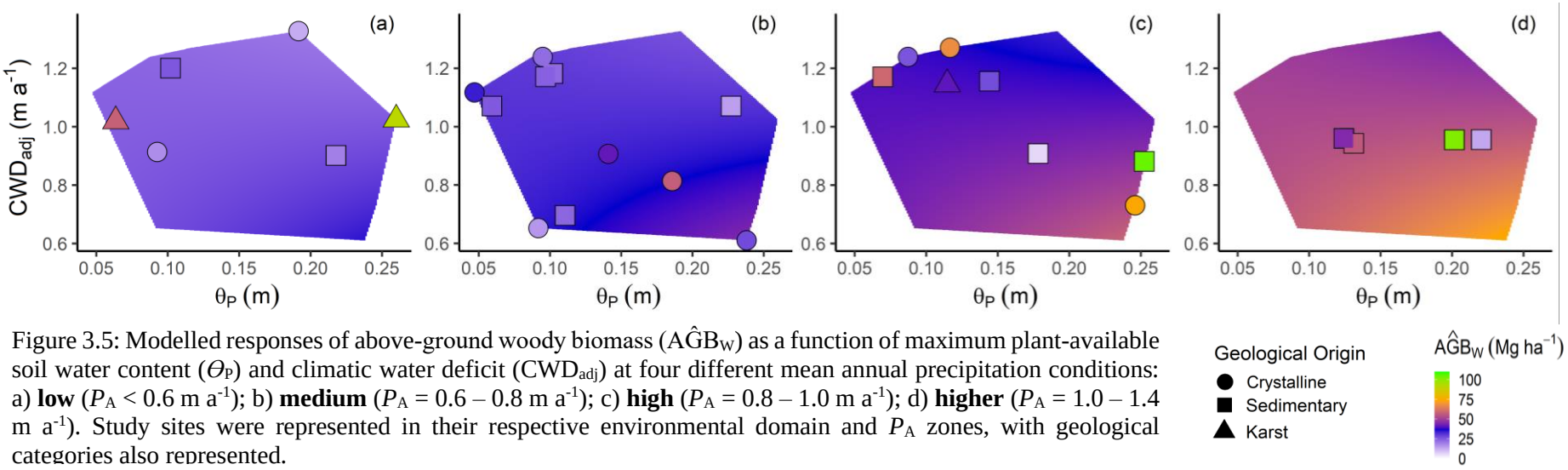

Figure 3.5: Modelled responses of above-ground woody biomass ($\hat{AGB}_W$) as a function of maximum plant-available soil water content (Θ_P) and climatic water deficit (CWD_{adj}) at four different mean annual precipitation conditions: a) **low** (P_A < 0.6 m a^{-1}); b) **medium** (P_A = 0.6 – 0.8 m a^{-1}); c) **high** (P_A = 0.8 – 1.0 m a^{-1}); d) **higher** (P_A = 1.0 – 1.4 m a^{-1}). Study sites were represented in their respective environmental domain and P_A zones, with geological categories also represented.

For this relationship, only S_{SED} sites were observed in the highest precipitation zone (Figure 3.5-d), which covers only intermediate levels of CWD_{adj} (0.8 – 1.0 m a^{-1}).

Finally, predictions of $A\hat{G}B_W$ levels as influenced by P_A were evaluated for four different $[Ca]_{ex}$ and Θ_P combinations (Figure 3.6). Across the full P_A gradient, the following environmental conditions were simulated: a) both $[Ca]_{ex}$ and Θ_P + 2 SD above their dataset mean (50.67 $mmol_c$ kg^{-1} and 0.27 m^3 m^2, respectively); b) $[Ca]_{ex}$ and Θ_P + 1 SD above their dataset mean (32.65 $mmol_c$ kg^{-1} and 0.21 m^3 m^2, respectively); c) $[Ca]_{ex}$ and Θ_P at their dataset mean (14.62 $mmol_c$ $kg^{-1}$and 0.15 m^3 m^2, respectively); and d) Θ_P -1 SD below the dataset mean (0.08 m^3 m^2) with $[Ca]_{ex}$ set to 1 $mmol_c$ kg^{-1} (as a standard deviation subtraction for $[Ca]_{ex}$ would generate negative values). This is shown in Figure 3.6, which shows that, although $A\hat{G}B_W$ increases with P_A levels, this relationship tends to become sharper as the soil conditions become more favourable [i.e. better nutritional levels (calcium) and greater maximum plant-available soil water content]. According to the model predictions, different Caatinga stands may show ca. threefold variation in $A\hat{G}B_W$ depending upon the prevailing Θ_P and $[Ca]_{ex}$, with the same relative differences at all evaluated P_A zones.

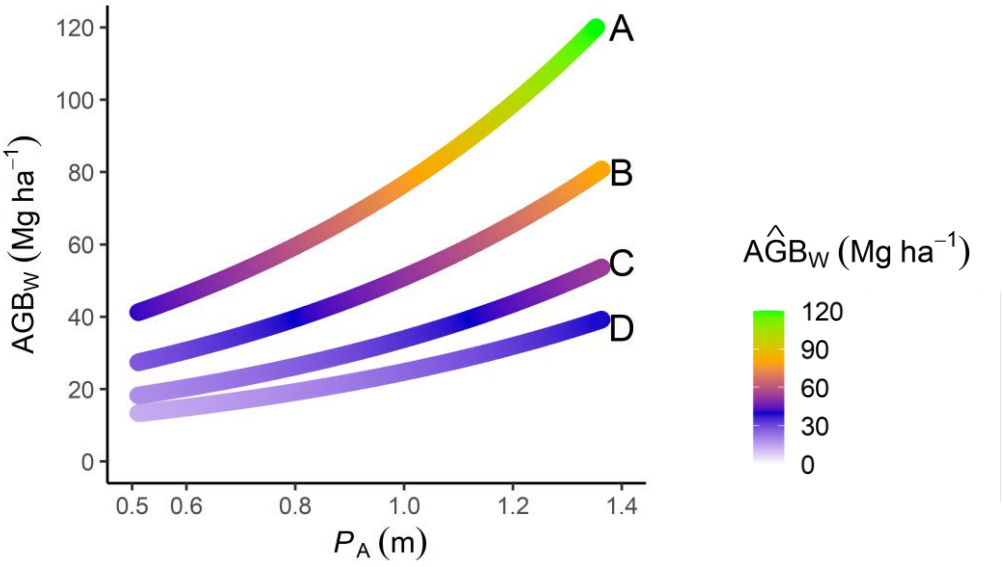

Figure 3.6: Modelled responses of above-ground woody biomass ($A\hat{G}B_W$) as a function of P_A at four different edaphic conditions: **A) higher** maximum plant-available soil water content (Θ_P) and higher exchangeable calcium ($[Ca]_{ex}$); i.e both variables with + 2 SD in relation to their average; **B) high** maximum plant-available soil water content (Θ_P) and high exchangeable calcium ($[Ca]_{ex}$); i.e. both variables with + 1 SD in relation to the average; **C) medium** maximum plant-available soil water content (Θ_P) and medium exchangeable calcium ($[Ca]_{ex}$); both at their means; **D) low** maximum plant-available soil water content (Θ_P) and low exchangeable calcium ($[Ca]_{ex}$); i.e. both variables with – 1 SD in relation to their average.

3.3.2 Assessing alternative models

To evaluate the ecological significance of climatic and edaphic drivers over AGB_W, an alternative set of models was tested. Initially, a model taking into account only the climatic terms expressed by Eqn. (3.5) was built:

$$\log(AGB_w) = \beta_0 + \beta_1 P_A + \beta_2 CWD_{adj} + \beta_3 T_{MAX} + (1|site) + \varepsilon \quad \text{Eqn. (3.5)}$$

As shown in Figure 3.7-a, a purely climatic model had negligible predictive power considering all data together, with $r^2_m = 0.07$ and AICc = 94.52.

Following the same approach, a model considering only soil chemical terms was tested,

$$\log(AGB_w) = \beta_0 + \beta_1 [Ca]_{ex} + \beta_2 \log[N]_t + \beta_3 \log[P]_t + (1|site) + \varepsilon \quad \text{Eqn. (3.6)}$$

Despite showing a better performance relative to the 'only climate model' of Eqn. (3.5), the model fit was relatively poor ($r^2_m = 0.16$; AICc = 91.26; Figure 3.7-b).

Subsequently, the complexity of the model was increased by adding all climatic and edaphic terms (both chemical and physical; the latter represented by the plant-available soil water; θ_P) without any interactive terms, as expressed by Eqn. (3.7):

$$\log(AGB_w) = \beta_0 + \beta_1 P_A + \beta_2 [Ca]_{ex} + \beta_3 CWD_{adj} + \beta_4 T_{MAX} + \beta_5 \log[N]_t + \beta_6 \log[P]_t + \beta_7 \theta_P + (1|site) + \varepsilon \quad \text{Eqn. (3.7)}$$

The model fit of Eqn. (3.7) had a better performance than the previous models, however, yielding higher AICc values ($r^2_m = 0.30$; AICc = 96.6). In addition, all possible models among variables in Eqn. (3.7) were tested using the *dredge* function of the *MuMin* package). Subsequentially, those models with Δ AICc < 4 were selected. From that analysis, it was found that AICc ranged from 85.0 to 88.98, and r^2_m ranged from 0.26 to 0.29. In simple terms, any model from the selected set can perform better than running the model as in Eqn. (3.7).

As there is no available straightforward method for calculating the r^2_m of averaged models, the r^2_m reported in Figure 3.7-c refers to the r^2_m of the AICc best-ranked model in the set.

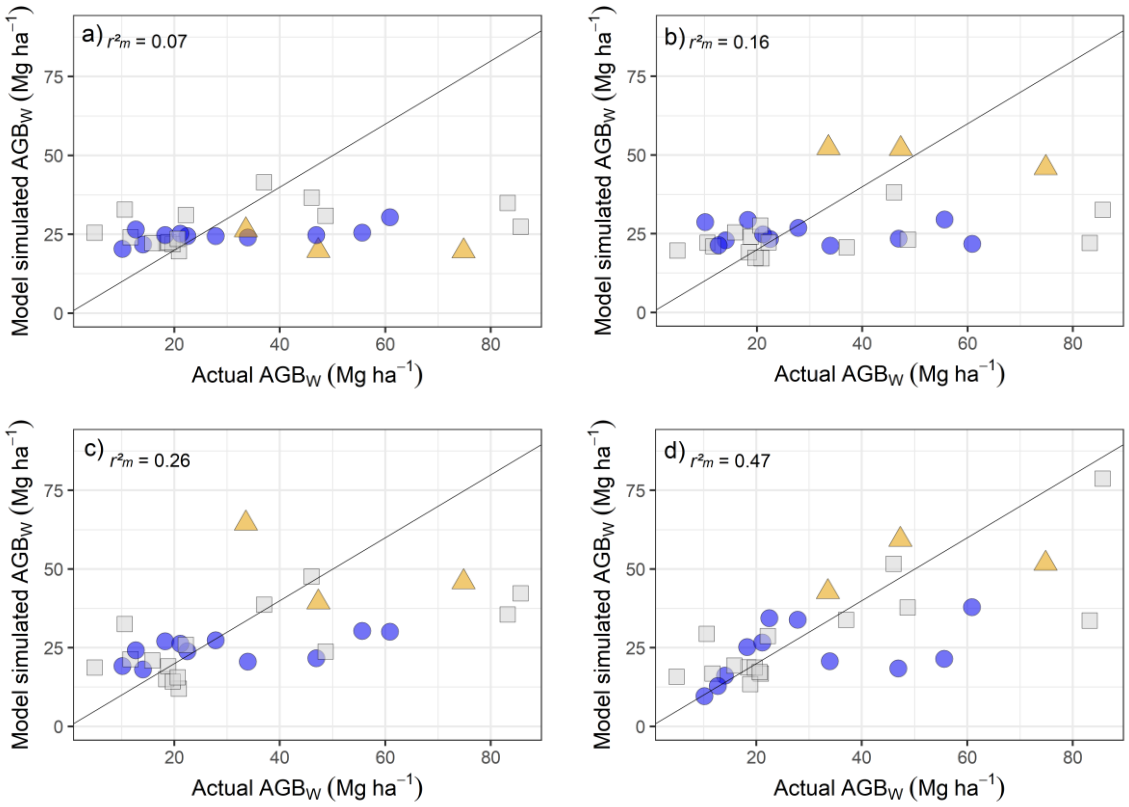

Figure 3.7: Differences of predictive ability among models with increasing complexity in accounting for AGB_W of Caatinga stands. **a)** 'Only climate model': $log(AGB_w) = \beta_0 + \beta_1 P_A + \beta_2 CWD_{adj} + \beta_3 T_{MAX} + (1|site) + \varepsilon$; **b)** 'Only soil model': $log(AGB_w) = \beta_0 + \beta_1 [Ca]_{ex} + \beta_2 log[N]_T + \beta_3 log[P]_T + (1|site) + \varepsilon$; **c)** 'No interactions model': $log\ (AGB_w) = \beta_0 + \beta_1 P_A + \beta_2 [Ca]_{ex} + \beta_3 CWD_{adj} + \beta_4 T_{MAX} + \beta_5 log[N]_T + \beta_6 log[P]_T + \beta_7 \theta_P + (1|site) + \varepsilon$; **d)** 'Full model': $log(AGB_w) = \beta_0 + \beta_1 \theta_P + \beta_2 P_A + \beta_3 [Ca]_{ex} + \beta_4 CWD_{adj} + \beta_5 \theta_P \times CWD_{adj} + \beta_6 [Ca]_{ex} \times CWD_{adj} + \beta_7 T_{MAX} + \beta_8 log[N]_T + \beta_9 log[P]_T + (1|site) + \varepsilon$. Marginal r^2 (r^2_m) values are provided. The respective geological affiliations of the study sites are shown.

Finally, the most complex tested model of Eqn (3.4), which includes potential interactive effects, yielded an r^2_m= 0.49 and AICc = 86.0. Then, when running all possible combinations among the terms in the model of Eqn. (3.4) and selecting those models with Δ AICc < 4, AICc values ranged from 84.9 to 88.8 and r^2_m ranged from 0.10 to 0.49, with the r^2_m value reported in Figure 3.7-d relative to the model with the lowest AICc in the set evaluated. Conditional r^2 (r^2_c, including random effects) was 0.88 for the lowest AICc model in the set.

3.3.3 Assessing AGB_W in geologically distinct stands

Table 3.1 shows the relationship between AGB_W and each individual selected soil and climate predictors (*log-linear* relationships). Considering the three geological classes together (S_{SED} + S_{CRY} + S_{KAR}), several soil predictors showed significant effects, with coefficients (β) representing changes in $\log(AGB_W)$ for standard deviation change in the predictors, i.e. $[Ca]_{ex}$ (β_1 = 0.256; r^2 = 0.13; p = 0.04), $\sum_B$ (β_1 = 0.258; r^2 = 0.13; p = 0.04), I_E (β_1 = 0.297; r^2 = 0.17; p = 0.02) and f_{sand} (β_1 = -0.278; r^2 = 0.15; p = 0.03), with no effects of any of the climatic or soil water storage variables detected (p > 0.1). No individual predictor at p < 0.05 could be considered superior to any other since the observed ΔAICc range was small for the significant relationships (≤ 2 for any comparison). Considering sites on the three geological classes separately, only effects related to soil were observed for the S_{SED}, i.e. $[Ca]_{ex}$ (β_1 = 0.385; r^2 = 0.25; p = 0.04), $[Mg]_{ex}$ (β_1 = 0.367; r^2 = 0.23; p = 0.05), $\sum_B$ (β_1 = 0.408; r^2 = 0.23; p = 0.03), I_E (β_1 = 0.434; r^2 = 0.28; p = 0.02), with the ΔAICc range not exceeding two units. Concerning the S_{CRY}, only P_A emerged as a significant predictor (β_1 = 0.432, r^2 = 0.50; p = 0.005). Moreover, the AIC_C value for P_A was 25.9, which means that the 'only P_A model' at S_{CRY} sites was superior compared to any other linear simple model. Because P_A was centred and scaled before the analysis, when P_A is on its average for those sites (P_A = 0.76 m a^{-1}), the model prediction for AGB_W = exp(3.2042) = 24.74 Mg ha^{-1} (model intercept), and an increase of 0.1 m a^{-1} in P_A represents an increase of exp(0.4321) = 1.54 Mg ha^{-1} in AGB_W.

Given that only three independent observations are available for S_{KAR} sites, inferences regarding causal relationships of environmental variables *versus* AGB_W in these study sites are necessarily imprecise. At these sites, total SOC (β_1 = -0.376; r^2 = 0.66; p = 0.021) and f_{sand} were significantly associated with AGB_W (β_1 = 0.359; r^2 = 0.61; p = 0.032). Figure 3.8 shows the more significant relationships found between AGB_W and tested predictors. Regression assumptions (i.e. homoscedasticity and normality of residuals) were met and spatial structures (Moran's I) in the residuals were not detected at p < 0.05.

Table 3.1: Individual predictors of above-ground woody biomass (AGB_W) according to site geology. Regression parameters were estimated through linear mixed- models (LMM). $[X]_{ex}$ = concentration of exchangeable cations in the brackets; $\sum_{B}$ = soil sum of bases; I_E = soil effective cations exchange capacity; $[X]_T$ = total concentration of elements in the brackets; pH_{H2O} = water-measured soil pH; f_{sand}, f_{silt}, f_{clay} = soil sand, silt and clay fractions; Θ_P = maximum plant-available soil water; Depth = soil depth; P_A = mean annual precipitation; CWD_{adj} = long-term mean annual climatic water deficit (multiplied by -1); ψ = precipitation seasonality index; T_{MAX} = mean annual temperature of the warmest month. Note: predictors were standardised, then coefficients (β) represent changes in log (AGB_W) per standard deviation changes in the predictor variables; significant relationships at $p \leq 0.05$ are shown in bold.

Variable	All (S_{SED} + S_{CRY} + $S_{KAR;}$ n = 29)					Sedimentary ($S_{SED;}$ n = 15)					Crystalline ($S_{CRY;}$ n = 11)					Karst ($S_{KAR;}$ n = 3)				
	β_1	SE	r^2	p	AICc	β_1	SE	r^2	p	AICc	β_1	SE	r^2	p	AICc	β_1	SE	r^2	p	AICc
$[Ca]_{ex}$	**0.256**	**0.120**	**0.13**	**0.042**	**86.90**	**0.385**	**0.385**	**0.25**	**0.040**	**46.10**	0.009	0.178	0.00	0.963	34.40	-0.292	0.155	0.42	0.108	12.30
$[Mg]_{ex}$	0.221	0.123	0.10	0.082	88.00	**0.367**	**0.174**	**0.23**	**0.051**	**46.60**	-0.140	0.173	0.05	0.437	33.70	0.116	0.207	0.07	0.613	14.60
$[K]_{ex}$	0.202	0.124	0.08	0.114	88.50	0.305	0.182	0.16	0.114	47.90	0.084	0.176	0.02	0.644	34.10	-0.225	0.286	0.25	0.286	13.60
$[Na]_{ex}$	-0.054	0.129	0.01	0.679	90.90	0.200	0.191	0.07	0.312	49.40	-0.282	0.157	0.22	0.100	31.50	-0.283	0.158	0.39	0.123	12.50
$[Al]_{ex}$	0.060	0.129	0.01	0.645	90.90	0.127	0.195	0.03	0.525	50.10	0.258	0.160	0.18	0.845	32.00	-0.280	0.159	0.38	0.128	12.60
$\sum_B$	**0.258**	**0.120**	**0.13**	**0.040**	**86.80**	**0.408**	**0.167**	**0.28**	**0.028**	**45.50**	-0.054	0.177	0.01	0.765	34.30	-0.234	0.171	0.27	0.219	13.50
I_E	**0.297**	**0.117**	**0.17**	**0.017**	**85.30**	**0.434**	**0.163**	**0.31**	**0.018**	**44.70**	0.008	0.178	0.00	0.966	34.40	-0.237	0.170	0.28	0.213	13.40
$[P]_T$	0.171	0.125	0.06	0.184	89.30	0.212	0.190	0.08	0.283	49.30	-0.308	0.152	0.26	0.068	30.90	-0.018	0.217	0.00	0.938	14.90
$[C]_T$	0.141	0.127	0.04	0.274	89.90	0.149	0.194	0.04	0.455	49.90	0.087	0.176	0.02	0.632	34.10	**-0.376**	**0.121**	**0.66**	**0.021**	**9.40**
$[N]_T$	0.224	0.123	0.10	0.077	87.90	0.251	0.187	0.11	0.198	48.80	-0.039	0.178	0.00	0.830	34.30	-0.170	0.194	0.15	0.444	14.20
pH_{H2O}	0.190	0.124	0.07	0.137	88.80	0.124	0.195	0.03	0.534	50.10	-0.072	0.177	0.01	0.693	34.20	-0.047	0.216	0.01	0.841	14.90
f_{sand}	**-0.278**	**0.119**	**0.15**	**0.026**	**86.10**	-0.299	0.182	0.15	0.121	48.00	-0.069	0.177	0.01	0.705	34.20	**0.359**	**0.129**	**0.61**	**0.032**	**10.10**
f_{silt}	0.303	0.117	0.18	0.303	85.00	0.341	0.177	0.20	0.073	47.20	0.194	0.168	0.10	0.273	33.10	-0.095	0.210	0.05	0.681	14.70
f_{clay}	0.151	0.151	0.04	0.242	89.70	0.189	0.192	0.06	0.340	49.60	-0.058	0.177	0.01	0.750	34.30	-0.220	0.176	0.24	0.301	13.70
Θ_P	0.095	0.128	0.02	0.464	90.50	-0.019	0.198	0.00	0.925	50.50	0.182	0.170	0.09	0.307	33.30	0.309	0.149	0.46	0.084	11.90
$Soil_{depth}$	-0.120	0.127	0.03	0.354	90.20	-0.207	0.190	0.07	0.294	49.40	0.148	0.173	0.06	0.410	33.70	0.127	0.205	0.08	0.578	14.60
P_A	0.185	0.125	0.07	0.148	89.00	0.330	0.180	0.19	0.081	47.30	**0.432**	**0.122**	**0.50**	**0.005**	**25.90**	-0.287	0.156	0.40	0.116	12.40
CWD_{adj}	-0.034	0.129	0.00	0.793	91.00	0.000	0.200	0.00	0.999	50.50	-0.089	0.176	0.02	0.622	34.10	-0.279	0.159	0.38	0.129	12.60
ψ	0.199	0.124	0.08	0.119	88.60	0.202	0.191	0.07	0.305	49.40	0.230	0.164	0.15	0.188	32.60	-0.283	0.158	0.39	0.122	12.50
T_{MAX}	-0.005	0.129	0.00	0.969	91.10	0.010	0.197	0.00	0.969	50.50	0.026	0.178	0.02	0.888	34.30	-0.246	0.168	0.30	0.194	13.30

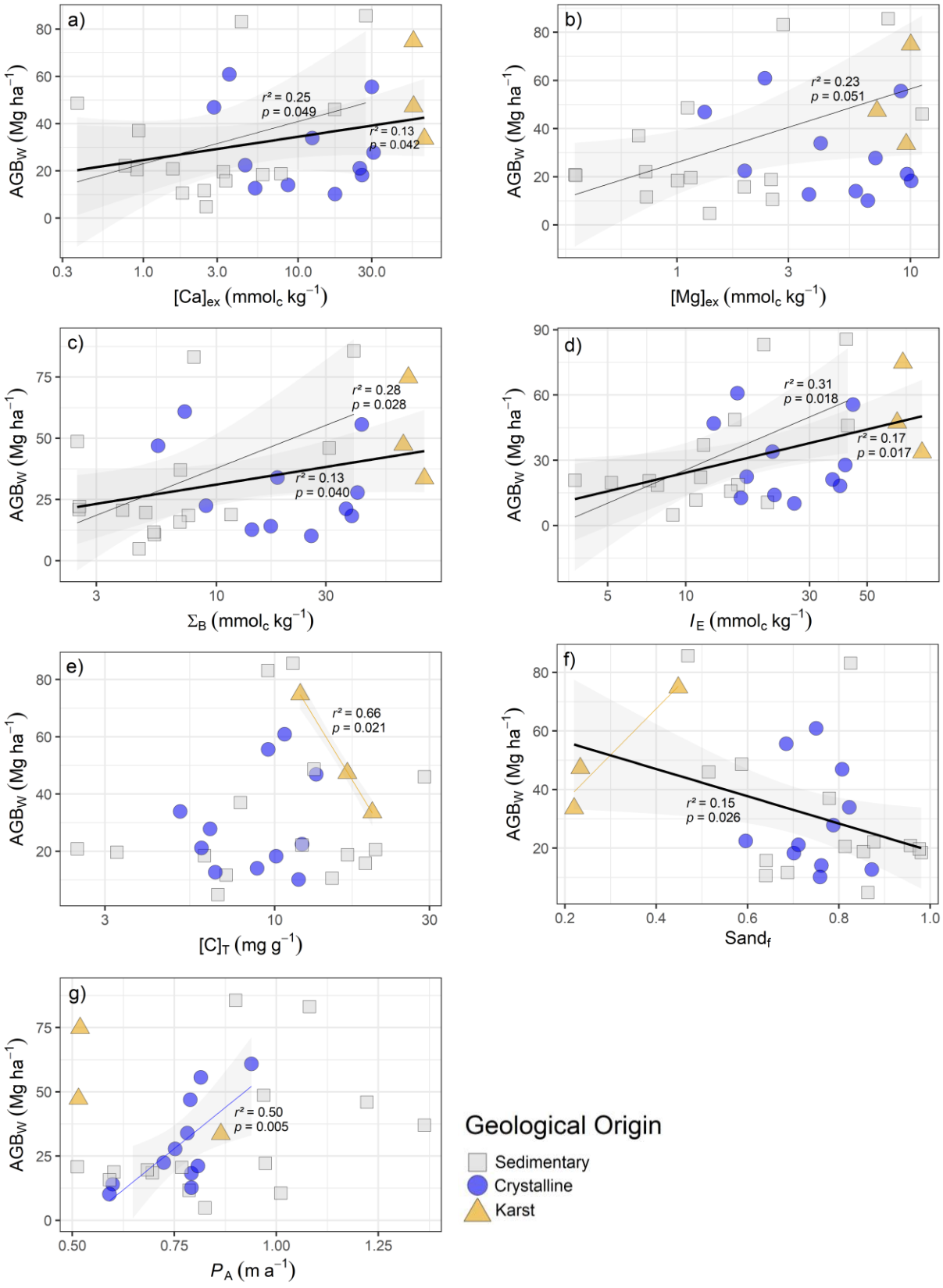

Figure 3.8: Observed variations in AGB_W as a function of selected edaphic and climatic predictors: a) $[Ca]_{ex}$; b) $[Mg]_{ex}$, c) $\sum_B$; d) I_E; e) $[C]_t$, f) $Sand_{fraction}$; g) P_A. Data points were discriminated according to their respective geological affiliations. Thinner lines represent linear fits for specific geological affiliations and coarser lines represent model fits at the entire sampling level. Shaded bands represent 0.95 confidence intervals.

3.3.4 Community-weighted trait means (CWM) and functional diversity

The community-weighted mean wood density (CWM_{wd}) was significantly lower at the S_{KAR} sites compared to both the S_{CRY} and S_{SED} sites (Figure 3.9-a). On the contrary, the differences in the community-weighted mean maximum diameter (CWM_{dmax}) were not significant at $p \leq 0.05$ (Figure 3.9-b). Regarding the differences in the functional diversity indexes, only F_{Ric} was significantly higher in S_{CRY} compared to S_{SED} (Figure 3.9-c). Functional divergence (F_{Div}) was, in general, moderate to high and F_{Eve} was generally low to moderate in all categories (Figure 3.9-d; Figure 3.9-e).

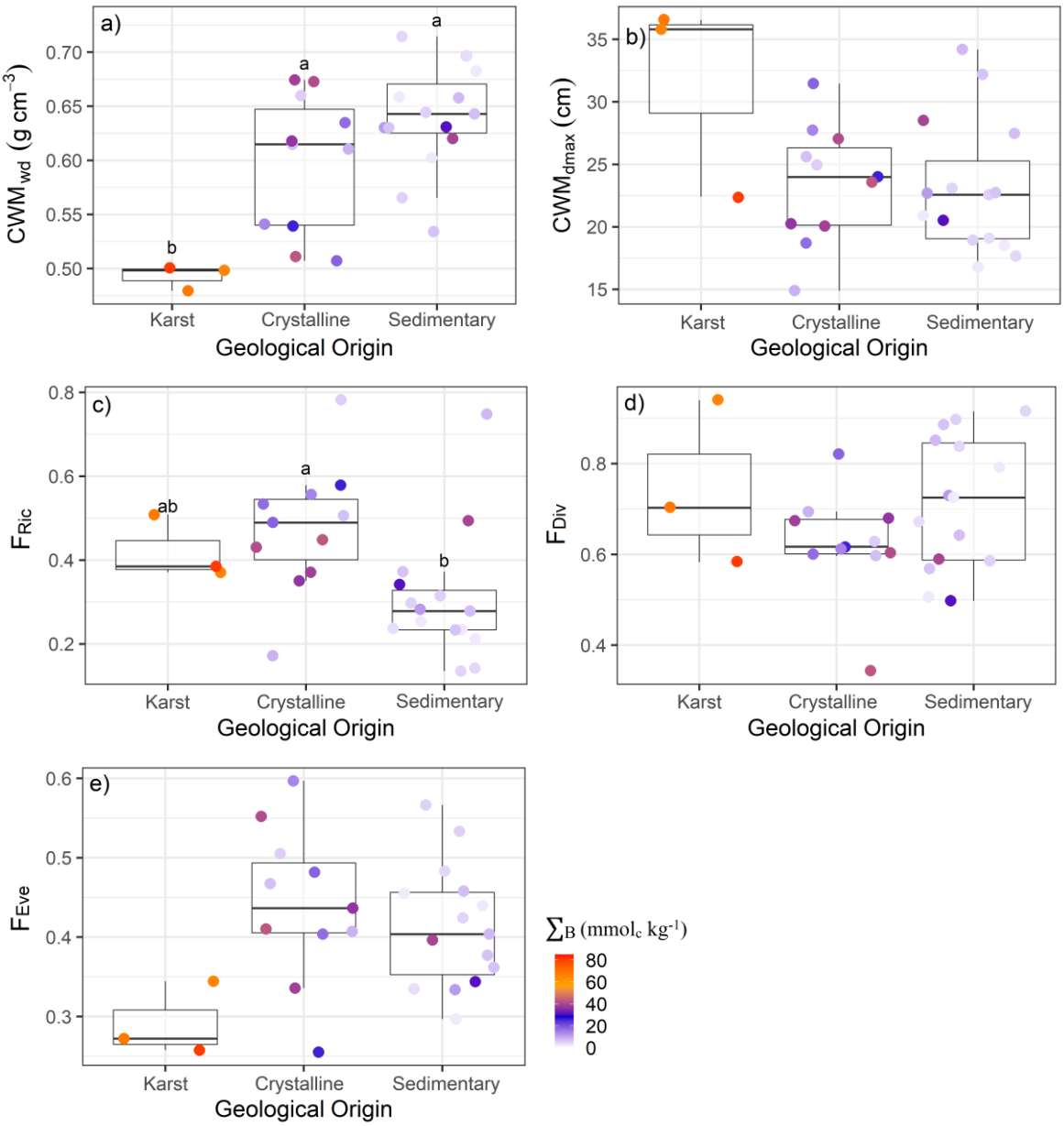

Figure 3.9: Community-weighted trait means and functional diversity indexes according to geological affiliations. a) Community-weighted mean wood density (wd); b) Community-weighted mean maximum diameter (dmax); c) Functional richness (F_{Ric}); d) Functional divergence (F_{Div}); c) Functional evenness (F_{Eve}).

Ordinary least squares linear regressions resulted in that AGB_W, considering all study sites together, was weakly associated with both (r^2 = 0.20; p = 0.009; Figure 3.10-a) and F_{Ric} (r^2 = 0.17; p = 0.015; Figure 3.10-b).

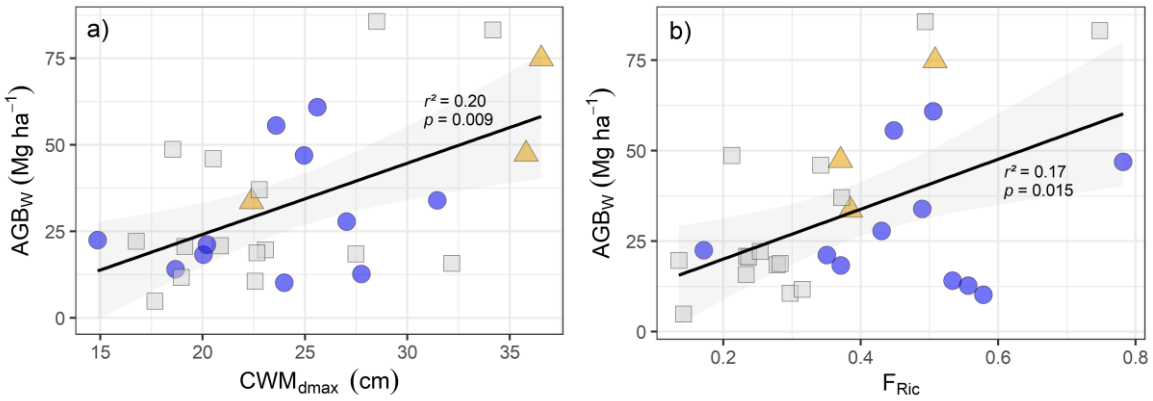

Figure 3.10: a) Predictive ability of CWM_{dmax} to explain variations in AGB_W; b) Predictive ability of functional richness (F_{Ric}) to explain variations in AGB_W. Shaded bands represent 0.95 confidence intervals. Respective soil geological affiliations are shown.

Finally, a series of bivariate correlations between functional properties, soil chemical properties and soil texture (Table 3.2) showed that CWM_{wd} was inversely associated with CWM_{dmax} (ρ = -0.49; *p-value* = 0.007), $[Ca]_{ex}$ (ρ = -0.50; *p-value* = 0.005), $[Mg]_{ex}$ (ρ = -0.43; *p-value* = 0.02), $\sum_B$ (ρ = -0.55, *p-value* = 0.002), $[K]_{ex}$ (ρ = -0.36; *p-value* = 0.052); I_E (ρ = -0.55, *p-value* = 0.002), $[Fe]_T$ (ρ = -0.43; *p-value* = 0.023), $[Zn]_T$ (ρ = -0.40; *p-value* = 0.023), $silt_f$ (ρ = -0.56; *p-value* = 0.023), and positively correlated with soil $sand_f$ (ρ = 0.50; *p-value* = 0.006). In turn, CWM_{dmax} was positively associated with F_{Ric} (ρ = 0.53; *p-value* = 0.003), $[Ca]_{ex}$ (ρ = 0.45; *p-value* = 0.015), and $\sum_B$ (ρ = 0.44; *p-value* = 0.016). Functional richness (F_{Ric}) was positively associated with $[Ca]_{ex}$ (ρ = 0.47; *p-value* = 0.010), $[Mg]_{ex}$ (ρ = 0.49; *p-value* = 0.007), $[K]_{ex}$ (ρ = 0.41; *p-value* = 0.027), $[Na]_{ex}$ (ρ = 0.38; *p-value* = 0.040), $\sum_B$ (ρ = 0.55; *p-value* = 0.002), I_E (ρ = 0.53; *p-value* = 0.003) and $[Zn]_T$ (ρ = 0.37; *p-value* = 0.146). Functional evenness (F_{Eve}) was inversely associated with $[C]_T$ (ρ = -0.53; *p-value* = 0.003), $[N]_T$ (ρ = -0.63; *p-value* = 0.000), $[Mn]_T$ (ρ = -0.44; *p-value* = 0.016). Finally, F_{Div} was negatively correlated with $[K]_{ex}$ (ρ = -0.49; *p-value* = 0.007) (Table 3.2).

Table 3.2: Spearman's rank correlation coefficient (ρ) amongst stand-level functional metrics (namely CWM_{wd}, CWM_{dmax}, F_{Ric}, F_{Eve} and F_{Div}) and selected soil chemical and physical properties, i.e. $[Ca]_{ex}$, $[Mg]_{ex}$, $[K]_{ex}$, $[Na]_{ex}$, $[Al]_{ex}$, $\sum_B$, I_E, soil pH_{H20}, $sand_f$, $silt_f$, $clay_f$, $[C]_T$, $[N]_T$, soil C/N ratio, $[P]_T$, $[Fe]_T$, $[Mn]_T$ and $[Zn]_T$. Significant correlations at $p \leq 0.05$ are shown in bold. The red colour represents negative correlations and blue represents positive correlations. Significant correlations at $p \leq 0.05$ are shown in bold.

Variable	CWM_{wd}	CWM_{dmax}	F_{Ric}	F_{Eve}	F_{Div}
CWM_{wd}	–	**-0.49**	-0.33	0.18	0.10
CWM_{dmax}	**-0.49**	–	**0.53**	0.03	0.14
F_{Ric}	-0.33	**0.53**	–	-0.02	-0.33
F_{Eve}	0.18	0.03	-0.02	–	0.00
F_{Div}	0.10	0.14	-0.33	0.00	–
$[Ca]_{ex}$	**-0.50**	**0.45**	**0.47**	-0.29	-0.16
$[Mg]_{ex}$	**-0.43**	0.29	**0.49**	-0.26	-0.11
$[K]_{ex}$	**-0.36**	0.16	**0.41**	-0.29	**-0.49**
$[Na]_{ex}$	-0.13	-0.24	**0.38**	0.04	-0.32
$[Al]_{ex}$	0.21	-0.33	-0.13	0.14	0.08
$\sum_B$	**-0.55**	**0.44**	**0.55**	-0.32	-0.23
I_E	**-0.55**	0.31	**0.53**	-0.32	-0.15
pH_{H2O}	-0.32	0.31	0.29	-0.17	-0.16
$[P]_T$	-0.32	0.14	0.19	-0.33	-0.19
$[C]_T$	-0.16	-0.08	-0.05	**-0.53**	0.10
$[N]_T$	-0.26	0.06	0.11	**-0.63**	0.01
Soil C/N	0.22	-0.14	-0.27	0.07	0.30
$[Fe]_T$	**-0.42**	-0.01	0.13	-0.24	-0.14
$[Mn]_T$	-0.29	0.13	0.21	**-0.44**	-0.11
$[Zn]_T$	**-0.40**	0.16	**0.37**	-0.17	-0.01
$Sand_f$	**0.50**	-0.06	-0.14	0.30	0.13
$Silt_f$	**-0.56**	0.24	0.20	-0.32	-0.17
$Clay_f$	-0.23	-0.20	0.07	-0.25	-0.07

3.4 Discussion

3.4.1 Study particularities

In this chapter, the most influential environmental drivers on stand-level AGB_W of Caatinga's seasonally dry communities were explored. To my knowledge, this work is the first to encompass study plots over a biome-wide geographical extension using standardised soil and vegetation sampling protocols in the Caatinga. Such a large spatial scale also implies that the task of disentangling environmental forces accounting for AGB_W in the Caatinga is not straightforward. This is because this region, despite having a common prevailing hot semiarid climate, is extremely patchy in terms of geodiversity (including both land-forms and geological substrates or parent materials, as shown in detail in Chapters 1 and 2). In addition, intricate evolutionary processes gave rise to a highly diversified flora and distinct physiognomies (QUEIROZ, 2006; QUEIROZ, 2017; FERNANDES et al., 2022), which means that the dry-adapted plant species of each community could respond differently to environmental effects.

As pointed out by CASTANHO et al. (2020a), for any study of above-ground biomass in the Caatinga, it is necessary to specify which factors are under evaluation. In a broad sense, these factors are environmental drivers (soil + climate; macro variability), land-use effects on a given stand (meso variability) and successional age (micro variability) (*sensu* CASTANHO et al., 2020a). This study aimed to evaluate the influence of environmental drivers in modulating AGB_W. As mentioned in Section 1.8, Caatinga has a long history of human disturbances (AB' SABER, 1974). Therefore, there is a high probability that at least some stands evaluated here must have undergone impactful human interferences in the past. However, considering that most stands evaluated here are within protected areas at least for a few decades, it is assumed that vegetation expression, to some extent, reflects the maximum environmental potential. Nevertheless, the impact of selective timber logging and sporadic grazing cannot be fully disregarded. Furthermore, the post-disturbance recovery of SDTFs is expected to be relatively rapid (3 – 5 decades), which might be attributable to the simpler structure of this vegetation type compared to moister forests (BECKNELL et al., 2012).

3.4.2 Biome-wide AGB_W is driven by complex interactions

The fundamental hypothesis that stand-level AGB_W in the Caatinga is driven by complex interactions among climate and soil both chemical and physical properties was tested with interesting patterns highlighted in Figures 3.4 and 3.5. The results presented here show that, indeed, when considered in a multivariate context, P_A and soil cation levels (calcium) accounted more expressively for AGB_W in both conditional and full average models, while the interaction terms, i.e. $[Ca]_{ex} \times CWD_{adj}$ and $\theta_P \times CWD_{adj}$, had lower but still meaningful effect sizes in the full average model.

Despite high temperatures potentially triggering tree mortality through carbon starvation and hydraulic failure (MCDOWELL et al., 2018), with an associated lower AGB_W over time, there was no evidence that higher T_{MAX} has an influence on AGB_W across the evaluated stands. The most likely reason for the ability of Caatinga trees to cope with high-temperature events is that these species have evolved to tolerate high-temperature and through mechanisms of both avoidance (e.g. changes in leaf morphology) and tolerance (e.g. accumulation of osmoprotectants) to conserve the photosynthetic machinery (MATHUR; AGRAWAL; JAJOO, 2014; JAJOO; ALLAKHVERDIEV, 2017). Despite the tendency to high temperatures in the Caatinga throughout the year, the typical drought-deciduous leaf habit of Caatinga species implies that, during the drier months, resources should be allocated to other plant processes instead of sustaining the high-cost leaves and photosynthetic apparatus.

Variations in total P and N appeared to be less important in determining AGB_W in the studied stands. Although they had small effect sizes in the conditional averaged model, the coefficients for both nutrients approached zero in the full average model and had low relative importance values. I recognise that measures of availability of both N and P are lacking in this study and fertilisation experiment studies such as those presented in Kaspari et al. (2008) or the undergoing Amazon Fertilisation Experiment (AFEX) would be of great interest to determine how these nutrients affect productivity and biomass accumulation in the long term. Total soil P has been suggested as a reasonable surrogate for the general availability of P (QUESADA et al., 201). Ecosystem buffering capacity has been described in which P from less bioavailable pools can become available if available P becomes scarce in the soil (KITAYAMA; MAJALAP-LEE; AIBA, 2000; QUESADA et al., 2010).

Similarly, N cannot be ruled out in driving AGB_W. Caatinga has been described as a hotspot for N fixation, although *in situ* and experimental research revealed that a small

proportion of potentially nodulating species effectively do so (FREITAS et al., 2010; SILVA et al., 2017). Furthermore, high foliar N concentrations and high foliar $\delta^{15}N$ have been reported in Caatinga, which is suggested to be the result of the high availability of N (FREITAS et al., 2010; MARTINELLI et al., 2021). It should be noted that all Caatinga sites included in the study by Martinelli et al. (2021) are also part of this study. Although Caatinga soils are generally assumed to be fertile, the sampling includes some fairly infertile soils (e.g. Hyperdystric Arenosol in CJU-01). Thus, the premise that high soil general fertility is linked to high higher N pools may not be necessarily observed in the field. However, N availability in the Caatinga seems somewhat controversial. This is because, although some potential indicators of high N-availability such as high $\delta^{15}N$ signals reported from both soils and leaves of Caatinga (e.g. FREITAS et al., 2010; MARTINELLI et al., 2021), N_2O emissions in the Caatinga were reported to be even lower than in Cerrado (RIBEIRO et al., 2016; MARTINELLI et al., 2021). In addition, as for tropical savannas (LLOYD et al., 2009), it is not clear to what extent N or P may limit photosynthetic rates in Caatinga. Photosynthetic capacity was shown to correlate with foliar N and P in tropical savannas, especially in drier areas (DOMINGUES et al., 2010). At the same time, higher foliar N and C/N ratios were found in the Caatinga compared to other Brazilian biomes (MARTINELLI et al., 2021). In general, deciduous trees require a high amount of nutrients (LLOYD et al., 2009) and have already been shown to resorb N much more efficiently from senescing leaves than evergreen shrubs and trees (AERTS, 1996). However, the extent to which nutrient use efficiency, i.e. nutrient resorption from senescing leaves (VITOUSEK, 1982; 1984) takes place in Caatinga is still little studied.

Mean annual precipitation (P_A) became relevant in driving AGB_W only in a multivariate context. This was, in part, contrary to the initial expectation as in the words of BECKNELL et al. (2012), *'..., the ecology and climate of SDTF suggest that water availability, even expressed through a coarse index like mean annual precipitation, is highly likely to play a role in SDTF biomass content'*. However, the P_A range in this study is within the dry-end spectrum of global SDTFs, that is, 17 of 29 study plots had $P_A \leq 0.8$, with only four study plots with $P_A \geq 1.0$ m. Menezes et al. (2021) pointed out that Caatinga forests are even drier than the hilly Mexican 'very dry deciduous forests' studied by LEBRIJA-TREJOS et al. (2008), in which P_A is around 0.9 m. The P_A of 0.9 m has also been suggested as a threshold level for AGB_W by BECKENELL et al. (2012), who found a lower and higher AGB_W below and above this mark, respectively (in this study, there were no differences in AGB_W according to this threshold;

results not shown). Therefore, it is plausible that the effects of P_A on driving AGB_W become more pronounced at higher P_A levels than observed in this study. Furthermore, the results presented here suggest that P_A is indeed important over a biome-range level, but its effect is conditioned by other abiotic factors.

Regarding the maximum climatological water deficit tested in this study (CWD), even the wettest site in the dataset showed a negative annual balance of -0.6 m. Maximum climatological water deficit (CWD) has been demonstrated to influence allometric relationships in tropical trees (CHAVE et al., 2014) and represents to what degree a certain place is water-stressed. Despite the small effect sizes of CWD and associated interactions with soil chemical and physical parameters, it was decided to proceed with model simulations, since coefficients were high in those models where these terms were retained. Therefore, it is suggested that soil properties also mediate vegetation responses to climate on small scales (MAIA et al., 2020a).

The influence of other cations (that were not included in the main model of Eqn. (3.4) on AGB_W cannot be ruled out. For example, potassium might play a key role in modulating tropical woody vegetation (SCHRODT et al., 2015; LLOYD et al., 2015). Similarly, magnesium can alter vegetation growth under severe deficiency. This is because this element is involved in several biochemical and physiological processes, acting in photosynthesis, synthesis of proteins and acid nucleic acids, and enzyme activation, in addition to improving the problems of aluminium toxicity (CHEN et al., 2018). Although relatively high exchangeable aluminium is found in some S_{SED} sites, no evidence of its potential negative effects was found. Detrimental aluminium effects (DELHAIZE; RYAN, 1995) have been observed in castor (*Ricinus communis* L.) under experimental conditions in Caatinga (LIMA et al., 2014), but should rarely affect vegetation performance under moderate to high soil pH conditions common to this region. Exchangeable sodium appeared only in small amounts (only two study soils exceeded 1 $mmol_c\,kg^{-1}$). Six important woody native species of Caatinga had a high capacity to tolerate low to moderate salinity levels, while only one specie (*Myracrodruon urundeuva* M. Allem.) could tolerate a high salinity level (BESSA et al., 2017).

Concerning the potential beneficial effects of calcium itself [included in the main model of Eqn. (3.4)], in addition to the fundamental role of calcium in providing structural support for plant cells, it is known that calcium also has an equally important role in several mechanisms associated with responses to plant abiotic stress. For example, exogenous calcium

ion treatment considerably improves antioxidant activities in grasses under heat stress (JIANG; HUANG, 2001), also conferring greater osmoprotecion by increasing glycine betaine (an important osmoprotectant) in *Catharanthus roseus* under water deficit (JALEEL et al., 2007). Furthermore, several mechanisms involving calcium signal decoding elements have been described. Such mechanisms refer to a complex and regulated signalling network, in which plants can respond specifically to different abiotic stresses and these responses are known to be largely mediated by the cytosolic concentration of Ca^{2+} (SONG et al., 2008; SHARMA; KUMAR, 2021). In turn, extracellular and calcium cytosolic concentration $[Ca^{2+}]_{cyt}$ are controlled by the soil $[Ca^{2+}]$ as well as transpiration rates in *Arabidopsis thaliana* (SONG et al., 2008). Calcium-mediated stress-induced responses were also studied in roots (WILKINS et al., 2016), and the authors pointed out that calcium is also important for exocytosis in growth and that roots also have to endure various abiotic stresses as they exploit the soil in search of water and nutrients. Therefore, regardless of the mechanisms considered to justify the importance of calcium, and contrary to the potential nutrient imbalance and calcium toxicity as suggested by PRADO-JUNIOR et al. (2016), results here suggest that calcium is of pivotal importance for the semi-arid Caatinga (Figure 3.4). That is, under similar (high) water stress conditions (higher CWD_{adj}), soils that afford greater calcium availability seem to be able to maintain a higher AGB_W over time.

Lastly, the interactive effect between maximum plant-available soil water (Θ_P) and maximum climatological water deficit (CWD_{adj}) suggests that soils with higher Θ_P are likely to mitigate the negative effects of suboptimal precipitation regimes. Precipitation seasonality and soil moisture gradients were also found to be the most important variables determining manifold vegetation parameters in sites including transitions between Caatinga, Atlantic Forest, and Cerrado (TERRA et al., 2018). Therefore, a higher Θ_P may represent an important buffering agent by which plants can benefit even after the end of wet season rains. I recognise the limitations of using a pedotransfer function instead of a field-measured water-holding capability. However, the index used here is believed to provide much better information compared to the commonly used coarse textural fractions to represent soil water-holding capacity per unit volume. Furthermore, the field-measured maximum effective soil depth (rarely measured in the field) embedded in Θ_P should reflect the size of the reservoir from which plants can potentially extract water.

3.4.3 Is the effect of climatic and edaphic factors the same for stands of different geological affiliations?

Several studies have already pointed out that Caatinga plant communities are particularly associated with geologically distinct substrates (e.g., ANDRADE-LIMA, 1981; DA COSTA et al., 2015; QUEIROZ, 2006; MORO et al., 2016; QUEIROZ et al., 2017; FERNANDES et al., 2022). Furthermore, the community composition of stands growing in karst and dunes environments is recognised by their unique species composition and high levels of endemism (QUEIROZ et al., 2017; FERNANDES et al., 2020). These differences in community compositions are thought to reflect species' suitability to edaphic conditions, but also reflect the available regional pool of species (i.e. geographical proximity).

The present-day assembly of plant lineages was identified to be primarily the result of ancient biogeographical changes, with later post-climate-induced changes in the vegetation responsible for most *in situ* speciation events (FERNANDES et al., 2022). Furthermore, the main pathway of species in Caatinga must have occurred from surrounding regions (i.e. Atlantic Forest and Cerrado), mostly represented by lineages carrying drought tolerance traits (FERNANDES et al., 2022). Nevertheless, another key point behind the suitability of the environment to host such species is that, beyond the critical environmental filter that Caatinga species are subjected to (i.e. relatively low water availability), species thrive in distinct geologically-determined edaphic conditions.

The results presented in Figure 3.8 and Table 3.1 suggest that different community compositions overlying geologic-edaphically distinct substrates may be primarily limited by different resources. To help understand these results, it is worth mentioning that much of the research on resource limitation in plant ecology has been put forward through economics analogies (*sensu* BLOOM; CHAPIN; MOONEY, 1985). From this perspective, it seems reasonable to assume that light availability, i.e. photon flux density (PFD), should rarely limit the typical open canopies communities with low cloud coverage of the seasonally dry Caatinga. On the other hand, the importance of water or nutrients in limiting a given community should be determined by the relative availability of each resource. Hence, plants should adjust in both the short and long-term (acclimation and genetic adaptation, respectively) to achieve a similar benefit-to-cost ratio related to the expenditure of each resource (BLOOM; CHAPIN; MOONEY, 1985). This conceptual framework may help explain why biomass stocks are not higher considering geological affiliations (Figure 2.1). That is, despite the generally higher

availability of nutrients in S_{CRY} - and S_{KAR}-associated communities, the latter does not have relatively higher biomass or, still, plants from nutrient-poor sites can adjust their physiology according to available resources.

In addition, nutritional needs can vary significantly across species, genotypes of a species, among tissues of a single plant, and according to ontogenetic stages (BLOOM; CHAPIN; MOONEY, 1985). Therefore, determining the limitations across plant communities is a difficult task. Plants have evolved to tolerate varying levels of resource availability, and a community dominated by a given (or a set of) species is expected to also show varying physiological traits to cope with the available nutrient supplies (CHAPIN; VITOUSEK; VAN CLEVE, 1986).

Concerning water availability, several mechanisms to cope with water stress have been extensively studied and include morphological, physiological, and biochemical adaptations such as activation of osmotic-stress signalling, ion transport, stomatal closure, leaf drop (inducing lower leaf area), improving water use efficiency - WUE (OSAKABE et al., 2014; MESQUITA; DANTAS; CAIRO, 2018). Similarly to nutrients, species may have different levels of tolerance to water stress. For example, MESQUITA; DANTAS; CAIRO (2018), experimentally studying six native species of the same site, found that all species have undergone a decrease in transpiration rate and stomatal conductance under lower soil moisture conditions. However, only two species (*Myracrodruon urundeuva* M. Allem. and *Cnidoscolus bahianus* (ULE) Pax & Hoffm.) had significant negative effects on net photosynthesis. An interesting example of species adaptation to a constrained environment in the current dataset is the dominance of the sclerophyllous *Copaifera coriaceae* in both plots at the sedimentary *'Dunas de São Francisco'*, for which P_A does not exceed 0.7 m a^{-1} and the aridity index is high (AI ≈ 0.28, AI = precipitation/potential evapotranspiration; SOUZA et al., 2021). Sclerophylly is a trait commonly associated with drought tolerance but was also reported to predominate in P-deficient soils of humid and semiarid regions (MEDINA; GARCIA; CUEVAS, 1990). Therefore, the dominance of *C. coriaceae* in the studied sand dunes may be attributable to the potential capacity of this species to thrive in both water- and P-limited environments.

In the last instance, the weighted composition of a given community and associated functional properties are expected to reflect its general resistance or tolerance to drought stress, as well as its capacity to cope with nutrient-poor environments. Therefore, the AGB_W and predictor relationships of Figure 3.8 and Table 3.1 indicate that soil cation concentrations play

a significant role in AGB_W throughout the biome, including different community compositions. The soil sand content was also influential when considering all sites together, probably reflecting nutrient levels, but also because fast-draining sandy soils are known to induce greater water stress in plants in seasonal environments (MAIA et al., 2020a). Furthermore, sandier textures have been associated with increased mechanical instability (QUESADA et al., 2012).

The positive effect of both exchangeable $[Ca]_{ex}$ and $[Mg]_{ex}$ (also reflected in $\sum_B$ and I_E) at S_{SED} sites can be interpreted as an indication that these cations can be relatively more limiting than water in these environments. Both calcium and magnesium are essential for plants, participating in several physiological and biochemical processes (Section 3.4.2). On the contrary, stands growing on mostly nutrient-rich S_{CRY} terrains appeared to be more limited by rainfall total amounts, with the relationship found between AGB_W and P_A being considerably strong (r^2 = 0.50; p = 0.005), interestingly close to the relationship presented in a global synthesis of AGB_W in dry forests (BECKNELL et al., 2012), who found r^2 = 0.55 (p < 0.000) for the same relationship. However, the slope of their relationship was much higher, where an increase of 1.0 m a^{-1} in P_A accounted for an increase of 187 Mg ha^{-1} in AGB_W, with these values being comparable to the relationship found in the global compilation of MARTÍNEZ-YRÍZAR (1995). Considering that AGB_W appeared to respond sharply to increases in P_A in both studies (BECKNELL et al., 2012; MARTÍNEZ-YRÍZAR, 1995), it is arguable that their evaluated stands probably grow on more nutrient-rich soils, even though their studies did not incorporate the relevant soil information. Moreover, most stands included in BECKNELL et al. (2012) had mean annual rainfall levels close to the maximum limit according to Murphy and Lugo's (1986) definition of SDTFs (i.e. 2000 mm a^{-1}) and with a much higher AGB_W (100 – 334 Mg ha^{-1}) than the values commonly found in the dry Caatinga.

Another implicit aspect of soil water availability is the fact that a reduction in the soil water supply is expected to impair significantly nutrient availability and this can be summarised in a few underlying reasons (*sensu* BLOOM; CHAPIN; MOONEY, 1985): (1) the movement of water towards the roots is diminished and, as a consequence, mass flow of nutrients onwards the roots also decreases; (2) As a result of soil drying, contact of roots and soil particles decreases due to shrinkage of both limiting nutrient diffusion; (3) Increased soil cation concentrations leads to the formation of less soluble cation-bonded compounds; (4) mineralisation rates are also expected to decrease, likely reducing the release of nutrients from organic matter to the soil. Therefore, since the supply of nutrients is generally relatively higher

in S_{CRY} sites, increased water availability can be expected to improve the nutritional status of these ecosystems.

Given that only three independent observations are available for the S_{KAR} category, I am unable to provide conclusive results about the environmental drivers of AGB_W in the S_{KAR} sites. However, it is still noteworthy that AGB_W in GBR-01 (Cambisol) was 58% higher than in GBR-02 (Leptosol). Although these study plots share virtually the same climatic conditions and very close edaphic properties, the soil was markedly shallower in GBR-02. Therefore, it may potentially be a case of bad anchorage to large trees, which often leads to lower AGB_W (QUESADA et al., 2012). Within the S_{KAR} sites, PFF-01 showed the lowest AGB_W even with annual precipitation being 0.3 m higher than the other S_{KAR} stands. This could potentially be due to adverse soil morphological properties (i.e. high rock and gravel levels; shallow depth), community characteristics or even potential uncounted human interference since PFF-01 was close to several small farms surrounding the municipalities of Mossoró and Baraúna, Rio Grande do Norte.

3.4.4 AGB_W, functional diversity and soil properties

Complementary bivariate analyses showed that the community-weighted mean wood density (CWM_{wd}) was not associated with AGB_W, while the mean maximum stem diameter (CWM_{dmax}) accounted for a small but significant variation in AGB_W ($r^2 = 0.20$; $p = 0.009$, Figure 3.10-a). Furthermore, among the components of functional diversity (F_{Ric}, F_{Div}, and F_{Eve}), only F_{Ric} was related to AGB_W ($r^2 = 0.17$; $p = 0.015$; Figure 3.10-b). These results are partially in agreement with Prado-Junior et al. (2016), who found that CWM_{wd} also accounted for only a low proportion of the variance in the initial standing AGB_W, and with F_{Div} and F_{Eve} accounting for variations in AGB_W instead of F_{Ric} found in this work. It should be noted that the functional diversity indexes used in the study by Prado-Junior et al. (2016) also included CWM_{sla} (specific leaf area), although this trait appeared to influence only the growth of surviving trees throughout their recensus.

Higher functional richness is assumed to imply niche complementarity, in which species can take advantage of resources in different manners. For example, assuming that tree diameter is, in general, allometrically associated with other vegetative characteristics (e.g. tree height, crown area, roots depth), a range of species' maximum stem diameter is very likely to reflect life histories and resource partitioning in a given community (VILÀ et al., 2013;

PRADO-JUNIOR et al., 2016). The results presented here suggest that relationships found for a given set of communities (and/or at smaller spatial scales) may not necessarily reflect the same patterns of trait economic spectrum on broader geographical scales or when considering other communities.

Although wood density presumably influences biomass storage (since high wood-density trees hold more biomass per unit of wood volume), this influence did not translate into differences in standing AGB_w in this study. This lack of ability of CWM_{wd} in predicting AGB_w was maintained even alternatively using the global allometric equation for dry forests, which includes wood density as an input variable (CHAVE et al., 2014). The CWM_{wd} itself had an inverse relationship with CWD_{dmax}, indicating a trend for thicker trees of low wood density or the inverse, likely reflecting different plant life histories. For example, the ecological meaning of high (or low) wood density can be broadly interpreted from the physical and biochemical points of view. In this respect, and contrary to the general idea that high wood densities provide higher strength (i.e. resistance to stem breakage), Larjavaara and Muller-Landau, 2010) showed that this may not always be true. This is because the resistance to stem breakage is proportional to the construction costs, and the latter also depends on the diameter of the trunk. Therefore, trunks with varying wood density but the same length can have identical construction costs, and trees with low wood density are more resistant to stem breakage compared to high wood density trees under the same construction costs (LARJAVAARA; MULLER-LANDAU, 2010). However, higher costs of maintaining respiration were shown to be associated with thicker trunk diameter (BOSC; DE GRANDCOURT; LOUSTAU, 2003; LARJAVAARA; MULLER-LANDAU, 2010), the latter unlikely being the most appropriate strategy for a Caatinga tree.

In addition to the physical aspects related to wood density, inverse correlations between CWM_{wd} and soil $[Ca]_{ex}$, $[Mg]_{ex}$, $[K]_{ex}$, $\sum_B$, I_E, $[Fe]_T$, $[Zn]_T$ and $silt_f$, and a positive correlation with $sand_f$ (Table 3.2) were found. Interestingly, the lowest CWM_{wd} was observed in S_{KAR} stands and with a clear trend for higher wood density values in S_{SED} sites, the latter with relatively lower cations availability (Chapter 2, Table 2.2). This indicates a greater abundance of individuals with low wood density in soils with greater availability of metallic cations. Potential mechanisms underlying these relationships have already been comprehensively characterised in detail by QUESADA et al. (2012) in the context of tropical rainforests. Regarding the semiarid Caatinga, these relationships are thought to reflect primarily water-economy strategies. For instance, S_{KAR} GBR-01 and GBR-02 are within the sites with the

lowest mean annual precipitation levels in the dataset (both showing P_A 0.51 m a^{-1}) and are fairly dominated by the low wood density *Commiphora leptophloeos* (Mart.). As wood density is generally well correlated with xylem density (SARMIENTO et al., 2011), those individuals with low wood density can exhibit greater sapwood water capacitance compared to individuals with high wood density, and therefore, greater availability of osmotically active cations may improve the capacitive efficiency of these plant cells (QUESADA et al., 2012). Similarly, given that an inverse association between wood density and parenchymatic tissues (responsible for storing water, nutrients and carbohydrates) can be established, an inverse association between wood density and osmotically active cations can also be reasonably expected (LIRA-MARTINS et al., 2019). This association has been suggested as an evolutionary strategy for plants to cope with potential cavitation in xylem conduits given the high susceptibility of low-wood-density plants to embolism (LIRA-MARTINS et al., 2019). Despite the less apparent causal effect of both $[Zn]_T$ $[Fe]_T$ on reflecting lower values of wood density, Zn has already been shown to improve the activity of osmoregulation substances under drought stress (WU et al., 2015). In contrast, stands with lower availability of osmotically active cations tended to exhibit high CWM_{wd} values, which is likely to reflect a long-term strategy for lower susceptibility to hydraulic failure. Finally, the inverse relationship between CWM_{wd} and soil $silt_f$ and wood density and the positive relationship with $sand_f$ are likely to reflect the nutrient relationships described above. Furthermore, soil texture is expected to correlate with mechanical stability, which in turn was shown to also affect wood density (QUESADA et al., 2012).

The community-weighted mean maximum stem diameter (CWM_{dmax}) was positively associated with F_{Ric}, indicating that stands with thicker adults are also those that fill more niche space. Regarding the relationships between CWM_{dmax} and soil properties, only $[Ca]_{ex}$ and $\sum_B$ were positively associated with CWM_{dmax}, suggesting that only soil bases, rather than I_E (which includes $[Al]_{ex}$), are important for secondary growth in plants. The relationship between eutrophic soils and stem growth was recently observed by Anglélico et al. (2021), who found individuals of *Enterolobium contortisiliquum* (Vell.) with greater stem diameter in eutrophic soils compared to oligotrophic soils in the Brazilian Cerrado. Furthermore, in their study, the cell fibres and pits between the cell vessels were higher in eutrophic soils than in oligotrophic soils, providing evidence that soil conditions influence the wood anatomical characteristics.

Except for $[Al]_{ex}$, F_{Ric} was positively related to all soil cation metrics evaluated (including I_E) and $[Zn]_T$ of the soil. This result suggests that the varying levels of these cations

in the soils reflect physiological adjustments of the trees to achieve the most cost-effective balance between secondary growth and woody density. Indeed, environmental gradients are expected to influence community functional traits, which are determined by the distribution of resources (LIU et al., 2012). Therefore, it seems reasonable to expect that the varying availability levels of these elements provide means for both acquisitive and conservative species to establish, which is reflected in higher F_{Ric}. Jager et al. (2015) observed a coordinated variation of several independent plant traits according to soil fertility degree in a warm forest in New Zealand.

Functional evenness (F_{Eve}) was negatively associated with soil $[C]_T$, $[N]_T$, and $[Mn]_T$. Although in the first evaluation there did not appear to be any causal relationship, this is hypothesised to potentially reflect organic matter quality. For instance, given that the recalcitrance of soil organic carbon (SOC) is influenced by the quality of organic matter produced by the vegetation (WANG et al., 2015), stands with low F_{Eve} may indicate that the niche space is mostly filled towards species with thinner stems of high wood density, these being potentially associated with the 'slow' leaf traits described by Jager et al., 2015 (that is, low SLA, low P and N and high thickness and dry matter content – LDMC). All of these traits are likely to influence the recalcitrance of carbon compounds and their residence time in soils, which in turn may reflect higher SOC values over time.

Functional divergence (F_{Div}) was negatively correlated with soil $[K]_{ex}$. If, as soil $[K]_{ex}$ values increase, traits of the most abundant species occur towards the centre of the niche space (low F_{Div}) (MASON et al., 2005), then the niche differentiation should be relatively small. This also means that competition for resources should be higher in those communities showing low F_{Div} (MASON et al., 2005). Finally, considering the functional traits and diversity metrics explored here, even though only CWM_{wd} and F_{Ric} were significantly different across geological categories (Figure 3.9), several soil properties when considered on a continuous basis, had marked associations with all functional metrics included in this study. This provides evidence for the multi-driven influence of soil properties on the vegetation function and how this may result in variations in biomass stocks over time.

3.5 Conclusions

This work encompassed a biome-wide spatial scale that allowed evaluating complex environmental interactions that account for variations in AGB_W. Specifically, AGB_W was found to be a product of climate and soil properties. Indeed, along the entire mean annual precipitation gradient observed in this work, changes in soil properties [i.e. from less to more favourable conditions in terms of nutrients availability and maximum plant-available soil water] were associated with an approximately three-fold increase in above-ground woody biomass (Figure 3.6). Furthermore, soil properties are suggested to be more limiting in sedimentary environments, whereas water availability appeared to be more influential in crystalline environments. Soil properties were also shown to have and 'indirect influence', by modulating community trait means and functional metrics, with CWM_{dmax} and F_{Ric} weakly predicting AGB_W. Alternative hypothesis of 'biomass ratio' and 'niche complementarity', based on the two traits evaluated, were considered less supported as drivers of AGB_W variations in the Caatinga, which is suggested to be primarily driven by environmental controls.

Supplementary topic

S3.1 – Biomass equations

Woody volume estimates are critical when leading a forest inventory or making management decisions in plantations, with native forest inventories usually showing more obstacles, such as species diversity (i.e., the allometric behaviour varies from species to species) and variable ages between trees (NAZARENO et al., 2021). However, despite the hindrances to obtaining reliable woody estimates, allometric equations have traditionally been used in ecology with a relatively safe margin of error.

Allometric equations remain relatively scarce for Caatinga trees, and there is no 'silver bullet' to obtain fully reliable estimates for the entire region. Most studies apply the Caatinga-specific equation (SAMPAIO; SILVA, 2006) or the global equation for dry forests (CHAVE et al., 2014), widely used at a global level in the tropics. Recent studies proposed using averaged values of the mentioned equations as a manner to reduce biomass estimates uncertainties (e.g. MAIA et al., 2020a; MAIA et al., 2020b). Sampaio and Silva's work provides multiple possibilities to predict AGB_W, i.e., equations based only on stem diameter at the breast height (DBH) or stem diameter at ground level (DGL), or different combinations of stem area at ground level (AGL) and stem area at breast height (ABH) with total tree height (H) and woody density (p).

Regarding only DGL or DBH equations available in the work of Sampaio and Silva (2005), either equation was considered suitable for calculating above-ground biomass as the authors found a very strong relationship between each other ($r^2 = 0.92$). It is noteworthy that some authors claim that the DGL equation should be preferred in Caatinga since it allows for easier measurements in common multitrunked trees of Caatinga, the reason why it is widely used in phytosociological studies across the region (RODAL; SAMPAIO; FIGUEIREDO, 2013).

Further comparison was made between Sampaio and Silva's DBH equations and the global equation for dry forests (CHAVE et al., 2014), widely used to estimate biomass in the tropics. Biomass values estimated through the global equation for dry forests for each standing tree were obtained through the *BIOMASS* package version 2.1.6 (RÉJOU-MÉCHAIN et al., 2021). Taking into account the two available ways to calculate tree biomass, a slightly modified equation from RÉJOU-MÉCHAIN ET AL. (2021) was used, whereby the inputs are wood density, diameter at breast height (DBH), and *E* (a measure of environmental stress estimated from the site coordinates). Wood density values for each species were obtained from the global

wood density database (CHAVE et al., 2009; ZANNE et al., 2009), and attributed to family, genus, or species when available. Botanical names were checked and adjusted according to the Brazilian Flora 2021 with the *flora* package version 0.3.5 (CARVALHO, 2020). On average, the AGB values generated with the Sampaio and Silva DBH equation were 19% higher than the Chave and co-workers' equation, the equations being highly correlated (r = 0.96).

Regardless of the differences observed when using these alternative equations, the DGL Sampaio and Silva equation was adopted in this work, supported by the fact that it was developed in the same region of this study, also achieving the best fits in their original work. Furthermore, specific equations for *cacti* and palm species were used to avoid overestimation of AGB_W values in some cases (a difference of 8 Mg ha^{-1} was recorded in SJO-01 when using the general equation of Sampaio and Silva for Caatinga species for *cacti* individuals). Figure S3.1 shows the relative difference in AGB_W calculated using the chosen equation and three other alternative methods. It should be noted that, depending on the allometric equation, differences in AGB values are found. First, assuming an inclusion criterion of DGL or DBH ≥ 5 cm, it can be expected that differences in stem count will occur. Often, a tree with DGL = 5 cm (or slightly higher) shows DBH < 5 cm, commonly resulting in a higher stem count for DGL rather than DBH. The opposite might also happen where trees usually branch at a certain height (e.g., higher than 30 cm), which is the case for five of the study sites. Despite such a pattern, a comparison between Sampaio and Silva's DGL and DBH equations using original data resulted in a nearly perfect correlation (r = 0.99; p < 0.000), even though the values obtained using the DBH equation were, on average, approximately 38% higher (without using specific equations for palm trees and cactus). This discrepancy can be attributable to the α parameters of these equations (0.0644; 0.1730 for DGL and DBH equations, respectively), thereby even small changes in both α and b coefficients might represent a significant difference in tree volumes, especially for large trees (SAMPAIO; SILVA, 2005).

Another source of variation might be attributable to the presence of *cacti* species. Of course, the difference should be minimal at stands where *cacti* rarely occur or are absent (which is usually not the case for many Caatinga areas). However, where *cacti* species occur in a larger proportion, one might overestimate AGB_W values up to 8 Mg ha^{-1} (as noted in SJO-01) if the general equation for trees is used. It is, in part, due to the columnar format (MAUSETH; KIESLING; OSTOLAZA, 2002) and specific allometric relationships present in most *cacti* species. For example, a strong anisometric relationship was shown for *Cereus giganteus*, i.e. taller specimens tended to be markedly thinner than younger, shorter counterparts (NIKLAS; BUCHMAN, 1994).

Since only 35 palm trees individuals are present in the dataset, it would not be expected to influence the AGB_W values at the plot levels significantly. In any case, palms are also known to show peculiar allometric relationships, and their heights do not necessarily vary proportionately with diameter. This should reflect a series of mechanical architecture strategies of palm species (RICH, 1986, ALVES; MARTINS; SANTOS, 2004).

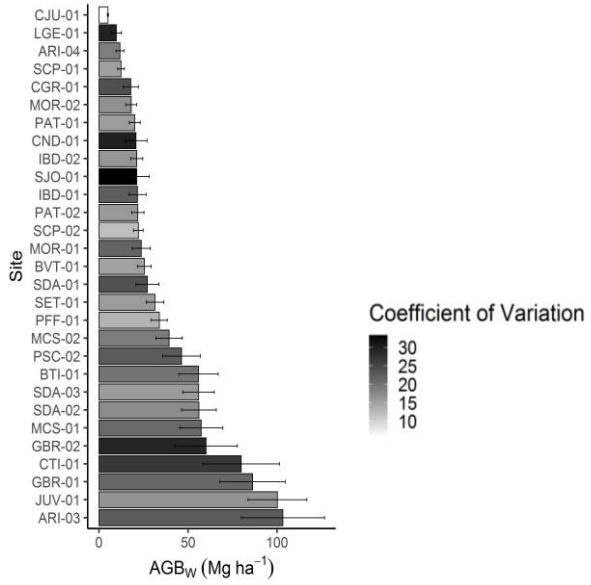

Figure S3.1: AGB_W average values ± standard deviations and coefficient of variation (CV%) relative to alternative equations.

Finally, most of the differences found in AGB_W estimates using the pantropical equation for dry forests (which uses DBH as diameter input) might be due to woody densities (p) entrances as well as the environmental stress factor (*E*). The former may vary significantly between and within tree species in dry forests, with recent work assuming a general average value of 0.55 g cm^{-3} for all Caatinga species (CASTANHO et al., 2020a). This value was used in satellite retrieval for carbon stock estimates for the entire biome (CASTANHO et al., 2020a), nearly achieving AGB_W as for the Caatinga-specific equation. However, we must observe that Caatinga species commonly (by no means always) attain higher wood density values. For example, the nine tree species used for Sampaio and Silva (2005) to develop their allometric equation showed an average woody density of 0.87 g cm^{-3}, but the authors also noted that several Caatinga species hold low wood densities values (such as *Jatropha Molissima* Pohl). Therefore, it is argued that, if possible, appropriate values of the average wood density should be weighted according to the assemblage of species in each community. The average wood densities retrieved from the global wood density database ranged from 0.50 to 0.72 g cm^{-3}, with most sites showing average values ≥ 0.60 g cm^{-3}. Furthermore, environmental stress factor (*E*)

has been shown to influence tropical trees' allometry and is obtained according to climatic water deficit, temperature seasonality, and precipitation seasonality (see CHAVE et al., 2014). Since *E* varied from 0.32 to 1.10 between the study sites, it can be expected that AGB_W estimates using the pantropical equation for dry forests can vary significantly compared to other equations that do not include these parameters.

Chapter 4

Concluding remarks

Chapter 4 – Concluding remarks

This work arose from the unique opportunity to sample soils and vegetation in a considerable part of the geographical extent of the Caatinga Domain. As highlighted throughout this thesis, the marked environmental heterogeneity in the region implies that, in addition to the semiarid climate under which vegetation is subjected, vegetation structure, attributes and composition are likely to be influenced by landscape-scale features in the Caatinga. Specifically, finer-scale environmental factors such as the geologically-derived soil properties and geomorphological features can be expected to account for variations in vegetation properties unexplained by the climate itself. Indeed, soil properties have long been overlooked in vegetation studies in Caatinga. Undertaking soil and vegetation standard protocols, it was shown that at the biome scale, not only climate or soils separately should influence vegetation structure. Instead, complex interactions between soil and climate accounted for variations in above-ground biomass.

Several mechanisms may be involved in vegetation responses to landscape features. For example, water storage capacity in the critical zone (the interactive environment of soil, air, water, rock and living organisms) has already been shown to be determined by underlying lithologies, also leading to differences in the composition of adjacent communities (HAHM et al., 2019). Studies involving ground-water storage and dynamics may bring more clarity for understanding differences in vegetation structure, composition and the mechanisms by which water shortage is ameliorated, thus allowing plant communities to survive during the drier periods in seasonal environments.

Geology (lithology) was associated with differences in several soil properties. However, the results were partially in agreement with what was previously hypothesised. For instance, properties associated with the soil sortive complex, i.e. soil exchangeable cations, soil pH, base and aluminium saturation and weathering metrics (including total reserve of bases) were more evidentially influenced by the underlying geological strata. On the other hand, except for S_{KAR} soils, total soil phosphorus did not present significant differences between geological classes. Phosphorus fractionation studies are still rare in Caatinga and can reveal patterns of P compartmentalisation in organic and inorganic pools with varying bioavailability levels. Similarly, soil organic carbon (accounting for the presence of pedogenic carbonate) had no significant influence from both geological and soil classes. These results suggest that organic carbon dynamics in Caatinga soils should be much more associated with carbon build-up and decomposition processes rather than a pedogenetic control. In this sense, a series of tools can be used in the future to help understand organic matter dynamics. For example, the use of

magnetic susceptibility (MS) can be used as a proxy. This method measures the magnetisation ability of a given material in a presence of a magnetic field. Therefore, not only the presence of ferrimagnetic minerals can be measured through this method, but also organic matter (OM) since it has a strong influence on MS. In addition, a magnetised phase of iron minerals such as goethite, ferrihydrite and hematite takes place only in the presence of organic matter (HANESCH; STANJEK; PETERSEN, 2006). This approach would shed some light on the mechanisms behind the formation of organo-mineral complexes and mineral transformations, potentially improving our ability to evaluate soil organic matter dynamics and isotope patterns. Future studies could also test the influence of the plant material quality on soil carbon storage and turnover. This approach has already been successfully undertaken (QUIDEAU et al., 2001) and can bring new information on how carbon storage and turnover are conditioned.

The assumption that the nitrogen cycle is strongly modulated by climatic conditions in water-limited environments was confirmed in this study. For instance, it was found that low total annual rainfall amounts, combined with a more regular distribution throughout the year are likely to provide favourable conditions for nitrogen transformations in the soils, as suggested by higher $\delta^{15}N$ values measured under these conditions. Nevertheless, the influence of the effective cation exchange capacity on soil $\delta^{15}N$ values under more humid conditions provides evidence that the nitrogen cycle can be also affected by soil properties even in semiarid environments. Machine learning techniques can be useful to elucidate the influence of soil properties on isotopic discrimination processes under a ‘pedo-isotopic view’.

Finally, the influence of soil properties (especially soil cations) on vegetation attributes, i.e. maximum stem diameter and wood density suggests that, although phylogenetic and climatic controls can also be expected, soil properties influence species’ strategies and performance. In the last instance, beyond the intuitive importance of water availability in the dry Caatinga, soil properties can also be considered of essential relevance for vegetation structure, and functioning, presumably affecting species’ evolutionary path in the long-term. The relationships found in this work are also thought to reflect vegetation trade-offs between investment in secondary growth and water-economy strategies.

References

AB'SÁBER, A. N. O domínio morfoclimático semi-árido das caatingas brasileiras. **Geomorfologia**, São Paulo, n. 43, p. 1–39, 1974.

AB'SÁBER, A. N.; MARIGO, L. C. **Ecosistemas do Brasil**. São Paulo: Metalivros, 2006.

ABREU, C. A. de; LOPES, A. S.; SANTOS, G. C. G. dos. Micronutrients. In: NOVAIS, R. F.; V. ALVAREZ, V. H. A.; BARROS, N. F. De; FONTES, R. L. F.; CANTARUTTI, R. B.; NEVES, J. C. L. (Eds.). **Fertilidade de Solo**. 1. ed. Viçosa. p. 645–736.

ACIEGO PIETRI, J. C.; BROOKES, P. C. Relationships between soil pH and microbial properties in a UK arable soil. **Soil Biology and Biochemistry**, v. 40, n. 7, p. 1856–1861, 2008.

AERTS, R. Nutrient Resorption from Senescing Leaves of Perennials: Are there General Patterns? **The Journal of Ecology**, v. 84, n. 4, p. 597, 1996. Available at: https://www.jstor.org/stable/2261481?origin=crossref

AGBENIN, J. O.; TIESSEN, H. Phosphorus transformations in a toposequence of lithosols and cambisols from semi-arid northeastern brazil. **Geoderma**, v. 62, n. 4, p. 345–362, 1994.

ALBUQUERQUE, U. P. de; DE LIMA ARAÚJO, E.; EL-DEIR, A. C. A.; DE LIMA, A. L. A.; SOUTO, A.; BEZERRA, B. M.; FERRAZ, E. M. N.; MARIA XAVIER FREIRE, E.; SAMPAIO, E. V. D. S. B.; LAS-CASAS, F. M. G.; DE MOURA, G. J. B.; PEREIRA, G. A.; DE MELO, J. G.; ALVES RAMOS, M.; RODAL, M. J. N.; SCHIEL, N.; DE LYRA-NEVES, R. M.; ALVES, R. R. N.; DE AZEVEDO, S. M.; TELINO, W. R.; SEVERI, W. Caatinga revisited: Ecology and conservation of an important seasonal dry forest. **The Scientific World Journal**, v. 2012, n. August, p. 1–18, 2012.

ALBUQUERQUE, A. S.; FREIRE, F. J.; BARBOSA, M. D.; MARANGON, L. C.; FELICIANO, A. L. P. Efficiency of biological utilization of micronutrients by forests species in hypoxerophytic caatinga. **Floresta e Ambiente**, v. 25, n. 4, 2018.

ALCÂNTARA, L. R. P. de; COUTINHO, A. P.; NETO, S. M. D. S.; DE GUSMÃO DA CUNHA RABELO, A. E. C.; ANTONINO, A. C. D. Computational modeling of the hydrological processes in caatinga and pasture areas in the brazilian semi-arid. **Water (Switzerland)**, v. 13, n. 13, 2021.

ALKMIM, F. F.; MARTINS-NETO, M. A. Brazil. In: SELLEY, R. C; COCKS, L. R. M.; PLIMER, I. R. (org.). **Encyclopedia of geology**. Oxford: Elsevier, 2004. v. 1, p. 306-327.

ALLEN, K.; DUPUY, J. M.; GEI, M. G.; HULSHOF, C.; MEDVIGY, D.; PIZANO, C.; SALGADO-NEGRET, B.; SMITH, C. M.; TRIERWEILER, A.; VAN BLOEM, S. J.; WARING, B. G.; XU, X.; POWERS, J. S. Will seasonally dry tropical forests be sensitive or resistant to future changes in rainfall regimes? **Environmental Research Letters**, v. 12, n. 2, 2017.

ALMEIDA, F. F. M. De; HASUI, Y.; NEVES, B. B. de B.; FUCK, R. A. **Províncias estruturais brasileiras. Actas**, 1977.

ALMEIDA, F. F. M.; HASUI, Y.; DE BRITO NEVES, B. B.; FUCK, R. A. Brazilian structural provinces: An introduction. **Earth Science Reviews**, v. 17, n. 1–2, p. 1–29, 1981.

ALVES, L. F.; MARTINS, F. R.; SANTOS, F. A. M. Alometria de uma palmeira Neotropical, Euterpe edulis Mart. **Acta Botanica Brasilica**, v. 18, n. 2, p. 369–374, 2004.

AMUNDSON, R.; AUSTIN, A. T.; SCHUUR, E. A. G.; YOO, K.; MATZEK, V.; KENDALL, C.; UEBERSAX, A.; BRENNER, D.; BAISDEN, W. T. Global patterns of the isotopic composition of soil and plant nitrogen. **Global Biogeochemical Cycles**, v. 17, n. 1, 2003.

ANDRADE-LIMA, D. The caatingas dominium. **Revista Brasilera de Botânica.**, v. 4, n. 1, p. 149–163, 1981.

ANDRADE, G. O. De. **Alguns Aspectos do Quadro Natural do Nordeste**, Série B: Brasil. SUDENE. Estudos Regionais. 2, 1977.

ANGÉLICO, T. dos S.; MARCATI, C. R.; ROSSI, S.; DA SILVA, M. R.; SONSIN-OLIVEIRA, J. Soil effects on stem growth and wood anatomy of tamboril are mediated by tree age. **Forests**, v. 12, n. 8, p. 1–14, 2021.

APGAUA, D. M. G.; PEREIRA, D. G. S.; SANTOS, R. M.; MENINO, G. C. O.; PIRES, G. G.; FONTES, M. A. L.; TNG, D. Y. P. Floristic variation within seasonally dry tropical forests of the Caatinga Biogeographic Domain, Brazil, and its conservation implications. **International Forestry Review**, v. 17, n. Special Issue 2, p. 33–44, 2015.

ARANIBAR, J. N.; OTTER, L.; MACKO, S. A.; FERAL, C. J. W.; EPSTEIN, H. E.; DOWTY, P. R.; ECKARDT, F.; SHUGART, H. H.; SWAP, R. J. Nitrogen cycling in the soil-plant system along a precipitation gradient in the Kalahari sands. **Global Change Biology**, v. 10, n. 3, p. 359–373, 2004.

ARAÚJO-FILHO, J. C. De. Relação Solos e Paisagem no Bioma Caatinga. **Anais do Simpósio Brasileiro de Geografia Física Aplicada**, v. 14, p. 23, 2011. Available at: http://www.alice.cnptia.embrapa.br/alice/handle/doc/896995

ARAÚJO-FILHO, J. C. de; CORREIA, R. C.; CUNHA, T. J. F.; NETO, M. B. de O.; ARAÚJO, J. L. P.; SILVA, M. M. de L. Ambientes e solos do Semiárido: potencialidades, limitações e aspectos socioeconômicos. In: **Tecnologias de Convivência com o Semiárido Brasileiro**. Fortaleza: Banco do Nordeste do Brasil S. A., 2019. p. 17–84.

ARAÚJO-FILHO, J. C. de; RIBEIRO, M. R.; BURGOS, N.; MARQUES, F. A. Solos da Caatinga. In: CURI, N.; KER, J. C.; NOVAIS, R. F.; VIDAL-TORRADO, P.; SCHAEFER, C. E. G. R. (Eds.). **Pedologia - Solos dos Biomas Brasileiros**. [s.l.] : Sociedade Brasileira de Ciência do Solo, 2017. p. 227–260.

ARAÚJO, M. S. B.; SCHAEFER, C. E. R.; SAMPAIO, E. V. S. B. Soil phosphorus fractions from toposequences of semi-arid Latosols and Luvisols in northeastern Brazil. **Geoderma**, v. 119, n. 3–4, p. 309–321, 2004.

BACHMAN, G. O.; MACHETTE, M. N. Calcic soils and calcretes in the southwestern United States. **Open-File Report 77-794**, p. 168, 1977.

BAISDEN, W. T.; AMUNDSON, R.; COOK, A. C.; BRENNER, D. L. Turnover and storage of C and N in five density fractions from California annual grassland surface soils. **Global Biogeochemical Cycles**, v. 16, n. 4, p. 64-1-64–16, 2002.

BALDOCK, J. A.; SKJEMSTAD, J. O. Role of the soil matrix and minerals in protecting natural organic materials against biological attack. **Organic Geochemistry**, v. 31, n. 7–8, p. 697–710, 2000.

BARALOTO, C.; RABAUD, S.; MOLTO, Q.; BLANC, L.; FORTUNEL, C.; HÉRAULT, B.; DÁVILA, N.; MESONES, I.; RIOS, M.; VALDERRAMA, E.; FINE, P. V. A. Disentangling stand and environmental correlates of aboveground biomass in Amazonian forests. **Global Change Biology**, v. 17, n. 8, p. 2677–2688, 2011.

BARTON, K.; BARTON, M. K. MuMIn: Multi-Model Inference. **R package** version 1.47.1, 2022. Available at: https://cran.r-project.org/package=MuMIn

BAUMAN, D.; DROUET, T.; DRAY, S.; VLEMINCKX, J. Disentangling good from bad practices in the selection of spatial or phylogenetic eigenvectors. **Ecography**, v. 41, n. 10, p. 1638–1649, 2018a.

BAUMAN, D.; DROUET, T.; FORTIN, M. J.; DRAY, S. Optimizing the choice of a spatial weighting matrix in eigenvector-based methods. **Ecology**, v. 99, n. 10, p. 2159–2166, 2018b.

BAUMGARTNER, S.; BAUTERS, M.; BARTHEL, M.; DRAKE, T. W.; NTABOBA, L. C.; BAZIRAKE, B. M.; SIX, J.; BOECKX, P.; VAN OOST, K. Stable isotope signatures of soil nitrogen on an environmental-geomorphic gradient within the Congo Basin. **Soil**, v. 7, n. 1, p. 83–94, 2021.

BECKNELL, J. M.; KUCEK, L. K.; POWERS, J. S. Aboveground biomass in mature and secondary seasonally dry tropical forests: A literature review and global synthesis. **Forest Ecology and Management**, v. 276, p. 88–95, 2012. a. Available at: http://dx.doi.org/10.1016/j.foreco.2012.03.033

BEEK, K. J.; BRAMAO, D. L. Nature and Geography of South American Soils. In: OYE, P. V. **Biogeography and Ecology in South America**. p. 82–112. 1968.

BELLÈ, S. L.; RIOTTE, J.; SEKHAR, M.; RUIZ, L.; SCHIEDUNG, M.; ABIVEN, S. Soil organic carbon stocks and quality in small-scale tropical, sub-humid and semi-arid watersheds under shrubland and dry deciduous forest in southwestern India. **Geoderma**, v. 409, 115606, 2022.

BELNAP, J. CRUSTS | Biological. In: **Reference Module in Earth Systems and Environmental Sciences**. [s.l.] : Elsevier, 2013. p. 1–10.

BELNAP, J.; WEBER, B.; BÜDEL, B. **Biological Soil Crusts as an Organizing Principle in Drylands**. [s.l.] : Springer, 2016. Available at: http://link.springer.com/10.1007/978-3-319-30214-0_1

BESSA, M. C.; LACERDA, C. F.; AMORIM, A. V.; BEZERRA, A. M. E.; LIMA, A. D. Mechanisms of salt tolerance in seedlings of six woody native species of the Brazilian semi-arid. **Revista Ciência Agronômica**, v. 48, n. 1, p. 157–165, 2017.

BIONDI, C. M.; NASCIMENTO, C. W. A. Do; FABRICIO NETA, A. de B.; RIBEIRO, M. R. Teores de Fe, Mn, Zn, Cu, Ni e Co em solos de referência de Pernambuco. **Revista Brasileira de Ciência do Solo**, v. 35, n. 3, p. 1057–1066, 2011.

BIZZI, L. A.; SCHOBBENHAUS, C.; MOHRIAK, W. U. Bacias Sedimentares da Margem Continental Brasileira Base de Dados. In: BIZZI, L. A.; SCHOBBENHAUS, C.; VIDOTT, R. M.; GONÇALVES, J. H. (Eds.). **Geologia, Tectônica e Recursos Minerais do Brasil**. Brasília: CPRM, 2003. p. 87–94.

BJORNSTAD, O. N.; CAI, J. **Package 'ncf': Spatial Covariance Functions**. Available at: https://cran.r-project.org/package=ncf

BLOOM, A. J.; CHAPIN, F. S.; MOONEY, H. A. Resource Limitation in Plants - An Economic Analogy. **Annual review of ecology and systematics. Vol. 16**, p. 363–392, 1985.

BLOOM, A. J.; SMITH, S. Mineral Nutrition. In: TAIZ, L.; ZEIGER, E.; MØLLER, I. M.; MURPHY, A. (Eds.). **Plant Physiology and Development**. Sixth ed. [s.l.] : Sinauer Associates, 2015. p. 119–142.

BOJÓRQUEZ-QUINTAL, E.; ESCALANTE-MAGAÑA, C.; ECHEVARRÍA-MACHADO, I.; MARTÍNEZ-ESTÉVEZ, M. Aluminum, a friend or foe of higher plants in acid soils. **Frontiers in Plant Science**, v. 8, n. October, p. 1–18, 2017.

BOSC, A.; DE GRANDCOURT, A.; LOUSTAU, D. Variability of stem and branch maintenance respiration in a Pinus pinaster tree. **Tree Physiology**, v. 23, n. 4, p. 227–236, 2003.

BOWEN, N. L. **The Evolution of the Igneous Rocks**. New York: Dover Publications, INC., 1928.

BRONICK, C. J.; LAL, R. Soil structure and management: A review. **Geoderma**, v. 124, n. 1–2, p. 3–22, 2005.

BROWN, S.; LUGO, A. E. The Storage and Production of Organic Matter in Tropical Forests and Their Role in the Global Carbon Cycle. **Biotropica**, v. 14, n. 3, p. 161, 1982.

BRUUN, T. B.; ELBERLING, B.; CHRISTENSEN, B. T. Lability of soil organic carbon in tropical soils with different clay minerals. **Soil Biology & Biochemistry**, v. 42, n. 6, p. 888–895, 2010. Available at: http://dx.doi.org/10.1016/j.soilbio.2010.01.009

BUENO, M. L.; DEXTER, K. G.; PENNINGTON, R. T.; PONTARA, V.; NEVES, D. M.; RATTER, J. A.; DE OLIVEIRA-FILHO, A. T. The environmental triangle of the Cerrado Domain: Ecological factors driving shifts in tree species composition between forests and savannas. **Journal of Ecology**, v. 106, n. 5, p. 2109–2120, 2018.

BURNHAM, K. P.; ANDERSON, D. R.; HUYVAERT, K. P. AIC model selection and multimodel inference in behavioral ecology: Some background, observations, and comparisons. **Behavioral Ecology and Sociobiology**, v. 65, n. 1, p. 23–35, 2011.

CAIXETA, J. M.; BUENO, G. V.; MAGNAVITA, L. P.; FEIJÓ, F. J. Bacias do Recôncavo, Tucano e Jatobá. **Boletim de Geociências da Petrobras**, v. 8, n. 1, p. 167–172, 1994.

CARVALHO, G. flora: Tools for Interacting with the Brazilian Flora 2020. **R package** version 0.3.4., 2020. Available at: http://www.github.com/gustavobio/flora BugReports

CASTANHO, A. D. A.; COE, M.; ANDRADE, E. M.; WALKER, W.; BACCINI, A.; CAMPOS, D. A.; FARINA, M. A close look at above ground biomass of a large and heterogeneous seasonally dry tropical forest-caatinga in north east of Brazil. **Anais da Academia Brasileira de Ciencias**, v. 92, n. 1, p. 1–18, 2020a.

CASTANHO, A. D. A.; COE, M. T.; BRANDO, P.; MACEDO, M.; BACCINI, A.; WALKER, W.; ANDRADE, E. M. Potential shifts in the aboveground biomass and physiognomy of a seasonally dry tropical forest in a changing climate. **Environmental Research Letters**, v. 15, n. 3, 2020b.

CEMIC, L. **Thermodynamics in Mineral Sciences: An Introduction**. Springer. 386 p. 2005

CHAPIN, F. S.; VITOUSEK, P. M.; VAN CLEVE, K. The nature of nutrient limitation in plant communities. **American Naturalist**, v. 127, n. 1, p. 48–58, 1986.

CHATURVEDI, R. K.; RAGHUBANSHI, A. S. Species Composition, Distribution, and Diversity of Woody Species in a Tropical Dry Forest of India. **Journal of Sustainable Forestry**, v. 33, n. 8, p. 729–756, 2014. Available at: http://dx.doi.org/10.1080/10549811.2014.925402

CHAVE, J.; COOMES, D.; JANSEN, S.; LEWIS, S. L.; SWENSON, N. G.; ZANNE, A. E. Towards a worldwide wood economics spectrum. **Ecology Letters**, v. 12, n. 4, p. 351–366, 2009.

CHAVE, J.; RÉJOU-MÉCHAIN, M.; BÚRQUEZ, A.; CHIDUMAYO, E.; COLGAN, M. S.; DELITTI, W. B. C.; DUQUE, A.; EID, T.; FEARNSIDE, P. M.; GOODMAN, R. C.; HENRY, M.; MARTÍNEZ-YRÍZAR, A.; MUGASHA, W. A.; MULLER-LANDAU, H. C.; MENCUCCINI, M.; NELSON, B. W.; NGOMANDA, A.; NOGUEIRA, E. M.; ORTIZ-MALAVASSI, E.; PÉLISSIER, R.; PLOTON, P.; RYAN, C. M.; SALDARRIAGA, J. G.; VIEILLEDENT, G. Improved allometric models to estimate the aboveground biomass of tropical trees. **Global Change Biology**, v. 20, n. 10, p. 3177–3190, 2014.

CHEN, Y.; LIAN, B.; YIN, Z.; TANG, Y. Weathering of carbonate rocks by biological soil crusts in karst areas. **Journal of Earth Science**, v. 25, n. 4, p. 662–667, 2014.

CHEN, Z. C.; PENG, W. T.; LI, J.; LIAO, H. Functional dissection and transport mechanism of magnesium in plants. **Seminars in Cell and Developmental Biology**, v. 74, p. 142–152, 2018. Available at: https://doi.org/10.1016/j.semcdb.2017.08.005

CLARHOLM, M.; SKYLLBERG, U.; ROSLING, A. Organic acid induced release of nutrients from metal-stabilized soil organic matter - The unbutton model. **Soil Biology and Biochemistry**, v. 84, p. 168–176, 2015. Available at: http://dx.doi.org/10.1016/j.soilbio.2015.02.019

CLARK, D. A.; CLARK, D. B. Landscape scale variation in forest structure and biomass in a tropical forest. **Forest Ecology and Management**, 14: 185-198. 2000.

COSTA, F. R. C.; SCHIETTI, J.; STARK, S. C.; SMITH, M. N. The other side of tropical forest drought: do shallow water table regions of Amazonia act as large-scale hydrological refugia from drought? **New Phytologist**, 2022.

CPRM, S. G. do B. Diagnóstico do Município de Buriti dos Lopes. **Projeto Cadastro de Fontes de Abastecimento por Água Subeterrânea**, n. Piauí, 2004.

CRAINE, J. M.; ELMORE, A. J.; WANG, L.; AUGUSTO, L.; BAISDEN, W. T.; BROOKSHIRE, E. N. J.; CRAMER, M. D.; HASSELQUIST, N. J.; HOBBIE, E. A.; KAHMEN, A.; KOBA, K.; KRANABETTER, J. M.; MACK, M. C.; MARIN-SPIOTTA, E.; MAYOR, J. R.; MCLAUCHLAN, K. K.; MICHELSEN, A.; NARDOTO, G. B.; OLIVEIRA, R. S.; PERAKIS, S. S.; PERI, P. L.; QUESADA, C. A.; RICHTER, A.; SCHIPPER, L. A.; STEVENSON, B. A.; TURNER, B. L.; VIANI, R. A. G.; WANEK, W.; ZELLER, B. Convergence of soil nitrogen isotopes across global climate gradients. **Scientific Reports**, v. 5, p. 1–8, 2015.

CROSS, A. F.; SCHLESINGER, W. H. A literature review and evaluation of the Hedley fractionation: Applications to the biogeochemical cycle of soil phosphorus in natural ecosystems. **Geoderma**, v. 64, n. 3–4, p. 197–214, 1995.

DA CONCEIÇÃO, D. M.; DE ANDRADE, L. S.; CISNEROS, J. C.; IANNUZZI, R.; PEREIRA, A. A.; MACHADO, F. C. New petrified forest in Maranhão, Permian (Cisuralian) of the Parnaíba Basin, Brazil. **Journal of South American Earth Sciences**, v. 70, p. 308–323, 2016. Available at: https://linkinghub.elsevier.com/retrieve/pii/S0895981116300840

DA COSTA, G. M.; CARDOSO, D.; DE QUEIROZ, L. P.; CONCEIÇÃO, A. A. Local changes in floristic richness in two ecorregions of the caatinga. **Rodriguesia**, v. 66, n. 3, p. 685–709, 2015.

DA SILVA, J. M. C.; LEAL, I. R.; TABARELLI, M. **Caatinga: The Largest Tropical Dry Forest Region in South America**. Cham: Springer International Publishing, 2017. Available at: http://link.springer.com/10.1007/978-3-319-68339-3

DAN, W.; NIANPENG, H.; QING, W.; YULIANG, L.; QIUFENG, W.; ZHIWEI, X.; JIANXING, Z. Effects of Temperature and Moisture on Soil Organic Matter Decomposition Along Elevation Gradients on the Changbai Mountains, Northeast China. **Pedosphere**, v. 26, n. 3, p. 399–407, 2016. Available at: http://dx.doi.org/10.1016/S1002-0160(15)60052-2

DAVIDSON, E. A.; JANSSENS, I. A. Temperature sensitivity of soil carbon decomposition and feedbacks to climate change. **Nature**, v. 440, n. 7081, p. 165–173, 2006.

DE SOUZA, C. R.; MOREL, J. D.; SANTOS, A. B. M.; DA SILVA, W. B.; MAIA, V. A.; COELHO, P. A.; REZENDE, V. L.; DOS SANTOS, R. M. Small-scale edaphic heterogeneity as a floristic–structural complexity driver in Seasonally Dry Tropical Forests tree communities. **Journal of Forestry Research**, v. 31, n. 6, p. 2347–2357, 2019.

DE SOUZA, L. Q.; DE FREITAS, A. D. S.; SAMPAIO, E. V. de S. B.; MOURA, P. M.; MENEZES, R. S. C. How much nitrogen is fixed by biological symbiosis in tropical dry forests? 1. Trees and shrubs. **Nutrient Cycling in Agroecosystems**, v. 94, n. 2–3, p. 171–179, 2012.

DELHAIZE, E.; RYAN, P. R. Aluminum Toxicity and Tolerance in Plants. **Plant Physiology**, v. 107, n. 2, p. 315–321, 1995.

DELVAUX, B.; HERBILLON, A. J.; VIELVOYE, L. Characterization of a weathering sequence of soils derived from volcanic ash in Cameroon. Taxonomic, mineralogical and agronomic implications. **Geoderma**, v. 45, n. 3–4, p. 375–388, 1989.

DEXTER, K. G.; PENNINGTON, R. T.; OLIVEIRA-FILHO, A. T.; BUENO, M. L.; SILVA DE MIRANDA, P. L.; NEVES, D. M. Inserting Tropical Dry Forests Into the Discussion on Biome Transitions in the Tropics. **Frontiers in Ecology and Evolution**, v. 6, n. July, p. 1–7, 2018.

DHALIWAL, S. S.; NARESH, R. K.; MANDAL, A.; SINGH, R.; DHALIWAL, M. K. Dynamics and transformations of micronutrients in agricultural soils as influenced by organic matter build-up: A review. **Environmental and Sustainability Indicators**, v. 1–2, n. May, p. 100007, 2019.

DÍAZ, S.; FARGIONE, J.; CHAPIN, F. S.; TILMAN, D. Biodiversity loss threatens human well-being. **PLoS Biology**, v. 4, n. 8, p. 1300–1305, 2006.

DIRZO, R.; YOUNG, H.; MOONEY, H. Seasonally Dry Tropical Forest Ecology and. In: DIRZO, R.; YOUNG, H.; CABALLOS, G.; MOONEY, H. . (Eds.). **Seasonally Dry Tropical Forests: Ecology and Conservation**. [s.l: s.n.]. p. 159–172.

DOMINGUES, T. F.; MEIR, P.; FELDPAUSCH, T. R.; SAIZ, G.; VEENENDAAL, E. M.; SCHRODT, F.; BIRD, M.; DJAGBLETEY, G.; HIEN, F.; COMPAORE, H.; DIALLO, A.; GRACE, J.; LLOYD, J. Co-limitation of photosynthetic capacity by nitrogen and phosphorus in West Africa woodlands. **Plant, Cell and Environment**, v. 33, n. 6, p. 959–980, 2010.

DORMANN, C. F.; ELITH, J.; BACHER, S.; BUCHMANN, C.; CARL, G.; CARRÉ, G.; MARQUÉZ, J. R. G.; GRUBER, B.; LAFOURCADE, B.; LEITÃO, P. J.; MÜNKEMÜLLER, T.; MCCLEAN, C.; OSBORNE, P. E.; REINEKING, B.; SCHRÖDER, B.; SKIDMORE, A. K.; ZURELL, D.; LAUTENBACH, S. Collinearity: A review of methods to deal with it and a simulation study evaluating their performance. **Ecography**, v. 36, n. 1, p. 27–46, 2013.

DRAY, A. S.; BAUMAN, D.; BLANCHET, G.; BORCARD, D.; CLAPPE, S.; GUENARD, G.; JOMBART, T.; LAROCQUE, G.; LEGENDRE, P.; MADI, N.; WAGNER, H. H. **R Package** 'adespatial'. 2021.

DRIESSEN, P.; DECKERS, J.; SPAARGAREN, O.; NACHTERGAELE, F. **Lecture notes on the major soils of the world**. FAO, Rome.

DRYFLOR. Plant diversity patterns in neotropical dry forests and their conservation implications. **Science**, v. 353, n. 6306, p. 1383–1387, 2016. Available at: https://www.sciencemag.org/lookup/doi/10.1126/science.aaf5080

DUSSIN, I. A.; DUSSIN, T. M. Supergrupo Espinhaço: Modelo de Evolução Geodinâmica. **Geonomos**, p. 1–8, 1995.

ELRYS, A. S.; ALI, A.; ZHANG, H.; CHENG, Y.; ZHANG, J.; CAI, Z. C.; MÜLLER, C.; CHANG, S. X. Patterns and drivers of global gross nitrogen mineralization in soils. **Global Change Biology**, v. 27, n. 22, p. 5950–5962, 2021.

ERNANI; ALMEIDA; SANTOS, 2007. IX Potássio In: NOVAIS et al. (2007): **Fertilidade do Solo**, Sociedade Brasileira de Ciência do Solo, 2007.

FAN, Y.; MIGUEZ-MACHO, G.; JOBBÁGY, E. G.; JACKSON, R. B.; OTERO-CASAL, C. Hydrologic regulation of plant rooting depth. **Proceedings of the National Academy of Sciences of the United States of America**, v. 114, n. 40, p. 10572–10577, 2017.

FAVARIN, A.; LAFORET, M. R.; ARCANJO, R. História. **Embrapa Solo e Suas Origens**. Available on: https://www.embrapa.br/solos/historia. Acessed in 25/03/2022.

FEIG, G. T.; MAMTIMIN, B.; MEIXNER, F. X. Soil biogenic emissions of nitric oxide from a semi-arid savanna in South Africa. **Biogeosciences**, v. 5, n. 6, p. 1723–1738, 2008.

FERNANDES, M. F.; CARDOSO, D.; and QUEIROZ, L. P. (2020). An updated plant checklist of the Brazilian Caatinga seasonally dry forests and woodlands reveals high species richness and endemism. **J. Arid Environ**. 174:104079. doi: 10.1016/j.jaridenv.2019.104079

FERNANDES, M. F.; CARDOSO, D.; PENNINGTON, R. T.; DE QUEIROZ, L. P. The Origins and Historical Assembly of the Brazilian Caatinga Seasonally Dry Tropical Forests. **Frontiers in Ecology and Evolution**, v. 10, n. February, p. 1–13, 2022.

FERREIRA, E. P. Gênese e Classificação de Solos em Ambiente Cárstico na Chapada do Apodi. 2013. **Dissertation**. UFRRJ, 2013.

FERREIRA, E. P.; DOS ANJOS, L. H. C.; PEREIRA, M. G.; VALLADARES, G. S.; CIPRIANO-SILVA, R.; DE AZEVEDO, A. C. Genesis and classification of soils containing carbonate on the apodi plateau, Brazil. **Revista Brasileira de Ciencia do Solo**, v. 40, p. 1–20, 2016.

FIANTIS, D.; NELSON, M.; SHAMSHUDDIN, J.; GOH, T. B.; VAN RANST, E. Determination of the Geochemical Weathering Indices and Trace Elements Content of New Volcanic Ash Deposits from Mt. Talang (West Sumatra) Indonesia. **Eurasian Soil Science**, v. 43, n. 13, p. 1477–1485, 2010.

FICK, S. E.; HIJMANS, R. J. WorldClim 2: new 1-km spatial resolution climate surfaces for global land areas. **International Journal of Climatology**, v. 37, n. 12, p. 4302–4315, 2017.

FONTES, M. P. F. Intemperismo de rochas e minerais. In: KER, J. C.; CURI, N.; SCHAEFER, C. E. R.; VIDAL-TORRADO, P. (Eds.). **Pedologia - Fundamentos**. 1st. ed. Viçosa: SBCS, 2012. p. 343.

FRAGA, V. da S.; SALCEDO, I. H. Declines of Organic Nutrient Pools in Tropical Semi-Arid Soils under Subsistence Farming. **Soil Science Society of America Journal**, v. 68, n. 1, p. 215–224, 2004.

FRANCHINI, J. C.; DEBIASI, H.; SACOMAN, A.; NEPOMUCENO, A. L.; FARIAS, J. R. B. Manejo do solo para redução das perdas de produtividade pela seca. **Embrapa, Documentos 314**, n. 314, p. 39, 2009.

FREITAS, A. D. S.; SAMPAIO, E. V. S. B.; SANTOS, C. E. R. S.; FERNANDES, A. R. Biological nitrogen fixation in tree legumes of the Brazilian semi-arid caatinga. **Journal of Arid Environments**, v. 74, n. 3, p. 344–349, 2010. Available at: http://dx.doi.org/10.1016/j.jaridenv.2009.09.018

FREITAS, A. D. S.; DE SÁ BARRETTO SAMPAIO, E. V.; MENEZES, R. S. C.; TIESSEN, H. ^{15}N natural abundance of non-fixing woody species in the Brazilian dry forest (caatinga). **Isotopes in Environmental and Health Studies**, v. 46, n. 2, p. 210–218, 2010.

FREITAS, A. D. S.; DE SAMPAIO, E. V. S. B.; DA SILVA, B. L. R.; DE ALMEIDA CORTEZ, J. S.; MENEZES, R. S. C. How much nitrogen is fixed by biological symbiosis in tropical dry forests? 2. Herbs. **Nutrient Cycling in Agroecosystems**, v. 94, n. 2–3, p. 181–192, 2012.

FREITAS, A. D. S.; SAMPAIO, E. V. de S. B.; RAMOS, A. P. de S.; BARBOSA, M. R. de V.; LYRA, R. P.; ARAÚJO, E. L. Nitrogen isotopic patterns in tropical forests along a rainfall gradient in Northeast Brazil. **Plant and Soil**, v. 391, n. 1–2, p. 109–122, 2015.

FROMM, J. Wood formation of trees in relation to potassium and calcium nutrition. **Tree Physiology**, v. 30, n. 9, p. 1140–1147, 2010.

GAISER, T.; GRAEF, F.; CORDEIRO, J. C. Water retention characteristics of soils with contrasting clay mineral composition in semi-arid tropical regions. **Australian Journal of Soil Research**, v. 38, n. 3, p. 523–536, 2000.

GARCIA-MONTIEL, D. C.; NEILL, C.; MELILLO, J.; THOMAS, S.; STEUDLER, P. A.; CERRI, C. C. Soil Phosphorus Transformations Following Forest Clearing for Pasture in the Brazilian Amazon. **Soil Science Society of America Journal**, v. 64, n. 5, p. 1792–1804, 2000.

GAVIRIA, J.; TURNER, B. L.; ENGELBRECHT, B. M. J. Drivers of tree species distribution across a tropical rainfall gradient. **Ecosphere**, v. 8, n. 2, 2017.

GEI, M. G.; POWERS, J. S. Nutrient Cycling in Tropical Dry Forests. In: SÁNCHEZ-AZOFEIFA, A.; POWERS, J. S.; FERNANDES, G. W.; QUESADA, M. (Eds.). **Tropical Dry Forests in the Americas**. Boca Raton: CRC Press, 2014. p. 141–156.

GOLDICH, S. S. A Study in Rock-weathering. **Journal of Geology**, n. 3, 1938.

GREEN, J. K.; SENEVIRATNE, S. I.; BERG, A. M.; FINDELL, K. L.; HAGEMANN, S.; LAWRENCE, D. M.; GENTINE, P. Large influence of soil moisture on long-term terrestrial carbon uptake. **Nature**, v. 565, n. 7740, p. 476–479, 2019. Available at: http://dx.doi.org/10.1038/s41586-018-0848-x

GRIME, J. P. Benefits of plant diversity to ecosystems: immediate, filter and founder effects. **Journal of Ecology**, v. 86, p. 902–910, 1998.

GÜNTNER, A.; BRONSTERT, A. Representation of landscape variability and lateral redistribution processes for large-scale hydrological modelling in semi-arid areas. **Journal of Hydrology**, v. 297, n. 1–4, p. 136–161, 2004.

GUO, F.; YOST, R. S.; HUE, N. V.; EVENSEN, C. I.; SILVA, J. A. Changes in Phosphorus Fractions in Soils under Intensive Plant Growth. **Soil Science Society of America Journal**, v. 64, n. 5, p. 1681–1689, 2000.

GUSWA, A. J. Effect of plant uptake strategy on the water-optimal root depth. **Water Resources Research**, v. 46, n. 9, p. 1–5, 2010.

HAHM, W. J.; REMPE, D. M.; DRALLE, D. N.; DAWSON, T. E.; LOVILL, S. M.; BRYK, A. B.; BISH, D. L.; SCHIEBER, J.; DIETRICH, W. E. Lithologically Controlled Subsurface Critical Zone Thickness and Water Storage Capacity Determine Regional Plant Community Composition. **Water Resources Research**, [s. l.], v. 55, n. 4, p. 3028–3055, 2019.

HANESCH, M.; STANJEK, H.; PETERSEN, N. Thermomagnetic measurements of soil iron minerals: The role of organic carbon. **Geophysical Journal International**, [s. l.], v. 165, n. 1, p. 53–61, 2006.

HARRISON, X. A.; DONALDSON, L.; CORREA-CANO, M. E.; EVANS, J.; FISHER, D. N.; GOODWIN, C. E. D.; ROBINSON, B. S.; HODGSON, D. J.; INGER, R. A brief introduction to mixed effects modelling and multi-model inference in ecology. **PeerJ**, v. 2018, n. 5, p. 1–32, 2018.

HASUI, Y. Compartimentação Geológica do Brasil. In: HASUI, Y.; CARNEIRO, C. D. R.; ALMEIDA, F. F. M. De; BARTORELI, A. (Eds.). **Geologia do Brasil**. [s.l.] : Beca, 2012. p. 112–122.

HE, X.; AUGUSTO, L.; GOLL, D. S.; RINGEVAL, B.; WANG, Y.; HELFENSTEIN, J.; HUANG, Y.; YU, K.; WANG, Z.; YANG, Y.; HOU, E. Global patterns and drivers of soil total phosphorus concentration. **Earth System Science Data**, v. 13, n. 12, p. 5831–5846, 2021.

HEDIN, L. O.; BROOKSHIRE, E. N. J.; MENGE, D. N. L.; BARRON, A. R. The nitrogen paradox in tropical forest ecosystems. **Annual Review of Ecology, Evolution, and Systematics**, [s. l.], v. 40, p. 613–635, 2009.

HEDLEY, M. J.; STEWART, J. W. B.; CHAUHAN, B. S. Changes in Inorganic and Organic Soil Phosphorus Fractions Induced by Cultivation Practices and by Laboratory Incubations. **Soil Science Society of America Journal**, v. 46, n. 5, p. 970–976, 1982.

HODNETT, M. G.; TOMASELLA, J. Marked differences between van Genuchten soil water -retention parameters. **Geoderma**, v. 108, p. 155–180, 2002.

HÖGBERG, P. Tansley Review No. 95 ^{15} natural abundance in soil-plant systems. **New Phytologist**, v. 137, n. 2, p. 179–203, 1997.

HOULTON, B. Z.; MARKLEIN, A. R.; BAI, E. Representation of nitrogen in climate change forecasts. **Nature Climate Change**, v. 5, n. 5, p. 398–401, 2015.

HU, L.; SU, Y.; HE, X.; WU, J.; ZHENG, H.; LI, Y.; WANG, A. Response of soil organic carbon mineralization in typical Karst soils following the addition of 14C-labeled rice straw and CaCO 3. **Journal of the Science of Food and Agriculture**, v. 92, n. 5, p. 1112–1118, 2012.

IBGE. **Biomas e Sistema Costeiro-Marinho do Brasil: compatível com a escala 1:250.000**, Brazilian Institute of Geography and Statistics. Rio de Janeiro. 2019a.

IBGE. **Macrocaracterização dos Recursos Naturais do Brasil**. Rio de Janeiro. Brazilian Institute of Geography and Statistics. Rio de Janeiro. 2019 b. Available at: https://biblioteca.ibge.gov.br/visualizacao/livros/liv101648.pdf

IUSS Working Group WRB. 2015. World Reference Base for Soil Resources 2014, update 2015. International soil classification system for naming soils and creating legends for soil maps. **World Soil Resources Reports No. 106**. FAO, Rome.

JACKSON, M.L. Chemical composition of soils. In: Bear, F (Ed.), **Chemistry of the soil**. 2nd ed. Van Nostrand Reinhold Co. N.Y. p. 71-141, 1969.

JACKSON, R. B.; CANADELL, J.; EHLERINGER, J. R.; MOONEY, H. A.; SALA, O. E.; SCHULZE, E. D. A global analysis of root distributions for terrestrial biomes. **Oecologia**, v. 108, n. 3, p. 389–411, 1996.

JACOMINE, P. K. T.; SILVA, F. B. R. e; FORMIGA, R. A.; ALMEIDA, J. C.; BELTRÃO, V. de A.; PESSÔA, S. C. P.; FERREIRA, R. C.; FERREIRA, R. C. Levantamento Exploratório - Reconhecimento de Solos do Estado do Rio Grande do Norte. **Boletim técnico n.° 21**, n. MA/DNPEA-SUDENE/DRN, 1971.

JACOMINE, P. K. T.; CAVALCANTI, A. C.; BURGOS, N.; PESSOA, S. C. P.; SILVEIRA, C. O. Da. Levantamento Exploratório - Reconhecimento de Solos do Estado de Pernambuco - Volume II. **Boletim Técnico n.°26**, n. MA/DNPEA-SUDENE/DRN, p. 354, 1972a.

JACOMINE, P. K. T.; RIBEIRO, M. R.; MONTENEGRO, J. C.; SILVA, A. P. De; FILHO, H. F. R. de M. Levantamento Exploratório - Reconhecimento de Solos do Estado da Paraíba. **Boletim Técnico n.°15**, n. MA/DNPEA-SUDENE/DRN, p. 683, 1972b.

JACOMINE, P. K. T.; ALMEIDA, J. C.; MEDEIROS, L. A. R. Levantamento Exploratório - Reconhecimento de Solos do Estado do Ceará - Volume I. **Boletim Técnico n.° 28**, n. MA/DNPEA-SUDENE/DRN, p. 301, 1973a.

JACOMINE, P. K. T.; CAVALCANTI, A. C.; BURGOS, N.; PESSOA, S. C. P.; SILVEIRA, C. O. Da. Levantamento Exploratório - Reconhecimento de Solos do Estado de Pernambuco - Volume I. **Boletim Técnico n.°26**, n. MA/DNPEA-SUDENE/DRN, p. 359, 1973b.

JACOMINE, P. K. T.; CAVALCANTI, A. C.; PESSÔA, S. C. P.; SILVEIRA, C. O. Da. Levantamento Exploratório de Reconhecimento de Ssolos do Estado de Alagoas. **Boletim Técnico n.° 35**, n. EMBRAPA/SUDENE-DRN, p. 531, 1975.

JACOMINE, P. K. T.; CAVALCANTI, A. C.; RIBEIRO, M. R.; MONTENEGRO, J. O.; BURGOS, N.; FILHO, H. F. R. de M.; FORMIGA, R. A. Levantamento Exploratório - Reconhecimento de Solos da Margem Esquerda do Rio São Francisco - Estado da Bahia. **Boletim Técnico n.° 38**, n. MA/DNPEA-SUDENE/DRN, p. 439, 1976.

JACOMINE, P. K. T.; CAVALCANTI, A. C.; SILVA, F. B. R. e; MONTENEGRO, J. O.; FORMIGA, R. A.; BURGOS, N.; FILHO, H. F. R. de M. Levantamento Exploratório - Reconhecimento de Solos da Margem Direita do Rio São Francisco - Estado da Bahia - Volume I. **Boletim Técnico n° 52**, n. EMBRAPA/DNPEA-SUDENE/DRN, p. 735, 1977.

JACOMINE, P. K. T.; CAVALCANTI, A. C.; FORMIGA, R. A.; SILVA, F. B. R. e; BURGOS, N.; MEDEIROS, L. A. R.; LOPES, O. F.; FILHO, H. F. R. de M.; PESSÔA, S. C. P.; LIMA, P. C. De. Levantamento Exploratório - Reconhecimento de Solos do Norte de Minas Gerais (Área de Atuação da Sudene). **Boletim Técnico n° 60**, v. 1, n. MA/DNPEA-SUDENE/DRN, p. 407, 1979.

JACOMINE, P. K. T.; CAVALCANTI, A. C.; BURGOS, N.; PESSOA, S. C. P.; SILVEIRA C. O. da; et al. **Mapa Exploratório - Reconhecimento de Solos do Estado do Piauí**, 1983.

JACOMINE, P. K. T.; CAVALCANTI, A. C.; PESSTA, S. C. P.; BURGOS, N.; MEDEIROS, L. A. R.; LOPES, O. F.; FILHO, H. F. R. de M. Levantamento Exploratório - Reconhecimento de Solos do Estado do Maranhão - Volume I. **Boletim Técnico n.° 35**, n. MA/DNPEA-SUDENE/DRN, 1986.

JAGER, M. M.; RICHARDSON, S. J.; BELLINGHAM, P. J.; CLEARWATER, M. J.; LAUGHLIN, D. C. Soil fertility induces coordinated responses of multiple independent functional traits. **Journal of Ecology**, v. 103, n. 2, p. 374–385, 2015.

JAJOO, A.; ALLAKHVERDIEV, S. I. High-temperature Stress in Plants: Consequences and Strategies for Protecting Photosynthetic Machinery. In: SHABALA, S. (Ed.). **Plant Stress Physiology**. 2nd. ed. University of Tasmania, Australia: CABI, 2017. p. 138–154.

JALEEL, C. A.; MANIVANNAN, P.; SANKAR, B.; KISHOREKUMAR, A.; GOPI, R.; SOMASUNDARAM, R.; PANNEERSELVAM, R. Water deficit stress mitigation by calcium chloride in Catharanthus roseus: Effects on oxidative stress, proline metabolism and indole alkaloid accumulation. **Colloids and Surfaces B: Biointerfaces**, v. 60, n. 1, p. 110–116, 2007.

JAHN, R., BLUME; H-P, ASIO, V. B.; SPAARGAREN; O AND SCHAD, P (2006) **Guidelines for soil description**. FAO, Rome, 97 p.

JARAMILLO, V. J.; MURRAY-TORTAROLO, G. N. Tropical dry forest soils: global change and local-scale consequences for soil biogeochemical processes. In: BUSSE, M.; GIARDINA, C.; MORRIS, D.; PAGE-DUMROESE, D. (Eds.). **Global Change and Forest Soils**. 1. ed. [s.l: s.n.]. v. 36p. 109–130.

JARBAS, T.; CUNHA, F.; PETRERE, V. G.; MONTEIRO, A.; MENDES, S.; MELO, R. F. De; BATISTA, M.; NETO, D. O. Principiais Solos do Semiárido Tropical Brasileiro: caracterização, potencialidades, limitações, fertilidade e manejo. **Semiárido Brasileiro: Pesquisa, Desenvolvimento e Inovação.**, p. 402, 2010.

JENNY, H. **The Soil Resource**. Origin and Behaviour. In. BILLINGS, W. D.; GOLLEY, F.; LANGE, O. L.; OLSON, J. S.; REMMERT, K. Ecological Studies. Springer New York, NY. v. 37. 1980.

JIANG, Y.; HUANG, B. Effects of calcium on antioxidant activities and water relations associated with heat tolerance in two cool-season grasses. **Journal of Experimental Botany**, v. 52, n. 355, p. 341–349, 2001.

KASPARI, M.; GARCIA, M. N.; HARMS, K. E.; SANTANA, M.; WRIGHT, S. J.; YAVITT, J. B. Multiple nutrients limit litterfall and decomposition in a tropical forest. **Ecology Letters**, v. 11, n. 1, p. 35–43, 2008.

KENZO, T.; SANO, M.; YONEDA, R.; CHANN, S. Comparison of wood density and water content between dry evergreen and dry deciduous forest trees in central Cambodia. **Japan Agricultural Research Quarterly**, v. 51, n. 4, p. 363–374, 2017.

KER, J. C. Latossolos Do Brasil: Uma Revisão. Geonomos, [s. l.], v. 5, n. 1, p. 17–40, 1997.

ING, D. A.; DAVIES, S. J.; NOOR, N. S. M. Growth and mortality are related to adult tree size in a Malaysian mixed dipterocarp forest. **Forest Ecology and Management**, v. 223, n. 1–3, p. 152–158, 2006.

KIRSTEN, M.; MIKUTTA, R.; VOGEL, C.; THOMPSON, A.; MUELLER, C. W.; KIMARO, D. N.; BERGSMA, H. L. T.; FEGER, K. H.; KALBITZ, K. Iron oxides and aluminous clays selectively control soil carbon storage and stability in the humid tropics. **Scientific Reports**, v. 11, n. 1, p. 1–12, 2021. Available at: https://doi.org/10.1038/s41598-021-84777-7

KITAYAMA, K.; MAJALAP-LEE, N.; AIBA, S. Soil phosphorus fractionation and phosphorus-use efficiencies of tropical rainforests along altitudinal gradients of Mount Kinabalu, Borneo. **Oecologia**, v. 123, n. 3, p. 342–349, 2000. Available at: http://link.springer.com/10.1007/s004420051020

LAIO, F.; D'ODORICO, P.; RIDOLFI, L. An analytical model to relate the vertical root distribution to climate and soil properties. **Geophysical Research Letters**, v. 33, n. 18, p. 1–5, 2006.

LALIBERTÉ, E., LEGENDRE, P. & SHIPLEY, B. (2014) FD: Measuring Functional Diversity from Multiple Traits, and Other Tools for Functional Ecology. **R package** version 1.0-12. Available at http://cran.r-project.org/.

LARJAVAARA, M.; MULLER-LANDAU, H. C. Rethinking the value of high wood density. **Functional Ecology**, v. 24, n. 4, p. 701–705, 2010.

LAURANCE, W. F.; FEARNSIDE, P. M.; LAURANCE, S. G.; DELAMONICA, P.; LOVEJOY, T. E.; RANKIN-DE MERONA, J. M.; CHAMBERS, J. Q.; GASCON, C. Relationship between soils and Amazon forest biomass. **Forest Ecology and Mangement**, v. 118, p. 127–138, 1999.

LAVOREL, S.; GRIGULIS, K.; MCINTYRE, S.; WILLIAMS, N. S. G.; GARDEN, D.; DORROUGH, J.; BERMAN, S.; QUÉTIER, F.; THÉBAULT, A.; BONIS, A. Assessing functional diversity in the field - Methodology matters! **Functional Ecology**, v. 22, n. 1, p. 134–147, 2008.

LE QUÉRÉ, C.; ANDRES, R. J.; BODEN, T.; CONWAY, T.; HOUGHTON, R. A.; HOUSE, J. I.; MARLAND, G.; PETERS, G. P.; VAN DER WERF, G. R.; AHLSTRÖM, A.; ANDREW, R. M.; BOPP, L.; CANADELL, J. G.; CIAIS, P.; DONEY, S. C.; ENRIGHT, C.; FRIEDLINGSTEIN, P.; HUNTINGFORD, C.; JAIN, A. K.; JOURDAIN, C.; KATO, E.; KEELING, R. F.; KLEIN GOLDEWIJK, K.; LEVIS, S.; LEVY, P.; LOMAS, M.; POULTER, B.; RAUPACH, M. R.; SCHWINGER, J.; SITCH, S.; STOCKER, B. D.; VIOVY, N.; ZAEHLE, S.; ZENG, N. The global carbon budget 1959-2011. **Earth System Science Data**, v. 5, n. 1, p. 165–185, 2013.

LEBRIJA-TREJOS, E.; BONGERS, F.; PÉREZ-GARCÍA, E. A.; MEAVE, J. A. Successional change and resilience of a very dry tropical deciduous forest following shifting agriculture. **Biotropica**, v. 40, n. 4, p. 422–431, 2008.

LIMA, J. R.; MAGALHÃES, A. R. Secas no Nordeste: registros históricos das catástrofes econômicas e humanas do século 16 ao século 21. **Revista Parcerias Estratégicas**, Brasília-DF, v. 23, n. 46, p. 191-212, jan./jun. 2018.

LIMA, R. L. S. de; SEVERINO, L. S.; FERREIRA, G. B.; DE AZEVEDO, C. A. V.; SOFIATTI, V.; ARRIEL, N. H. C. Soil exchangeable aluminum influencing the growth and leaf tissue macronutrients content of castor plants. **Revista Caatinga**, v. 27, n. 4, p. 10–15, 2014.

LIRA-MARTINS, D.; HUMPHREYS-WILLIAMS, E.; STREKOPYTOV, S.; ISHIDA, F. Y.; QUESADA, C. A.; LLOYD, J. Tropical tree branch-leaf nutrient scaling relationships vary with sampling location. **Frontiers in Plant Science**, v. 10, n. July, 2019.

LIU, X.; SWENSON, N. G.; WRIGHT, S. J.; ZHANG, L.; SONG, K.; DU, Y.; ZHANG, J.; MI, X.; REN, H.; MA, K. Covariation in plant functional traits and soil fertility within two species-rich forests. **PLoS ONE**, v. 7, n. 4, 2012.

LLOYD, J.; DOMINGUES, T. F.; SCHRODT, F.; ISHIDA, F. Y.; FELDPAUSCH, T. R.; SAIZ, G.; QUESADA, C. A.; SCHWARZ, M.; TORELLO-RAVENTOS, M.; GILPIN, M.; MARIMON, B. S.; MARIMON-JUNIOR, B. H.; RATTER, J. A.; GRACE, J.; NARDOTO, G. B.; VEENENDAAL, E.; ARROYO, L.; VILLARROEL, D.; KILLEEN, T. J.; STEININGER, M.; PHILLIPS, O. L. Edaphic, structural and physiological contrasts across Amazon Basin forest-savanna ecotones suggest a role for potassium as a key modulator of tropical woody vegetation structure and function. **Biogeosciences**, v. 12, n. 22, p. 6529–6571, 2015.

LLOYD, J.; GOULDEN, M. L.; OMETTO, J. P.; PATIÑO, S.; FYLLAS, N. M.; QUESADA, C. A. Ecophysiology of forest and savanna vegetation. In: KELLER, M.; BUSTAMANTE, M.; GASH, J.; DIAS, P. S. (Eds.). **Amazonia and Global Change**. Washington D. C.: American Geophysical Union, 2009. p. 463–484.

LLOYD, J.; TAYLOR, J. A. On the Temperature Dependence of Soil Respiration. **Functional Ecology**, v. 8, n. 3, p. 315–323, British Ecological Society. 1994.

LOHBECK, M.; POORTER, L.; MARTINEZ-RAMOS, M.; BONGERS, F.; CRAFT, N. J. B. Biomass is the main driver of changes in ecosystem process rates during tropical forest succession. **Ecology**, v. 96, n. 5, p. 1242–1252, 2015.

LÜ, L.; WANG, R.; LIU, H.; YIN, J.; XIAO, J.; WANG, Z.; ZHAO, Y.; YU, G.; HAN, X.; JIANG, Y. Effect of soil coarseness on soil base cations and available micronutrients in a semi-arid sandy grassland. **Solid Earth**, v. 7, n. 2, p. 549–556, 2016.

LÜTZOW, M. V.; KÖGEL-KNABNER, I.; EKSCHMITT, K.; MATZNER, E.; GUGGENBERGER, G.; MARSCHNER, B.; FLESSA, H. Stabilization of organic matter in temperate soils: Mechanisms and their relevance under different soil conditions - A review. **European Journal of Soil Science**, v. 57, n. 4, p. 426–445, 2006.

MABESOONE, J. M.; NEUMANN, V. H. Sedimentary Basins of Brazilian Borborema and São Francisco Tectonic Provinces Since Mesoproterozoic. In: MABESOONE, J. M.; NEUMANN, V. H. (Eds.). **Cyclic Development of Sedimentary Basins**. [s.l.] : Elsevier, 2005. p. 191–236.

MAIA, V. A.; DE SOUZA, C. R.; DE AGUIAR-CAMPOS, N.; FAGUNDES, N. C. A.; SANTOS, A. B. M.; DE PAULA, G. G. P.; SANTOS, P. F.; SILVA, W. B.; DE OLIVEIRA MENINO, G. C.; DOS SANTOS, R. M. Interactions between climate and soil shape tree community assembly and above-ground woody biomass of tropical dry forests. **Forest Ecology and Management**, v. 474, n. May, p. 118348, 2020a.

MAIA, V. A.; MIRANDA SANTOS, A. B.; DE AGUIAR-CAMPOS, N.; DE SOUZA, C. R.; DE OLIVEIRA, M. C. F.; COELHO, P. A.; MOREL, J. D.; DA COSTA, L. S.; FARRAPO, C. L.; ALENCAR FAGUNDES, N. C.; PIRES DE PAULA, G. G.; SANTOS, P. F.; GIANASI, F. M.; DA SILVA, W. B.; DE OLIVEIRA, F.; GIRARDELLI, D. T.; ARAÚJO, F. de C.; VILELA, T. A.; PEREIRA, R. T.; ARANTES DA SILVA, L. C.; DE OLIVEIRA MENINO, G. C.; GARCIA, P. O.; LEITE FONTES, M. A.; DOS SANTOS, R. M. The carbon sink of tropical seasonal forests in southeastern Brazil can be under threat. **Science Advances**, v. 6, n. 51, p. 1–12, 2020b.

MARENGO, J. A.; CUNHA, A. P.; ALVES, L. M. A seca de 2012-15 no semiárido do Nordeste do Brasil no contexto histórico. Revista Climanálise, [s. l.], v. 4, n. 1, p. 49–54, 2016. Available at: http://climanalise.cptec.inpe.br/~rclimanl/revista/pdf/30anos/marengoetal.pdf

MARIN-SPIOTTA, E.; SILVER, W. L.; SWANSTON, C. W.; OSTERTAG, R. Soil organic matter dynamics during 80 years of reforestation of tropical pastures. **Global Change Biology**, v. 15, n. 6, p. 1584–1597, 2009.

MARKESTEIJN, L.; IRAIPI, J.; BONGERS, F.; POORTER, L. Seasonal variation in soil and plant water potentials in a Bolivian tropical moist and dry forest. **Journal of Tropical Ecology**, v. 26, n. 5, p. 497–508, 2010.

MARQUES, J. . J. .; TEIXEIRA, W. G.; SCHULZE, D. G.; CURI, N. Mineralogy of soils with unusually high exchangeable Al from the western Amazon Region. **Clay Minerals**, v. 37, n. 4, p. 651–661, 2002.

MARTINELLI L.A., PICCOLO MC, TOWNSEND AR, VITOUSEK PM, CUEVAS E, MCDOWELL W, ROBERTSON GP, SANTOS OC, TRESEDER K. 1999. Nitrogen stable isotopic composition of leaves and soil: tropical versus temperate forests. **Biogeochemistry** 46 (1–3): 45–65. 1999.

MARTINELLI, L. A.; NARDOTO, G. B.; SOLTANGHEISI, A.; REIS, C. R. G.; ABDALLA-FILHO, A. L.; CAMARGO, P. B.; DOMINGUES, T. F.; FARIA, D.; FIGUEIRA, A. M.; GOMES, T. F.; LINS, S. R. M.; MARDEGAN, S. F.; MARIANO, E.; MIATTO, R. C.; MORAES, R.; MOREIRA, M. Z.; OLIVEIRA, R. S.; OMETTO, J. P. H. B.; SANTOS, F. L. S.; SENA-SOUZA, J.; SILVA, D. M. L.; SILVA, J. C. S. S.; VIEIRA, S. A. Determining ecosystem functioning in Brazilian biomes through foliar carbon and nitrogen concentrations and stable isotope ratios. **Biogeochemistry**, v. 154, n. 2, p. 405–423, 2021. Available at: https://doi.org/10.1007/s10533-020-00714-2

MARTÍNEZ-YRÍZAR, A., 1995. Biomass distribution and primary productivity of tropical dry forests. In: Bullock, S.H., Mooney, H.A. (Eds.), **Seasonally Dry Tropical Forests**. Cambridge University Press, Cambridge, pp. 326–345.

MASON, N. W. H.; MOUILLOT, D.; LEE, W. G.; WILSON, J. B. Functional richness, functional evenness and functional divergence: The primary components of functional diversity. **Oikos**, v. 111, n. 1, p. 112–118, 2005.

MATHUR, S.; AGRAWAL, D.; JAJOO, A. Photosynthesis: Response to high temperature stress. **Journal of Photochemistry and Photobiology B: Biology**, v. 137, p. 116–126, 2014. Available at: http://dx.doi.org/10.1016/j.jphotobiol.2014.01.010

MAUSETH, J.; KIESLING, R.; OSTOLAZA, C. **A Cactus Odyssey**. Journeys in the wilds of Bolivia, Peru, and Argentina. Timber Press, Portland, Oregon. 2002.

MAX, A.; WING, J.; WESTON, S.; WILLIAMS, A.; KEEFER, C.; ENGELHARDT, A.; COOPER, T.; MAYER, Z.; ZIEM, A.; SCRUCCA, L.; HUNT, T.; KUHN, M. M. Classification and Regression Training. '**Caret package**' version 6.0-86.

MAZEROLLE, M. J.; Model Selection and Multimodel Inference Based on (Q)AIC(c). **'AICmodavg' R package** version 2.3-1. 2020.

MCDOWELL, N.; ALLEN, C. D.; ANDERSON-TEIXEIRA, K.; BRANDO, P.; BRIENEN, R.; CHAMBERS, J.; CHRISTOFFERSEN, B.; DAVIES, S.; DOUGHTY, C.; DUQUE, A.; ESPIRITO-SANTO, F.; FISHER, R.; FONTES, C. G.; GALBRAITH, D.; GOODSMAN, D.; GROSSIORD, C.; HARTMANN, H.; HOLM, J.; JOHNSON, D. J.; KASSIM, A. R.; KELLER, M.; KOVEN, C.; KUEPPERS, L.; KUMAGAI, T.; MALHI, Y.; MCMAHON, S. M.; MENCUCCINI, M.; MEIR, P.; MOORCROFT, P.; MULLER-LANDAU, H. C.; PHILLIPS, O. L.; POWELL, T.; SIERRA, C. A.; SPERRY, J.; WARREN, J.; XU, C.; XU, X. Drivers and mechanisms of tree mortality in moist tropical forests. **New Phytologist**, v. 219, n. 3, p. 851–869, 2018.

MCGILL, W. B.; COLE, C. V. Comparative Aspects of Cycling of Organic C, N, S and P Through Soil Organic Matter. **Geoderma**, v. 26, p. 267–286, 1981.

MCKEY, D. Legumes and nitrogen: The evolutionary ecology of a nitrogen-demanding lifestyle. **Advances in Legume Systematics 5: The Nitrogen Factor**, v. 5, n. JANUARY 1994, p. 211–228, 1994.

MCLAREN, K. P.; MCDONALD, M. A. The effects of moisture and shade on seed germination and seedling survival in a tropical dry forest in Jamaica. **Forest Ecology and Management**, v. 183, n. 1–3, p. 61–75, 2003.

MEDINA, E.; GARCIA, V.; CUEVAS, E. Sclerophylly and Oligotrophic Environments: Relationships Between Leaf Structure, Mineral Nutrient Content, and Drought Resistance in Tropical Rain Forests of the Upper Rio Negro Region. **Biotropica**, v. 22, n. 1, p. 51, 1990.

MEIADO, M. V.; SILVA, F. F. S. Da; BARBOSA, D. C. de A.; FILHO SIQUEIRA, J. A. De. Diaspores of the caatinga: a review. In: FILHO, J. A. de S.; CONCEIÇÃO, A. A.; RAPINI, A. et al. (Eds.). **Flora of the Caatingas of the São Francisco River – Natural History and Conservation.** Rio de Janeiro. v. Chapter 9p. 306–365.

MELFI, A. J.; CERRI, C. C.; KRONBERG, B. I.; FYFE, W. S.; MCKINNON, B. Granitic weathering: a Brazilian study. **Journal of Soil Science**, v. 34, n. 4, p. 841–851, 1983.

MENEZES, R. S. C.; SALES, A. T.; PRIMO, D. C.; ALBUQUERQUE, E. R. G. M. De; JESUS, K. N. De; PAREYN, F. G. C.; SANTANA, M. da S.; SANTOS, U. J. Dos; MARTINS, J. C. R.; ALTHOFF, T. D.; NASCIMENTO, D. M. Do; GOUVEIA, R. F.; FERNANDES, M. M.; LOUREIRO, D. C.; ARAÚJO FILHO, J. C. De; GIONGO, V.; DUDA, G. P.; ALVES, B. J. R.; IVO, W. M. P. de M.; ANDRADE, E. M. De; PINTO, A. de S.; SAMPAIO, E. V. de S. B. Soil and vegetation carbon stocks after land-use changes in a seasonally dry tropical forest. **Geoderma**, v. 390, n. January, 2021.

MENEZES, R.S.M.; GARRIDO, M.S.; PEREZ-MARIN, A.M., 2005. Fertilidade dos solos no semi-árido. In **Proceedings of the XXX Congresso Brasileiro de Ciência do Solo**. Recife: Sociedade Brasileira de Ciência do Solo. 30 p. CD-ROM. 2005

MENEZES, R.; SAMPAIO, E.; GIONGO, V.; PÉREZ-MARIN, A. Biogeochemical cycling in terrestrial ecosystems of the Caatinga Biome. **Brazilian Journal of Biology**, v. 72, n. 3 (suppl.), p. 643–653, 2012.

MESQUITA, A. C.; DANTAS, B. F.; CAIRO, P. A. R. Ecophysiology of caatinga native species under semi-arid conditions. **Bioscience Journal**, v. 34, n. 6, p. 81–89, 2018.

MILANI, E. J.; THOMAZ FILHO, A. Sedimentary Basins of the South America. **Tectonic Evolution of South America**, n. November, p. 389–449, 2000.

MILES, L.; NEWTON, A. C.; DEFRIES, R. S.; RAVILIOUS, C.; MAY, I.; BLYTH, S.; KAPOS, V.; GORDON, J. E. A global overview of the conservation status of tropical dry forests. **Journal of Biogeography**, v. 33, n. 3, p. 491–505, 2006. Available at: https://onlinelibrary.wiley.com/doi/10.1111/j.1365-2699.2005.01424.x

MOINET, G. Y. K.; MOINET, M.; HUNT, J. E.; RUMPEL, C.; CHABBI, A.; MILLARD, P. Temperature sensitivity of decomposition decreases with increasing soil organic matter stability. **Science of the Total Environment**, v. 704, p. 135460, 2020. Available at: https://doi.org/10.1016/j.scitotenv.2019.135460

MONGER, H. C.; MARTINEZ-RIOS, J. J.; KHRESAT, S. A. Arid and Semiarid. In: HILLEL, D.; ROSENZWEIG, C.; POWLSON, D.; SCOW, K.; SINGER, M.; SPARKS, D. (Eds.). **Encyclopedia of Soils in the Enviorment - Vol 4.** 1 edition ed. New York, NY: Academic Press, 2005. p. 375.

MOONEY, H. A.; BULLOCK, S. H.; MEDINA, E. Introduction. In: MOONEY, H. A.; BULLOCK, S. H.; MEDINA, E. (Eds.). **Seasonally Dry Tropical Forests**. [s.l.] : Cambridge University Press, 1995. p. 1–8.

MOONLIGHT, P. W.; BANDA-R K, PHILLIPS O. L., et al. Expanding tropical forest monitoring into Dry Forests: The DRYFLOR protocol for permanent plots. The DryFlor field manual for plot establishment and remeasurement (supporting information). **Plants, People, Planet**, 2020;00:1-6. Available at: https://doi.org/10.1002/ppp3.10112

MOORE, S.; ADU-BREDU, S.; DUAH-GYAMFI, A.; ADDO-DANSO, S. D.; IBRAHIM, F.; MBOU, A. T.; GRANDCOURT, A.; VALENTINI, R.; NICOLINI, G.; DJAGBLETEY, G.; OWUSU-AFRIYIE, K.; GVOZDEVAITE, A.; OLIVERAS, I.; RUIZ-JAEN, M. C.; MALHI, Y. Forest biomass, productivity and carbon cycling along a rainfall gradient in West Africa. **Global Change Biology**, v. 24, n. 2, p. e496–e510, 2018. Available at: https://onlinelibrary.wiley.com/doi/10.1111/gcb.13907

MORENO-JIMÉNEZ, E.; PLAZA, C.; SAIZ, H.; MANZANO, R.; FLAGMEIER, M.; MAESTRE, F. T. Aridity and reduced soil micronutrient availability in global drylands. **Nature Sustainability**, v. 2, n. 5, p. 371–377, 2019. Available at: http://www.nature.com/articles/s41893-019-0262-x

MORO, M. F.; NIC LUGHADHA, E.; DE ARAÚJO, F. S.; MARTINS, F. R. A Phytogeographical Metaanalysis of the Semiarid Caatinga Domain in Brazil. **Botanical Review**, v. 82, n. 2, p. 91–148, 2016. Available at: http://dx.doi.org/10.1007/s12229-016-9164-z

MORO, M. F.; NIC LUGHADHA, E.; FILER, D. L.; ARAÚJO, F. S. De; MARTINS, F. R. A catalogue of the vascular plants of the Caatinga Phytogeographical Domain: a synthesis of floristic and phytosociological surveys. **Phytotaxa**, v. 160, n. 1–118, p. 0, 2014. Available at: https://biotaxa.org/Phytotaxa/article/view/phytotaxa.160.1.1

MORO, M. F.; SILVA, I. A.; DE ARAÚJO, F. S.; LUGHADHA, E. N.; MEAGHER, T. R.; MARTINS, F. R. The role of edaphic environment and climate in structuring phylogenetic pattern in seasonally dry tropical plant communities. **PLoS ONE**, v. 10, n. 3, p. 1–18, 2015.

MOSHI, A. O.; WILD, A.; GREENLAND, D. J. Effect of Organic Matter on the Charge and Phosphate Adsorption Characteristics of Kikuyu Red Clay From Kenya. **Geoderma**, v. 11, n. 4, p. 275–285, 1974.

MOURA, M. S. B. de M.; SOBRINHO, J. E.; SILVA, T. G. F. Da; SOUZA, W. M. De. Aspectos Meteorólogicos do Semiárido Brasileiro. In: XIMENES, L. F.; SILVA, M. S. L. Da; BRITO, L. T. de L. (Eds.). **Tecnologias de Convivência com o Semiárido Brasileiro**. Fortaleza: Banco do Nordeste do Brasil, 2019. p. 85–104.

MURPHY, P. G.; LUGO, A. E. Ecology of Tropical Dry Forest. **Annual review of ecology and systematics. Vol. 17**, v. 17, n. 1, p. 67–88, 1986. b. Available at: https://www.annualreviews.org/doi/10.1146/annurev.es.17.110186.000435

NAJAFI-GHIRI, M.; REZABIGI, S.; HOSSEINI, S.; BOOSTANI, H. R.; OWLIAIE, H. R. Potassium fixation of some calcareous soils after short term extraction with different solutions. **Archives of Agronomy and Soil Science**, v. 65, n. 7, p. 897–910, 2019. Available at: https://doi.org/10.1080/03650340.2018.1537485

NAKAGAWA, S.; SCHIELZETH, H. A general and simple method for obtaining R2 from generalized linear mixed-effects models. **Methods in Ecology and Evolution**, v. 4, n. 2, p. 133–142, 2013.

NANZYO, M.; KANNO, H. **Inorganic constituents in soil: Basics and visuals**. Springer Open. 181 p. 2018.

NARDOTO, G. B.; OMETTO, J. P. H. B.; EHLERINGER, J. R.; HIGUCHI, N.; BUSTAMANTE, M. M. D. C.; MARTINELLI, L. A. Understanding the influences of spatial patterns on N availability within the Brazilian Amazon forest. **Ecosystems**, v. 11, n. 8, p. 1234–1246, 2008.

NAZARENO, L. S. Q.; RIBEIRO, A.; SOUSA, M. V. C.; VIEIRA, C. W.; FERRAZ FILHO, A. C. Wood volume estimation strategies for trees from a Dry Forest/Savannah transition area in Piauí, Brazil. **Southern Forests**, v. 83, n. 2, p. 111–119, 2021.

NELSON, D. W. AND SOMMERS, L. E.: Total carbon and total nitrogen, in: **Methods of Soil Analysis: Part 3 – Chemical Methods**, edited by: Sparks, D. L., SSSA Book Series No 5, American Society of Agronomy/Soil Science Society of America, Madison, WI, 961–1010, 1996.

NIKLAS, K. J.; BUCHMAN, S. L. The Allometry of Saguaro Height Author (s): Karl J . Niklas and Stephen L . Buchman Published by : Wiley Stable URL : https://www.jstor.org/stable/2445478 THE ALLOMETRY OF SAGUARO HEIGHT1. **American Journal of Botany**, v. 81, n. 9, p. 1161–1168, 1994.

NZIGUHEBA, G.; BÜNEMANN, E. K. Organic phosphorus dynamics in tropical agroecosystems. In: TURNER, B. L.; FROSSARD, E.; BALDWIN, D. (Eds.). **Organic Phosphorus in the Environment**. [s.l: s.n.]. p. 243–268.

O'DONNELL, M. S.; IGNIZIO, D. A. Bioclimatic Predictors for Supporting Ecological Applications in the Conterminous United States. **U.S Geological Survey Data Series 691**, p. 10, 2012.

OCÓN, J. P.; IBANEZ, T.; FRANKLIN, J.; PAU, S.; KEPPEL, G.; RIVAS-TORRES, G.; SHIN, M. E.; GILLESPIE, T. W. Global tropical dry forest extent and cover: A comparative study of bioclimatic definitions using two climatic data sets. **PLOS ONE**, v. 16, n. 5, 2021. Available at: https://dx.plos.org/10.1371/journal.pone.0252063

OLIVEIRA, O. F. De. Caatinga of Northeastern Brazil: Vegetation and Floristic Aspects. In: RIET-CORREA, F.; PFISTER, J.; SCHILD, A. L.; WIERENGA, T. (Eds.). **Poisoning by Plants, Mycotoxins, and Related Toxins**. [s.l.] : CAB International, 2011. p. 2–24.

OLIVEIRA, D. P.; SARTOR, L. R.; SOUZA JÚNIOR, V. S.; CORRÊA, M. M.; ROMERO, R. E.; ANDRADE, G. R. P.; FERREIRA, T. O. Weathering and clay formation in semi-arid calcareous soils from Northeastern Brazil. **Catena**, v. 162, n. March 2017, p. 325–332, 2018. Available at: https://doi.org/10.1016/j.catena.2017.10.030

OLIVEIRA, A. P. De; DUSI, D. M. de A.; WALTER, B. M. T.; GOMES, A. C. M. M.; NORONHA, S. E. De; BRAGA, M. B.; COELHO, C. M.; BARROS, L. M. G. Evaluation of Cerrado species for aluminium tolerance. **Embrapa - Boletim de Pesquisa e Desenvolvimento**, v. 355, n. February, p. 26, 2019a.

OLIVEIRA, G. de C.; FRANCELINO, M. R.; ARRUDA, D. M.; FERNANDES-FILHO, E. I.; SCHAEFER, C. E. G. R. Climate and soils at the Brazilian semiarid and the forest-Caatinga problem: New insights and implications for conservation. **Environmental Research Letters**, v. 14, n. 10, 2019b.

OLIVEIRA, M. T.; MATZEK, V.; MEDEIROS, C. D.; RIVAS, R.; FALCÃO, H. M.; SANTOS, M. G. Stress tolerance and ecophysiological ability of an invader and a native species in a seasonally dry tropical forest. **PLoS ONE**, v. 9, n. 8, 2014.

OLSEN, S AND SOMMERS, L. (1982) Phosphorus. In: **Methods of Soil Analysis 2nd Edition** (ed. A Page), pp 403-427. American Society of Agronomy/Soil Science Society of America, Madison.

PALM, C.; SANCHEZ, P.; AHAMED, S.; AWITI, A. Soils: A contemporary perspective. **Annual Review of Environment and Resources**, v. 32, p. 99–129, 2007.

PALMER, D. S ELLEY , R. C., C OCKS . L. R. M. & P LIMER , I. R. (eds) 2004. Encyclopedia of Geology (5 volumes), Volume 1 : xxxvii+594 pp; Volume 2 : xxxvii+545 pp.; Volume 3 : xxxvii+659 pp.; Volume 4 : xxxvii+692 pp.; Volume 5 : xxxvii+807 pp. Amsterdam: Elsevier. In: SELLEY, R. C.; PLIMER, L. R. M.; I. R. (ORG.) (Eds.). **Geological Magazine**. [s.l.] : Oxford:Elsevier, 2005. v. 142p. 314–315.

PAN, F.; LIANG, Y.; ZHANG, W.; ZHAO, J.; WANG, K. Enhanced nitrogen availability in karst ecosystems by oxalic acid release in the rhizosphere. **Frontiers in Plant Science**, v. 7, n. MAY2016, p. 1–9, 2016.

PANSU, M.; GAUTHEYROU, J. **Handbook of Soil Analysis - Mineralogical, Organic and Inorganic Methods**. New York: Springer, 2006.

PARAHYBA, R. da B. V.; DOS SANTOS, M. C.; NETO, F. C. R.; JACOMINE, P. K. T. Pedogenesis of Planosols in a toposequence of the agreste region of Pernambuco, Brazil. **Revista Brasileira de Ciência do Solo**, v. 34, n. 6, p. 1991–2000, 2010.

PARKER, A. An Index of Weathering for Silicate Rocks. **Geological Magazine**, v. 107, n. 6, p. 501–504, 1970.

PATEIRO-LÓPEZ, M. B; RODRÍGUEZ-CASAL, A. Generalization of the Convex Hull of a Sample of Points in the Plane '**Alphahull package**' version 2.5. 2022.

PELLA, E.: Elemental organic analysis, Part 2, State of the art, **Am. Lab**., 22, 28–32, 1990.

PEÑA-CLAROS, M.; POORTER, L.; ALARCÓN, A.; BLATE, G.; CHOQUE, U.; FREDERICKSEN, T. S.; JUSTINIANO, M. J.; LEAÑO, C.; LICONA, J. C.; PARIONA, W.; PUTZ, F. E.; QUEVEDO, L.; TOLEDO, M. Soil Effects on Forest Structure and Diversity in a Moist and a Dry Tropical Forest. **Biotropica**, v. 44, n. 3, p. 276–283, 2012.

PENNINGTON, T. R.; PRADO, D. E.; PENDRY, C. A. Neotropical seasonally dry forests and Quaternary vegetation changes. **Journal of Biogeography**, v. 27, n. 2, p. 261–273, 2000. Available at: http://doi.wiley.com/10.1046/j.1365-2699.2000.00397.x

PENNINGTON, R. T.; LEWIS, G.; RATTER, J. An Overview of the Plant Diversity, Biogeography and Conservation of Neotropical Savannas and Seasonally Dry Forests. In: PENNINGTON, R. T.; LEWIS, G. P.; RATTER, J. A. (Eds.). **Neotropical Savannas and Seasonally Dry Forests**. The System ed. [s.l.] : CRC Press, 2006. p. 1–29.

PENNINGTON, R. T.; LAVIN, M.; OLIVEIRA-FILHO, A. Woody plant diversity, evolution, and ecology in the tropics: Perspectives from seasonally dry tropical forests. **Annual Review of Ecology, Evolution, and Systematics**, v. 40, p. 437–457, 2009.

PEULVAST, J. P.; BÉTARD, F. A history of basin inversion, scarp retreat and shallow denudation: The Araripe basin as a keystone for understanding long-term landscape evolution in NE Brazil. **Geomorphology**, [s. l.], v. 233, p. 20–40, 2015. Available at: http://dx.doi.org/10.1016/j.geomorph.2014.10.009

PINHEIRO, E. A. R.; COSTA, C. A. G.; DE ARAÚJO, J. C. Effective root depth of the Caatinga biome. **Journal of Arid Environments**, v. 89, p. 1–4, 2013. Available at: http://dx.doi.org/10.1016/j.jaridenv.2012.10.003.

PINHEIRO, E. A. R.; DE VAN LIER, Q. J.; BEZERRA, A. H. F. Hydrology of a water-limited forest under climate change scenarios: The case of the Caatinga biome, Brazil. **Forests**, v. 8, n. 3, 2017.

POORTER, L. et al. Biomass resilience of Neotropical secondary forests. **Nature**, v. 530, n. 7589, p. 211–214, 2016. Available at: http://dx.doi.org/10.1038/nature16512

PORDER, S.; HILLEY, G. E. Linking chronosequences with the rest of the world: Predicting soil phosphorus content in denuding landscapes. **Biogeochemistry**, v. 102, n. 1, p. 153–166, 2011.

PORDER, S.; RAMACHANDRAN, S. The phosphorus concentration of common rocks-a potential driver of ecosystem P status. **Plant Soil**, v. 367, n. 1–2, p. 41–55, 2013.

POULTER, B.; FRANK, D.; CIAIS, P.; MYNENI, R. B.; ANDELA, N.; BI, J.; BROQUET, G.; CANADELL, J. G.; CHEVALLIER, F.; LIU, Y. Y.; RUNNING, S. W.; SITCH, S.; VAN DER WERF, G. R. Contribution of semi-arid ecosystems to interannual variability of the global carbon cycle. **Nature**, v. 509, n. 7502, p. 600–603, 2014. Available at: http://dx.doi.org/10.1038/nature13376

POWERS, J. S.; SALUTE, S. Macro- and micronutrient effects on decomposition of leaf litter from two tropical tree species: Inferences from a short-term laboratory incubation. **Plant and Soil**, v. 346, n. 1, p. 245–257, 2011.

PRADO-JUNIOR, J. A.; SCHIAVINI, I.; VALE, V. S.; ARANTES, C. S.; VAN DER SANDE, M. T.; LOHBECK, M.; POORTER, L. Conservative species drive biomass productivity in tropical dry forests. **Journal of Ecology**, v. 104, n. 3, p. 817–827, 2016.

PRADO, D. E.; GIBBS, P. E. Patterns of Species Distributions in the Dry Seasonal Forests of South America. **Annals of the Missouri Botanical Garden**, v. 80, n. 4, p. 902–927, 1993. Available at: https://www.jstor.org/stable/2399937?origin=crossref

QGIS Development Team (2022). **QGIS Geographic Information System**. Open Source Geospatial Foundation Project. http://qgis.osgeo.org

QUIDEAU, S. A.; CHADWICK, O. A.; BENESI, A.; GRAHAM, R. C.; ANDERSON, M. A. A direct link between forest vegetation type and soil organic matter composition. **Geoderma**, [s. l.], v. 104, n. 1–2, p. 41–60, 2001.

QUEIROZ, L. P. de. The Brazilian Caatinga: Phytogeographical Patterns Inferred from Distribution Data of the Leguminosae. In: PENNINGTON, R. T.; LEWIS, G. P.; RATTER, J. A. (Eds.). **Neotropical Savannas and Seasonally Dry Forests**. The System ed. [s.l.] : CRC Press, 2006. p. 121–158.

QUEIROZ, L. P. de; CARDOSO, D.; FERNANDES, M. F.; MORO, M. F. Diversity and Evolution of Flowering Plants of the Caatinga Domain. In: SILVA, J. M. C. Da; LEAL, I. R.; TABARELLI, M. (Eds.). **Caatinga: The Largest Tropical Dry Forest Region in South America**. [s.l.] : Springer, 2017. p. 23–64.

QUESADA, C. A.; LLOYD, J.; SCHWARZ, M.; PATIÑO, S.; BAKER, T. R.; CZIMCZIK, C.; FYLLAS, N. M.; MARTINELLI, L.; NARDOTO, G. B.; SCHMERLER, J.; SANTOS, A. J. B.; HODNETT, M. G.; HERRERA, R.; LUIZÃO, F. J.; ARNETH, A.; LLOYD, G.; DEZZEO, N.; HILKE, I.; KUHLMANN, I.; RAESSLER, M.; BRAND, W. A.; GEILMANN, H.; FILHO, J. O. M.; CARVALHO, F. P.; FILHO, R. N. A.; CHAVES, J. E.; CRUZ, O. F.; PIMENTEL, T. P.; PAIVA, R. Variations in chemical and physical properties of Amazon forest soils in relation to their genesis. **Biogeosciences**, v. 7, n. 5, p. 1515–1541, 2010.

QUESADA, C. A. N.; PAZ, C.; OBLITAS MENDOZA, E.; LAWRENCE PHILLIPS, O.; SAIZ, G.; LLOYD, J. Variations in soil chemical and physical properties explain basin-wide Amazon forest soil carbon concentrations. **Soil**, v. 6, n. 1, p. 53–88, 2020. a. Available at: https://soil.copernicus.org/articles/6/53/2020/

QUESADA, C. A.; PHILLIPS, O. L.; SCHWARZ, M.; CZIMCZIK, C. I.; BAKER, T. R.; PATIÑO, S.; FYLLAS, N. M.; HODNETT, M. G.; HERRERA, R.; ALMEIDA, S.; ALVAREZ DÁVILA, E.; ARNETH, A.; ARROYO, L.; CHAO, K. J.; DEZZEO, N.; ERWIN, T.; DI FIORE, A.; HIGUCHI, N.; HONORIO CORONADO, E.; JIMENEZ, E. M.; KILLEEN, T.; LEZAMA, A. T.; LLOYD, G.; LÖPEZ-GONZÁLEZ, G.; LUIZÃO, F. J.; MALHI, Y.; MONTEAGUDO, A.; NEILL, D. A.; NÚÑEZ VARGAS, P.; PAIVA, R.; PEACOCK, J.; PEÑUELA, M. C.; PEÑA CRUZ, A.; PITMAN, N.; PRIANTE FILHO, N.; PRIETO, A.; RAMÍREZ, H.; RUDAS, A.; SALOMÃO, R.; SANTOS, A. J. B.; SCHMERLER, J.; SILVA, N.; SILVEIRA, M.; VÁSQUEZ, R.; VIEIRA, I.; TERBORGH, J.; LLOYD, J. Basin-wide variations in Amazon forest structure and function are mediated by both soils and climate. **Biogeosciences**, v. 9, n. 6, p. 2203–2246, 2012.

R CORE TEAM (2021). **R: A language and environment for statistical computing**. R Foundation for Statistical Computing, Vienna, Austria. URL https://www.R-project.org/.

RATKE, R. F.; CAMPOS, A. R.; INDA, A. V.; BARBOSA, R. S.; BEZERRA DA SILVA, Y. J. A.; AZEVEDO NÓBREGA, J. C.; LOPES DA SILVA, J. B. Agricultural potential and soil use based on the pedogenetic properties of soils from the cerrado-caatinga transition. **Semina:Ciencias Agrarias**, v. 41, n. 4, p. 1119–1134, 2020.

RÉJOU-MÉCHAIN, A. M.; CHAVE, J.; HÉRAULT, B.; FELDPAUSCH, T.; VERLEY, P. **Package ' BIOMASS** '. 2021.

RIBEIRO, K.; SOUSA-NETO, E. R. De; CARVALHO, J. A. De; SOUSA LIMA, J. R. De; MENEZES, R. S. C.; DUARTE-NETO, P. J.; DA SILVA GUERRA, G.; OMETTO, J. P. H. B. Land cover changes and greenhouse gas emissions in two different soil covers in the Brazilian Caatinga. **Science of the Total Environment**, v. 571, p. 1048–1057, 2016. Available at: http://dx.doi.org/10.1016/j.scitotenv.2016.07.095

RICH, P. M. Mechanical Architecture of Arborescent Rain Forest Palms. **Principes**, v. 30, n. 3, p. 117–131, 1986.

RIGHI, D.; MEUNIER, A. Origin and Mineralogy of Clays. In: VELDE, B. (Ed.). **Origin and Mineralogy of Clays**. Paris. p. 523. 1995.

RIVERO-VILLAR, A.; RUIZ-SUÁREZ, G.; TEMPLER, P. H.; SOUZA, V.; CAMPO, J. Nitrogen cycling in tropical dry forests is sensitive to changes in rainfall regime and nitrogen deposition. **Biogeochemistry**, v. 153, n. 3, p. 283–302, 2021.

RODAL, M. J. N. .; SAMPAIO, E. V. S. B.; FIGUEIREDO, M. A. **Manual sobre métodos de estudo florístico e fitossociológico: Ecossistema Caatinga**. [s.l.] : SBB, 2013. Available at: http://www.botanica.org.br/ebook/man_sob_met_est_flo_fit.pdf

ROGGY, J. C.; PREVOST, M.; GARBAYE, J.; DOMENACH, A. M. Nitrogen cycling in the tropical rainforest of French Guiana: Comparison of two sites with contrasting soil types ^{15}N. **Journal of Tropical Ecology** 15: 1-22. 1999.

RÖMHELD, V.; MARSCHNER, H. Function of Micronutrients in Plants. In: MORTVEDT, J. J.; COX, F. R.; SHUMAN, L. M.; WELCH, R. M. (Eds.). **Micronutrients in Agriculture**. 2. ed. Madison: Soil Science Society of America, Inc., 1991. p. 297–324.

SALCEDO, I. H.; Biogeoquímica do fósforo em solos da região semi-árida do NE do Brasil. **Revista Geografia**, v. 23, n. 3, p. 159-184, 2006.

SALDARRIAGA, J. G.; WEST, D. C.; THARP, M. L.; UHL, C. Long-Term Chronosequence of Forest Succession in the Upper Rio Negro of Colombia and Venezuela. **The Journal of Ecology**, v. 76, n. 4, p. 938, 1988.

SAMPAIO, E. V. S. B. Overview of the Brazilian Caatinga. In: MOONEY, H. A.; BULLOCK, S. H.; MEDINA, E. (Eds.). **Seasonally Dry Tropical Forests**. [s.l.] : Cambridge University Press, 1995. p. 35–63.

SAMPAIO, E. V. S. B. Caracterização do bioma caatinga: características e potencialidades. In: GARIGLIO, M. A.; CESTARO, E. V. de S. B. S. L. A.; KAGEYAMA, P. Y. (Eds.). **Uso sustentável e conservação dos recursos florestais da caatinga.** Brasília: MMA, 2010. p. 29–48.

SAMPAIO, E. V. S. B.; SILVA, G. C. Biomass Equations for Brazilian semiarid caatinga plants. **Acta Botanica Brasilica**, v. 19, n. 4, p. 935–943, 2005.

SANCHEZ, P. A. **Properties and Management of Soils in the Tropics**. 2. ed. New York: Cambridge University Press, 2019.

SANCHEZ, P. A.; UEHARA, G. Management Considerations for Acid Soils with High Phosphorus Fixation Capacity. In: **The Role of Phosphorus in Agriculture**. [s.l: s.n.]. p. 471–514.

SANTANA, A. S. de; SANTOS, G. Impactos da seca de 2012-2017 na região semiárida do Nordeste: notas sobre a abordagem de dados quantitativos e conclusões qualitativas. **In: Boletim Regional, Urbano e Ambiental**. [s.l: s.n.]. p. 119–129. 2020.

SANTOS, F. L. S.; VASCONCELOS, V.; JESUS, K.; NEVES, G.; COUTO JUNIOR, A. F.; SAMPAIO, E. V; OMETTO, J. P.; MENEZES, R. S. C.; NARDOTO, G. B. Climatic controls on the soil nitrogen isotopic composition across the physiographic regions of the Pernambuco state, northeast Brazil. **Geoderma Regional**, v. 30, n. February 2021, 2022.

SANTOS, H. G.; JACOMINE, P. K. T.; ANJOS, L. H. C.; OLIVEIRA, V. A.; LUMBRERAS, J. F.; COELHO, M. R.; ALMEIDA, J. A.; FILHO., J. C. A.; CUNHA, T. J. F.; OLIVEIRA, J. B. **Sistema Brasileiro de Classificação de Solos** (SiBCS). EMBRAPA. 2018.

SANTOS, J. C.; LEAL, I. R.; ALMEIDA-CORTEZ, J. S.; FERNANDES, G. W.; TABARELLI, M. Caatinga: The Scientific Negligence Experienced by a Dry Tropical Forest. **Tropical Conservation Science**, v. 4, n. 3, p. 276–286, 2011. Available at: http://journals.sagepub.com/doi/10.1177/194008291100400306

SÄRKINEN, T.; IGANCI, J. R. V.; LINARES-PALOMINO, R.; SIMON, M. F.; PRADO, D. E. Forgotten forests - issues and prospects in biome mapping using Seasonally Dry Tropical Forests as a case study. **BMC Ecology**, v. 11, n. 1, p. 27, 2011. Available at: http://bmcecol.biomedcentral.com/articles/10.1186/1472-6785-11-27

SARMIENTO, C.; PATIÑO, S.; TIMOTHY PAINE, C. E.; BEAUCHÊNE, J.; THIBAUT, A.; BARALOTO, C. Within-individual variation of trunk and branch xylem density in tropical trees. **American Journal of Botany**, v. 98, n. 1, p. 140–149, 2011.

SCHENK, H. J.; JACKSON, R. B. The global biogeography of roots. **Ecological Monographs**, v. 72, n. 3, p. 311–328, 2002.

SCHJØNNING, P.; JENSEN, J. L.; BRUUN, S.; JENSEN, L. S.; CHRISTENSEN, B. T.; MUNKHOLM, L. J.; OELOFSE, M.; BABY, S.; KNUDSEN, L. The Role of Soil Organic Matter for Maintaining Crop Yields: Evidence for a Renewed Conceptual Basis. **Advances in Agronomy**, v. 150, p. 35–79, 2018.

SCHOBBENHAUS, C.; NEVES, B. B. B. A geologia do Brasil no contexto da plataforma Sul-americana. **Geology, Tectonics and Mienral Resources of Brazil**, n. December, p. 5–54, 2003.

SCHRODT, F.; DOMINGUES, T. F.; FELDPAUSCH, T. R.; SAIZ, G.; QUESADA, C. A.; SCHWARZ, M.; ISHIDA, F. Y.; COMPAORE, H.; DIALLO, A.; DJAGBLETEY, G.; HIEN, F.; SONKÉ, B.; TOEDOUMG, H.; ZAPFACK, L.; HIERNAUX, P.; MOUGIN, E.; BIRD, M. I.; GRACE, J.; LEWIS, S. L.; VEENENDAAL, E. M.; LLOYD, J. Foliar trait contrasts between African forest and savanna trees: Genetic versus environmental effects. **Functional Plant Biology**, v. 42, n. 1, p. 63–83, 2015.

SCHROO, H. A study of highly phos-phatic soils in a karst region of the humid tropics. **Netherlands Journal of Agricultural Science**, v. 11, n. 3, p. 209–231, 1963.

SCHULTE, E. E. Fertilizer Sources of Iron. **Understanding Plant Nutrients**, v. 9, n. 92, p. 2, 2004. Available at: http://corn.agronomy.wisc.edu/Management/pdfs/a3554.pdf

SCHULZE, D. G. CLAY MINERALS. In: **Encyclopedia of Soils in the Environment**. Chichester, UK: Elsevier, 2005. v. 3p. 246–254.

SHAHID, M.; FERRAND, E.; SCHRECK, E.; DUMAT, C. Behavior and impact of zirconium in the soil-plant system: Plant uptake and phytotoxicity. **Reviews of Environmental Contamination and Toxicology**, v. 221, p. 107–127, 2013.

SHARMA, D.; KUMAR, A. **Calcium signaling network in abiotic stress tolerance in plants**. [s.l.] : Elsevier Inc., 2021. v. 2 Available at: http://dx.doi.org/10.1016/B978-0-12-821792-4.00003-5

SHUMAN, L. M. Chemical Forms of Micronutrients in Soils. In: **Micronutrients in Agriculture**. p. 113–144. 2018.

SIEFERT, A.; RAVENSCROFT, C.; ALTHOFF, D.; ALVAREZ-YÉPIZ, J. C.; CARTER, B. E.; GLENNON, K. L.; HEBERLING, J. M.; JO, I. S.; PONTES, A.; SAUER, A.; WILLIS, A.; FRIDLEY, J. D. Scale dependence of vegetation-environment relationships: A meta-analysis of multivariate data. **Journal of Vegetation Science**, v. 23, n. 5, p. 942–951, 2012.

SILVA, F.B.R., RICHE, G.R., TONNEAU, J.P., SOUZA NETO, N.C., BRITO, L.T.L., CORREIA, R.C., CAVALCANTE, A.C., SILVA, A.B., ARAUJO FILHO, J.C. and LEITE, A.P. **Zoneamento agroecológico do Nordeste: diagnóstico do quadro natural e agrossocioeconômico**. Petrolina: EMBRAPA-CPATSA. 325 p. 1993

SILVA, A. F. da; FREITAS, A. D. S.; COSTA, T. L.; FERNANDES-JÚNIOR, P. I.; MARTINS, L. M. V.; SANTOS, C. E. de R. e S.; MENEZES, K. A. S.; SAMPAIO, E. V. de S. B. Biological nitrogen fixation in tropical dry forests with different legume diversity and abundance. **Nutrient Cycling in Agroecosystems**, v. 107, n. 3, p. 321–334, 2017.

SILVA, J. M. C. DA, BARBOSA, L. C. F., LEAL, I. R., & TABARELLI, M. (2017). The caatinga: Understanding the challenges. In **Caatinga** (pp. 3–19). Cham: Springer International Publishing. https://doi.org/10.1007/978-3-319-68339-3_1.

SILVEIRA, M. M. L. Da; ARAÚJO, M. do S. B.; SAMPAIO, E. V. de S. B. Phosphorus Distribution in Different Soil Orders in the Semi-arid States of Paraíba and Pernambuco, Brazil. **Revista Brasileira de Ciência do Solo**, v. 30, n. 2, p. 281–291, 2006.

SINGH, M.; SARKAR, B.; BISWAS, B.; BOLAN, N. S.; CHURCHMAN, G. J. Relationship between soil clay mineralogy and carbon protection capacity as influenced by temperature and moisture. **Soil Biology and Biochemistry**, v. 109, p. 95–106, 2017. Available at: http://dx.doi.org/10.1016/j.soilbio.2017.02.003

SINGH, M.; SARKAR, B.; SARKAR, S.; CHURCHMAN, J.; BOLAN, N.; MANDAL, S.; MENON, M.; PURAKAYASTHA, T. J.; BEERLING, D. J. Stabilization of Soil Organic Carbon as Influenced by Clay Mineralogy. In: **Advances in Agronomy**. 1. ed. [s.l.] : Elsevier Inc., 2018. v. 148p. 33–84.

SIYUM, Z. G. Tropical dry forest dynamics in the context of climate change: syntheses of drivers, gaps, and management perspectives. **Ecological Processes**, v. 9, n. 1, p. 25, 2020. Available at: https://ecologicalprocesses.springeropen.com/articles/10.1186/s13717-020-00229-6

SMECK, N. E. Phosphorus dynamics in soils and landscapes. **Geoderma**, v. 36, n. 3–4, p. 185–199, 1985.

SMITH, D.B., SOLANO, FEDERICO, WOODRUFF, L.G., CANNON, W.F., AND ELLEFSEN, K.J., 2019, Geochemical and mineralogical maps, with interpretation, for soils of the conterminous United States: **U.S. Geological Survey Scientific Investigations Report 2017**-5118, https://doi.org/10.3133/sir20175118.

SONG, W. Y.; ZHANG, Z. Bin; SHAO, H. B.; GUO, X. L.; CAO, H. X.; ZHAO, H. Bin; FU, Z. Y.; HU, X. J. Relationship between calcium decoding elements and plant abiotic-stress resistance. **International Journal of Biological Sciences**, v. 4, n. 2, p. 116–125, 2008.

SOUTO, P. C.; BAKKE, I. A.; SOUTO, J. S.; OLVEIRA, V. M. De. Cinética Da Respiração Edáfica Em Dois Ambientes Kinetics of the Soil Respiration in Two Different Sites. **Revista Caatinga**, [s. l.], v. 22, n. 1985, p. 52–58, 2009.

SOUZA, D. G.; SFAIR, J. C.; DE PAULA, A. S.; BARROS, M. F.; RITO, K. F.; TABARELLI, M. Multiple drivers of aboveground biomass in a human-modified landscape of the Caatinga dry forest. **Forest Ecology and Management**, v. 435, n. July 2018, p. 57–65, 2019. Available at: https://doi.org/10.1016/j.foreco.2018.12.042

SOUZA, J. J. L. L. de; B. I.; XAVIER, R. A.; PACHECO, A. A.; PESSENDA, L. C. R.; DOS SANTOS BRITO, E. Archaeoanthrosol formation in the Brazilian semiarid. **Catena**, v. 193, n. March, p. 104603, 2020. Availae at: https://doi.org/10.1016/j.catena.2020.104603

SOUZA, J. J. L. L. de; SOUZA, B. I.; XAVIER, R. A.; CARDOSO, E. C. M.; DE MEDEIROS, J. R.; DA FONSECA, C. F.; SCHAEFER, C. E. G. R. Organic carbon rich-soils in the brazilian semiarid region and paleoenvironmental implications. **Catena**, v. 212, n. July 2021, 2022.

SOUZA, I. M.; HUGHES, F. M.; FUNCH, L. S.; DE QUEIROZ, L. P. Nocturnal and diurnal pollination in Copaifera coriacea, a dominant species in sand dunes of the middle São Francisco River Basin, Northeastern Brazil. **Plant Ecology and Evolution**, v. 154, n. 2, p. 207–216, 2021.

SPARKS, D. L. Dynamics of K in soils and their role in management of K nutrition. **Potassium for sustainable crop production**, n. Gurgaon, Haryana, India, p. 79–101, 2002.

SPRENT, J. I. **Legume Nodulation: A Global Perspective**. [s.l.] : John Wiley & Sons, Ltd, 2009.

SULLIVAN, M. J. P. et al. Long-term thermal sensitivity of earth's tropical forests. **Science**, v. 368, n. 6493, p. 869–874, 2020.

SWAP, R.; GARSTANG, M.; GRECO, S.; TALBOT, R.; KALLBERG, P. Saharan dust in the Amazon Basin. **Tellus, Series B**, v. 44 B, n. 2, p. 133–149, 1992.

SWAP, R. J.; ARANIBAR, J. N.; DOWTY, P. R.; GILHOOLY, W. P.; MACKO, S. A. Natural abundance of 13C and 15N in C3 and C4 vegetation of southern Africa: Patterns and implications. **Global Change Biology**, v. 10, n. 3, p. 350–358, 2004.

SZYJA, M.; MENEZES, A. G. de S.; OLIVEIRA, F. D. A.; LEAL, I.; TABARELLI, M.; BÜDEL, B.; WIRTH, R. Neglected but Potent Dry Forest Players: Ecological Role and Ecosystem Service Provision of Biological Soil Crusts in the Human-Modified Caatinga. **Frontiers in Ecology and Evolution**, v. 7, n. December, p. 1–18, 2019.

TAIZ L. & ZEIGER E. (2014). **Plant physiology and development:6th revised edition**. SINAUER Associates Inc. U.S.

TERRA, M. de C. N. S.; SANTOS, R. M. Dos; JÚNIOR, J. A. do P.; MELLO, J. M. De; SCOLFORO, J. R. S.; FONTES, M. A. L.; SCHIAVINI, I.; REIS, A. A. Dos; BUENO, I. T.; MAGNAGO, L. F. S.; STEEGE, H. Ter. Water availability drives gradients of tree diversity, structure and functional traits in the Atlantic-Cerrado-Caatinga transition, Brazil. **Journal of Plant Ecology**, v. 11, n. 6, p. 803–814, 2018.

TIESSEN, H. AND MOIR, J. O.: Total and Organic Carbon, in: **Soil Sampling and Methods of Analysis**, edited by: Carter, M. R., 187– 199, Lewis Publishers, Boca Raton, FL, 1993.

TIESSEN, H.; SALCEDO, I. H.; SAMPAIO, E. V. S. B. Nutrient and soil organic matter dynamics under shifting cultivation in semi-arid northeastern Brazil. **Agriculture, Ecosystems and Environment**, v. 38, n. 3, p. 139–151, 1992.

TIESSEN, H.; SAMPAIO, E. V. S. B.; SALCEDO, I. H. Organic matter turnover and management in low input agriculture of NE Brazil. **Nutrient Cycling in Agroecosystems**, v. 61, n. 1–2, p. 99–103, 2001.

TILMAN, D.; ISBELL, F.; COWLES, J. M. Biodiversity and ecosystem functioning. **Annual Review of Ecology, Evolution, and Systematics**, v. 45, p. 471–493, 2014.

TILMAN, D.; KNOPS, J.; WEDIN, D.; REICH, P.; RITCHIE, M.; SIEMANN, E. The influence of functional diversity and composition on ecosystem processes. **Science**, v. 277, n. 5330, p. 1300–1302, 1997.

TISDALL, J. M.; OADES, J. M. Organic matter and water-stable aggregates in soils. **Journal of Soil Science**, v. 33, n. 2, p. 141–163, 1982.

UPADHYAY, S.; RAGHUBANSHI, A. S. **Determinants of soil carbon dynamics in urban ecosystems**. [s.l.] : Elsevier Inc., 2020. Available at: http://dx.doi.org/10.1016/B978-0-12-820730-7.00016-1

VAN GENUCHTEN, M. T. A Closed-form Equation for Predicting the Hydraulic Conductivity of Unsaturated Soils. **Soil Science Society of America Journal**, v. 44, n. 5, p. 892–898, 1980.

VELLOSO, A. L.; SAMPAIO, E. V. S. B.; GIULIETTI, A. M.; BARBOSA, M. R. V.; CASTRO, A. A. J. F.; QUEIROZ, L. P. De; FERNANDES, A.; OREN, D. C.; CESTARO, L. A.; CARVALHO, A. J. E. De; PAREYN, F. G. C.; SILVA, F. B. R. Da; MIRANDA, E. E. De; KEEL, S.; GONDIM, R. S. Ecorregiões - Propostas para o Bioma Caatinga. In: VELLOSO, A. L.; SAMPAIO, E. V. S. B.; PAREYN, F. G. . (Eds.). **Resultados do Seminário de Planejamento Ecorregional da Caatinga**. Aldeia - PE: The Nature Consevancy do Brasil, Associação Plantas do Nordeste, 2001. p. 75.

VILÀ, M.; CARRILLO-GAVILÁN, A.; VAYREDA, J.; BUGMANN, H.; FRIDMAN, J.; GRODZKI, W.; HAASE, J.; KUNSTLER, G.; SCHELHAAS, M. J.; TRASOBARES, A. Disentangling Biodiversity and Climatic Determinants of Wood Production. **PLoS ONE**, v. 8, n. 2, 2013.

VILAGROSA, A.; CHIRINO, E.; PEGUERO-PINA, J. X.; BARIGAH, T. S.; CHOCARD, H.; et al.. Xylem cavitation and embolism in plants living in water-limited ecosystems. In: **Plant responses to drought stress**, Springer, 466 p., 2012, 978-3-642-32652-3. 10.1007/978-3-642-32653-0_3 . hal-00964859

VITOUSEK, P. Nutrient cycling and nutrient use efficiency. **The American Naturalist**, v. 119, n. 4, 1982.

VITOUSEK, P. M. Litterfall , Nutrient Cycling , and Nutrient Limitation in Tropical Forests. **Ecological Society of America**, v. 65, n. 1, p. 285–298, 1984.

VITOUSEK, P. M.; SANFORD, R. L. Nutrient cycling in moist tropical forest. **Annual Review of Ecology & Systematics 17**: 137-167. 1986.

VITOUSEK, P. M.; SHEARER, G.; KOHL, D. H. Foliar ^{15}N natural abundance in Hawaiian rainforest: patterns and possible mechanisms. **Oecologia**, v. 78, n. 3, p. 383–388, 1989.

WAKEEL, A.; FAROOQ, M.; QADIR, M.; SCHUBERT, S. Potassium substitution by sodium in plants. **Critical Reviews in Plant Sciences**, v. 30, n. 4, p. 401–413, 2011.

WALKER, T. W.; SYERS, J. K. The fate of phosphorus during pedogenesis. **Geoderma**, v. 15, n. 1, p. 1–19, 1976.

WANG, H.; BOUTTON, T. W.; XU, W.; HU, G.; JIANG, P.; BAI, E. Quality of fresh organic matter affects priming of soil organic matter and substrate utilization patterns of microbes. **Scientific Reports**, v. 5, n. May, p. 1–13, 2015.

WEIL R. R., & BRADY N. C. **The nature and properties of soils, global edition** (15th ed.). Pearson Education (2016).

WELTZIN, J. F.; LOIK, M. E.; SCHWINNING, S.; WILLIAMS, D. G.; FAY, P. A.; HADDAD, B. M.; HARTE, J.; HUXMAN, T. E.; KNAPP, A. K.; LIN, G.; POCKMAN, W. T.; SHAW, M. R.; SMALL, E. E.; SMITH, M. D.; SMITH, S. D.; TISSUE, D. T.; ZAK, J. C. Assessing the Response of Terrestrial Ecosystems to Potential Changes in Precipitation. **BioScience**, v. 53, n. 10, p. 941–952, 2003.

WHITE, J. G.; ZASOSKI, R. J. Mapping soil micronutrients. **Field Crops Research**, v. 60, n. 1–2, p. 11–26, 1999.

WICKHAM H (2016). ggplot2: Elegant Graphics for Data Analysis. **R Package.** Springer-Verlag New York. ISBN 978-3-319-24277-4, https://ggplot2.tidyverse.org.

WILKINS, K. A.; MATTHUS, E.; SWARBRECK, S. M.; DAVIES, J. M. Calcium-mediated abiotic stress signaling in roots. **Frontiers in Plant Science**, v. 7, n. AUG2016, p. 1–17, 2016.

WILSON, M. J. The origin and formation of clay minerals in soils: past, present and future perspectives. **Clay Minerals**, v. 34, n. 1, p. 7–25, 1999.

WU, S.; HU, C.; TAN, Q.; LI, L.; SHI, K.; ZHENG, Y.; SUN, X. Drought stress tolerance mediated by zinc-induced antioxidative defense and osmotic adjustment in cotton (Gossypium Hirsutum). **Acta Physiologiae Plantarum**, v. 37, n. 8, 2015.

ZANNE, A.E. et al., 2009. Towards a Worldwide Wood Economics Spectrum https://doi.org/10.5061/dryad.234 (**Dryad Digital Repository**).

ZOMER, R. J.; TRABUCCO, A. **Global Aridity Index and Potential Evapo-Transpiration (ET_0) Database v3**. n. March, p. 1–6, 2022.